2014-04-28

Equation of State Based Thermal Compositional Reservoir Simulator for Hybrid Solvent/Thermal Processes

Heidari, Mohammadreza

UNIVERSITY OF CALGARY

Equation of State Based Thermal Compositional Reservoir Simulator for Hybrid Solvent/Thermal Processes

by

Mohammadreza Heidari

A THESIS

SUBMITTED TO THE FACULTY OF GRADUATE STUDIES

IN PARTIAL FULFILMENT OF THE REQUIREMENTS FOR THE

DEGREE OF DOCTOR OF PHILOSOPHY

DEPEARTMENT OF CHEMICAL AND PETROLEUM ENGINEERING

CALGARY, ALBERTA

APRIL, 2014

Abstract

In the earlier generations of thermal compositional simulators, several assumptions are used for representing the characteristics of dead oil and steam mixtures. The K-Value approach is used for phase splitting and equilibrium ratios are considered to be functions of only temperature and pressure. Phase properties such as density, enthalpy and internal energy are calculated from correlations using ideal solution assumption. Excess properties such as excess enthalpy and density and mutual solubility of water in oil phase and vice versa are neglected in such models.

These assumptions may work well for simple fluid mixtures with pure steam injection but could produce false results in more complicated processes such as the hybrid processes involving injection of hydrocarbons with steam. In such processes, where a hydrocarbon is added to the steam, equilibrium ratios change with the variation of composition, and neglecting this effect may lead to thermodynamically inconsistent or wrong results. Solubility of water in oil phase increases with temperature and it could become significantly high in some cases.

In this study, a new 3-D, fully implicit, equation of state (EOS) based thermal compositional simulator capable of modeling hybrid and thermal processes of heavy oil recovery was developed. By using an equation of state, our goal is to correctly model the thermodynamic and compositional effects on the phase behavior. Water is allowed to be soluble in all phases and mutual solubility of oil and water is taken into account in this simulator and its effect on the oil recovery can be investigated. Thermal expansion, fluid compressibility, solvent extraction, and steam distillation are calculated by an EOS based thermodynamic model. Steam properties are calculated from EOS or steam tables.

A new isenthalpic multiphase flash calculation was also developed and was integrated in the thermal compositional simulator. The flash calculation method uses a modified Rachford-Rice monotonic objective function and the negative flash concept for phase distribution and phase identification. Therefore phase stability analysis is not necessary and the flash method is not computationally expensive. The new isenthalpic multiphase flash calculation shows no difficulty in handling difficult situations such as narrow boiling point regions and appearance and disappearance of different phases which is common in thermal processes.

Acknowledgements

I would like to take this opportunity to express my gratitude, regards and sincere thanks to my supervisor, Professor Brij B. Maini for his continuous guidance and support throughout my study at the University of Calgary and completion of this project.

I am also thankful to the member of my dissertation committee Professor Ian D. Gates and Dr.Hassan Hassanzadeh for their comments and suggestions during this study.

I am very grateful to Dr. Abdoljalil Varavei for his technical inputs, helpful discussions, and great suggestions.

I would also like to acknowledge the financial support from Schlumberger Regional Technology Center, Calgary, Canada. Without this support this achievement would not be possible.

To love of my life, Maryam

Table of Contents

List of Tables

List of Figures and Illustrations

List of Symbols, Abbreviations and Nomenclature

Symbol	Definition
A	Dimensionless parameter used in the EOS
A_r	First coefficient of rock heat capacity
a	Mixture parameter used in the EOS
a_i	Pure component parameter used in the EOS
a_{oi}	Pure component viscosity coefficient
B	Dimensionless parameter used in the EOS
B_r	Second coefficient of rock heat capacity
b	Mixture parameter used in the EOS
b_i	Pure component parameter used in the EOS
b_{oi}	Pure component viscosity coefficient
C_f	Pore volume compressibility factor
C_{pi}^o	Pure component ideal gas state heat capacity
C_v	Constant volume heat capacity
cf	Conversion factor
D_{ij}	Diffusion coefficient of pure component
d	Diffusion length in heat loss model
d_{ij}	Binary interaction coefficient
d'_{ij}	Parameter used in fugacity equation
E	Energy
E_c	Energy stored in the cap-rock
ew	Relative permeability exponent for water
eg	Relative permeability exponent for gas
eow	Relative permeability exponent for oil w.r.t water
eog	Relative permeability exponent for oil w.r.t gas
F_j	Phase mole fraction
f	Degree of freedom
f_a	Accumulation term of residual

f_f	Flow term of residual
f_{ij}	Fugacity of component *i* in phase *j*
f_{ir}	Fugacity of component *i* in reference phase
f_s	Sink/Source term of residual
f_w	Fractional flow
G	Geometric factor
H_{sys}	System total molar enthalpy
H^t	Total enthalpy of fluid mixture
h_j	Phase molar enthalpy
h_{ij}	Component molar enthalpy in phase j
h_{mix}	Mixture molar enthalpy
h	molar enthalpy
h^0	Ideal gas state phase molar enthalpy
I	Parameter used in the heat loss model
K_i	Equilibrium ratio of a pure component
k_i^I	Equilibrium ratio of a pure component of phase I
k_i^{II}	Equilibrium ratio of a pure component of phase II
K_w^*	Parameter used in MRR equation
K_w^z	Parameter used in MRR equation
K_i^{go}	Equilibrium ratio of a pure component between oil and gas phases
K_i^{wo}	Equilibrium ratio of a pure component between oil and water phases
K_T	Heat conduction of rock
k_x	Permeability in x-direction
k_y	Permeability in y-direction
k_z	Permeability in z-direction
k	Absolute permeability
k_{rj}	Relative permeability of phase j
k_{row}	Relative permeability of oil in presence of water
k_{roiw}	Endpoint Relative permeability of oil in presence of water
k_{rgro}	Endpoint Relative permeability of gas at residual oil saturation
k_{rwro}	Endpoint Relative permeability of water at residual oil saturation
k_{rog}	Endpoint Relative permeability of oil in presence of water

k_{roig}	Endpoint Relative permeability of oil in presence of gas
$kv1$	First coefficient for K-Value of pure component
$kv2$	Second coefficient for K-Value of pure component
$kv3$	Third coefficient for K-Value of pure component
$kv4$	Forth coefficient for K-Value of pure component
$kv5$	Fifth coefficient for K-Value of pure component
L	Liquid phase mole fraction
L_g	Gas phase mole ratio
L_o	Oil phase mole ratio
L_w	Water phase mole ratio
M_w	Molecular weight
N_c	Number of components
N_i	Total mole number of pure component
nb	Number of grid-blocks
n_{ij}	Mole number of component *i* in phase *j*
Np	Number of phases
$nlay$	Number of layers
P	Pressure
P_0	Reference pressure
P_{cons}	Constraint pressure
p	Parameter used in the heat loss model
p_{bh}	Bottom-hole pressure
p_{bhref}	Bottom-hole pressure for reference layer
P_{ci}	Critical pressure for pure component
P_{cog}	Capillary pressure oil-gas phase
P_{cow}	Capillary pressure oil-water phase
q	Parameter used in the heat loss model
q_{cons}	Rate constraint
q_h	Molar enthalpy rate of injection or production
q_i	Total molar flow rate of component *i*
q_{ij}	Molar flow rate of component *i* in phase *j*
q_t	Total molar flow rate
R	Gas constant

r_e	Equivalent well radius
r_w	Well-bore radius
S_j	Phase Saturation
S_{jir}	Irreducible phase saturation
S_{orw}	Residual oil saturation to water
S_{jc}	Critical phase saturation
S_{org}	Residual oil saturation to gas
S_f	Skin factor
T	Temperature
T_{ci}	Component critical temperature
T_D	Dimensionless Temperature in Lauwerier problem
T_{ij}	Pure component transmissibility in phase *j*
T_{ref}	Reference temperature
T_{ri}	Component reduced temperature
t	Time
t_{sw}	Front time in water flooding
U_j	Molar internal energy of phase j
U_r	Rock internal energy
u_j	Darcy's velocity
V	Vapor phase mole fraction
V^*	Parameter used in free water flash calculation
$\bar{V}$	Parameter used in free water flash calculation
V_b	Bulk volume
V_J	Phase j volume
V_{max}	Parameter used in free water flash calculation
V_{min}	Parameter used in free water flash calculation
V_p	Pore volume
v_j	Phase molar volume
W	Aqueous phase mole fraction
w_i	Aqueous pure component mole fraction
WI	Well index
X_D	Dimensionless length in Lauwerier problem
X_p	Primary variable

X_g	Gas ratio in PER method
X_o	Oil Ratio in PER method
X_w	Water Ratio in PER method
x_i	Liquid pure component mole fraction
x_{ij}	Component mole fraction in phase j
x_{Sw}	Front location in water flooding
y_i	Vapor pure component mole fraction
Y_D	Dimensionless length in Lauwerier problem
Z_j	Phase compressibility factor
ZH	Global mole fraction-Enthalpy
ZT	Global mole fraction-Temperature
z	Distance from boundary in z-direction
z_i	Pure component global mole fraction
z_{ref}	Reference depth

Greek Symbols

δ	Differentiator
$\bar{\delta}$	Time differentiator
δ_1	First numerical constant in EOS
δ_2	Second numerical constant in EOS
Ω_a	Equation of state parameters
Ω_b	Equation of state parameters
θ	Parameter used in the heat loss model
θ_0	Parameter used in the heat loss model
α	Thermal diffusivity of cap and base rock
κ	Thermal conductivity of rock
λ_j	Phase mobility
μ_j	Phase viscosity
μ_{oi}	Oleic pure component viscosity
ρ_j	Phase molar density
ρ_r	Rock density
Φ_j	Phase potential

φ_{ij}	Pure component fugacity in phase j
ϕ	porosity
ϕ_0	Reference porosity
ω_i	Acentric factor
τ_D	Dimensionless time in Lauwerier problem
∞	infinity
∇	gradient
Δ	Increment

Acronyms

ADI	Alternative direction method
API	American petroleum Institute
CSR	Compact Sparse Row
EOS	Equation of State
ES-SAGD	Expanded solvent SAGD
GMRES	General Minimized ReSidual
IMPES	Implicit pressure Explicit saturation
QNSS	Quasi Newton Successive Substitution
MRR	Modified Rachford-Rice
RR	Rachford-Rice
SAGD	Steam Assisted Gravity Drainage
SRK	Soave Redlich-Kwong
VAPEX	Vapor Extraction
VLE	Vapor-Liquid equilibrium
VLLE	Vapor-Liquid-Liquid equilibrium

Chapter One: **INTRODUCTION**

Steam-Assisted Gravity Drainage (SAGD) is the most famous thermal recovery process in Alberta and has been tested successfully in many cases and widely used as a recovery technique for heavy oil and bitumen. SAGD is an expensive process and requires large energy input in the form of steam to produce each barrel of recovered oil. In addition to using large amount of fresh water, it also emits lots of greenhouse gases to the environment. Co-injecting steam and hydrocarbon additives is an attractive option since it reduces the amount of steam required per barrel of recovered oil by taking the advantages of both heating and dilution for viscosity reduction. It offers the potential of higher oil rate and recovery with lower energy and water consumption along with reduced greenhouse gas emission.

The combination of steam and solvent in the hybrid processes increases the production rate and reduces the greenhouse gas emissions but on the other hand it makes the process more complex because of the occurrence of heat and mass transfer simultaneously. In fact, the role of hydrocarbon additive in the steam chamber and its effect on the performance of this gravity drainage process is not well understood. Depending on operating condition and phase behavior of hydrocarbon additive, it can act as a pressure carrier and insulator as well as a solvent for reducing heavy oil viscosity

There are many published papers on the both experimental and simulation of SAGD and different aspects of this process have been investigated. However, very few studies have been done on the simulation and experimental studies of the hybrid processes. Most of the published simulation papers on the hybrid processes have relied on commercial simulators such as CMG SATRS and ECLIPSE Thermal.

In the development of early generations of thermal compositional simulators several assumptions were used for representing the characteristic of dead oil and steam mixtures. The early thermal compositional reservoir simulators started with the black oil concept and later limited compositional capability was added to the simulators. In order to calculate the thermodynamic properties of fluid mixture correlations were used instead of equation of states and for phase

splitting K-Value approach was chosen. Phase properties such as density, enthalpy, internal energy, thermal expansion, and fluid compressibility were calculated from correlations and ideal fluid assumption. The excess properties such as excess enthalpy and excess density were neglected in such simulators.

1.1 **Compositional dependency of equilibrium ratios**

Dependency of equilibrium ratios to the composition is neglected in K-Value approach. This is good assumption for SAGD cases where equilibrium ratios have week dependency on the oil composition variations. In hybrid processes were hydrocarbon is added to the steam or in HOT VAPEX process were pure hydrocarbon is injected to the reservoir, equilibrium ratios change with the variation of composition and neglecting this effect may lead to thermodynamically inconsistent or wrong results. In the K-Value approach the equilibrium equations for components are not solved and it is not necessary that the equilibrium conditions have been satisfied when a time step reaches to convergence.

1.2 **Mutual solubility of different phases**

Mutual solubility of water in oil phase and vice versa has been neglected in these models. In some commercial simulators, i.e.; ECLIPSE Thermal, the water component only exists in the water and vapor phases, and mutual solubility of water and oil are assumed negligible. However, the solubility of water in the oil phase increases with temperature, and it could be significantly high in some cases (Griswold and Kasch (1942), Nelson (1956), McKeta and Katz (1948), Tsonopoulos and Wilson (1983), and Heidman et al. (1985)). Production of emulsion has been observed in most of the experimental SAGD models, which is an indicator of solubility of water in the oil phase at high temperatures (Chung and Butler (1988)).

1.3 **Phase property calculations**

Viscosity reduction by heating/dilution is only a part of total recovery of hybrid thermal/solvent process. Steam distillation, solvent extraction, and thermal expansion are other mechanisms that contribute in the total recovery. The co-injection of intermediate components as an additive to

steam even makes these mechanisms more important in comparison to simple steam injection and it requires proper calculation of thermodynamic properties. Integration of an equation of state package to a reservoir simulator enables the simulator to calculate all of the phase properties from equation of state, and therefore the calculations would be thermodynamically consistent. Excess enthalpies are also calculated in the equation of state package and equilibrium ratios are calculated from equilibrium at each Newton's iteration level.

1.4 **Molecular diffusion and dispersion effect**

Effect of molecular diffusion and dispersion on thermal and non-thermal processes have been neglected in the many published studies in the literature. Firstly, because it is assumed the molecular diffusion or physical dispersion is not dominant compared to convection and secondly, due to lack of such a functionality in the commercial simulators. Both analytical and numerical models of VAPEX simulations showed the effect of dispersion in VAPEX process (Das and Butler (1996, 1998), Das (2005), Yazdani (2007)). The experimental oil production in VAPEX was reported to be ten times higher than the calculated one by using conventional molecular diffusion based theory (Karmaker and Maini (2003), Yazdani and Maini (2005)). The dispersion coefficient can change with composition, temperature and pressure and it can be much larger than the molecular diffusion coefficient. There is no commercial simulator capable of accounting for the variation of dispersion coefficient with composition in thermal processes to quantify the effect of this mechanism on the recovery.

1.5 **Multiphase flash calculation**

The integration of equations of state (EOS) with compositional reservoir simulators has been done during past decades. However, for thermal compositional simulation another path was selected. One of the major components in developments of thermal compositional simulators with ability of handling the PVT properties of reservoir by using equation of state is a robust and efficient multiphase flash calculation. The current multiphase flash calculations are mostly designed for a single cell calculation. Therefore, their main purpose is to provide answer for a single cell. Most of these algorithms are robust enough but not efficient enough for reservoir

simulators. In reservoir simulators, the multiphase flash calculation must be performed repeatedly in thousands to millions of grid blocks at each Newton's iteration level. Thus, such a multiphase flash calculation method must have both robustness and speed to make the reservoir simulation efficient.

The current multiphase flash calculation algorithms generally use Newton-Raphson method and they are heavily dependent on stability analysis. In a reservoir simulator, where energy is a primary variable, an isenthalpic flash calculation is necessary to calculate phase splitting, mole fraction of each component in different phases, phase mole fractions, and temperature of the mixture.

The isenthalpic flash calculation are even more difficult than the isothermal flash calculation because temperature in not known a priori. Therefore, a stability test to determine number of phases is only as good as the initial guess for temperature. In an isenthalpic flash calculation the number of phases might change between different Newton's iterations and it requires another stability analysis. Therefore the current algorithms that are based on the stability analysis become computationally very expensive and development of an efficient and robust multiphase flash calculation is essential.

1.6 **Proposed work**

Currently there is no commercial simulator available to quantify the effect of the simplifying assumptions discussed above on hybrid processes and most of the published papers on the hybrid processes rely on the current simulators, which employ these simplifying assumptions.

The purpose of this research is to develop a 3-D, fully implicit, equation of state based thermal compositional simulator capable of modeling any non-reactive hybrid and thermal process of heavy oil recovery such as; SAGD, ES-SAGD, HOT VAPEX, Steam flooding, and hot water injection. By using an equation of state our goal is to correctly model the thermodynamic and compositional effects on the phase behaviour.

Water is allowed to be soluble in all phases and mutual solubility of oil and water would be taken into account in our proposed simulator and its effect on the oil recovery would be investigated. Thermal expansion, fluid compressibility, solvent extraction, and steam distillation are calculated in our thermodynamic model instead of using any simplistic correlations or formulae which are often used in the current commercial simulators. Steam properties are calculated from EOS or steam table.

The effect of molecular diffusion is investigated in the new simulator since an important objective of developing the new simulator is adding these terms to the conservation equations of each component. By adding this term, we will be able to quantify the effect of diffusion in comparison with the convection in hybrid and thermal processes.

1.7 **Thesis outline**

In Chapter two a brief review on previous works on thermal compositional simulation development is provided. In addition, a literature survey on mutual solubility of oleic and aqueous phases and multiphase flash calculation is presented.

Chapter three presents mathematical formulations of the numerical model, variable selection, calculation schemes of thermodynamic properties and rock-fluid properties. It also covers the heat loss model, wellbore model, the solution technique, sparse matrix storage method and the linear solver.

A review of the current isenthalpic flash calculation and the development of a new isenthalpic multiphase flash calculation is described in detail in chapter four. The new method is validated against current standard algorithm for accuracy and the validation results are presented in this chapter. In the results section of this chapter the new method is compared with the industry standard algorithms for accuracy, robustness and speed.

Chapter five consists of analytical and numerical validation of the developed equation of state based thermal compositional reservoir simulator. The numerical model has several features and these features were validated against several analytical and well-known numerical models.

In chapter six several thermal recovery cases are extracted from open published data and used in thermal and hybrid process simulations. The results of these simulations were compared with the current industry standard simulators.

Chapter seven provides conclusions of this study and recommendations for future work.

Chapter Two: **LITERATUR REVIEW**

The development of thermal reservoir simulators goes back to more than four decades ago. Early simulators were more simplistic and tried to model thermal processes based on the black oil approach without distillation. Basically, they solved mass balance of phases instead of compositions. The oleic phase was assumed to be non-volatile and a condensation term was added to both water and steam mass balance equations to handle the inter-phase mass transfer between water and steam phases. Adding the condensation term to water and steam mass balance equation introduced more computational complexity to the system. The early models had to make more assumptions and make the model more simplistic to compensate for the lack of computation speed.

2.1 **Thermal simulators**

One of the earliest thermal simulators was developed by Shutler (1969). He developed a simplified one dimensional thermal model for linear steam flooding process simulation and later extended the model into a two dimensional version Shutler (1970). In this model, the heat conduction was modeled in 2-D and convective heat transfer only in the direction of flow. Heat conduction in vertical direction is necessary to model heat loss to over/underburden layers. The mass balance equation of phases, the heat balance equation plus a component mass balance equation of an inert gas comprised the full set of governing equations.

He assumed that the non-condensable gas has no effect on water-steam equilibrium. Internal energy was assumed equal to enthalpy and diffusion was neglected. A stage wise procedure was used to calculate the primary variables and it consisted of three major steps;

- All of the mass conservation equations are solved simultaneously to calculate pressure and saturation for the next time step. The temperature and gas composition is assumed constant in this step.
- The energy equation is solved by a non-iterative ADI (Adaptive Direction Method) procedure and the temperature is obtained. Pressure and saturations are from step one.

- The gas compositions are calculated while pressure, saturations and temperatures are constant and already calculated in step 1 and 2.

Abdalla and Coats (1971) implemented the Implicit Pressure Explicit Saturation technique (IMPES) to develop a thermal simulator for steam flooding process. This was a dead oil thermal simulator since they assumed the oil phase to be non-volatile and they ignored the mutual solubility of oil and water. There was also no inert gas in the system unlike the Shutler's model (1969, 1970). Water was present only in the gas and water phases. Pressure was solved implicitly in the flow equations first and in the next step saturation and temperature for steam free blocks were computed from material balance and energy equations. The rate of condensation term was treated differently from the Shutler (1969) model. In steam free blocks, where the temperature would be less than the steam saturation temperature, all steam coming in from adjacent blocks condensed. For blocks with steam, the saturated temperature was calculated from steam table assuming it to be equal to saturation temperature of steam at the prevailing pressure. In these blocks the calculated temperature was plugged into the energy balance equation to calculate the residuals, then the condensation term was calculated to make the residuals zero. The IMPES method is computationally less expensive than fully implicit methods. However it suffers from instability problems when equations are highly non-linear.

Vinsome (1974) 2-D model is also similar to the Abdalla and Coats (1971) model in terms of governing equations. Unlike Abdalla and Coats (1971) model, in this model they accounted for the gravity term in Darcy's equations and internal energy was used instead of enthalpy. Heat loss to surrounding was modeled by a semi-analytical model.

Coats et al. (1974) improved his previous model to handle the instability problem. In the new model mass balance and energy balance equations are solved together and simultaneously to calculate pressure, temperature and saturations. In this model transmissibility of water is treated implicitly to reduce instability. The condensation term was removed by combining the mass balance equation of water and steam phases. They also removed another assumption from

previous work and internal energy was not assumed equal to enthalpy. This model was also a dead oil thermal model, therefore there is no distillation effect involved in this model.

In 1976 Coats (1976) developed the first sequential thermal compositional simulator to capture steam distillation effect on steam flooding process. Molar fractions of hydrocarbon in the gas and oil phase were related by equilibrium ratios. Raoult's Law was used to compute the mole fraction of water in vapor phase. Equilibrium ratios are only function of temperature and pressure. Mutual solubility of water and oil was neglected in this model. In the first sequence pressure is solved in reduced linear system and in the next sequence temperature and saturations and mole fractions are solved by linear algebra. The biggest problem of this model was material balance error in the presence of light hydrocarbons in the model.

Ito's (1977) model is a 1-D model, very similar to Abdalla and Coats (1971) model with exception that the heat loss to cap and base rock was calculated differently in this model.

Later Coats (1978) improved the instability problem of his compositional model by introducing variable substitution technique for the first time. He used fully implicit scheme to eliminate stability issues. The fully implicit model had larger time steps and less cumulative number of time steps in comparison with the sequential model. In this model, transmissibility, capillary pressure and well rates are treated implicitly for saturation and composition. If a grid block is free of steam or gas then transmissibility is treated implicitly for temperature in this block because the temperature becomes the primary variable in these blocks. For the blocks with free gas or steam, transmissibility is treated explicitly for temperature.

Ferrer and Farouq-Ali (1977) developed a 2-D, three-phase compositional simulator. This model is very similar to the Coats (1976) model except that the heat of vaporization was used in their model for calculation of gas phase enthalpy. They also neglected the work term in internal energy equation and assumed internal energy is equal to enthalpy.

Farouq-Ali (1977) developed a two dimensional in-situ combustion model which considered concentration of oxygen, nitrogen and carbon dioxide in the gas phase and neglected the presence of coke in the system. In this model transmissibility is treated explicitly and sink/source

terms are treated implicitly with respect to saturation. They reported serious time step limitation when rate of oxidation is high.

Crookston et al. (1979) developed first thermal compositional simulator which handles multiple reaction in the system. The main purpose for developing this model was in-situ combustion simulation. The model included four chemical reactions: oxidation of light oil and heavy oil, thermal cracking of heavy oil, and oxidation of coke. In this model the relative permeability in transmissibility term is obtained from the latest iteration. However densities, viscosities and enthalpies are from last time step. All of sink/source terms and reaction rates are calculated in the current time with respect to all of primary variables. Crookston et al. (1979) did not use variable substitution in their model instead they did not allow the phases to disappear completely. In this situation a minimum saturation for each phase is set and it never goes below that. This model works as long as gas phase in the system does not disappear completely or there is an inert gas in the system. Abou-Kassem and Aziz (1985) used the same approach and developed a solution for handling phase appearance and disappearance in thermal simulators which does not have the restriction of Crookston et al. (1979) approach.

Coats (1980) developed a fully implicit model to simulate in-situ combustion process. In this model an arbitrary number of components can be used and water exists in water and gas phase and coke only exist in the solid phase. Raoult's law was used to calculate water composition in vapor phase. They compared their model with Crookston et al. (1979) model for 1-D combustion problem set up by Crookston et al. (1979) and reported a significant improvement in both computation speed and time step size.

Abou-Kassem and Aziz (1982) developed a model which was very similar to Ferrer and Farouq-Ali (1977) model. The model is a 2-D model and they tried to remove following limitations of Ferrer and Farouq-Ali (1977) model;

- Lateral heat loss is allowed
- Internal energy is not equal to enthalpy

In this model, for the first time a nine point finite difference scheme was used, therefore this model suffers less from grid orientation problem. In reservoir simulators, five point finite difference scheme is used commonly and grid orientation sometimes has significant effect on the results of simulation.

Rubin and Vinsome (1980) developed a model with five components capable of modeling in-situ combustion. In this model they used a variable alignment technique to achieve optimum diagonal dominance of Jacobian matrix. Pressure is aligned with continuity equation, water saturation with mass balance equation of water component, oil saturation with summation mass balance equation of oleic components, and temperature is aligned with energy equation. Oxygen is aligned with summation of the mass balance equation for non-condensable gases, and coke with mass balance for coke.

Grabowski et al. (1979) introduced four phase general purpose finite difference thermal simulator. This model has water, oil, gas, and solid phase and it also considers reaction in the system. Having solid phase and reaction functionality, the Grabowski et al. (1979) model was able to simulate in-situ combustion process as well. In fact this model was an extension of Rubin and Vinsome (1980) model and removes the restriction on the number of components. Also, an arbitrary number of reactions can be used in this model. Rubin and Buchanan (1985) improved functionality and performance of this simulator to a higher level.

Chan and Sarioglu (1992) presented a procedure for incorporating fracture characteristics in a thermal reservoir simulator. Cicek and Ertekin (1996) also developed a simulator for steam injection.

Luo and Baruffet (2005) introduced a thermal compositional simulator and considered solubility of water in oil phase. However they ignored solubility of oleic phase into the aqueous phase. Basically they assumed water to be a pure component. The main objective of their model was the investigation of the effect of water solubility in oleic phase and its impact on the oil recovery of steam injection processes. They also developed an algorithm for multi-phase (water/oil/gas) flash calculation to handle the phase splitting and implemented their model in the simulator. The oleic

phase in their model needed to be characterized with at least three pseudo components in order to achieve accurate results.

Huang (2007) developed a fully implicit thermal compositional simulator which was able to model steam injection, in-situ combustion and Steam-Assisted Gravity Drainage. This model consists of both single and dual porosity, and is capable of handling fractures. In this model they provided an algorithm for equation line up which can be used for any kind of thermal simulator. Type A primary variables were used in this model and the provided algorithm for aligning the primary variables with governing equations only works for this type of variables. He reported that by using this method of primary variable line up with equations, zero pivoting of Jacobian matrix is avoided.

All of latter thermal compositional simulation models have one common assumption, they use K-Value approach to handle phase equilibrium and equilibrium ratios are only functions of pressure and temperature. The first attempt to use equation of state (EOS) to calculate oleic and gaseous phase's properties was done by Ishimoto et al. (1985). Ishimoto's model was a one dimensional, fully implicit, compositional model and solved conservation of mass and energy equation using a fully implicit formulation. Raoult's law was used to find the mole fraction of water in the vapor phase. They used the global mass fraction of components as primary variable in addition to temperature and pressure. Pressure and temperature are aligned with the continuity equation and energy equation respectively. In narrow boiling point situations where temperature is not independent of pressure, steam quality was used as a primary variable.

Chien et al. (1989) proposed a general purpose compositional simulator with both options of EOS and K-Value to compute oleic and gaseous phase's properties. This model was flexible and allowed running it with or without the thermal option. This model allowed three different modes;

- No mutual solubility between water and hydrocarbon components
- Complete mutual solubility between hydrocarbon and water components
- Partial solubility, where water is soluble in oleic phase but water phase has only H_2O.

In this model Peng-Robinson EOS was used in the case of EOS option to handle phase equilibrium and to calculate the PVT dependent properties. Chien et al. (1989) model assumes the water phase behaves like an ideal solution and water component in the vapor phase behaves like an ideal gas. They also used ideal mixing to compute phase volumes.

Brantferger (1991) developed a fully implicit thermodynamically consistent thermal compositional simulator. He used SRK equation of state to compute thermodynamic properties of all three phases (aqueous/oleic/gaseous). He assumed water as non-ideal solution but they ignored mutual solubility of oil and water. He also used another assumption; there is always a heavy component in the system and the oleic phase never disappears completely.

Most of the reviewed EOS based thermal simulators have assumed there is no mutual solubility of water and oil phases. It is a valid assumption when temperatures is less than 170 ^{0}F .They use EOS to calculate oleic and gaseous phase's thermodynamic properties, and Raoult's law to compute gaseous and aqueous phase's properties.

In 2009, Varavei and Sepehrnoori (2009) developed a fully implicit, parallel, EOS based thermal compositional simulator. This model is capable of handling electrical heating as well. He used Type B primary variables. Primary variables in this model are listed as following;

- Global mole number per unit pore volume of each component, $N_i \;\; i = 1, \dots, Nc$
- Pressure, P
- Temperature or total enthalpy, T, H^t
- Equilibrium ratios of each component, $LnK_i \;\; i = 1, \dots, Nc$

Equation of state was used for equilibrium calculation among phases. In isothermal mode, this simulator is able to handle second oil rich liquid phase and equilibrium ratios are function of pressure, temperature and mole fraction of components.

2.2 **Primary variables**

Selection of type of primary variable is one of the key issues in development of a thermal compositional reservoir simulator. Aziz (1986) categorizes primary variables of isothermal reservoir simulator into two different groups;

- Type A variables
  - Pressure
  - $N_p - 1$ saturations
  - $N_p - N_c$ component mole fractions
- Type B variables
  - Pressure
  - $N_c - 1$ overall quantities; global component mole fractions

Type A variables are also called natural variables, however the same terminology as Aziz's is used for thermal simulator in this study. Selection of each type has its advantages and disadvantages and they will be discussed in this section.

Huang (2007) summarized the existing thermal compositional simulators in the literature based on the selection of primary variables. Table 2-1 lists thermal compositional simulators and their primary variables.

CMG STARS, Coats (1980), Rubin and Buchanan (1985), Crookston et al. (1979), Grabowski et al. (1979), and Youngren (1980) belongs to Type A primary variables. Chien et al. (1989) also belongs to Type A primary variables but it solves volume of phase instead of phase saturation in his formulation. CMG STARS has Type B primary variables option as well. User could choose ZT or ZH primary variable instead of Sxy option, which is the default option in CMG STARS.

Table 2-1: Summary of Type A and B primary variables

		Primary variables			
Type A	Sxy	Temperature	Pressure	Component mole fraction	Saturation
	VSxy	Temperature	Pressure	Component mole fraction	Volume
Type B	ZT	Temperature	Pressure	Component global mole fraction	
	ZTFg	Temperature	Pressure	Component global mole fraction	Flash constraint
	ZH	Total Enthalpy	Pressure	Component global mole fraction	
	NT	Temperature	Pressure	Component total mole number	
	NE	Internal Energy	Pressure	Component total mole number	
	NH	Total Enthalpy	Pressure	Component total mole number	

Buchanan (1985) added a flash constraint to primary variables and eliminated one of the components from primary variables. Buchanan (1985) model belongs to Type B of primary variables. Mifflin et al. (1991) model belongs to Type B and he used total mole number and temperature as primary variables. Naccache (1997) used internal energy (instead of temperature) and component molar density and Brantferger (1991) used total enthalpy and total mole number as primary variable and both of these models fit in Type B category. ECLIPSE Thermal uses same variable as Naccache's model (1997). Pressure always is a primary variable in both categories.

There are several advantages of using Type A variables. Natural variables of equations are solved and they could be used directly in property calculations, Jacobian generation is easier, and flash calculation for grid blocks is not necessary. On the other hand, it is common in thermal simulation that in some grids, temperature and pressure of grid block are not independent anymore (narrow boiling point) and implementation of the "variable substitution" method seems necessary. Another problem which is inherited with Type A formulation is phase appearance and

disappearance, it is necessary to keep track of each grid block in the reservoir to switch the primary variables (replacing the non-existing phase variables with the corresponding variables for the existing phases).

Type B variables are energy and a global property. The energy is conserved all the time and if it is chosen as primary variable, implementation of variable substitution technique is unnecessary. Selection of component global mole fraction or number instead of component mole fraction in each phase removes need of tracking of phase appearance and disappearance in the system; however generation of the Jacobian matrix is more complicated due to use of a series of the chain rule formulae.

2.3 **Mutual solubility of aqueous/liquid phases**

Mutual solubility of oil in water and water in oil is negligible for temperature below 170 ^{0}F. In thermal processes temperature goes much higher and solubility of water in oil phase and vice versa could be significant. Most of early thermal models ignored effect of mutual solubility on the thermodynamic properties and consequently on the final results, such as oil and water production. Experimental data of SAGD tests always show emulsion of water in oil and oil in water which indicates the mutual solubility of these two phases at elevated temperatures.

There are several published papers in the literature that examine the mutual solubility of oil/water. Griswold and Kasch (1942) investigated mutual solubility of water and oil at high temperatures and pressures. Their data show that for a 54.3 API naphta the solubility of water in oil is 16.18 mole % at 431.6 ^{0}F, for a 42 API kerosene the solubility of water in oil is 34.97 mole % at 431.6 ^{0}F, and for a 29.3 API lube oil the solubility of water in oil is 43.44 mole % at 537.8 ^{0}F. Their results also show that the solubility of water in oil phase increases with increase of temperature. Nelson (1956) also showed that the water solubility in oil is as high as 42 mole % at 540 ^{0}F.

Based on the Heidman et al. (1985) study, the solubility of water in liquid C8 is 38.7 mole % at 500 ^{0}F. Solubility of oil in water phase was investigated by Yaws et al. (1993), and Amirjafari and Campbell (1972) and they showed that the solubility of hydrocarbon in water is very small.

Garthofner (1979), and Glandt and Chapman (1995) studied the effect of water in oil solubility on oil viscosity. These results show that the mutual solubility of oil and water can be significant under thermal recovery conditions and should be accounted for.

Chapter Three: **MATHEMATICAL FORMULATION**

3.1 **Introduction**

In the mathematical development of this thermal compositional simulator the following assumptions were used.

- Equilibrium is instantaneous in each grid block
- Maximum three phases coexist in a grid block
- Lateral heat loss through the boundary of reservoir is negligible
- Multiphase Darcy's law can be used to calculate flux of each phase
- Rock density is constant, therefore rock mass within a grid block remains constant
- Oleic pressure is used to calculate phase equilibrium and thermodynamic properties
- There are no chemical reactions or sorption of any species

The primary equations in any thermal compositional simulators are mass balance equation for each component and energy balance equation. The secondary equations are all of the constraints. The followings equations represent the primary and secondary equations that need to be solved in any thermal compositional simulator.

- Component mass balance equation for species i :

$$\frac{\partial}{\partial t}\left[\phi\left(\sum_{j=1}^{np}\rho_j S_j x_{ij}\right)\right] = -\nabla\cdot\left(\sum_{j=1}^{np}\rho_j x_{ij} u_j\right) + \nabla\cdot\left(\sum_{j=1}^{np}\rho_j S_j D_{ij}\nabla x_{ij}\right) + q_i \qquad \textbf{3-1}$$

- Energy balance equation:

$$\frac{\partial}{\partial t}\left[\phi\left(\sum_{j=1}^{np}\rho_j S_j U_j\right) + (1-\phi)\rho_r U_r\right] = -\nabla\cdot\left(\sum_{j=1}^{np}\rho_j h_j u_j\right) + \nabla\cdot\left(K_T\nabla T\right) + q_H \qquad \textbf{3-2}$$

- Phase saturation constraint:

$$\sum_{j=1}^{np} S_j = 1 \qquad \textbf{3-3}$$

- Mole fraction of component constraint:

$$\sum_{i=1}^{nc} x_{ij} = 1 \qquad \textit{if phase j exist} \qquad \textbf{3-4}$$

- Equilibrium constraints for species i in two different phases:

$$f_{ij} = f_{ir} \qquad r \neq j \qquad \textbf{3-5}$$

- Multiphase Darcy's law:

$$u_j = -\frac{kk_{rj}}{\mu_j} \nabla \Phi_j \qquad \textbf{3-6}$$

- Capillary pressures:

$$P_{cog} = P_o - P_g \qquad \textbf{3-7}$$

$$P_{cow} = P_w - P_o \qquad \textbf{3-8}$$

Initial and boundary conditions are problem dependent and they will be defined differently for different problems. However some of these boundary and initial conditions are common for all of the reservoir simulation problems. For example uniform distribution of initial temperature and global mole fraction is considered for each grid block of reservoir.

$$T\left(x,y,z,t=0\right)=T_{init} \quad \textbf{3-9}$$

$$Z_i\left(x,y,z,t=0\right)=Z_{i0} \qquad i=1,N_c \quad \textbf{3-10}$$

Initial condition for pressure is defined at reference grid block and simulator calculates the rest of grid points according to their location with respect to the reference point and their head. The current simulator is volumetric reservoir simulator. Therefore all the grid blocks at the boundaries have zero mass flux rates. The heat flux rate at lateral boundaries is assumed to be negligible but the heat loss to overburden and underburden is allowed and it will be discussed in this chapter.

Number of total unknowns in such a system is:

- Component mole fraction in each phase : $N_c \times N_p$
- Phase saturation : N_p
- Pressure : P
- Temperature : T
- Total number of unknowns : $N_c \times N_p + N_p + 2$

The total number of equations in this system including primary and secondary equations is:

- Mass balance : N_c
- Energy balance : 1
- Saturation constraint : 1
- Component mole fraction constraint : N_p
- Equilibrium : $\left(N_p - 1\right) \times N_c$
- Total number of equations : $N_c \times N_p + N_p + 2$

This system of equations and unknowns is highly coupled and non-linear, and it is not necessary to calculate all of the system of equations and unknowns at the same time. It would be also very expensive and practically impossible. The degree of freedom for any thermodynamic system with all intensive parameters is:

- $f = N_c - N_p + 2$ **3-11**

In our system we have also $N_p - 1$ extensive primary variables which are the saturations of different phases, therefore the degree of freedom for this system would be:

- $f = N_c - N_p + 2 + N_p - 1 = N_c + 1$ **3-12**

It means that we only need to solve $N_c + 1$ equations and unknowns and the rest of variables are secondary variables and they are determined from constraint equations. The total number of primary equations is also $N_c + 1$ since there are N_c mass balance equations plus one energy balance equation.

3.2 **Primary variable selection**

Thermal compositional simulators are divided into two different types in terms of selection of primary variables.

- Type A: which uses natural variables as primary variables
  - P
  - T
  - S_j
  - x_{ij}
- Type B: which uses global variables as primary variables
  - P
  - H
  - Z_i

Selection of primary variable is very important part of the development of a thermal compositional simulator and it dictates the rest of development steps. Both types have their cons and pros and in the following sections some of the issues involve are discussed.

3.2.1 *Type A primary variables*

If Type A is used as primary variables, saturation and component mole fractions in phases plus pressure and temperature are updated at each Newton's iteration level. Phase properties such as molar density, molar enthalpy, internal energy etc. are calculated without performing any flash calculation. This is one of the biggest advantages of this method. In fact flash calculation and phase splitting is done mostly for hydrostatic head calculation in wellbore or determination of volumetric injection or production rates at surface conditions. Since the natural variables are explicitly presented in primary equations, the Jacobian matrix construction is much simpler and less error prone.

The biggest challenge with Type A primary variables is phase appearance and disappearance. Because mole fractions of components in each phase and saturation of phases are used as primary variable, therefore the existence of the primary variable depends on the existence of that phase in the grid block. In thermal compositional simulator grid blocks have different phases at different times of simulation depending on the grid conditions. Primary variables could be different from block to block.

Tracking of primary variable in each grid block and switching of primary variable from non-existing phase to existing phase adds extra work and level of difficulty in development of this method and makes coding more challenging.

Another problem with Type A variable arises when a grid block is in narrow boiling point state. In this situation temperature is no longer a primary variable and is a function of pressure. Then temperature cannot be aligned with energy equation and one of phase saturations is aligned with the energy equation instead of temperature. An alternative solution for this case is the use of system enthalpy as a primary variable and it will be always independent of pressure and will be

aligned to the energy equation. In the next sections narrow and wide boiling points are discussed further.

3.2.2 *Type B primary variables*

Type B reservoir simulators use global mole number or global mole fraction and energy plus pressure as primary variable. The biggest advantage of this method is using one set of primary variables and there is no need for variable switching or substitution. Since primary variables are global variables their existence is independent of the existence of individual phases. Energy, whether in form of enthalpy or internal energy is used as primary variable instead of temperature and energy is always independent of pressure. Then the narrow boiling point situation which is very common in thermal processes is handled without variable switching.

The drawback of using global variables is that at each Newton's iteration and for every single block in the reservoir a flash calculation must be performed to find the number of phases, component mole fractions and phase splitting. Because energy is a primary variable then the temperature is a secondary variable and it also will be calculated from isenthalpic flash calculation.

Type B simulators are heavily dependent on the flash calculation and a robust, fast and accurate flash calculation method is crucial in this type of simulators. Multiphase flash calculation is the Achilles' heel of these simulators and a bullet proof flash calculation method is a key component in the success of this category of reservoir simulators. In Chapter four a new multiphase flash calculation scheme that has been used in this simulator is discussed in detail.

The other problem with Type B method is that the Jacobian construction is more challenging. In these types of simulators, analytical derivatives are preferred to numerical one and extensive use of chain rules is inevitable in differentiation of the residual equation with respect to primary variables. It makes the Jacobian construction difficult and more error prone. The use of numerical differentiation is easier, but it requires more flash calculation for each shifted primary variable.

This method solves the phase appearance and disappearance problem, however severe time-step cut and slow convergence have been observed during the phase appearance and disappearance. The main problem happens with the saturation changes during phase appearance and disappearance since they are calculated as secondary variables. There are several methods to handle this situation in Type B simulator such as saturation chop proposed by John Appleyard (ECLIPSE, Technical Description, (2010)). This method is used in ECLIPSE Thermal, which uses Type B primary variables and has improved the speed and robustness of simulator significantly. Referring to ECLIPSE Thermal manual page, when a phase appears or disappears, or a phase saturation change is bigger than 0.2, saturation will be chopped and solution will be damped. The damping factor will be calculated and applied to the solution locally.

Phase splitting and flash calculation itself is a difficult problem to solve and adds extra cost to the simulator in terms of computation and storage. In these simulators, it is necessary to have a recovery method for the cases where a flash calculation for a specific grid block does not converge. In the current simulator we use both Type A and B primary variables. For Type B primary variables option, several isenthalpic flash calculation methods have been implemented and if any of them fails it switches to the other one. If none of them converge the time step will be cut and simulation will restarts. If there are several consecutive time steps cut then simulation will be terminated.

3.3 **Wide boiling point range**

As it is shown in Figure 3-1, gas and liquid phases exist together over a wide range of temperatures for a system with a given pressure and global mole fractions, feed. In reservoir simulation, reservoir cells which contain significant amount of non-condensable gases or very volatile hydrocarbons belong to this category. Flash calculation constraints are more sensitive to phase fraction and less sensitive to the temperature. Therefore, temperature is independent of pressure and it is aligned with energy equation. This is an ideal situation and simulation usually converges quickly and smoothly in such reservoir grids.

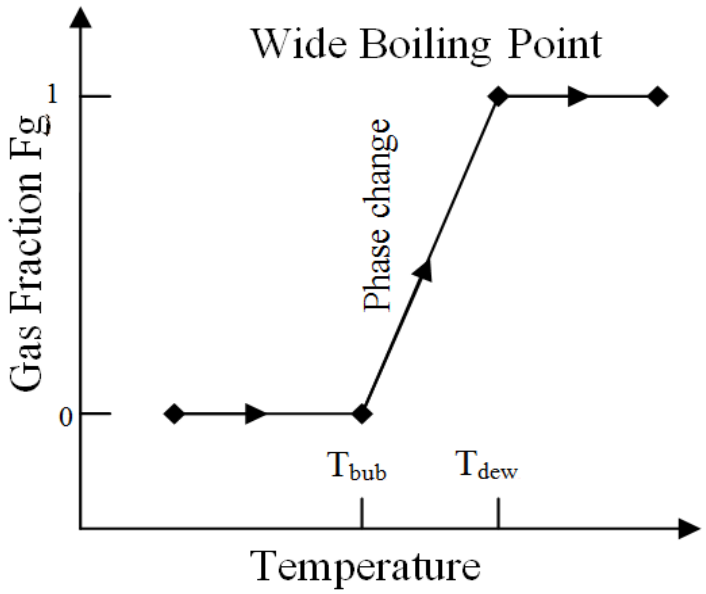

Figure 3-1: Wide boiling point example

3.4 **Narrow boiling point range**

Based on the phase rule, for N_c component in equilibrium in N_p phases in a thermodynamic system there are $f = N_c - N_p + 2$ degree of freedom. For example water at its saturation temperature is in equilibrium in two phases and its degree of freedom is equal to 1. The second case would be when there are two components and three phase system, once again the degree of freedom is equal to one. In both latter cases pressure and temperature are fixed and they cannot change independently. This situation happens most of the time in the steam simulators, for example when steam is injected into a reservoir. There are cases were dead oil is heated by steam and there are many cells in the reservoir in which there are three phases in equilibrium. This situation is called a narrow boiling point and handling of this state is difficult.

Figure 3-2 shows a narrow boiling point system. In narrow boiling point system phase change occurs very abruptly with an infinitesimal change in temperature and bubble point and dew point of system are almost identical.

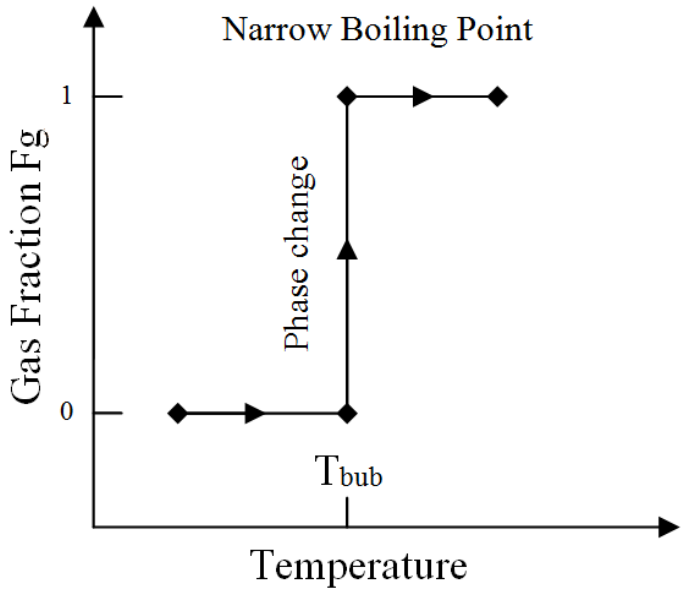

Figure 3-2: Narrow boiling point example

When a reservoir grid is in a narrow boiling point state, temperature is no longer a primary variable, and in this situation gas saturation is aligned with the energy equation. Temperature is calculated form saturation temperature of system at given pressure and global mole fractions. Figure 3-3 shows the same system, but gas fraction is plotted versus enthalpy of system, gas fraction does not change sharply with enthalpy. Bubble point enthalpy and dew point enthalpy are widely different, and if the enthalpy of mixture lies between these two enthalpies we have two phase equilibrium of gas and liquid.

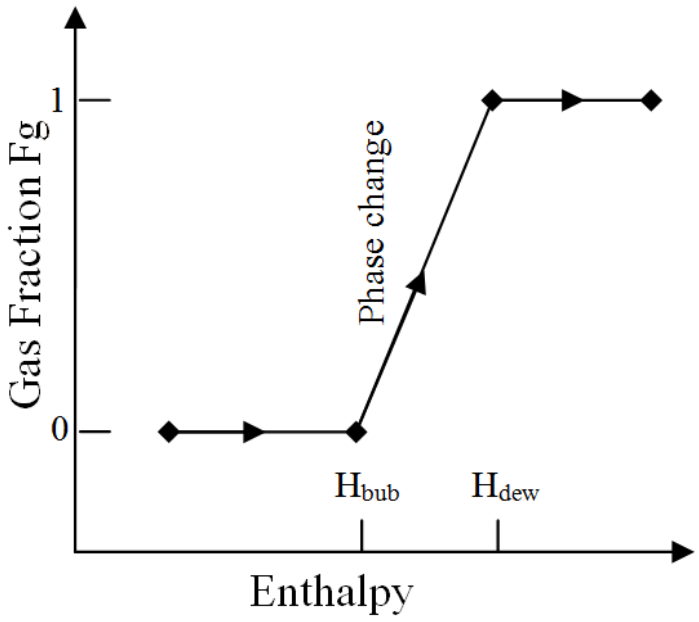

Figure 3-3: Narrow boiling point example, gas phase mole fraction versus total molar enthalpy

As is shown in Figure 3-3, gas fraction change with enthalpy happens over wider range of enthalpy in comparison with temperature. On the other hand, enthalpy remains independent of pressure and could be used as primary variable. In narrow boiling point system phase splitting can't be calculated by isothermal flash and special care must be applied to such systems.

An isenthalpic flash must be performed to find the phase fractions, molar fractions and temperature of system. Gas fraction change with enthalpy is not as sharp as the one with temperature and therefore enthalpy is more suitable as a primary variable for both flash and flow equation in narrow boiling point situations.

During a thermal process a reservoir grid state could change into variety of forms such as three-phase, two-phase or single phase. Any phase, aqueous, oleic or gaseous, could appear or disappear or may reappear under different conditions.

Abou-Kassem and Aziz (1985) provides three examples in which phase change take places under certain conditions;

- Gas phase may disappear if a saturated reservoir is re-pressurized, in this situation, steam is forced to condense and condensable gases dissolve in the oleic phase.
- Superheated steam created due to large pressure drop in an injection block. Water phase disappears in this case because of evaporation of water. Volatile hydrocarbons are also vaporized from oleic phase.
- Thermal cracking in processes such as in-situ combustion may cause total oleic phase disappearance in a reservoir grid block.

As it is seen, a change in the number of phases present could happen under many circumstances and proper handling of this situation is very important. There are several methods of handling such phase changes in the literature (Crookston et al. (1979), Forsyth et al. (1981), Grabowski et al. (1979), Coats (1978, 1980), Abou-Kassem and Aziz (1985)). Two of these methods are the most well-known, variable substitution and pseudo-equilibrium ratio method. Both of these methods work for simulators that use natural variables as primary variables (Type A).

In Type A reservoir simulators, phase appearance and disappearance is checked rigorously at each Newton's iteration level and then the primary variables are changed and aligned with different equations after determination of unknowns and state of the grid block. Constraint equations are also changed according to the state of the grid block. In fact in Type A reservoir simulators, the flash calculation is embedded in the formulation of phase change handling and equation alignment with primary variables.

3.5 **Variable substitution**

Variable substitution has been originally discussed by Coats (1978, 1980). Abou-Kassem (1996) provides four different scenarios that a grid block can exhibit during a thermal process and he discusses the variable substitution for each case separately;

- $S_o^{(v)} > 0$, $S_g^{(v)} > 0$ and $S_w^{(v)} > 0$, $(3 - phase\ LVW)$: Aqueous phase is in equilibrium with steam in gaseous phase. In this situation, temperature is not independent of pressure and is not a primary variable anymore. It is narrow boiling point situation and temperature is equal to the saturation temperature at prevailing pressure.
- $S_o^{(v)} > 0$, $S_g^{(v)} > 0$ and $S_w^{(v)} = 0, (2 - Phase\ LV)$: There is no aqueous phase in the system and water is superheated. Temperature is independent of pressure and is considered as primary variable and will substitute water saturation. The proper constraint equation in this case would be; $S_o^{(v)} + S_g^{(v)} = 1$.
- $S_o^{(v)} > 0$, $S_g^{(v)} = 0$ and $S_w^{(v)} > 0, (2 - phase\ LW)$: There is no gas phase in the system. Temperature is an independent of pressure and considered as unknown. In this case, temperature substitutes the gas saturation and $S_o^{(v)} + S_w^{(v)} = 1$ constraint will be used instead of $\sum_{i=1}^{nc} y_i = 1$ constraint.
- $S_o^{(v)} = 0$, $S_g^{(v)} > 0$ and $S_w^{(v)} > 0, (2 - phase\ VW)$: It means oil phase has disappeared and it does not exist in the grid block. In this situation, gas mole fraction substitutes the oil mole fraction as primary variable and $S_g^{(v)} + S_w^{(v)} = 1$ is used as the correct constraint. $\sum_{i=1}^{nc} y_i = 1$ constraint is still valid in this case.

3.6 **Pseudo Equilibrium Ratio (PER) method**

This method was originally introduced by Crookston et al. (1979) and later on was completed by Abou-Kassem and Aziz (1985). Variable substitution is very logic intensive and difficult for coding whereas this method handles phase appearance and disappearance without using variable substitution. Therefore only one set of equations and unknown are used during simulation. The pseudo-equilibrium ratios are defined as followings;

$$k_i = \begin{cases} \hat{k}_i X_o X_g \\ \hat{k}_i X_w X_g \end{cases} \quad \textbf{3-13}$$

where,

$$X_o = \frac{S_o}{S_o + \varepsilon_o} \quad \textbf{3-14}$$

$$X_w = \frac{S_w}{S_w + \varepsilon_w} \quad \textbf{3-15}$$

$$X_g = \frac{S_g + \varepsilon_g}{S_g + 10^{-30}} \quad \textbf{3-16}$$

and ε_o, ε_w, and ε_g are small numbers of the order of 10^{-5}. The function X_o, X_w, and X_g are approximately one except for small values of saturations, i.e. $S<10^{-3}$. In this method saturation of all of the phases can approach zero without becoming zero; it is like there is always a small amount non-condensable gas, dead oil and non-volatile water in the system which prevents the phase from complete disappearance. More details about this method can be found in the Crookston et al. (1979) and Abou-Kassem and Aziz (1985) papers.

3.7 **Property calculation**

Before solving the primary equations, many parameters and variables need to be computed. Some of these parameters are calculated from EOS and some of them are independent of EOS. In this study EOS dependent parameters and EOS independent variables are divided into two categories.

3.7.1 *EOS independent properties*

3.7.1.1 Porosity

Porosity of each grid block is a function of pressure and it is given by following equation;

$$\phi = \phi_0 \left[1 + C_f \left(P - P_0 \right) \right] \quad \textbf{3-17}$$

In this equation, ϕ_0 is reference porosity at reference pressure P_0. C_f is pore volume compressibility factor.

3.7.1.2 Rock heat capacity

Constant volume specific heat capacity is assumed to be only a function of temperature and variation of this function with respect to pressure is neglected. Constant volume heat capacity is defined as;

$$C_v = A_r + B_r T \quad \textbf{3-18}$$

Internal energy of rock is calculated as;

$$U_r = \int_{T_{ref}}^{T} C_v d\tau \quad \textbf{3-19}$$

After applying integration;

$$U_r = A_r\left(T - T_{ref}\right) + \frac{B_r}{2}\left(T^2 - T_{ref}^2\right) \qquad \textbf{3-20}$$

3.7.1.3 Relative permeability

Relative permeability of each phase can be defined as a table which changes with the saturation or by any type of analytical correlation. In this study, phase relative permeability is expressed by Corey's (1954) type function. To calculate phase relative permeability endpoints and phase exponents of phases are defined by user as input. Next correlations show the relative permeability of different phases.

$$\begin{aligned}
K_{rw} &= K_{rwro}\left(\frac{S_w - S_{wir}}{1 - S_{orw} - S_{wir}}\right)^{ew} \\
K_{row} &= K_{roiw}\left(\frac{1 - S_w - S_{orw}}{1 - S_{orw} - S_{wir}}\right)^{eow} \\
K_{rg} &= K_{rgro}\left(\frac{S_g - S_{gc}}{1 - S_{gc} - S_{org} - S_{wir}}\right)^{eg} \\
K_{rog} &= K_{roiw}\left(\frac{1 - S_g - S_{org} - S_{wir}}{1 - S_{org} - S_{wir}}\right)^{eog}
\end{aligned} \qquad \textbf{3-21}$$

Stone's (1973) model (Stone II) is used to compute relative permeability of oil phase changes with respect to water and gas saturation.

$$K_{ro} = K_{roiw}\left[\left(\frac{K_{row}}{K_{roiw}} + K_{rw}\right)\left(\frac{K_{rog}}{K_{roiw}} + K_{rg}\right) - K_{rw} - K_{rg}\right] \qquad \textbf{3-22}$$

Where, $ew, eg,$ are saturation exponent for water and gas phases. eow , eog are saturation exponent for oil phase for k_{row} , and k_{rog} respectively.

3.7.1.4 Thermal conductivity

Thermal conductivity of rock and different phases is expressed as constant value and thermal conductivity of mixture is calculated by a saturation weighted mixing rule as;

$$\kappa_{mix} = \phi\left(\kappa_o S_o + \kappa_g S_g + \kappa_w S_w\right) + \left(1-\phi\right)\kappa_r \qquad \textbf{3-23}$$

3.7.1.5 Viscosity

There are two options to define viscosity of different phases in this simulator; table of different component viscosities versus temperature or a formula.

- Viscosity of oleic phase

Viscosity of each component in oleic phase is defined as;

$$\mu_{oi} = a_{oi} \cdot \exp\left(\frac{b_{oi}}{T}\right) \qquad \textbf{3-24}$$

Where, a_{oi}, and b_{oi} are constants which are defined as input and T is absolute temperature. Viscosity of oleic phase is calculated be following mixing rule.

$$\mu_o = \prod_{i=1}^{nc} \mu_{oi}^{xi} \qquad \textbf{3-25}$$

- Viscosity of aqueous phase

Viscosity of aqueous phase is calculated similar to oleic phase. If water is the only component of aqueous phase, no mixing rule will apply.

- Viscosity of gaseous phase

For gas phase viscosity, we use a simple correlation similar to the one is used in CMG STARS.

$$\mu_g = 0.0136 + 3.8e^{-5}T \qquad \textbf{3-26}$$

T is in ^{0}C and viscosity of gaseous phase is function of temperature only and effect of pressure and composition is neglected. This is a valid assumption in thermal processes where changes of gas viscosity with pressure and composition are negligible in comparison with temperature.

3.7.2 *EOS dependent properties*

The Peng-Robinson EOS or SRK EOS can be used in the simulator. The general form of both equations is presented by equation 3-27;

$$P = \frac{RT}{v-b} - \frac{a}{\left(v+\delta_1 b\right)\left(v+\delta_2 b\right)} \qquad \textbf{3-27}$$

Where, δ_1 and δ_2 are numerical constants and *a* and *b* are mixture parameters and are given by the following mixing rules;

$$a = \sum_{i=1}^{nc}\sum_{j=1}^{nc} x_i x_j \sqrt{a_i a_j}\left(1-d_{ij}\right) \qquad \textbf{3-28}$$

$$b = \sum_{i=1}^{nc} x_i b_i \qquad \textbf{3-29}$$

Where, d_{ij} are interaction coefficients between *i* and *j*. The pure component properties, a_i and b_i are calculated from the critical properties and acentric factors of pure components.

$$a_i = \Omega_a \frac{R^2 T_{ci}^2}{P_{ci}} \left[1 + m_i \left(1 - \sqrt{\frac{T}{T_{ci}}} \right) \right]^2 \quad \textbf{3-30}$$

$$b_i = \Omega_b \frac{RT_{ci}}{P_{ci}} \quad \textbf{3-31}$$

The numerical constants and m_i are presented separately for PR EOS and SRK EOS.

- SRK equation of state (1972) ;

  $\delta_1 = 1, \quad \delta_2 = 0, \quad \Omega_a = 0.42748, \quad \Omega_b = 0.08664$

  $m_i = 0.48 + 1.574\omega_i - 0.176\omega_i^2$

- PR equation of state (1976) ;

  $\delta_1 = 1 + \sqrt{2}, \quad \delta_2 = 1 - \sqrt{2}, \quad \Omega_a = 0.45724, \quad \Omega_b = 0.07780$

  $m_i = 0.37464 + 1.54226\omega_i - 0.26992\omega_i^2$

3.7.2.1 Compressibility factor

The compressibility factor for each phase is expressed as;

$$Z = \frac{Pv}{RT} \quad \textbf{3-32}$$

By substituting this equation into SRK or PR EOS, a cubic form of equation of state in term of compressibility factor is derived.

$$Z^3-\left(\delta_1\delta_2B+1\right)Z^2+\left[A-\left(\delta_1+\delta_2\right)B-\left(1-2\delta_1\delta_2\right)B^2\right]Z-\left[AB+\delta_1\delta_2\left(B^2+B^3\right)\right]=0 \quad \textbf{3-33}$$

Dimensionless parameters, A, and B are defined as;

$$A=\frac{aP}{R^2T^2} \quad \textbf{3-34}$$

$$B=\frac{bP}{RT} \quad \textbf{3-35}$$

3.7.2.2 Volume

The molar volume of each phase is calculated after the compressibility factor is computed from the EOS. The molar volume is defined as;

$$v=\frac{ZRT}{P} \quad \textbf{3-36}$$

The molar density of each phase is related to the molar volume by;

$$\rho=\frac{1}{v} \quad \textbf{3-37}$$

3.7.2.3 Enthalpy

The molar enthalpy of each phase is determined from the EOS and it is given by;

$$h - h^0 = RT\left(Z-1\right) + \frac{T\,\partial a/\partial T - a}{\left(\delta_1 - \delta_2\right)b}\ln\left(\frac{Z+\delta_1 B}{Z+\delta_2 B}\right) \qquad \textbf{3-38}$$

where, h^0 is enthalpy of ideal solution and is calculated as following;

$$h^0 = \sum_{i=1}^{nc} x_i h_i^0 \qquad \textbf{3-39}$$

where,

$$h_i^0 = \int_{T_{ref}}^{T} C_{pi}^0 d\tau \qquad \textbf{3-40}$$

A third order polynomial equation is used to compute ideal gas state heat capacity;

$$C_{pi}^0 = C_{p1i}^0 + C_{p2i}^0 T + C_{p3i}^0 T^2 + C_{p4i}^0 T^3 \qquad \textbf{3-41}$$

Polynomial coefficients are determined from experiments or can be computed from a group contribution method, Reid et al. (1987).

3.7.2.4 Fugacity and fugacity coefficient

Fugacity coefficient in general form is expressed as;

$$\ln\varphi_i = \frac{b_i}{b}\left(Z-1\right) - \ln\left(Z-B\right) + \frac{A}{\left(\delta_1-\delta_2\right)B}\left(\frac{b_i}{b} - d_{ij}^{'}\right)\ln\left(\frac{Z+\delta_1 B}{Z+\delta_2 B}\right) \qquad \textbf{3-42}$$

where;

$$d_{ij}^{'} = \frac{2\sqrt{a_i}}{a} \sum_{j=1}^{nc} x_j \sqrt{a_j} \left(1 - d_{ij}\right) \qquad \textbf{3-43}$$

3.7.2.5 Internal energy

The phase internal energy is derived from the enthalpy and the molar volume of each phase by the following definition;

$$u = h - pv \qquad \textbf{3-44}$$

3.8 **Heat loss to overburden and underburden**

There are two well-known approaches in reservoir simulation to model heat loss into cap rock and base rock, analytical approach and numerical approach. One of the simplest analytical models was proposed by Vinsome and Westerveld (1980) and it is relatively accurate one dimensional heat loss model in semi-infinite space. In most of the reservoir simulations, cap rock and base rock are assumed as impermeable to fluid flow, therefore energy is delivered into the cap and base rock only by conduction. The Vinsome's model (1980) for heat loss has been implemented in most of commercial simulators. We also used Vinsome's model (1980) to capture heat loss effect on the thermal processes efficiency. In this section Visnome's model (1980) is described briefly.

Vinsome and Westerveld (1980) suggest that the temperature profile into cap or base rock can be adequately approximated by any flexible function with few parameters. They chose a fitting function for temperature profile into cap or base rock;

$$T(t,z)=\left(\theta+pz+qz^2\right)\exp\left(-\frac{z}{d}\right) \qquad \textbf{3-45}$$

Where, θ is the temperature at the interface between the reservoir rock and the cap or base rock, p and q are the fitting parameters and need to be determined, d is called diffusion length and it is defined as;

$$d=\frac{\sqrt{\kappa t}}{2} \qquad \textbf{3-46}$$

Alpha is heat diffusivity and it is given by;

$$\alpha=\frac{\kappa}{\rho_r C_v} \qquad \textbf{3-47}$$

Boundary conditions are stated by the followings;

$$\begin{aligned} T&=\theta\,@\,z=0\\ T&=\theta_0\,@\,z=\infty\\ T&=\theta_0\,@\,t=0 \end{aligned} \qquad \textbf{3-48}$$

As mentioned before, heat carries to the base or cap rock only by conduction. The equation of heat flow to the cap rock for example is;

$$\frac{\partial T}{\partial t}=\alpha\frac{\partial^2 T}{\partial z^2} \qquad \textbf{3-49}$$

The heat flow equation at the interface is expressed as;

$$\frac{\partial \theta}{\partial t} = \alpha \left. \frac{\partial^2 T}{\partial z^2} \right|_{z=0} \qquad \textbf{3-50}$$

Inserting the fitting equation for temperature profile into the heat flow equation at the interface and discretizing time results;

$$\frac{\theta - \theta^n}{\Delta t} = \alpha \left(\frac{\theta}{d^2} - \frac{2p}{d} + 2q \right) \qquad \textbf{3-51}$$

where, θ^n is the interface temperature at the beginning of the time step. They also used another physical feature which is conservation of cap rock energy to derive another equation.

$$\frac{\partial}{\partial t} \int_0^\infty T dz = \alpha \left. \frac{\partial T}{\partial z} \right|_{z=0} \qquad \textbf{3-52}$$

Once again if fitting function for temperature profile into the cap rock is plugged into the latter equation, we will have;

$$\frac{I - I^n}{\Delta t} = \alpha \left(\frac{\theta}{d} - p \right) \qquad \textbf{3-53}$$

where,

$$I = \theta d + pd^2 + 2qd^3 \qquad \textbf{3-54}$$

At this stage, we have two equations and two unknowns, therefore fitting parameters can be determined.

$$p = \frac{\alpha\Delta t \dfrac{\theta}{d} + I^n - \dfrac{d^3\left(\theta - \theta^n\right)}{\alpha\Delta t}}{3d^2 + \alpha\Delta t} \qquad \textbf{3-55}$$

$$q = \frac{2pd - \theta + \dfrac{d^2\left(\theta - \theta^n\right)}{\alpha\Delta t}}{2d^2} \qquad \textbf{3-56}$$

The heat loss rate into the cap or base rock is defined as;

$$\left.\frac{\partial T}{\partial z}\right|_{z=0} = -\left(\frac{\theta}{d} - p\right), \qquad \textbf{3-57}$$

and the energy stored in the cap rock is;

$$E_c = \frac{\kappa}{\alpha} d\left(\theta + pd + 2qd^2\right) \qquad \textbf{3-58}$$

3.9 **Wellbore model**

Treatment of wellbore model in a single-layer well is relatively a simple task but special considerations are necessary when multi-layer wellbores are being modeled. There are several models in the literature for handling wellbore model in reservoir simulators, such as STARS Flexible and Discretized wellbore, ECLIPSE Multi-Segmented well model, some Semi-Analytical models, and Sink/Source model. Wellbores are considered as boundary conditions of the reservoir model and in any numerical model boundary conditions must be carefully defined and handled since they will affect the solution and robustness of the model. On the other hand, at the end of any reservoir simulation, injection and production rate are the main outcome of the simulation, therefore accuracy and robustness of wellbore model is essential in any reservoir simulator.

In this simulator we use sink/source approach of treatment of wellbore model for injection and production of each component or energy into or from reservoir. Peaceman (1983) method is incorporated in our model to calculate geometric factor and equivalent drainage radius. In this simulator multi-layer and directional wells can be defined with two major control modes;

- Constant bottom hole pressure
- Constant volumetric flow rate at surface condition

The constant volumetric flow rate at surface condition includes; total liquid rate, water rate, oil rate, gas rate and steam rate. Any combination of the rate and pressure operation condition can be applied for both producer and injectors. Well model couples flow rate of each component or phase with flowing borehole pressure.

$$q_j = WI.\lambda_j \left(P_{bh} + head - P \right) \qquad \textbf{3-59}$$

Where, $\lambda_j$is mobility of each phase and WI is well index. Well index or geometric factor for linear 1-D and 2-D model for a grid block is calculated as;

$$WI_k = \frac{cf \cdot k_x \cdot \Delta y_i \Delta z_i}{\Delta x_i} \qquad \textbf{3-60}$$

where, *cf* is a conversion factor.

For three dimensional linear flows with anisotropy, WI is calculated based on the Peaceman (19783) well model.

$$WI_k = \frac{cf \cdot \sqrt{k_x k_y} \cdot \Delta z_i}{\ln\left(\frac{r_e}{r_w}\right) + S_f} \qquad \textbf{3-61}$$

where, r_e is an equivalent drainage radius and it is given by;

$$r_e = \frac{\left[\Delta x^2 \sqrt{\frac{k_y}{k_x}} + \Delta y^2 \sqrt{\frac{k_x}{k_y}}\right]^{1/2}}{\sqrt[4]{\frac{k_y}{k_x}} + \sqrt[4]{\frac{k_x}{k_y}}} \qquad \textbf{3-62}$$

WI in x and y direction is calculated similar to the one in z direction.

3.9.1 *Well residual equations*

The total molar rate for multi-layer well is computed by;

$$q_t = \sum_{k=1}^{nlay} WI_k \sum_{j=1}^{np} \left[\lambda_j \rho_j \left(P_{bh} + head - P \right) \right]_k \qquad \textbf{3-63}$$

The bottom-hole pressure of reference layer of each well is another primary variable which is needed to be calculated fully implicitly with the rest of primary variables. Well equation is added as another equation to close the system of equation and unknowns. There are two different category of operating constraint in simulators; rate control, pressure control. When constant bottom hole pressure is an operating condition, the calculation of sink/source term for each perforation or layer is straight forward. The sink/source term for component *i* in layer *k* in conservation of mass equation related to this component is expressed as;

$$q_{ik} = \sum_{j=1}^{np} \left[WI \lambda_j \rho_j x_{ij} \left(P_{bh} + head - P \right) \right]_k \qquad \textbf{3-64}$$

The energy sink/source term in energy equation for layer k is calculated as;

$$q_{hk} = \sum_{j=1}^{np} \left[WI \lambda_j \rho_j h_j \left(P_{bh} + head - P \right) \right]_k \qquad \textbf{3-65}$$

The well residual term is simple when constant bottom-hole is constraint and it is shown by equation 3-66.

$$R_w = P_{cons} - P_{bh} = 0 \qquad \textbf{3-66}$$

When operating condition of a well is constant rate at surface condition other actions must be done because;

- Specified rate is usually the volumetric rate at surface condition and it must be converted to molar rate
- Specified rate is assigned for the well and it must be recalculated for each perforation or layer

First an estimate of bottom-hole pressure is provided weather from the last Newton's iteration or it is calculated. If it is the first time and the bottom-hole pressure has not been defined yet it must be calculated and the following well residual equation needs to be solved;

$$R_w = q_{cons} - q_{calc} = 0 \qquad \textbf{3-67}$$

Calculated well flow rate is at standard condition and it has different forms depending on the specified constraint. For example, if total liquid rate is assigned as constraint, then the calculated well flow rate is total liquid rate at surface condition. This simulator supports oil, water, gas, liquid rate, and steam rate as constraint and residual equation for each separate case is briefly discussed in this section.

3.9.1.1 Oil flow rate at surface condition

$$R_w = q_{cons} - \left(\frac{L_o}{\rho_o}\right)^{ST} \sum_{k=1}^{nlay} WI_k \sum_{j=1}^{np} \left[\lambda_j \rho_j \left(P_{bh} + head - P\right)\right]_k = 0 \qquad \textbf{3-68}$$

3.9.1.2 Water flow rate at surface condition

$$R_w = q_{cons} - \left(\frac{L_w}{\rho_w}\right)^{ST} \sum_{k=1}^{nlay} WI_k \sum_{j=1}^{np} \left[\lambda_j \rho_j \left(P_{bh} + head - P\right)\right]_k = 0 \qquad \textbf{3-69}$$

3.9.1.3 Gas flow rate at surface condition

$$R_w = q_{cons} - \left(\frac{L_g}{\rho_g}\right)^{ST} \sum_{k=1}^{nlay} WI_k \sum_{j=1}^{np} \left[\lambda_j \rho_j \left(P_{bh} + head - P\right)\right]_k = 0 \qquad \textbf{3-70}$$

3.9.1.4 Total liquid flow rate at surface condition

$$R_w = q_{cons} - \left(\frac{L_o}{\rho_o} + \frac{L_w}{\rho_w}\right)^{ST} \sum_{k=1}^{nlay} WI_k \sum_{j=1}^{np} \left[\lambda_j \rho_j \left(P_{bh} + head - P\right)\right]_k = 0 \qquad \textbf{3-71}$$

Where, L_o , L_w , and L_g are mole fraction of oil, water and gas phases at standard condition respectively. Phase ratios and molar density of each phase at standard condition must be calculated at each Newton's iteration. An isothermal flash is performed for global mole fraction of produced stream at surface temperature and pressure to obtain the latter properties. The major challenge in this section would be the calculation of global mole fraction which is explained below.

The total molar rate of production will be calculated from equation 3-63 and component molar rate for each component is calculated as; $\sum_{k=1}^{nlay} WI_k \sum_{j=1}^{np} \left[\lambda_j \rho_j x_{ij} \left(P_{bh} + head - P\right)\right]_k$

Then global mole fraction is obtained from next expression;

$$z_i = \frac{\sum_{k=1}^{nlay} WI_k \sum_{j=1}^{np} \left[\lambda_j \rho_j x_{ij} \left(P_{bh} + head - P \right) \right]_k}{\sum_{k=1}^{nlay} WI_k \sum_{j=1}^{np} \left[\lambda_j \rho_j \left(P_{bh} + head - P \right) \right]_k} \qquad \textbf{3-72}$$

Bottom-hole pressure as a primary variable is aligned with the well residual equation in Newton-Raphson method and it will be updated for the next iteration until convergence is achieved. After convergence, well rates are calculated and updated and bottom-hole pressure is compared with constraint value to check the violation of operation condition. If well operating condition is pressure, then calculated rates will be compared with the constraint rate.

3.9.2 *Head calculation*

If several layers of perforations are used for production, flowing bottom-hole pressure of different layers must be determined with respect to the reference layer flowing bottom-hole pressure. In this simulator, effect of friction and acceleration terms on pressure is neglected. By this assumption, only gravity effect will remains and flowing bottom hole pressure for other layers is calculated as;

$$P_{bh}\big|_k = P_{bh}\big|_{ref} + \gamma_{ave} \left(z - z_{ref} \right) \qquad \textbf{3-73}$$

Where γ_{av} is the specific gravity of the fluid. To calculate the specific gravity it is necessary to calculate average density of fluid in each layer of wellbore. In this section we will explain the average density calculation in each layer of a multilayer well bore model. In a production well, average mass density of mixture is expressed by;

$$\rho_{ave}^{M} = MW_{ave}\rho_{ave} \quad \textbf{3-74}$$

where, ρ_{av} is average molar density of mixture in layer k, and $MW_{av}$is molecular weight of mixture in that layer. Subscripts k has been dropped for the sake of simplicity.

$$\frac{1}{\rho_{ave}} = \sum_{j=1}^{np} \frac{L_j}{\rho_j} \quad \textbf{3-75}$$

As it is clear from equation 3-75, molar density and phase fraction of each phase at layer k, are necessary to calculate mixture molar density of fluid. An isenthalpic flash is performed to calculate phase fraction and molar density of each phase at layer k.

Molar enthalpy of fluid, global mole fraction of each component and pressure are the main input of any isenthalpic flash calculation. The input data for isenthalpic flash calculation are obtained differently for injectors and producers and it will be discussed below.

3.9.2.1 Producer head calculation

Global mole fraction of each component is calculated based on the flow from reservoir toward the wellbore in layer k;

$$q_{tk} = \sum_{j=1}^{np} \lambda_j \rho_j \quad \textbf{3-76}$$

Total component inflow from reservoir to layer k of producer is;

$$q_{ik} = \sum_{j=1}^{np} \lambda_j \rho_j x_{ij} \qquad \textbf{3-77}$$

Then,

$$z_i = \frac{\sum_{j=1}^{np} \lambda_j \rho_j x_{ij}}{\sum_{j=1}^{np} \lambda_j \rho_j} \qquad \textbf{3-78}$$

Where, mobility, molar density, and component mole fraction are calculated at upstream conditions. Total molar enthalpy of system is also calculated in a similar method.

$$h_{mixk} = \frac{\sum_{j=1}^{np} \lambda_j \rho_j h_j}{\sum_{j=1}^{np} \lambda_j \rho_j} \qquad \textbf{3-79}$$

At this point we know all of necessary input for isenthalpic flash calculation, h_{mix}, z_i, and $P_{bh}|_k$. Well block temperature, phase fractions and molar density of each phase will be obtained from the isenthalpic flash for h_{mix}, z_i, and $P_{bh}|_k$. As it is seen, bottom hole flowing pressure is related to the head calculation and head calculation depends on the density of mixture which is also a function of pressure. This is a recursive process and the calculation must be repeated until it reaches to a unique solution.

3.9.2.2 Injector head calculation

Properties of injected fluid, such as; steam quality, injection temperature and pressure, injection rate or pressure, and global mole fraction of injected fluid is provided by user. Thermal properties of fluid are used to calculate the amount of energy which is delivered to the reservoir from injection well.

Heat loss from wellbore to the reservoir or overburden is neglected in this simulator and energy will be the same as injected enthalpy at the sand-face of reservoir. Similar to producer an isenthalpic flash is performed for global mole fraction of injected fluid, Z_i, injected enthalpy, and bottom hole pressure of layer k and phase fraction, mole fraction related to each phase, molar density and molar enthalpy of each phase at sand-face conditions is calculated. Mass density of mixture is calculated and the head will be determined. As it was pointed before, this is a recursive process and it is repeated until it converges to a unique solution.

The head calculation must be done at each time step and if there is any head difference between the layers. For horizontal wells with no rising part and with no inclination head will be always zero compare to the reference point. After determination of thermodynamic properties, the injection of each component in layer *k* is computed.

3.10 **Solution technique**

Partial differential equations, mass balance and heat balance equation, and constraint equations are discretized and converted to finite difference format. Transmissibility terms for convective flow of mass and heat, are discretized based on the one-point upstream weighting factor. However conductive heat flow and diffusive mass flow terms are discretized based on the harmonic average method. The residual form of governing equation in finite difference format is expressed as;

Mass balance equation of each component:

$$R_i = \frac{\partial}{\partial t}\left[V_p \left(\sum_{j=1}^{np} \rho_j S_j x_{ij} \right) \right] - \sum_{k=1}^{nnb} \sum_{j=1}^{np} T_j \rho_j x_{ij} \Delta\Phi_j - \sum_{k=1}^{nnb} \sum_{j=1}^{np} T_{Dj} \Delta x_{ij} - V_b \cdot q_i \qquad \textbf{3-80}$$

Energy balance equation:

$$R_h = \frac{\partial}{\partial t}\left[V_p \left(\sum_{j=1}^{np} \rho_j S_j U_j \right) + V_r U_r \right] - \sum_{k=1}^{nnb} \sum_{j=1}^{np} T_j \rho_j h_j \Delta\Phi_j - \sum_{k=1}^{nnb} \kappa \Delta T - V_b \cdot q_h \qquad \textbf{3-81}$$

Volume or saturation constraint:

$$R_s = \sum_{j=1}^{np} S_j - 1 \qquad \textbf{3-82}$$

Molar fraction constraint:

$$R_x = \sum_{i=1}^{nc} x_{ij} - 1 \qquad \textbf{3-83}$$

Phase equilibrium constraint:

$$R_{eq} = \ln f_{ij} - \ln f_{iR} \qquad i = 1, \ldots, N_c \qquad j = 1, \ldots, N_P \qquad \textbf{3-84}$$

This system of equations and unknowns is strongly coupled and highly non-linear. There is no analytical solution available to solve such a system and it has to be solved numerically. In this

simulation we used fully implicit method to solve this system of equations due to high level of non-linearity of variation of properties with primary variables. The Newton-Raphson method was used for linearization of system of equations. Constraint equation can be eliminated at matrix level in linear matrix solver package.

The Newton iteration can be expressed as:

$$\left(\frac{\partial \vec{R}}{\partial X_p}\right)^{\nu} \delta \vec{X}_p^{\nu} = -\vec{R}^{\nu} \qquad \textbf{3-85}$$

Primary variables are updated as following;

$$\vec{X}_p^{\nu+1} = \vec{X}_p^{\nu} + \delta \vec{X}_p^{\nu} \qquad \textbf{3-86}$$

Jacobian matrix is constructed by differentiation of each term in the residual equation with respect to primary variables. There are two major categories of differentiation in reservoir simulation: analytical and numerical differentiation. Each method has its own strong points and weaknesses. In our simulator both of these methods were used in construction of the Jacobian matrix.

Analytical differentiation was used in construction of Jacobian matrix in EOS approach of this simulator. Analytical derivatives are preferred for EOS simulators because there is no need to perform extra flash calculation to compute the derivatives. To calculate numerical derivatives of properties in EOS approach we need to calculate each property when any primary variable is shifted and it requires performing many flash calculations. Flash calculation itself is an expensive and time consuming task to do and it should be avoided as much as possible in a simulator. Derivatives of PVT dependent properties are calculated at flash calculation package

and they are presented in Appendix A. Derivatives of the rest of properties, such as relative permeability, viscosity, heat conductivity, rock energy, heat loss to surroundings, heater rates are calculated separately before Jacobian construction.

In K-Value approach we used numerical derivation. In K-Value approach Type A primary variables have been used and Sxy formulation was used to handle PVT properties, therefore there is no need of performing flash calculation. Numerical derivatives might not be as accurate as analytical solution but its implementation is much faster and simpler and the code is much shorter and cleaner. It is also very easy to add new features to a simulator. In fact the Jacobian construction remains untouched regardless of new features added to the simulator.

Construction of Jacobian matrix and right hand side matrix in this simulator is broken into three different pieces, accumulation term, flux term and sink/source terms (wells, heat loss, and heaters). Derivatives of accumulation and sink/source terms are only dependent on properties of the control volume and they are stored on the diagonal of Jacobian matrix. Derivatives of flux term include adjacent cells and these are stored on diagonal and off-diagonal of Jacobian matrix.

The following algorithm describes the stage wise Jacobian construction:

1. Calculate accumulation term of block l
2. If block includes sink/source term, calculate sink/source terms of block l
3. Find upstream direction for block l and its connections
4. Loop over number of connection of block l and calculate flux terms
5. Loop over primary variables
6. Shift primary variables
7. Repeat step 1-6 and construct accumulation, sink/source and flux derivatives
8. Derivatives of well equation with respect to the primary variables are calculated separately from the reservoir part.

The structure of Jacobian matrix is shown in Figure 3-4. As it is shown it consists of four different sections. The RR section includes derivatives of reservoir equations with respect to primary variables of reservoir. The RW section involves the derivatives of reservoir residual

equations of reservoir part with respect to primary variable of well; i.e. well bore flow pressure. Derivatives of well residual equations with respect to primary variables of reservoir and wellbore are presented in WR and WW parts of Figure 3-4.

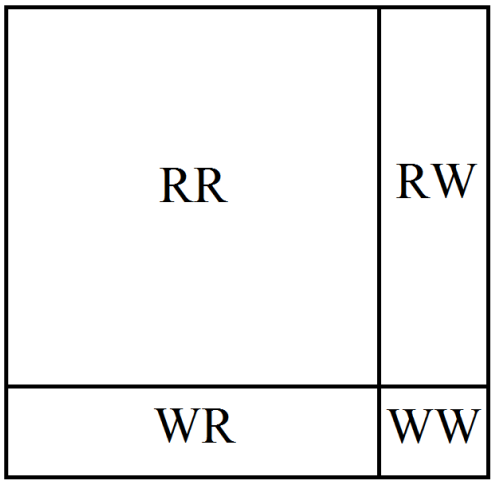

Figure 3-4: Jacobian matrix structure

The Jacobian matrix is a block diagonal and sparse matrix. It has many zero entries and it is very expensive to store this matrix in raw format. In this simulator Compressed Sparse Row (CSR) method (Saad (1990)) is used to store only non-zero elements of the Jacobian matrix. In CSR method only column index, row's beginning pointer and the non-zero element is stored. Figure 3-5 shows an example of CSR storage of 3x3 sparse matrix.

12	2	0
0	34	0
0	0	45

Value	12	2	34	45
I_col	1	2	2	3
I_row	1	3	4	

Figure 3-5: A 3x3 sparse matrix representation and its storage in CSR format

As it was mentioned before Jacobian matrix is a block diagonal, highly non-symmetric and sparse matrix and it is suitable to be solved by iterative matrix solvers. General Minimized RESidual method (GMRES) by Saad and Schultz (1986) was used in this simulator.

The GMRES uses Krylov subspace algorithm and this algorithm is often useless without pre-conditioning and the rate of convergence of linear solver could be very slow in difficult problems. Incomplete Lower Upper (ILU) method of preconditioning (Behie and Forsyth (1983)) with different level of fill-in was used in this simulator. All of the tested models in this work used level of fill-in equal to one or two. Generally speaking, more accurate ILU factorization method results in faster pre-conditioned Krylov subspace algorithm. On the other hand, more accurate ILU requires more space and time and it becomes computationally more expensive. Therefore an optimum number of fill-in must be used to have both of accuracy and speed of a linear solver.

Chapter Four: **PVT AND FLASH CALCULATION**

4.1 **Introduction**

Knowing the number of phases before running a VLE flash or VLLE flash calculation is a very difficult problem. Traditionally this problem has been solved either by conducting a two-phase flash or by making a saturation-pressure calculation; both methods are expensive and not entirely reliable. Michelsen (1982) and Trangenstein (1985) used Gibbs free energy of the mixture to establish thermodynamic stability of a phase. For a given composition, Gibbs free energy of a single phase is calculated, then a trivial composition of second phase is added to the single phase and Gibbs free energy of mixture is calculated again. If Gibbs free energy of mixture is less than the single phase one, then the single phase is not stable. Same procedure will apply on the new mixture to find actual number of phases in equilibrium.

Michelsen (1982) proposed stationary local point method to analyze phase stability and Trangenstein (1987) developed method of minimization of Gibbs free energy with respect to a trial phase composition. Mathematical calculation of these two methods is skipped in this report.

Multiphase flash calculation is the next step after determination of number of phases. Two phase flash calculation are well developed during past decades and there are several robust and efficient methods available in the literature, however multiphase flash calculation needs more development. Mathematically, the two-phase and multiphase flash calculation can be solved by either of following methods;

- satisfying the equal-fugacity and material-balance constraints with a successive-substitution or Newton-Raphson algorithm
- minimizing the mixture Gibbs free energy function

In case of two-phase flash calculation, Rachford and Rice (1952) proposed their well-behaved objective function and this method has been used extensively in many reservoir simulators. Baker et al. (1982) and Michelsen (1982) used tangent plane criterion of Gibbs free energy to calculate phase equilibrium. Peng and Robinson (1976), Heidmann (1974), and Nutakki et al.

(1988) solved multiphase flash equilibrium (VLLE) by using EOS and Newton Raphson method and they conclude that the method is not robust. Nelson (1987) used bubble point and dew point criteria for two phase flash and extend it for multiphase flash calculation and Chien (1994) improved Nelson's method for VLLE flash calculation. Stateva and Tsvetkov (1995) applied tangent plane criteria for Gibbs free energy in stability analysis and improved it for multi-phase flash calculation.

4.2 **Phase stability analysis of isenthalpic system**

As mentioned before, the lack of information about the number of phases in the solution of a thermodynamic system is a big problem. We need to know what numbers of phases exist to perform two phase flash or multiphase flash calculations. In isenthalpic problem it is even bigger problem than the iso-thermal processes since the temperature itself is an unknown and the traditional stability test which works based on the minimum Gibbs free energy surface at a particular temperature is not applicable anymore. Therefore determination of the number of phases from stability test in isenthalpic flash is impossible with the traditional stability methods. In fact what the stability test can provide is the number of phases at any initial guess of temperature of system, which may or may not be the same as number of phases in the final solution. One of the major problems associated with this problem is the appearance and disappearance of phase during the iterative solution procedure.

The earliest works on isenthalpic flash calculations were done by Boston and Brit (1978) and Prausnitz et al. (1980) and these were mainly for two phase systems. Michelsen (1987) proposed a stage-wise procedure for isenthalpic flash. In this procedure, the system is assumed at single phase initially and the number of phases is increased through the instability tests. This method is very similar to the stage-wise stability test for isothermal processes.

Brantferger (1991) presented a thermodynamically rigorous method to find the number of phases in an isenthalpic flash calculation. In this method, a Newton-type entropy maximization

algorithm is combined with a Gibbs stability test to find number of phases and then a multiphase flash calculation is preformed to calculate phase splits and temperature.

Agarwal et al. (1991) provided three methods for isenthalpic flash calculations. In the first method, scheme 1 a series of multiphase isothermal flash calculations is performed at different temperatures until energy equation convergence is achieved. In fact multiphase isothermal flash is performed in an inner loop while temperature is fixed. Since temperature is fixed a conventional stability is performed and correct number of phases at that fixed temperature is determined. Isothermal flash is performed and equilibrium condition is satisfied. Then energy equation is solved in an outer loop and temperature is updated using a secant method. Because this method is a sequential method, energy in outer loop is only a function of temperature and monotonically increasing and therefore it binds the temperature to lower and upper limits. If temperature does not lie between the temperature bounds it can bring it back in the limits. This is the main reason that why this method is very robust.

In the second method (scheme 2) the energy and material balance are solved simultaneously to obtain phase splits and temperature. This method was claimed to be three times faster than the first method but not as robust as the first method. The second method requires a very good initial guess and it diverges if the initial guess is not in the radius of convergence. On the other hand the first method is not as sensitive as the second method to initial guess. Another shortcoming of the first method is that it is unable to handle narrow boiling point areas where the degree of freedom is equal to unity. Narrow boiling point and wide boiling point were described in chapter three briefly.

This second method is a stage-wise procedure. First it is assumed that the system is single phase. Energy equation is solved to find temperature of single phase system at given pressure and system molar enthalpy. A secant method similar to the scheme 1 is used at this stage. Then a stability test is performed at calculated temperature on single phase system. If the system is stable at calculated temperature, then the system is single phase, otherwise a second phase is added to single phase and a two phase isenthalpic flash is performed until it converges. Another

stability test is performed at converged temperature on two phase system to see whether a three phase isenthalpic flash calculations is necessary or not.

In the third method (scheme 3) they used a hybrid scheme to take the advantage of both previous schemes, robustness of first scheme and speed of the second scheme. A series of isothermal flash calculation is performed until energy equation satisfy certain tolerance of convergence then the last calculated temperature is used as an initial guess for the scheme 2 and scheme 2 is repeated until its convergence is achieved. They reported 5 iterations were enough for the scheme 1 and then the results of schem1 are used for scheme 2.

4.3 **Formulation of isenthalpic flash calculations**

The goal of performing an isenthalpic flash is to find number of phases, phase compositions and fractions, and temperature for a given pressure, global mole fraction of components and energy. After defining the thermodynamic model there are total of N_p independent governing equations:

- $N_p - 1$ material balance equation
- 1 Energy equation

There are also total of N_p independent primary variables:

- $N_p - 1$ phase mole fractions
- Temperature

This close system needs to be solved to calculate primary and secondary variables. In this section the Agarwal et al. (1991) method is described in details. The equilibrium ratios (equilibrium ratios) are defined as:

$$K_{ij} = \frac{x_{ij}}{x_{iR}} \qquad \textbf{4-1}$$

where, x_{ij} is the mole fraction of component i in phase j and R is the reference phase. Reference phase can be different for different components and equilibrium ratio of the reference phase is equal to unity all the time. If F_j is mole fraction of phase j in the system then the compositions can be defined from material balance equations as;

$$x_{ij} = \frac{z_i K_{ij}}{\xi_i} \qquad \textbf{4-2}$$

where;

$$\xi_i = \sum_{j=1}^{np} F_j K_{ij} \qquad \textbf{4-3}$$

The summation of mole fraction of component in each phase must be equal to unity, therefore $N_p - 1$ independent material balance equation can be derived;

$$g_j = \sum_{i=1}^{nc} \frac{z_i \left(K_{ij} - K_{iR} \right)}{\xi_i} \qquad j = 1, ..., N_p - 1 \qquad \textbf{4-4}$$

The last equation is energy balance equation;

$$g_j \equiv H - H_{sys} = 0 \qquad \textbf{4-5}$$

Where, H_{sys} is the specified molar enthalpy of system. The total energy of system is also expressed in terms of partial molar enthalpies, phase molar fractions and component mole fractions as;

$$H = \sum_{j=1}^{np} F_j \sum_{i=1}^{nc} x_{ij} h_{ij} \qquad \textbf{4-6}$$

This close system of equation and unknowns can be solved by Newton-Raphson method. Derivatives of equilibrium ratios with respect to temperature are derived from following thermodynamic equilibrium equation;

$$lnK_{ij} + ln\varphi_{ij} - ln\varphi_{iR} = 0 \qquad j \neq R \qquad \textbf{4-7}$$

Equation 4-7 is derived from equality of fugacities and for a system with N_c component and N_p phases the total of $N_c(N_p - 1)$ equation for equilibrium ratios are constituted. Agarwal et al. (1991) provided the following algorithm for isenthalpic flash calculations;

1. Assume $K_{ij}^{(k)}$, $x_{ij}^{(k)}$, $F_j^{(k)}$ and $T^{(k)}$ are the k-th iteration values of K_{ij}, x_{ij}, F_j and T
2. Calculate $x_{ij}^{(k)}$ from equation 4-2
3. Calculate $lnK_{ij}^{(k)} + ln\phi_{ij}^{(k)} - ln\phi_{iR}^{(k)}$
4. Perform one QNSS iteration for K_{ij} and let the resulting value be $K_{ij}^{(k+\frac{1}{2})}$
5. Calculate $x_{ij}^{(k+\frac{1}{2})}$ from $F_j^{(k)}$ and $K_{ij}^{(k+\frac{1}{2})}$
6. Calculate $F_j^{(k+1)}$ and $T^{(k+1)}$ by performing one Newton's iteration on equations

7. Calculate $K_{ij}^{(k+1)}$ by assuming a linear model with respect to temperature, i.e.

$$lnK_{ij}^{(k+1)} = lnK_{ij}^{(k+\frac{1}{2})} + \left(\frac{\partial lnK_{ij}}{\partial T}\right)^{(k)} \left(T^{(k+1)} - T^{(k)}\right)$$

8. Let $k = k + 1$ and go to step 2 and proceed until convergence

The Agarwal et al. (1991) method also works with K-Value approach. In the EOS approach, an equation of state is used to calculate equilibrium ratios, however in K-Value approach, the equilibrium ratios are available from correlation or tables. In this approach phase enthalpies are also calculated from table or correlation by ideal solution assumption. Therefore derivatives of partial molar enthalpies and equilibrium ratios with respect to temperature are easy and straight forward to calculate and there is no need to solve any equilibrium condition.

ECLIPSE Thermal uses Type B primary variables and energy is one of the primary variables. Since energy is a primary variable this simulator is heavily dependent on isenthalpic flash calculations. Stone and Nolen (2009) provide very practical and robust isenthalpic multiphase flash calculations method which is used in ECLIPSE Thermal. The mutual solubility of water and oleic phases are neglected in this method and it is based on the K-values fluid characterization. Equilibrium ratios are only function of temperature and pressure.

The biggest challenge with isenthalpic flash calculation is that conventional stability test to find the number of phases in isothermal methods is not enough due to variation of temperature. The advantage of Stone and Nolen (2009) method is that they first perform a stability test based on the critical enthalpies and find the number of phases and then an isenthalpic flash calculation is performed to determine phase splits and temperature.

The major idea behind the phase envelope construction is simple. If sufficient heat is added to a mixture of liquid water and oil it boils and three phase system will be created. If more heat is added then one of the liquid phases disappears and only two phase system exist. By adding more heat to the system the remaining liquid phase also evaporates completely and only vapor phase

exist. Of course presence of non-volatile oil or non-condensable gas may prevent some of the later states from materializing. Therefore there are three critical temperatures in the system for appearances or disappearances of phases.

Then three critical enthalpies are calculated at these three critical temperatures, given pressure and the feed composition. If T_3 is the temperature where gas appears first, then the critical enthalpy at this temperature is called $h_{c,gas}$. T_2 is the temperature where the first liquid phase disappears and T_1 is temperature where the last liquid phase also evaporates completely. The second critical enthalpy at T_2 can be $h_{c,oil}/h_{c,wat}$ and the last critical enthalpy depends on what is the second critical enthalpy. If oil disappears first then $h_{c,oil}$ is the second critical enthalpy, otherwise $h_{c,wat}$ would be the second critical enthalpy. In fact these critical enthalpies are transitional enthalpies at phase boundaries and they are unique because enthalpy is increasing monotonically with temperature, i.e. $\partial h/\partial T > 0$.

Finally enthalpy of system is compared with these three critical enthalpies and numbers of phases are determined depending on the location of given enthalpy. At this moment the phase stability is established and numbers of phases are known. Depending on the number of phases a two or three phase isenthalpic flash calculation is performed and phase molar fractions, component mole fractions and temperature of the system are calculated.

Figure 4-1 shows a diagram of critical temperature sequences which is adapted from Stone and Nolen's (2009) original paper.

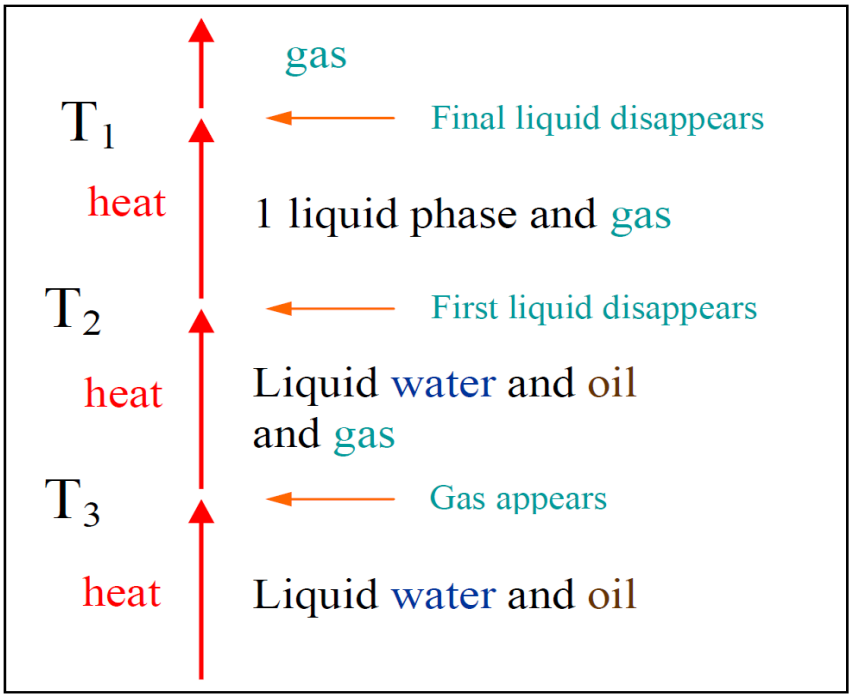

Figure 4-1: Phase appearance and disappearance diagram, adapted from Stone and Nolen (2009)

More details about the formulation of this method and calculation procedure can be found in the original paper. In current simulator, if K-Value approach with global primary variables is used then this method is employed to determine phase numbers and phase splits plus temperature.

4.4 **Multiphase flash calculation (VLLE)**

For multiphase flash calculation an objective function similar to Rachford-Rice function is defined. The equal fugacity constrains for each component in oleic/gaseous/aqueous phase is;

$$f_{iL} = f_{iV} = f_{iW} \qquad \textbf{4-8}$$

The objective functions for three-phase flash calculation are;

$$R_1(V,W)=\sum_{i=1}^{nc}(y_i-x_i)=\sum_{i=1}^{nc}\frac{z_i\left(k_i^{go}-1\right)}{1+V\left(k_i^{go}-1\right)+W\left(k_i^{wo}-1\right)}=0 \qquad \textbf{4-9}$$

$$R_2(V,W)=\sum_{i=1}^{nc}(w_i-x_i)=\sum_{i=1}^{nc}\frac{z_i\left(k_i^{wo}-1\right)}{1+V\left(k_i^{go}-1\right)+W\left(k_i^{wo}-1\right)}=0 \qquad \textbf{4-10}$$

Partial derivative of these two functions with respect to V and W are;

$$\begin{aligned}
\frac{\partial R_1(V,W)}{\partial V}&=-\sum_{i=1}^{nc}\frac{z_i\left(k_i^{go}-1\right)^2}{\left[1+V\left(k_i^{go}-1\right)+W\left(k_i^{wo}-1\right)\right]^2}\\
\frac{\partial R_1(V,W)}{\partial W}&=-\sum_{i=1}^{nc}\frac{z_i\left(k_i^{go}-1\right)\left(k_i^{wo}-1\right)}{\left[1+V\left(k_i^{go}-1\right)+W\left(k_i^{wo}-1\right)\right]^2}\\
\frac{\partial R_2(V,W)}{\partial V}&=-\sum_{i=1}^{nc}\frac{z_i\left(k_i^{go}-1\right)\left(k_i^{wo}-1\right)}{\left[1+V\left(k_i^{go}-1\right)+W\left(k_i^{wo}-1\right)\right]^2}\\
\frac{\partial R_2(V,W)}{\partial W}&=-\sum_{i=1}^{nc}\frac{z_i\left(k_i^{wo}-1\right)^2}{\left[1+V\left(k_i^{go}-1\right)+W\left(k_i^{wo}-1\right)\right]^2}
\end{aligned} \qquad \textbf{4-11}$$

The analytical derivatives show that only two of them are always less than zero. Unlike the Rachford-Rice equation for two phase flash, these objective functions are not monotonic and Newton-Raphson algorithm may lead to false or trivial solution sometimes. Newton-Raphson algorithm is very sensitive to the initial guess and having a good initial guess is very crucial for this method.

Recently, Lapene et al. (2010) proposed a new multiphase flash calculation specifically fitted for thermal compositional reservoir simulators. They used free water assumption and developed a novel modified monotonic Rachford-Rice objective function. Negative flash concept with this modified Rachford-Rice monotonic objective function was used to calculate phase ratios, equilibrium ratios, and component mole fraction of components in different phases.

The free-water assumption means that the solubility of hydrocarbon components in the water-rich liquid phase is neglected, that is, this phase consists of pure water. The free-water assumption is supported by the fact that the solubility of hydrocarbon (typically of the order of 10^{-4} mole fraction) in the water-rich phase is several orders of magnitude smaller than the solubility of water (typically of the order of10^{-2} mole fraction) in the hydrocarbon-rich phase.

Tang and Saha (2003) also used the same assumption and their proposed method was able to determine phase equilibrium by using nelson criteria. Iranshahr et al. (2009) also developed a multiphase flash calculation method based on the free water flash calculation and this method requires an additional assumption, i.e., the solubility of water in the hydrocarbon-rich liquid phase is also negligible. Moreover, the objective function is not guaranteed to be monotonic.

4.5 **Development of new isenthalpic multiphase flash calculations**

The current isenthalpic multiphase flash calculations methods such as Michelsen (1987) or Agarwal et al. (1991) are stage-wise methods which are dependent on stability analysis. The stability analysis is not only tedious and expensive but it is also a difficult task. In a reservoir simulator thousands to millions of flash calculations must be performed and the current available methods are not fast enough to be employed in a thermal compositional reservoir simulator.

In development of our new reservoir simulator, a new isenthalpic multiphase flash calculation was developed to handle thermodynamic part of reservoir simulator. This model follows the hybrid scheme of Agarwal et al. (1991). However there is no need to perform any stability test or stage-wise procedure to calculate temperature and phase splitting.

First, this model performs a series of isothermal flash in an inner loop using free water flash calculation method of Lapene et al. (2010). The Free water flash calculation model is implemented since the modified Rachford-Rice objective function is guaranteed to be monotonic. It also uses negative flash concept for phase distribution and phase identification, thus phase stability analysis is skipped. Lapene et al. (2010) tested their model with several

practical cases and the model showed accuracy and robustness as well as speed. For many cases where solubility of oil components in water phase is low, they reported that results did not show any significant deviation from true equilibrium. Lapene's et al. (2010) model should not be used for cases where solubility of hydrocarbon component in aqueous phase is high i.e., CO_2 sequestration.

Since the objective function is a monotonic function and it always returns a unique solution, it is easy to define appropriate boundaries to the flash calculation which return non-negative component mole fractions all the time.

Second, in the outer loop energy equation is solved and temperature is updated. As long as the thermodynamic system is in wide boiling point region this model finds solution very quickly. When there is a narrow boiling point region, phase change happens in a very narrow window of temperature, then the temperature does not change in outer loop after few iterations and residual of energy equation remains unchanged. At this point flash calculation doesn't converge in sequential method since energy equation is less sensitive to temperature and more sensitive to phase mole fractions. Basically the level of explicitness of sequential method would not find the real solution. Therefore flash calculation is switched to the fully implicit scheme.

Third, a system of energy equation and material balance equation is solved fully implicitly by Newton-Raphson method. Primary variables are temperature and phase mole fractions. We use the most updated temperature and phase molar fraction as initial guess for this system of equations and the fully implicit method converges to the solution usually within few iterations. In fact the good initial guess from the sequential scheme is the key factor in the success of the fully implicit scheme.

The switching criterion is not based on the number of iterations or any convergence tolerance but it is based on the absolute change of temperature. When the temperature change is less than 1.0E-4 K and absolute value of residual of energy equation is bigger than the 1.0E-4 J/mol then the isenthalpic flash calculation is switched from sequential scheme to fully implicit scheme.

One of the problems that the scheme 2 of Agarwal et al.'s method (1991) encountered is phase appearance and disappearance during Newton's iteration. If the initial guess of temperature is not in convergence radius or it is not close enough to the solution then phases could appear, disappear or reappear during Newton's iterations and extra care is required to handle these situations and the convergence of scheme 2 requires more iterations and stability tests, if it does not fail.

In all of the flash calculations that have been performed in this study we did not encounter any difficulty in regards to phase appearance or disappearance in the isenthalpic flash calculations after switching to the fully implicit scheme. Usually the number of phases remains unchanged during the second scheme and only temperature and phase molar fractions vary to minimize the residuals.

The main reason is that the sequential scheme usually finds the temperature very close to the final solution temperature and it also finds the correct number of phases. However energy equation does not converge because the phase mole fractions are not correct. Therefore, using most updated temperature and phase mole fraction of sequential scheme as initial guess only requires few iteration of the fully implicit scheme to adjust mostly phase mole fractions. Temperature change is not very significant in this stage.

The tolerance for energy and material balance equation residual is set equal to 1.E-8. If residual is less than the tolerance then the flash calculation is terminated and temperature, phase mole fractions and component mole fractions in each phase is extracted from the flash calculations.

This new isenthalpic flash calculation method takes advantages of robustness of sequential scheme and speed of the fully implicit scheme. It is not sensitive to initial guess and in all of the performed flash calculations in this study the initial guess for temperature was set to 15 ^{o}C.

The Wilson correlation (1969) was used for initialization of equilibrium ratios of flash calculation and except for few examples, all of the cases converged to the solution with this initialization. If the solution converges to the trivial solution then the flash calculation algorithm

checks this situation and it defines new set of initial equilibrium ratios. Once again the most updated equilibrium ratios of first scheme are very good candidate for these situations.

The equilibrium ratios from Wilson correlation work very well at moderate conditions and because this method is not sensitive to the initial guess one can start the flash calculation from a low temperature. After few iterations of sequential scheme temperature reaches to very close proximity of the solution and the most updated equilibrium ratios can be used as initial values for the second scheme.

In this chapter this new flash method will be tested against the Agarwal's et al. (1991) method and the robustness, number of iteration and sensitivity to initial guess of these two methods will be compared. In the next section mathematical derivation of the free water flash calculation model and its algorithm will be discussed.

4.5.1 *Free water flash calculation*

In the sequential method, series of iso-thermal flash calculation is performed in an inner loop. Iso-thermal flash calculation method of Lapene et al. (2010) is used and this method is described in details in this section. This section consists of two subsections. In the first section modified Rachford-Rice objective function is derived and phase identification and separation will be explained and in the second part the algorithm of free water flash calculation is described.

4.5.1.1 Derivation of Modified Rachford Rice objective function

The equal fugacity constraint for each component in oleic/gaseous/aqueous phase was presented in equation 4-8. The fugacity of each component relates to fugacity coefficient by the following expression;

$$\varphi_{iL} P x_i = \varphi_{iV} P y_i = \varphi_{iW} P w_i \qquad \textbf{4-12}$$

The equilibrium ratios are defined as;

$$k_i^I = \frac{y_i}{x_i} \qquad \textbf{4-13}$$

$$k_i^{II} = \frac{y_i}{w_i} \qquad \textbf{4-14}$$

The component material balance for W/L/V system is;

$$z_i = Lx_i + Vy_i + Ww_i \qquad \textbf{4-15}$$

The overall phase material balance constraint is defined as;

$$L + V + W = 1 \qquad \textbf{4-16}$$

In free water system, water component is distributed in all three phases and hydrocarbon components only distribute in vapor and oleic phase. Based on this assumption mole fraction of water component in the water phase is equal to unity. Material balance constraint for water component will be as;

$$z_w = Lx_w + Vy_w + W \qquad \textbf{4-17}$$

Water fraction is calculated by rearranging component material balance for water component and by plugging overall material balance into the latter equation; water phase fraction is expressed as;

$$W = \frac{z_w - x_w + z_w\left(x_w - y_w\right)}{1 - x_w} \qquad \textbf{4-18}$$

The component material balances for the rest of components are defined as;

$$z_i = \left(1 - V - W\right)x_i + Vy_i \qquad \textbf{4-19}$$

By using the equilibrium ratios and the latter equations, one can derive an equation for the component mole fraction in oleic phase.

$$x_i = \frac{z_i}{1 + V\left(k_i^I - 1\right) - W} \qquad \textbf{4-20}$$

Lapene et al. (2010) started from the classical Rachford-Rice equation to find a new monotonic objective function between new asymptotes. By adding $\frac{y_w - x_w}{1 - x_w}$ to both sides of Rachford-Rice equation and performing few simple algebraic steps they developed a new monotonic objective function. The final form of new modified Rachford-Rice objective function is;

$$G\left(V\right) = \sum_{i \neq w}^{nc} \frac{z_i\left(k_i^I - k_w^*\right)}{k_w^z + V\left(k_i^I - k_w^*\right)} = 0 \qquad \textbf{4-21}$$

where;

$$k_w^* = \frac{1-y_w}{1-x_w} \qquad \textbf{4-22}$$

$$k_w^z = \frac{1-z_w}{1-x_w} \qquad \textbf{4-23}$$

Analytical derivative of modified Rachford-Rice is always less than zero and function is guaranteed to be monotonic.

$$\frac{dG(V)}{dV} = -\sum_{i\neq w}^{nc} \frac{z_i \left(k_i^I - k_w^*\right)^2}{\left[k_w^z + V\left(k_i^I - k_w^*\right)\right]^2} \leq 0 \qquad \textbf{4-24}$$

In two phase flash calculation, V is in the range of [0, 1], In this method, V must be in the interval of [0, V*], where V* is the maximum phase ratio of vapor when oleic phase disappear. In this case V+W=1 and V* is defined as;

$$V^* = \frac{1-z_w}{1-y_w} \qquad \textbf{4-25}$$

Another useful physical restriction comes from the fact that amount of water in the vapor phase cannot exceed its global molar fraction. The maximum water mole fraction (y_w) in the vapor phase while all of aqueous phase disappear is less than or equal to z_w. Since W=0; then L=1-V, the volume of vapor phase in this situation is equal to;

$$\bar{V} = \frac{z_w - x_w}{y_w - x_w} \qquad \textbf{4-26}$$

4.5.1.2 Determination of water phase presence

As it was mentioned before, this new objective function monotonically decreases between adjacent asymptotes. The vertical asymptotes occur at;

$$V_i = \frac{k_w^z}{k_w^* - k_i^I} \quad \textbf{4-27}$$

In negative flash concept, all solution within the range of $[V_{min}, V_{max}]$ gives positive phase compositions. V_{max} and V_{min} are defined as;

$$V_{\min} = \max\left(\frac{k_w^z}{k_w^* - k_i^I}\right)_{k_i^I > k_w^*} \quad \textbf{4-28}$$

$$V_{\max} = \min\left(\frac{k_w^z}{k_w^* - k_i^I}\right)_{k_i^I < k_w^*} \quad \textbf{4-29}$$

When $k_w^* > k_{min}^I$ and $k_w^* < k_{max}^I$, V_{max} is greater than zero and V_{min} is less than zero. Since solution is within the range of $[V_{min}, V_{max}]$, it can be easily shown that;

$$V_{\min} < 0 < V < V_{\max} \quad \textbf{4-30}$$

Presence or absence of water is very important in this method. If water phase is absent then classical Rachford-Rice calculation will be performed. Assume V is a solution of modified Rachford-Rice in the window of negative flash $[V_{min}, V_{max}]$. Depending on the composition of water component in the oleic and vapor phase, the presence of water phase can be determined.

The following steps describe the method for determination of water phase presence in negative flash window;

1. First determine position of V with respect to $\bar{V}$;
   - $Case1: \quad V_{min} < \bar{V} < V_{max} \quad if\ G(\bar{V}) > 0 \quad then \quad V > \bar{V} \quad else \quad V < \bar{V}$
   - $Case2: \quad \bar{V} < V_{min} \quad then \quad V > \bar{V}$
   - $Case3: \quad V_{max} < \bar{V} \quad then \quad V < \bar{V}$
2. After position of V with respect to $\bar{V}$ was determined, determine presence or absence of water depending on the composition of water component in oleic and vapor phase;
   - $Case1: if\ V < \bar{V} \quad then \quad if \quad y_w < x_w \quad then \quad W = 0 \quad else \quad W > 0$
   - $Case2: if\ V > \bar{V} \quad then \quad if \quad y_w > x_w \quad then \quad W = 0 \quad else \quad W > 0$

4.5.1.3 Algorithm of free water flash calculation

Lapene et al. (2010) provided a very straight forward algorithm for successive substitution (SS) method and they used Peng-Robinson (PR) EOS to describe each phase. However any other accelerated or second order method or EOS can be used for phase equilibrium calculation.

1. Initialize equilibrium ratio (k_i^I) for non-water components; i.e.; Wilson correlation

$$k_i^I = \frac{P_{ci}}{P} exp\left[5.37(1+\omega_i)\left(1-\frac{T_{ci}}{T}\right)\right]$$

2. Initialize equilibrium ratio (k_i^I) for water component; i.e.; Peng Robinson for water.

$$k_i^I = 10^6 \frac{P_{ci}}{P}\frac{T}{T_{ci}}$$

3. Update water mole fractions; for the first iteration mole fraction of water in vapor phase can be calculated from Raoult's law.

$$y_w = k_w^{II}$$

$$x_w = \frac{k_w^{II}}{k_w^{I}}$$

4. Calculate minimum and maximum equilibrium ratio for hydrocarbon components. if $k_{min}^{I} > k_w^*$ or $k_{max}^{I} < k_w^*$ then solve a classical Rachford-Rice equation and go to step 6, otherwise go to the next step.
5. Calculate $\bar{V}$ and determine sign of $G(\bar{V})$, evaluate the position of $\bar{V}$ relative to V. Then predict absence or presence of water corresponding to sign of $G(\bar{V})$ and the relative position of water composition. If water is present solve modified Rachford-Rice equation, else solve classical Rachford-Rice equation.
6. Find V by solving classical Rachford-Rice equation by any method; e.g.; combined Bisection-Newton method.
7. Find V by solving modified Rachford-Rice equation by any method; e.g.; combined Bisection-Newton method.
8. If classical Rachford Rice equation was solved, calculate phase composition for all components including water. If modified Rachford-Rice equation was solved, calculate phase composition for all components excluding water. Then use equation 4-18 to calculate water mole fractions in different phases.
9. Evaluate fugacity coefficient by using EOS for each phase.
10. Evaluate convergence error; if convergence is achieved go to step 12, otherwise go to the next step.

$$s = \left[\sum_{i=1}^{nc}\left(\frac{f_{iL}}{f_{iV}} - 1\right)^2\right]^{0.5}$$

11. Update equilibrium ratios and go back to step 3

$$k_i^I = k_i^I \frac{f_{iL}}{f_{iV}}$$

- If modified Rachford-Rice equation was solved

$$k_w^{II} = k_w^{II} \frac{f_{wW}}{f_{wV}}$$

- If Rachford-Rice equation was solved,

$$k_w^{II} = y_w$$

12. Finally calculate the final distribution and assign final values for phase ratios. Set V to the appropriate limits if solution is out of physical range. If classical Rachford-Rice equation was solved and $V > 1$, set it to unity. If modified Rachford-Rice equation was solved and $V > V^*$, set $V = V^*$.

4.5.2 *Algorithm of new isenthalpic multiphase flash calculation*

In this section we provide the following algorithm for our new isenthalpic multiphase flash calculations;

1. Assume $T^{(k)}$ is the k-th iteration values of T
2. Perform free water isothermal flash calculation and calculate $K_{ij}^{(k)}$, $x_{ij}^{(k)}$, $F_j^{(k)}$
3. Calculate residual of energy equation

4. If $Res < tol1 \quad where, \ tol1 = 1.E-10$ terminate flash calculation
5. Solve energy equation and update $T^{(k+1)}$ by a secant method
6. Limit temperature to lower and upper bound if it is out of boundaries
7. If $\Delta T < (tol2 = 1.E-4) \ and \ Res > tol2$ switch to the fully implicit scheme otherwise go to step 1
8. Construct system of equations, energy and material balance equations
9. Calculate residual of system
10. If $Res < tol1$ then terminate flash calculation
11. Construct Jacobian matrix, $J = \frac{\partial R}{\partial Xp} \quad where \ Xp = T, V, W$
12. Solve linear system of equations by Newton-Raphson's method
13. Update primary variables, $T^{(k+1)}$, $F_j^{(k+1)}$
14. Update equilibrium ratios; $lnK_{ij}^{(k+1)} = lnK_{ij}^{(k)} + \left(\frac{\partial lnK_{ij}}{\partial T}\right)^{(k)} \left(T^{(k+1)} - T^{(k)}\right)$
15. Update component mole fraction of each phase, $x_{ij}^{(k+1)}$
16. Let $k = k + 1$ and go to step 8 and proceed until convergence

In the next section the new isenthalpic flash calculation is tested against commercial simulators and published data in the literature for validation and verifications. Several isenthalpic multiphase flash calculations with different feeds from published data are also performed at different enthalpies to investigate the results and performance of this new method.

4.6 **Validations and verifications**

The purpose of this section is to verify and validate the results of new isenthalpic flash calculation against current available algorithm which are used by industry. PVTSIM and CMG Winprop are two commercial simulator, which are used by industry and have been used in this study to verify and validate the accuracy of this new method. The isenthalpic flash calculation

method of Michelsen (1987) is used in PVTSIM and Agarwal et al. (1991) method is used in Winprop.

As mentioned before isothermal multiphase flash calculation of Lapene et al. (2010) model was used in the current isenthalpic flash calculation method. In this section first the Lapene et al. (2010) model is validated by recreating the provided examples in their original paper and versus commercial simulators for two synthetic cases. Then the isenthalpic flash validation examples are presented in the next section.

4.7 **Verification of isothermal multiphase flash calculation**

Three out of five of the examples in the Lapene et al. (2010) paper are recreated. They tested five cases to cover all possible phase distribution configurations. Three synthetic mixture containing hydrocarbon and water, and two reservoir fluid-water systems were tested. Peng-Robinson cubic EOS was used in all test cases.

4.7.1.1 Water/Nitrogen/C10/C20 mixture

The mixture was tested at T = 450 K and pressure range of 100-20000 kPa. Feed composition and component properties are given in Table 4-1. With increasing pressure, the phase sequence is VL/VLW/LW. Figure 4-2 presents comparison between our results and Lapene et al.'s results.

Table 4-1: Feed composition and component properties

Component Name	Mole Fraction	T_c (K)	P_c (kPa)	ω
H_2O	0.55	647.0	22050.0	0.344
N2	0.10	126.2	3400.0	0.040
C10	0.10	622.0	2530.0	0.443
C20	0.25	782.0	1460.0	0.816

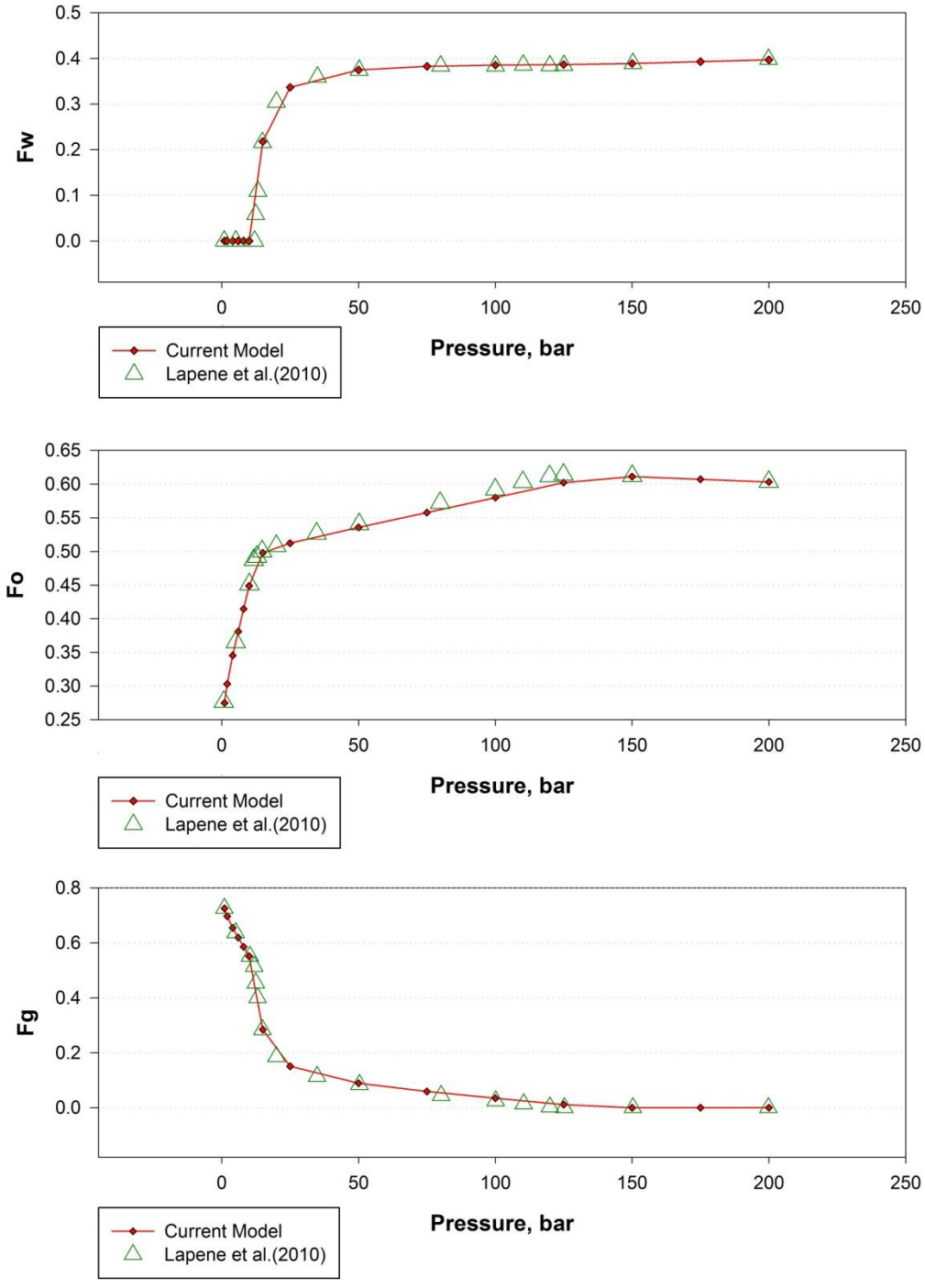

Figure 4-2: Comparison between results of this study and Lapene et al. (2010)

4.7.1.2 Reservoir fluid/water mixture

A real reservoir fluid plus water is tested. Mixture includes 18 components where composition, component properties, and binary interaction coefficient between components are given in Table 4-2. The summation of mole fractions in the original paper exceeds unity, i.e., Sum = 1.2, therefore mole fraction of each component was normalized to get summation equal to unity. In this case, two tests were done. The first test is an isothermal test, where temperature is kept at T equal to 450 K and pressure varies from 100 kPa to 50000 kPa. In the second test, which is an isobaric test, pressure is held at 5000 kPa and temperature changes in the interval of 200 K to 700 K. Phase sequence in the first test is VL/VLW/VW and in the second test by increasing temperature phase sequence is LW/VLW/VL/V. Figure 4-3 and 4-4 compare results of Lapene et al. (2010) model and this study.

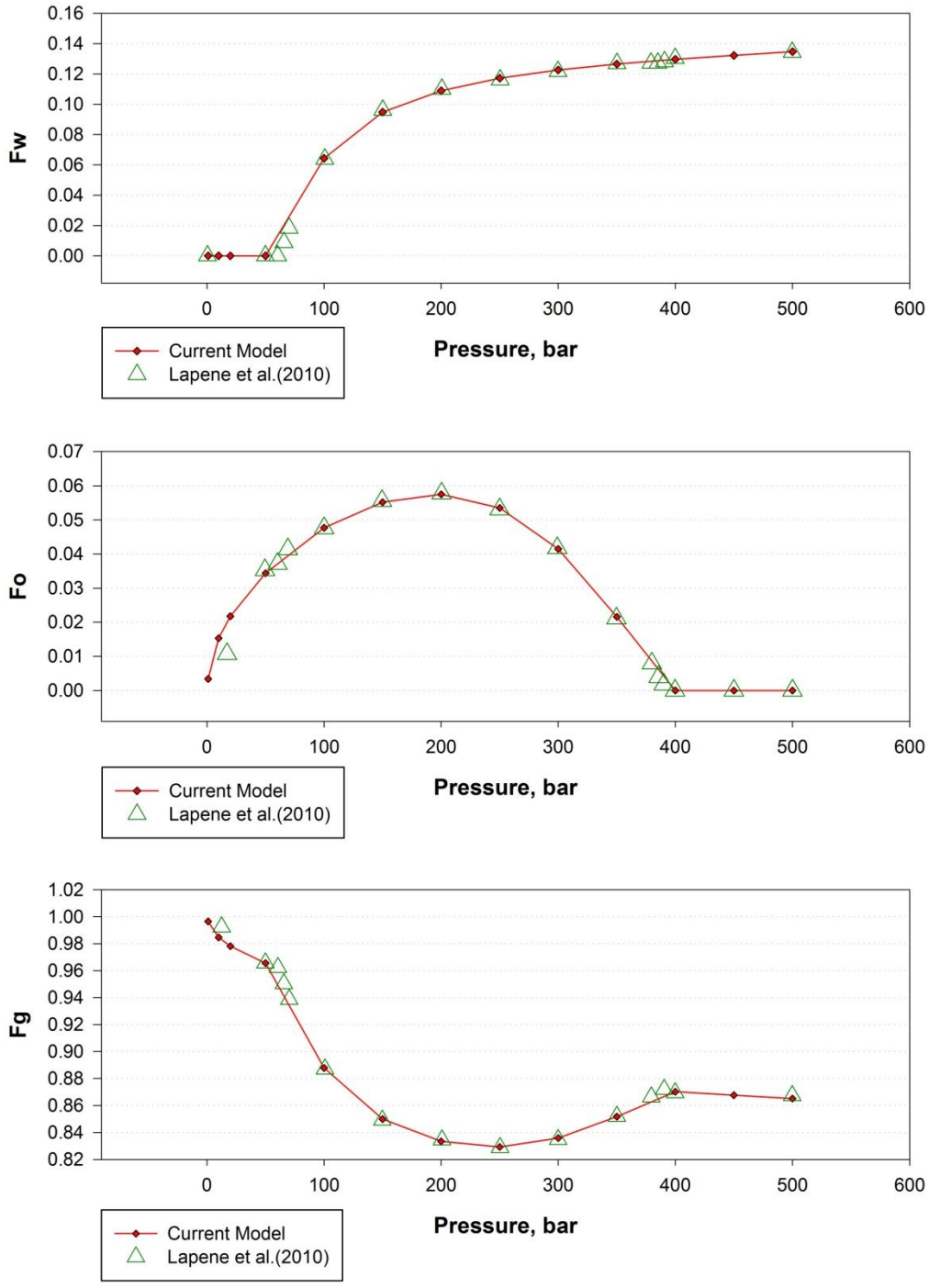

Figure 4-3: Comparison between this work and Lapene et al. (2010) at 450 K

Table 4-2: Composition and feed data

Component Name	Mole Fraction	Tc (K)	Pc (kPa)	ω	Binary interaction coefficient				
					H_2O	N2	CO_2	C1	C2
H_2O	0.1667	647.37	22120.00	0.344	0	0.4778	0.1896	0.485	0.492
N2	0.0022	126.20	3394.00	0.040	0.4778	0	0.1000	0.100	0.100
CO_2	0.03	304.21	7377.00	0.225	0.1896	0.1000	0	0.120	0.120
C1	0.6177	190.60	4600.00	0.012	0.4850	0.1000	0.1200	0	0
C2	0.0662	305.40	4884.00	0.091	0.4920	0.1000	0.1200	0	0
C3	0.0274	369.80	4246.00	0.145	0.5525	0.1000	0.1200	0	0
i-C4	0.0057	408.10	3648.00	0.176	0.5000	0.1000	0.1200	0	0
n-C4	0.0103	425.20	3800.00	0.193	0.5000	0.1000	0.1200	0	0
i-C5	0.0046	464.74	3477.00	0.223	0.5000	0.1000	0.1200	0	0
n-C5	0.0051	469.60	3374.00	0.227	0.5000	0.1000	0.1200	0	0
C6	0.0072	515.28	3257.00	0.264	0.5000	0.1000	0.1200	0	0
C7	0.0096	553.84	3100.00	0.290	0.5000	0.1000	0.1200	0	0
C8	0.0089	581.28	2850.00	0.324	0.5000	0.1000	0.1200	0.020	0
C9	0.0079	609.35	2650.00	0.379	0.5000	0.1000	0.1200	0.030	0
C10	0.0056	626.97	2460.00	0.436	0.5000	0.1000	0.1200	0.050	0.020
HVY	0.0138	658.15	2120.00	0.520	0.5000	0.1000	0.1200	0.070	0.040
HVY2	0.0094	778.15	1570.00	0.650	0.5000	0.1000	0.1200	0.085	0.050
HVY3	0.0018	998.15	1350.00	0.720	0.5000	0.1000	0.1200	0.070	0.040

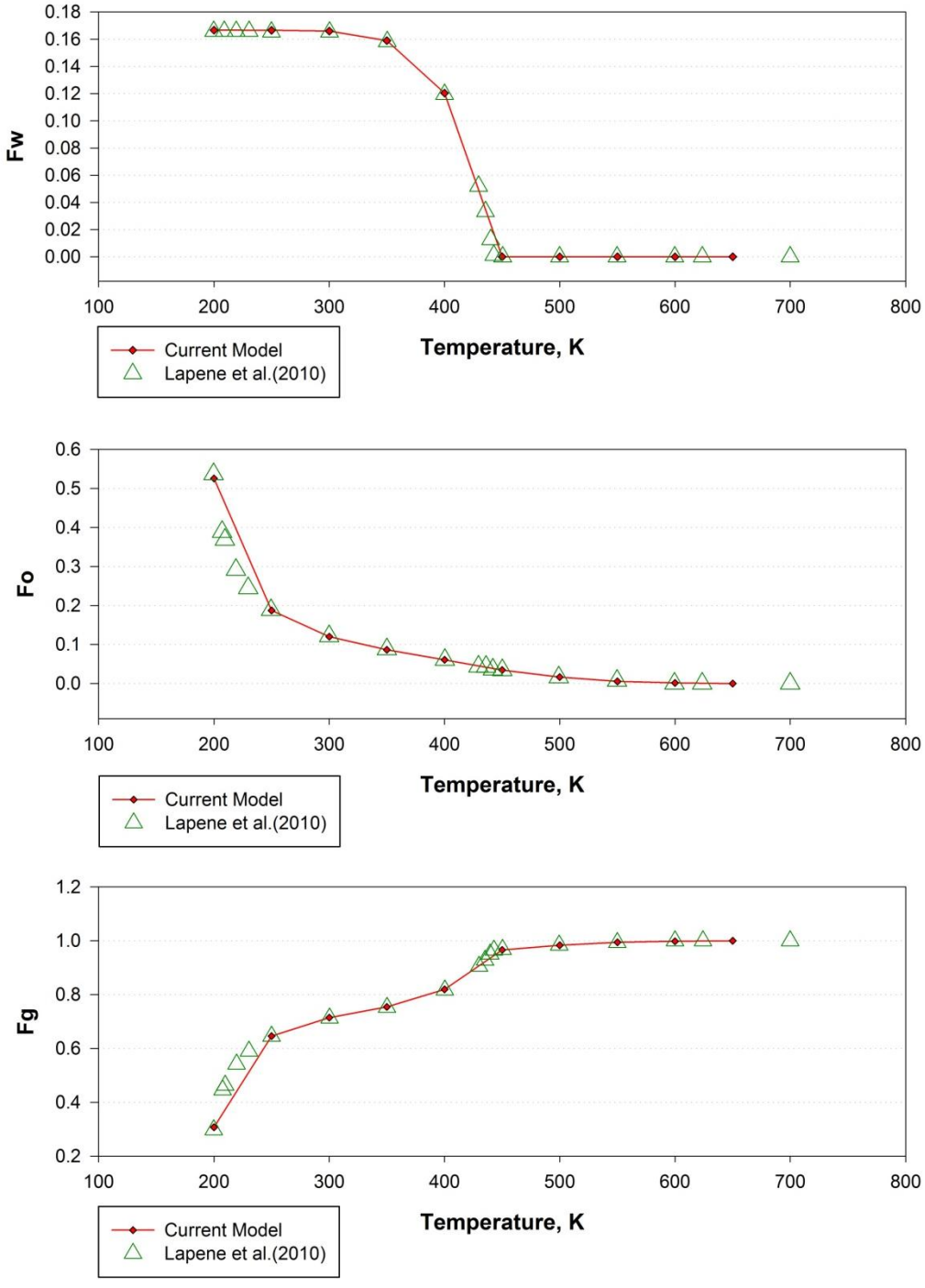

Figure 4-4: Comparison between this work and Lapene et al. (2010) at 5000 kPa

4.7.1.3 Heavy oil at high temperature

The last example in the Lapene et al. (2010) paper is extra heavy oil. This mixture is lumped into seven pseudo components and water. Composition and component properties of all seven pseudo components are presented in Table 4-3. Free water flash calculation was performed at P = 700 kPa and temperature varied from 438 K to 438.5 K. The phase sequence in this range of temperature is LW/VLW/VL. The three phase equilibrium occurs in very narrow window (approximately 0.1 K) which is a good example of narrow boiling point region. Figure 4-5 shows results of Lapene et al. (2010) paper and our flash calculation code. Note that the temperature scale is highly expanded in this case, the same behavior as in Lapene et al. (2010) results is observed, however the three phase equilibrium starts at 438.04 K in our case whereas it starts at 438.3 K at Lapene et al.'s case. In their paper they did not report the binary interaction coefficient between components and we assumed them to be zero in our case. Binary interaction coefficients could cause the deviation in our results.

Table 4-3: Composition and component properties

Component Name	Mole fraction	Tc (K)	Pc (kPa)	ω
H_2O	0.9834	647.37	22120.00	0.3440
C2-C11	0.0003	635.64	2411.00	0.4645
C12-C16	0.003	701.24	1925.00	0.6087
C17-C21	0.0026	772.05	1510.00	0.7880
C22-C27	0.0023	826.30	1229.00	0.9467
C28-C35	0.0019	879.55	994.00	1.1042
C36-C49	0.0017	936.97	779.00	1.2730
C50+	0.0048	1260.00	600.00	1.6500

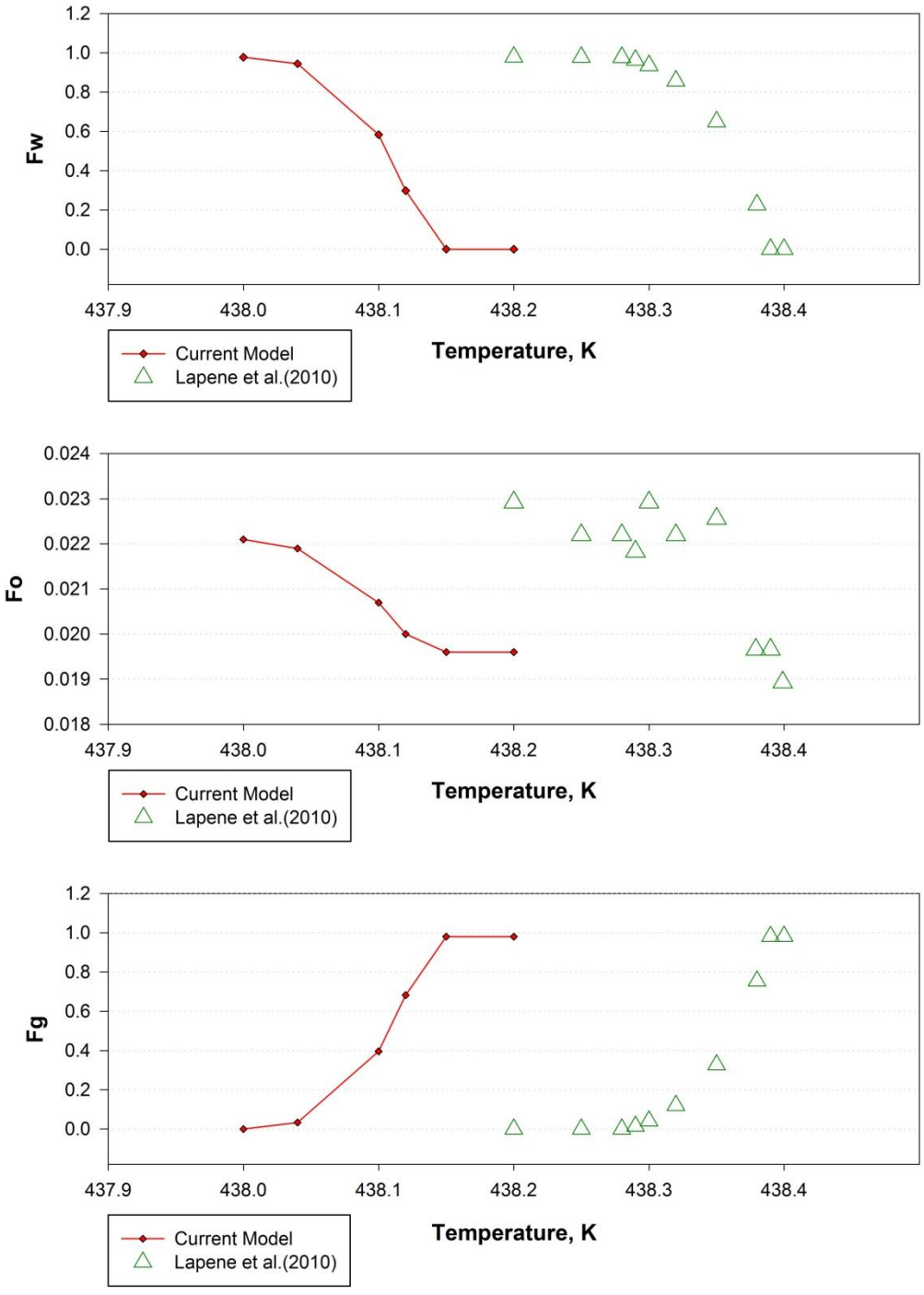

Figure 4-5: Comparison between results of this work and Lapene et al. (2010) for heavy oil case

4.7.1.4 Water\C6\C10\C15 mixture

After recreation of the three cases of original paper, the results of this method are compared with commercial PVT packages, i.e., CMG Winprop, and PVTSIM. In this part a very detailed comparison between the current code and PVT packages results was performed. Composition, components properties and binary interaction coefficient are provided in Table 4-4. SRK EOS is used instead of Peng-Robinson EOS in the next cases.

A synthetic mixture was tested for a range of temperature while pressure was kept constant at 500 kPa and for a pressure range while temperature kept constant at 438 K. These two tests were performed with PVTSIM and CMG Winprop. During the increasing pressure and temperature different phase sequences were observed. Phase mole fractions of each phase are plotted to compare the results of simulators and current code in Figure 4-6 and 4-7. Table 4-5 shows that, in the presence of free water, the solubility of water in oil phase increases as temperature increases. When the free water phase disappears, the mole fraction of water in liquid phase decreases with increasing temperature.

Table 4-4: Composition and component properties

Component Name	Mole fraction	Tc (K)	Pc (kPa)	ω
H_2O	0.55	647.3	22089.00	0.344
C6	0.1	507.4	2969.00	0.296
C10	0.1	594.906	2439.00	0.5764
C15	0.25	676.266	1824.00	0.7678

Binary Interaction Coefficient	H2O	C6	C10	C15
H_2O	0			
C6	0.48	0		
C10	0.48	0.00280	0	
C15	0.48	0.01097	0.02657	0

Table 4-5: Comparison between results of this study and commercial PVT packages at 500 kPa

		This Study			PVTSIM			WINPROP		
T(K)	Components	w_i	y_i	x_i	w_i	y_i	x_i	w_i	y_i	x_i
288	H_2O	1	0.0000	0.0003	1	0.0000	0.0003	1	0.0000	0.0002
	C_6	0	0.0000	0.1000	0	0.0000	0.1000	0	0.0000	0.1000
	C_{10}	0	0.0000	0.2999	0	0.0000	0.2999	0	0.0000	0.2999
	C_{15}	0	0.0000	0.5998	0	0.0000	0.5999	0	0.0000	0.5999
338	H_2O	1	0.0000	0.0025	1	0.0000	0.0025	1	0.0000	0.0024
	C_6	0	0.0000	0.0998	0	0.0000	0.0998	0	0.0000	0.0998
	C_{10}	0	0.0000	0.2993	0	0.0000	0.2993	0	0.0000	0.2993
	C_{15}	0	0.0000	0.5985	0	0.0000	0.5985	0	0.0000	0.5985
388	H_2O	1	0.0000	0.0130	1	0.0000	0.0130	1	0.0000	0.0128
	C_6	0	0.0000	0.0987	0	0.0000	0.0987	0	0.0000	0.0987
	C_{10}	0	0.0000	0.2961	0	0.0000	0.2961	0	0.0000	0.2962
	C_{15}	0	0.0000	0.5922	0	0.0000	0.5922	0	0.0000	0.5923
438	H_2O	0	0.8464	0.0283	0	0.8464	0.0283	0	0.8542	0.0278
	C_6	0	0.0619	0.0337	0	0.0619	0.0337	0	0.0629	0.0328
	C_{10}	0	0.0764	0.2502	0	0.0764	0.2502	0	0.0680	0.2593
	C_{15}	0	0.0152	0.6878	0	0.0152	0.6878	0	0.0149	0.6800
488	H_2O	0	0.6988	0.0212	0	0.6988	0.0212	0	0.7062	0.0210
	C_6	0	0.0634	0.0178	0	0.0634	0.0178	0	0.0640	0.0175
	C_{10}	0	0.1468	0.1578	0	0.1468	0.1578	0	0.1400	0.1733
	C_{15}	0	0.0910	0.8032	0	0.0911	0.8032	0	0.0898	0.7883

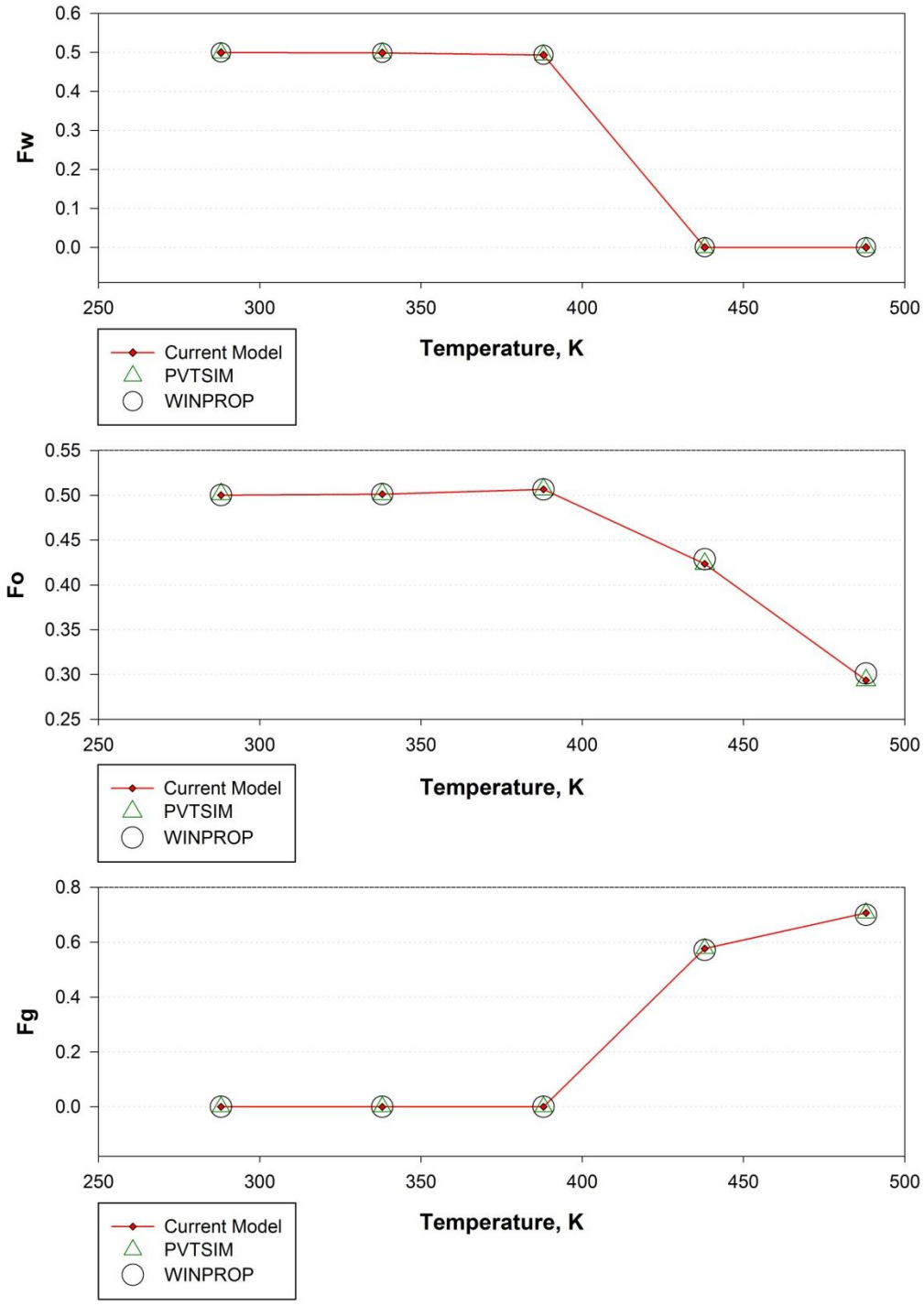

Figure 4-6: Comparison between results of this study and commercial PVT packages

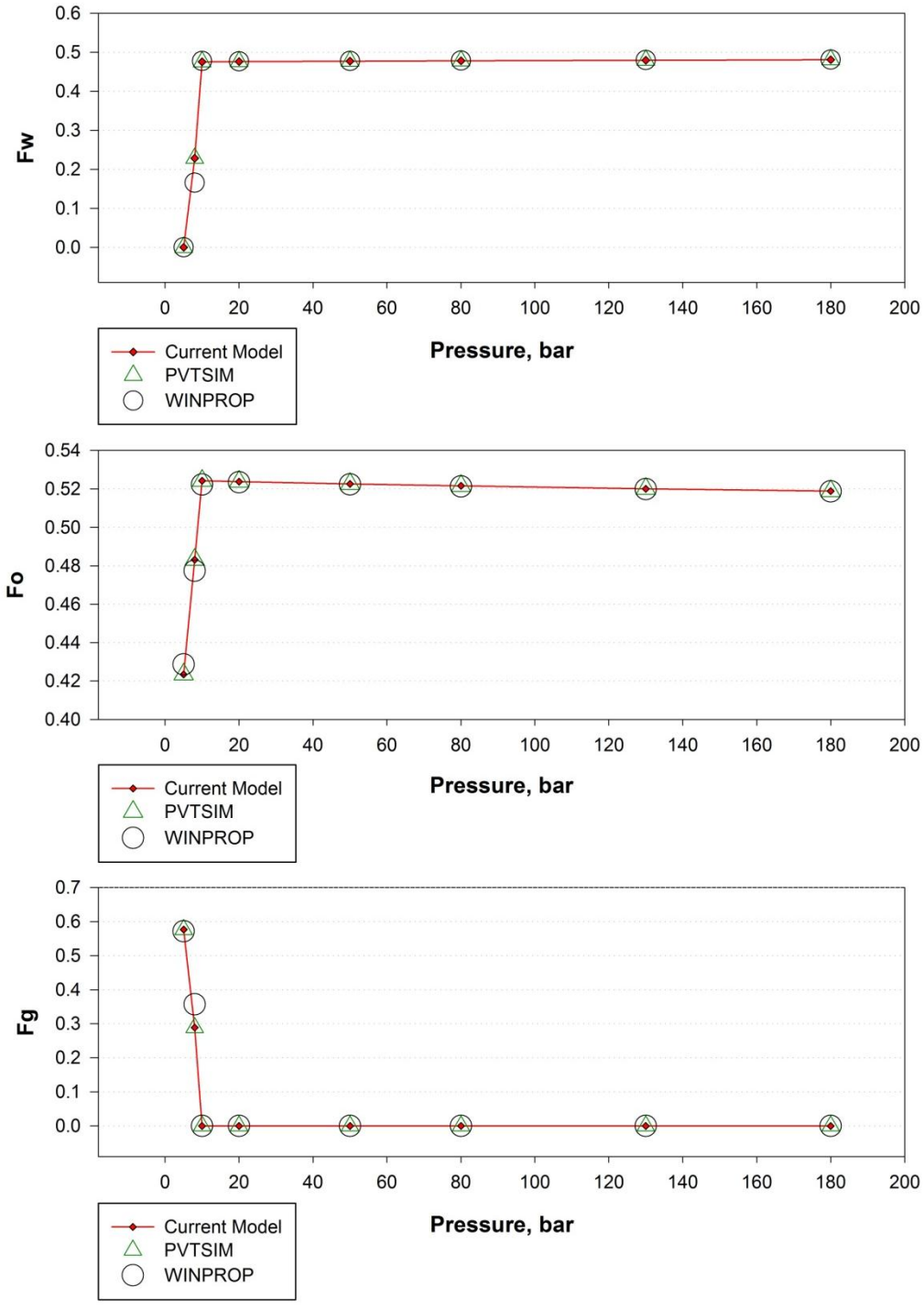

Figure 4-7: Comparison between results of this study and commercial PVT packages

4.7.1.5 Synthetic mixture (Water\C10\C15\C19\C25\$C26^{+}$)

Another synthetic mixture was introduced to perform more validation tests. The same tests were applied on this synthetic mixture. The synthetic mixture consists of water and five hydrocarbon components. Properties of these components are listed in Table 4-6. All of HC-HC binary interaction coefficients are equal to zero. H_2O-HC binary interaction coefficient is equal to 0.48. A wide range of pressure and temperature was used to challenge the current free water flash calculation model. In the first test, pressure changes in the range of 500 to 20000 kPa while temperature is kept at 488K. Phase equilibrium sequence in this pressure range varies from VL/L/LW. In Figure 4-8, the mole fractions of phases are plotted. In the second test pressure remains constant at 1500 kPa and temperature varies from 288 K to 538 K. Mixture goes from Liquid/Water to Vapor/Liquid state.

To validate the results of current model, the same test were conducted by the two commercial simulators and the results are almost identical. It is worth mentioning that the tolerance equal to $1.0E^{-15}$ was chosen for flash calculation and successive substitution method was used to perform the flash calculations.

Table 4-6: Composition and component properties

Component Name	Mole fraction	Tc (K)	Pc (kPa)	ω
H_2O	0.0915	647.300	22089.00	0.3440
C10	0.0004	594.906	2439.00	0.5764
C15	0.0009	676.266	1824.00	0.7678
C19	0.0009	726.653	1581.00	0.9046
C25	0.0023	791.757	1435.00	1.0755
C26+	0.9040	802.131	1420.00	1.1014

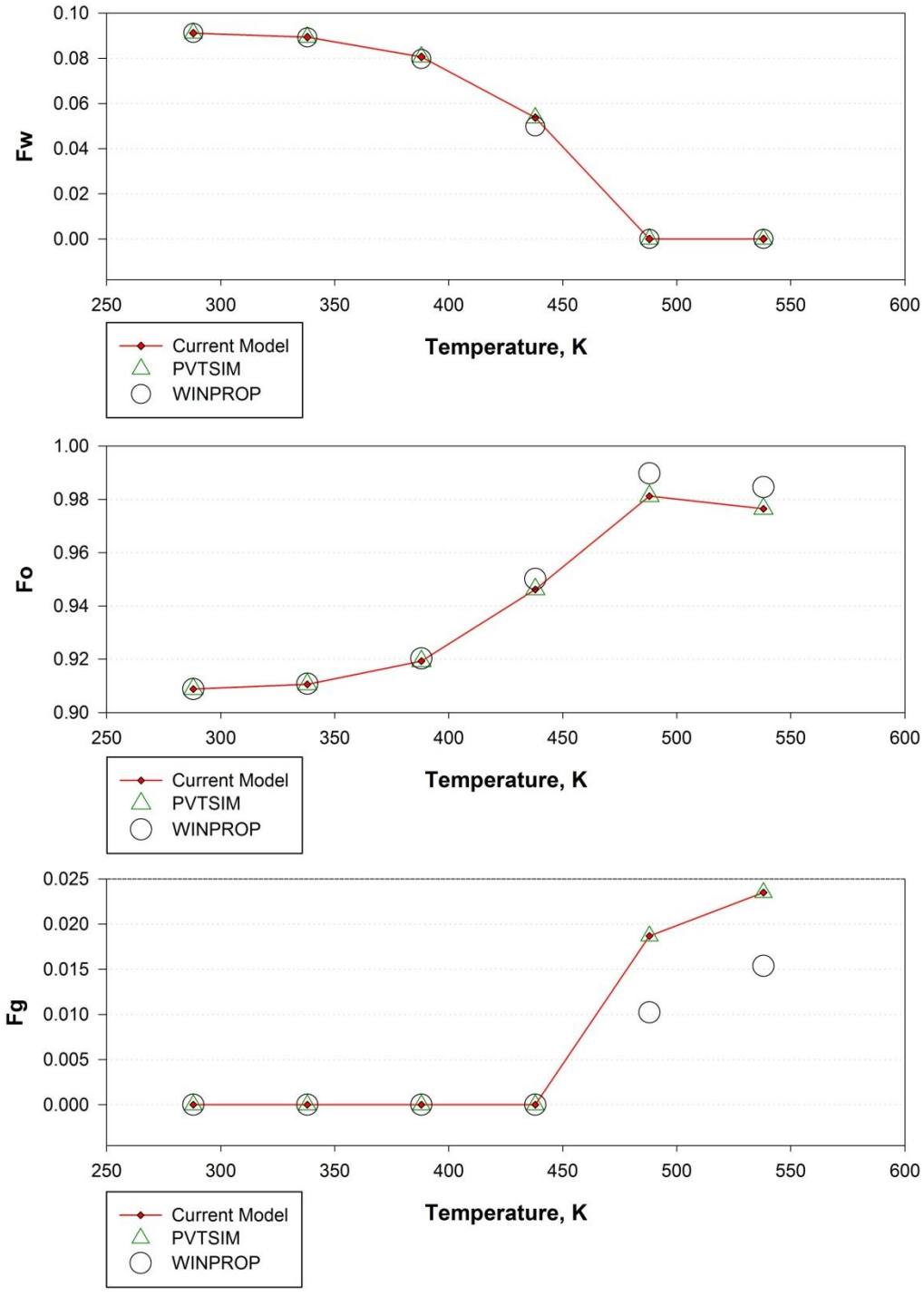

Figure 4-8: Comparison between results of this study and commercial PVT packages

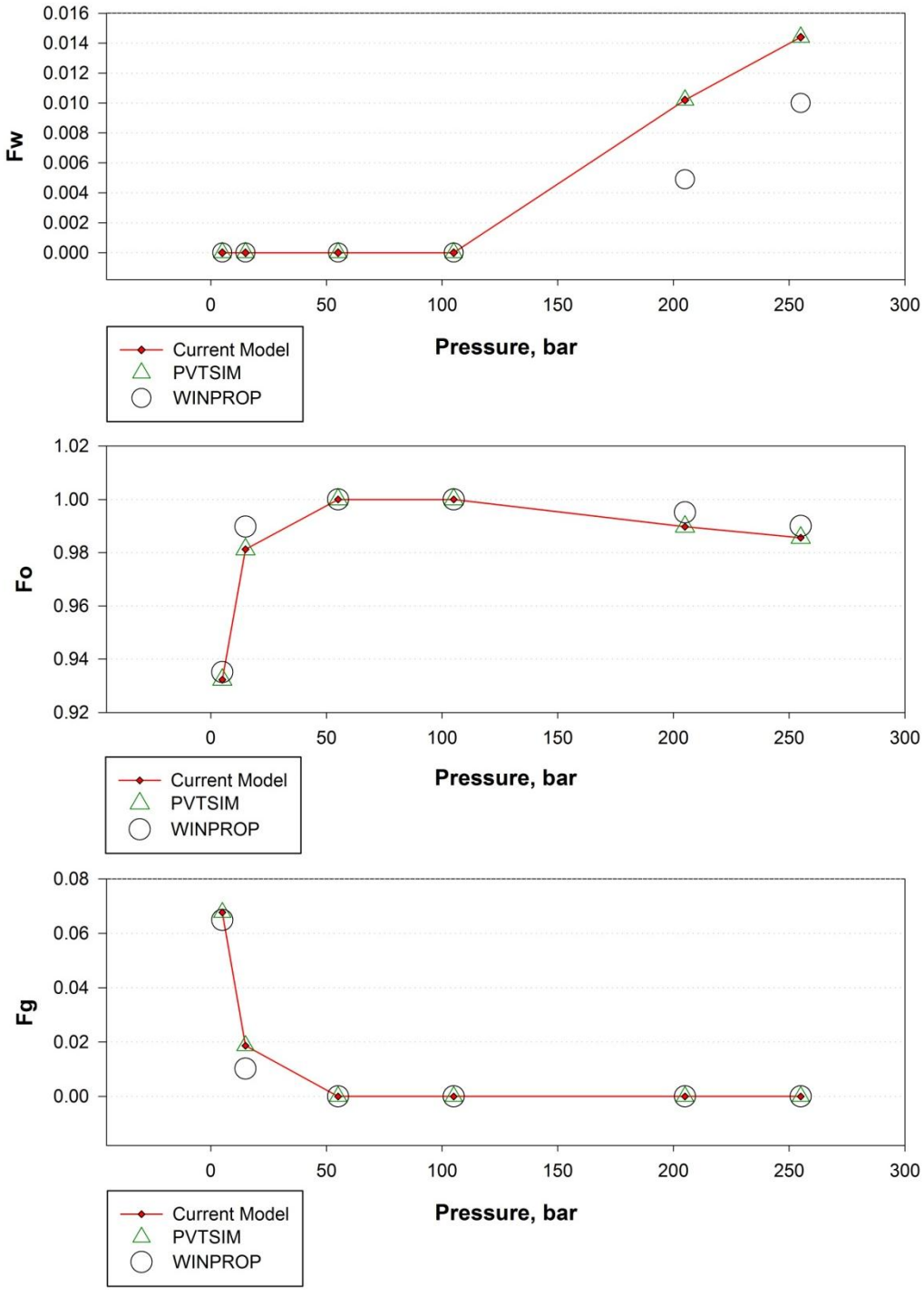

Figure 4-9: Comparison between results of this study and commercial PVT packages

4.8 **Verification of isenthalpic multiphase flash calculation**

The developed multiphase isenthalpic flash calculation method was validated with several examples from the literature. First, three examples from Agarwal et al.'s paper (1991) were extracted from the original paper. We had to choose only the examples which contain water component since the free water assumption is used. These three examples were run in CMG Winprop and their results were compared against the current simulator. Then in the second step, the same examples were run with PVTSIM but with different reference enthalpies. Two of these three examples are more difficult for isenthalpic flash calculations, since the phase change happens in very narrow boiling point region. Soave modification of Redlich and Kowng equation of state (1972) was used in all of verification and validations.

4.8.1.1 Example 1: mixture (Water/CO_2/C9/C41) vs. CMG Winprop

In this mixture the water component in the feed is equal to 98% and it includes CO_2. This mixture was selected because of three main reasons. First, it includes CO_2, and CO_2 has high solubility in water phase at high temperatures. We wanted to see the deviation of the results of current model which uses free water assumption against the cases were mutual solubility of component in all phases are considered. Second, water component global mole fraction is 98% and it is very common in the reservoir simulators to have a grid block with only traces of hydrocarbons. Third, the phase change occurs in a very narrow window of temperature and variation of enthalpy with temperature is very abrupt.

The synthetic mixture consists of water and three hydrocarbon components and properties of these components are listed in Table 4-7. A wide range of total molar enthalpy was used while feed composition and pressure were kept constant to cover different phase change regions. Figure 4-10 shows variation of vapor phase mole fraction versus temperature for CMG Winprop and the current model. The red line is CMG Winprop results and blue circles are current model. Total molar enthalpy is changing from -30000 to 30000 J/mol and pressure is equal to 7040 kPa. The results match very closely and the phase change occurs in a very narrow window of temperature.

Figure 4-11 plots variation of vapor phase mole fraction versus total molar enthalpy. It is clear that the variation of total molar enthalpy versus vapor phase mole fraction is not as steep as vapor phase mole fraction versus temperature.

CMG Winprop takes into account the solubility of other component in the water phase. In this new isenthalpic flash calculation method, first the sequential method is used and it finds the initial guess for temperature and phase fractions and this information is then used in the fully implicit scheme. In the fully implicit scheme we also take into account the mutual solubility of all phases, thus the results of this study and CMG Winprop are very close to each other.

Table 4-7: Composition and component properties for Example 1

Component Name	Mole fraction	Tc (K)	Pc (kPa)	ω
H_2O	0.9814	647.3000	22048.3200	0.3440
CO_2	0.0047	304.2000	7376.4600	0.2250
C9	0.0018	598.5000	2729.7000	0.3908
C41	0.0121	938.5000	788.3100	1.2725

Component Name	Cp1	Cp2	Cp3	Cp4
H_2O	33.75536	-0.005940	2.24E-05	-9.96E-09
CO_2	29.26153	-0.022360	0.000265	-4.15E-07
C9	-23.62510	0.780753	-0.000320	0.00
C41	-24.10940	3.004869	-0.001140	0.00

Binary Interaction Coefficients	H_2O	CO_2	C9	C41
H_2O	0			
CO_2	0.20	0		
C9	0.48	0.15	0	
C41	0.48	0.15	0.0294163	0

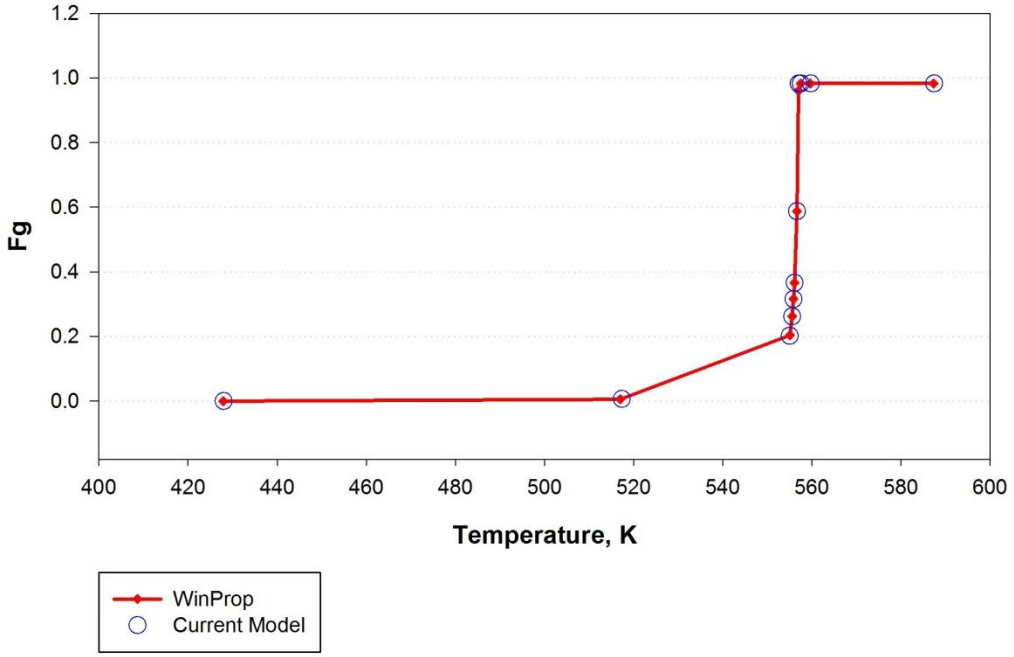

Figure 4-10: Variation of gas phase mole fraction versus temperature

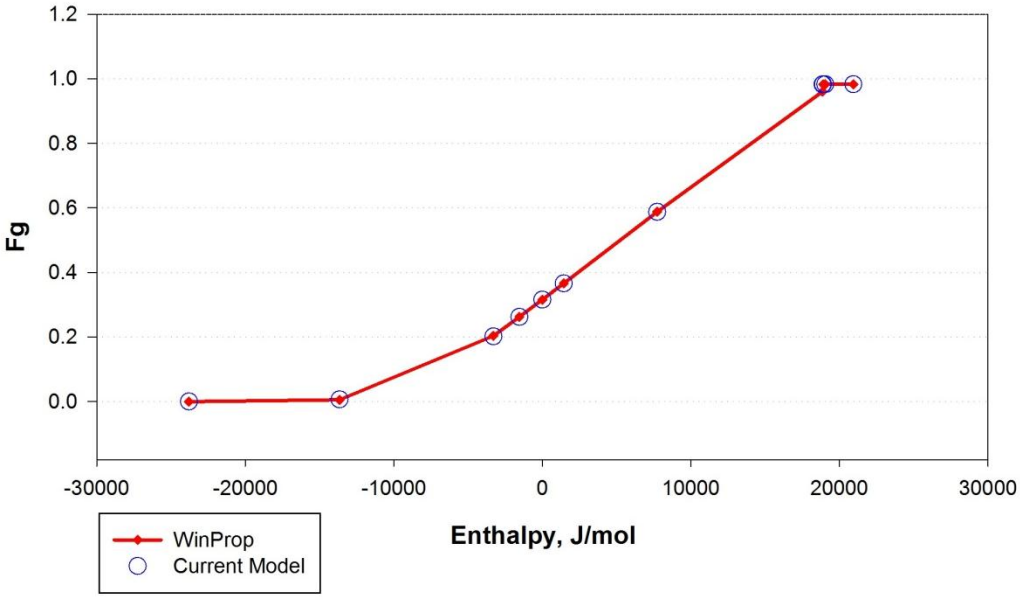

Figure 4-11: Variation of gas phase mole fraction versus total molar enthalpy

4.8.1.2 Example 1: mixture (Water, CO_2, C9, C41) vs. PVTSIM

The same mixture as example 1 is used and it has been validated against PVTSIM which uses Michelsen's (1987) model. Different reference enthalpy was used in this model; therefore the temperature range is different in this case in comparison with the first case.

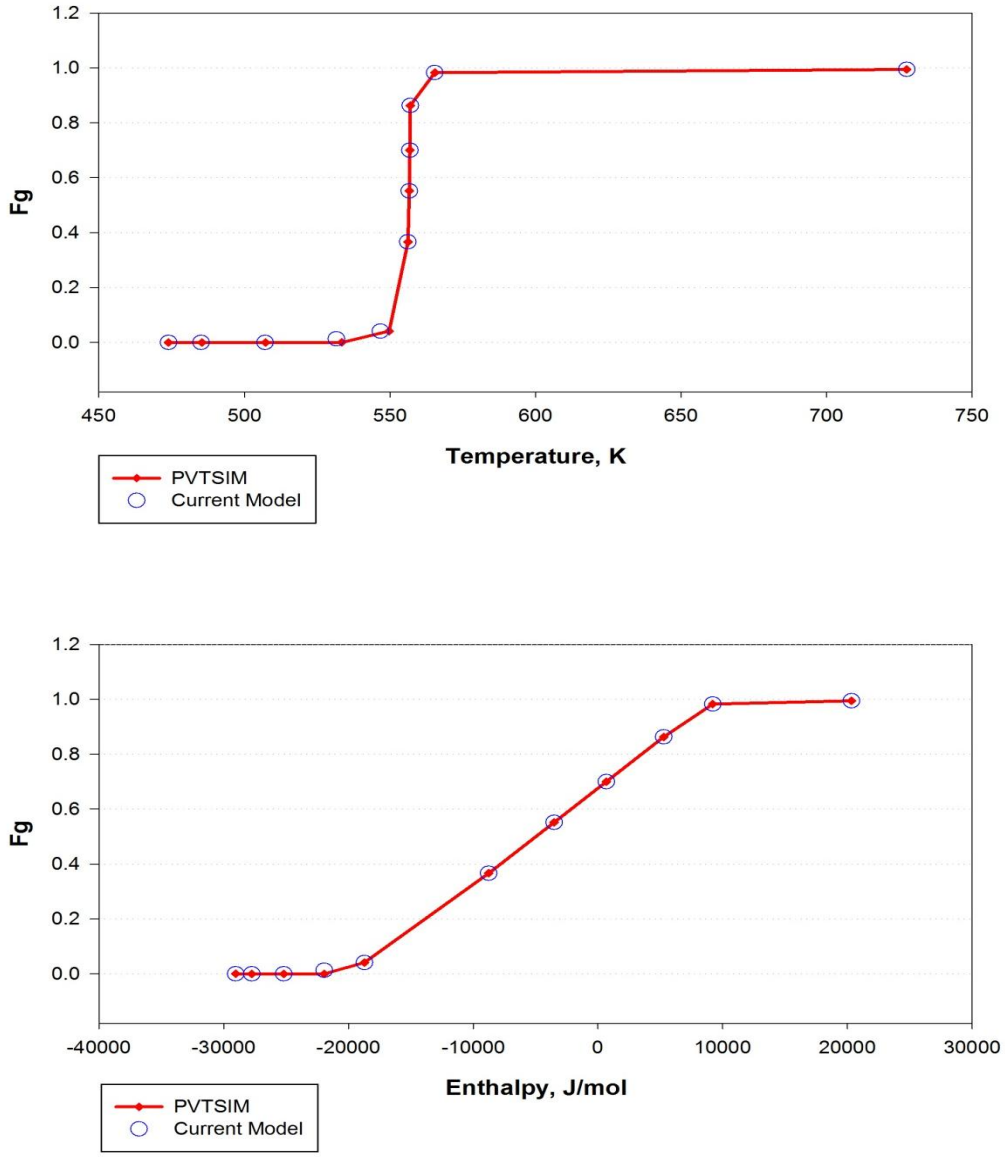

Figure 4-12: Variation of gas phase mole fraction versus temperature and total molar enthalpy

4.8.1.3 Example 2: mixture (Water, CO_2, C2, nC5, C8, C12) vs. CMG Winprop

In this mixture water component global mole fraction is equal to 13% and CO_2 is 80%. This mixture is close to example 1 but it has more CO_2 and less water. The heaviest component is C12 which is not as heavy as C41. In this example also a wide range of total molar enthalpy at constant pressure and feed composition were examined. This mixture consists of water and five other components and Table 4-8 presents the mixture's component properties. Figure 4-13 compares the results of this model against CMG Winprop which uses Agarwal et al.'s model (1991). Figure 4-13 shows that in the beginning there is LW equilibrium and by increasing the enthalpy of system first a sharp three phase LVW region occurs, after that water phase disappears and there is a wide range of LV equilibrium and finally only vapor phase remains in the system. The results of the current model are almost identical with the Agarwal et al.'s model (1991).

Table 4-8: Composition and component properties for Example 2

Component Name	Mole fraction	Tc (K)	Pc (kPa)	ω
H_2O	0.134	647.3	22048.3	0.344
CO_2	0.800	304.2	7376.1	0.225
C2	0.033	305.4	4883.6	0.098
nC5	0.011	469.6	3374.0	0.251
C8	0.011	570.5	2950.4	0.351
C12	0.011	663.9	2191.6	0.522

Component Name	Cp1	Cp2	Cp3	Cp4
H_2O	33.75536	-0.00594	2.24E-05	-9.96E-09
CO_2	29.26153	-0.02236	0.000265	-4.15E-07
C2	33.30586	-0.01113	0.000357	-3.76E-07
nC5	33.77337	0.24845	0.000253	-3.84E-07
C8	-20.53700	0.69221	-0.000280	0
C12	-26.45610	1.02055	-0.000410	0

Binary Interaction Coefficients	H_2O	CO_2	C2	nC5	C8	C12
H_2O	0					
CO_2	0.2000	0				
C2	0.4911	0.15	0			
nC5	0.5000	0.15	0.008578	0		
C8	0.4800	0.15	0.01796	0.001765	0	
C12	0.4800	0.15	0.033751	0.008637	0.002618	0

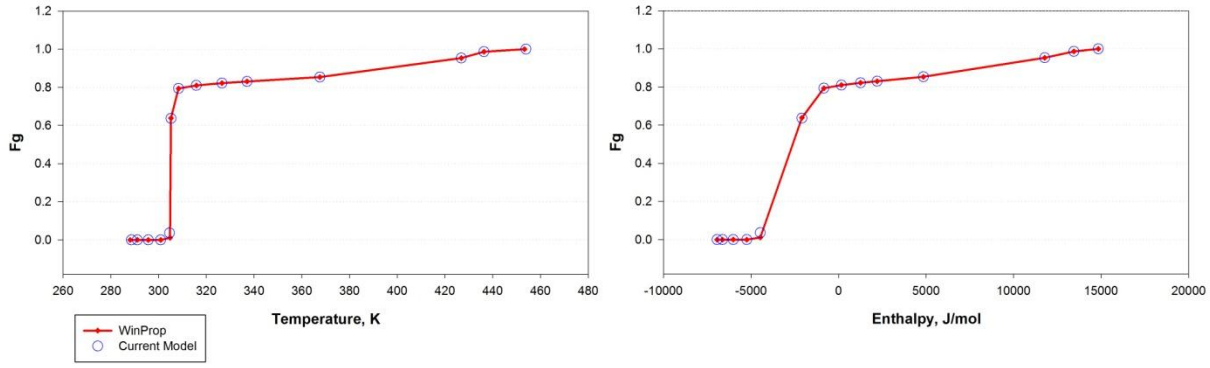

Figure 4-13: Variation of gas phase mole fraction versus temperature and total molar enthalpy

4.8.1.4 Example 2: mixture (Water, CO_2, C2, nC5, C8, C12) vs. PVTSIM

The same mixture as example 2 is used and it was tested for different molar enthalpy range but same pressure and feed composition and different reference enthalpy for ideal gas enthalpies. Figure 4-14 and 4-15 express variation of vapor phase mole fraction versus temperature and total molar enthalpy respectively. The result shows very good agreement between the current model and Michelsen's (1987) model. The reference temperature for ideal gas enthalpy is equal to 273.15 K.

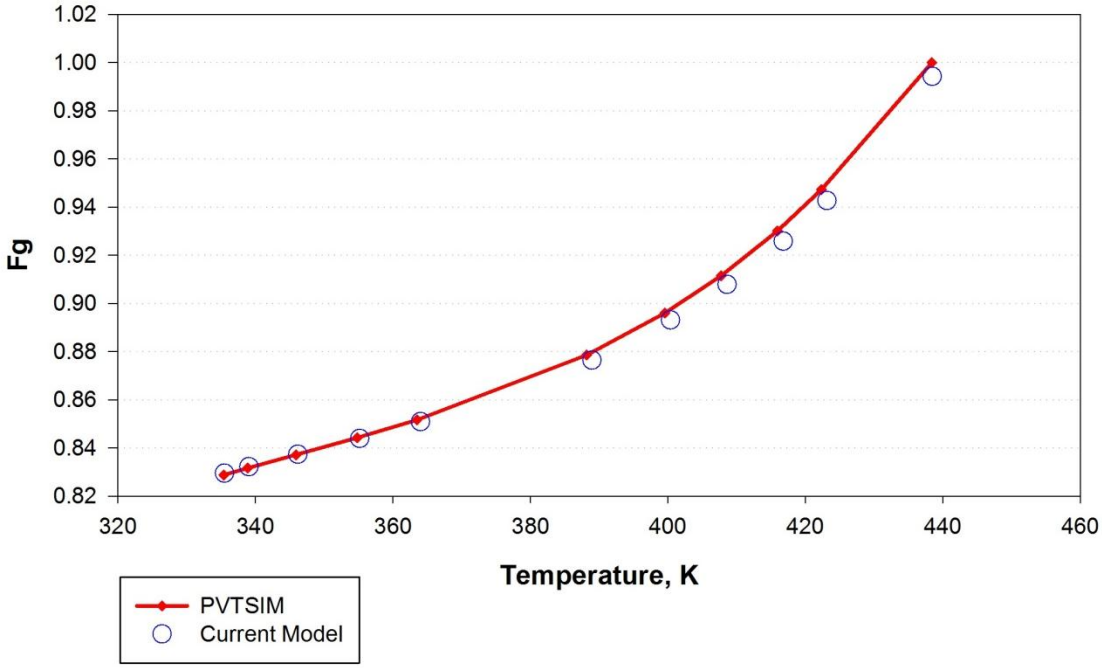

Figure 4-14: Variation of gas phase mole fraction versus temperature

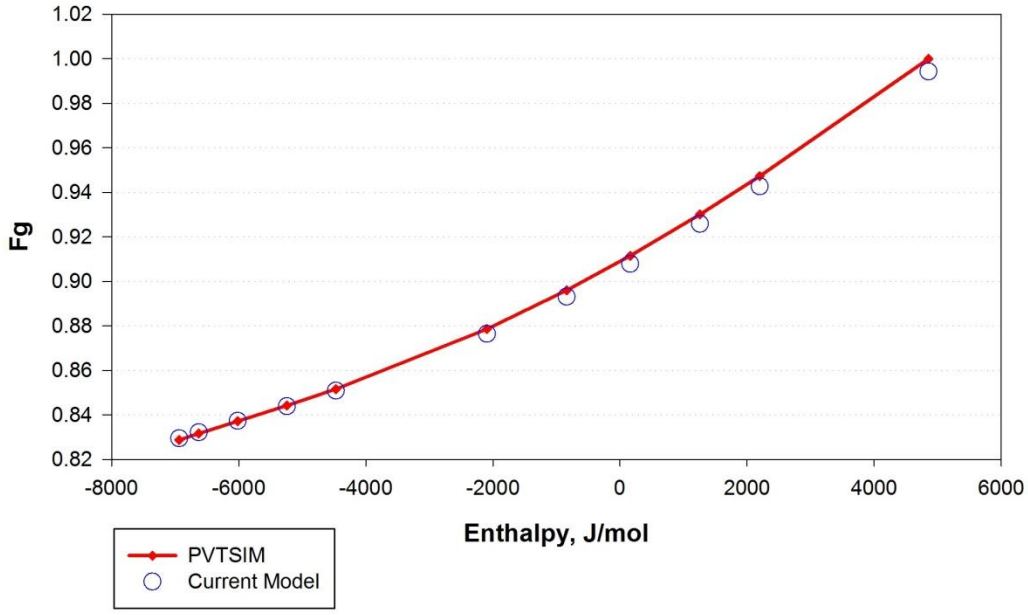

Figure 4-15: Variation of gas phase mole fraction versus total molar enthalpy

4.8.1.5 Example 3: mixture (Water, C1, C40) vs. CMG Winprop

This case is from example 11 of Agarwal's paper (1991). This example is very similar to typical fluid mixtures which are used in SAGD simulation. The mixture consists of water, a volatile component and an almost non-volatile component. The global mole fraction is equal for all three components; i.e.; equal to 0.3333. Properties of these components are listed in Table 4-9. Pressure is kept at 1000 kPa and total molar enthalpy changes from -55000 to 110000 J/mol. Once again the results of these model and CMG Winprop are very close.

Table 4-9: Composition and component properties for Example 3

Component Name	Mole fraction	Tc (K)	Pc (kPa)	ω
H_2O	0.3333	647.3	22048.32	0.344
C1	0.3333	190.6	4599.93	0.008
C40	0.3334	934.3	800.43	1.259

Component Name	Cp1	Cp2	Cp3	Cp4
H_2O	33.75536	-0.00594	2.24E-05	-9.96E-09
C1	36.14727	-0.05111	0.000221	-1.82E-07
C40	-24.03340	2.96444	-0.001120	0

Binary Interaction Coefficients	H_2O	C1	C40
H_2O	0		
C1	0.4907	0	
C40	0.4800	0.125465	0

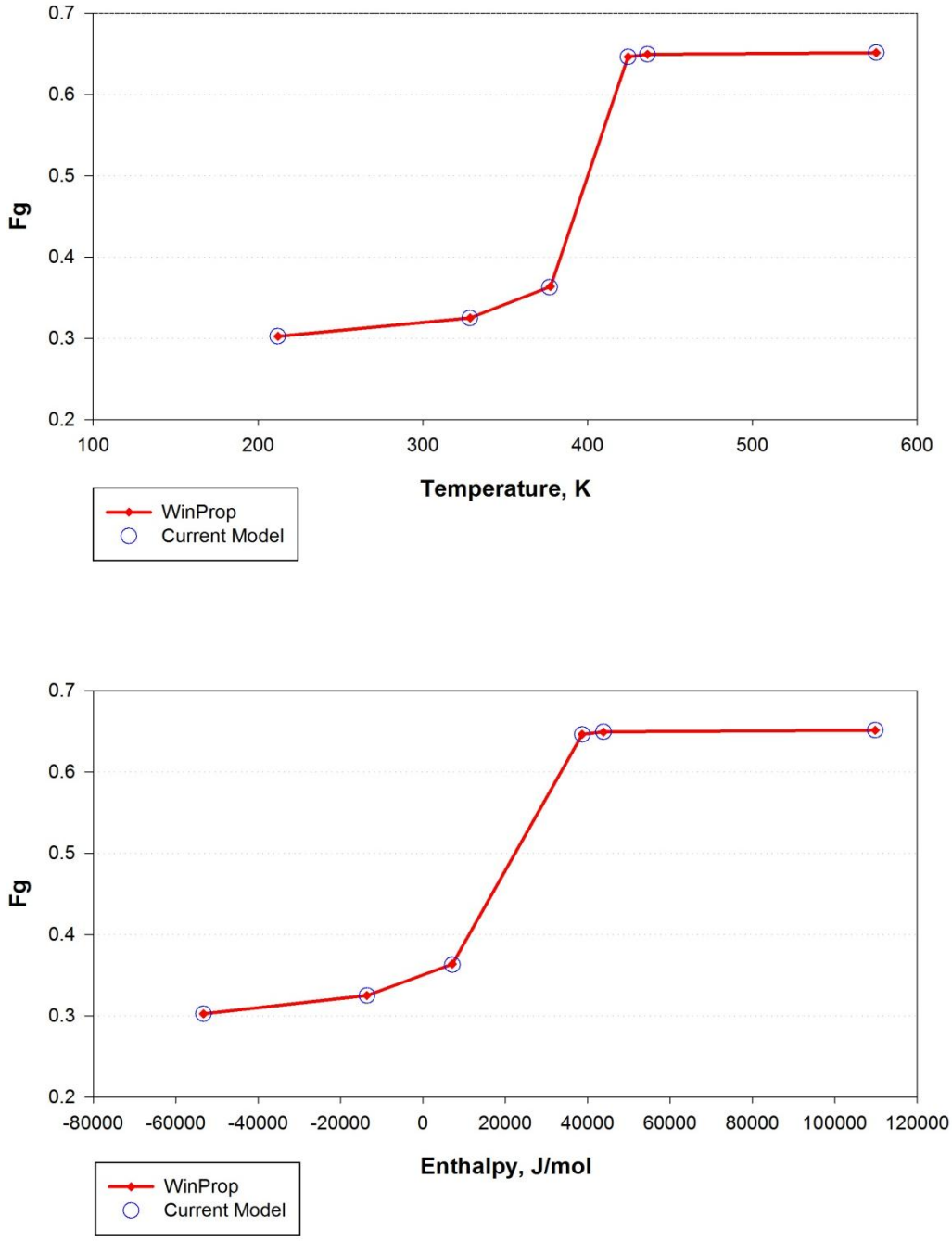

Figure 4-16: Variation of gas phase mole fraction versus temperature and total molar enthalpy

4.8.1.6 Example 3: mixture (Water, C1, C40) vs. PVTSIM

The same mixture as example 3 is used and it was tested the same pressure and feed composition. Figure 4-17 and 4-18 show variation of temperature and total molar enthalpy versus vapor phase mole fraction respectively. The result shows very good agreement between the current model and Michelsen's (1987) model. The reference temperature for ideal gas enthalpy is equal to 273.15 K.

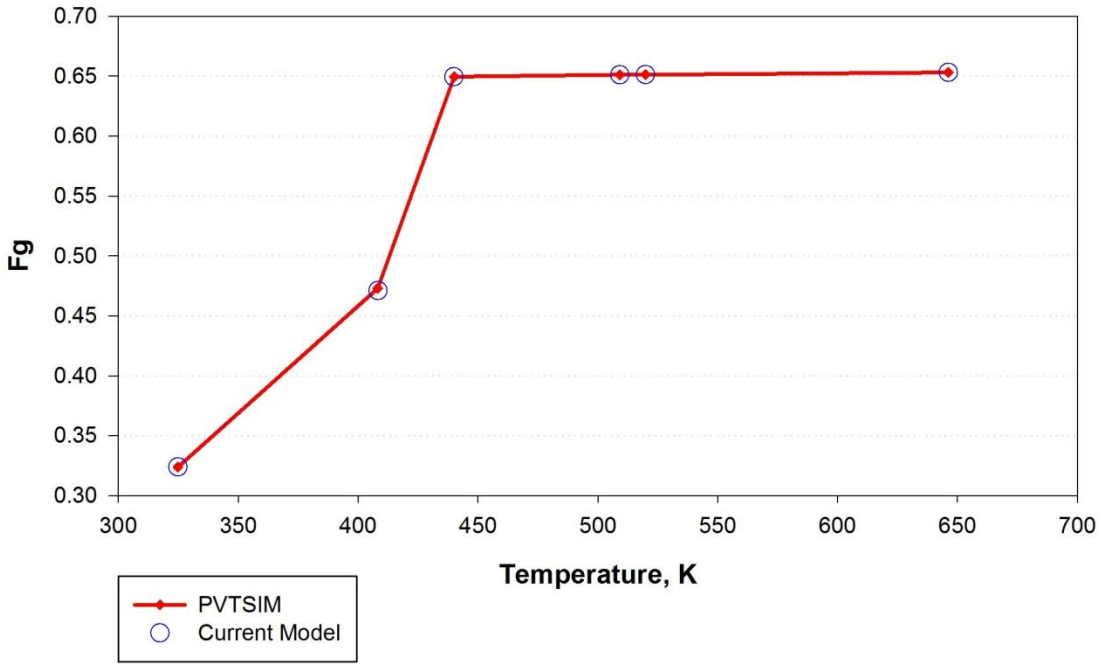

Figure 4-17: Variation of gas phase mole fraction versus temperature

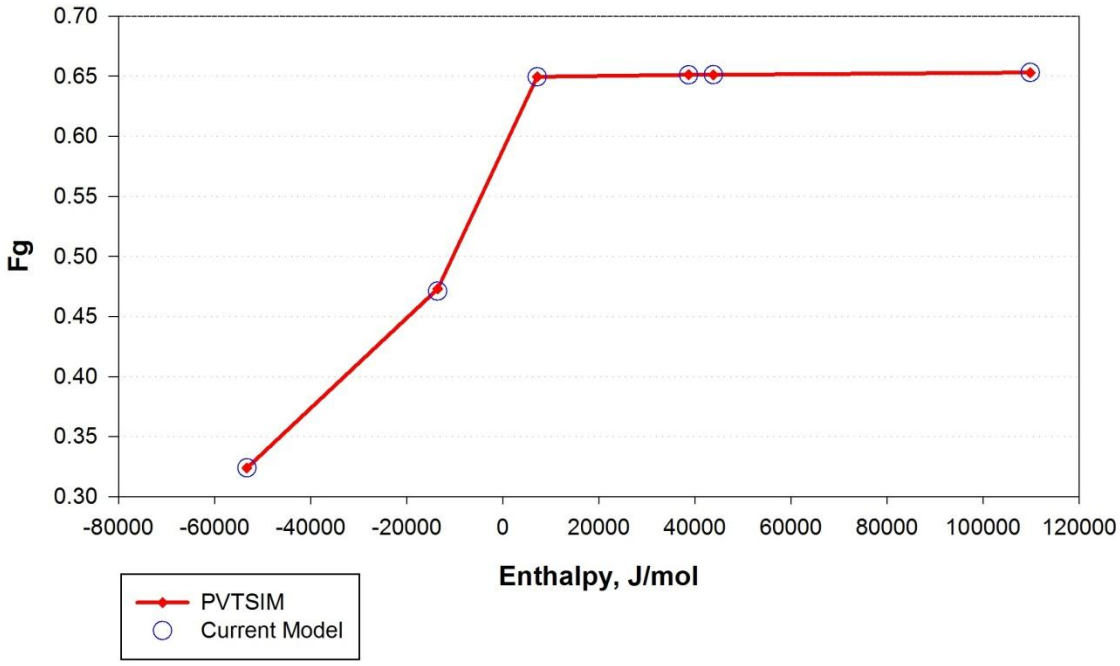

Figure 4-18: Variation of gas phase mole fraction versus total molar enthalpy

4.9 **Isenthalpic flash results and discussions**

In this section the new isenthalpic multiphase flash calculation method is used with several synthetic fluids. The synthetic mixtures are run for a wide range of total molar enthalpies at given constant pressure and feed composition. In the reservoir simulator, energy, pressure and feed composition at each grid block change with time at each Newton iteration level throughout the simulation due to injection and production of mass and energy. In thermal and hybrid processes where pure steam or combination of steam and small amount of solvent is injected into the reservoir, the global mole fraction of water component changes from its original value to values close to one in most of the reservoir grid blocks. In addition to global mole fraction, total energy of grid block also changes due to higher temperature of injected steam.

Thus several test cases were designed and tested to investigate the effect of change of global mole fraction and energy on phase splitting and temperature calculation during isenthalpic flash

calculation. In these tests the global mole fraction of water component is changing from low values to values up to 99%. This is commonly encountered in thermal simulators when hot steam is injected into the reservoir.

Another objective of these tests was to compare the robustness and speed of these method compared to the currently available algorithms such as Agarwal et al.'s model (1991). As it was mentioned in the last section this new isenthalpic flash calculation method is not sensitive to initial guess and a poor initial guess only requires more number of iteration to find the final solution. All three schemes of Agarwal et al. (1991) method are available in CMG Winprop and user has the ability to set the initial guess and also select the flash scheme. A single initial guess for temperature is used as initial guess and the sensitivity of CMG Winprop hybrid scheme to the initial guess is compared with the current algorithm.

In the other study the number of iterations for hybrid scheme of Agarwal et al. (1991) model is compared to the number of iteration of the current method. Once again the same initial guess is used for comparison between hybrid scheme of Agarwal's method (1991) and this method. The failure of each method also shows the sensitivity of these schemes to the initial guess.

It is worth mentioning that the Wilson correlation (1969) was used for initialization of equilibrium ratios in all comparison tests for the current isenthalpic flash calculation method. However any method of initialization can be implemented in the algorithm. Soave modification of Redlich and Kwong equation of state (1972) was used in all of the current studies.

4.9.1 *Case 1: mixture (H_2O/C1/C6/Bitumen)*

The synthetic mixture consists of water and three hydrocarbon and fluid properties are extracted from Gates et al. (2007) with few modifications and are presented in Table 4-10. Table 4-10 also presents the ideal gas specific heat capacity coefficients of each component. The ideal gas specific heat capacity coefficients are taken from CMG Winprop package. This mixture was tested for a range of total molar enthalpies and it was compared with CMG Winprop for

accuracy, speed and its sensitivity to initial guess. The global mole fraction of water component was changed twice and the mixture was tested for different ranges of total molar enthalpies.

Table 4-10: Composition and component properties for Case 1

Component	MW	Pc(kPa)	Tc(K)	ω	Mole fraction
H_2O	18.015	22088.85	647.37	0.344	0.9000
C1	16.043	4600.16	190.60	0.008	0.0002
C6	86.178	3289.00	507.40	0.275	0.0030
BITUMEN	570.000	999.06	976.00	1.124	0.0968

Component	C_{P1}	C_{P2}	C_{P3}	C_{P4}
H_2O	34.49058	-0.01426	4.73E-05	-3.57E-08
C1	37.93011	-0.06841	0.000272	-2.39E-07
C6	-5.96761	0.53462	-0.000200	0
BITUMEN	-19.84750	3.02670	-0.001140	0

Binary Interaction Coefficients	H_2O	C1	C6	BITUMEN
H_2O	0			
C1	0.4907	0		
C6	0.4800	0.025345	0	
BITUMEN	0.4800	0.132875	0.048416	0

4.9.1.1 Test 1: mixture with $Z(H_2O) = 90\%$

In the first test water with global mole fraction of 90% was used and the results of the current simulator are compared against hybrid scheme of Agarwal et al.'s model (1991) from CMG Winprop. There is a very good match between the results of two simulators. The initial guess equal to 288.15 K was used, pressure equal to 500 kPa and the simulation was run for a wide range of enthalpies from -46000J/mol to 26000 J/mol with 4000 J/mol increment . Fluid mixture changes from WL region to WLV region and after that to LV and single vapor phase V. As

shown in Figure 4-19, three phase region happens in a relatively narrow window and both methods were able to capture it. In Figure 4-20 the number of iterations to convergence for both simulators with the same initial guess is presented. In all tested enthalpies the current model takes fewer number of iteration except for two points.

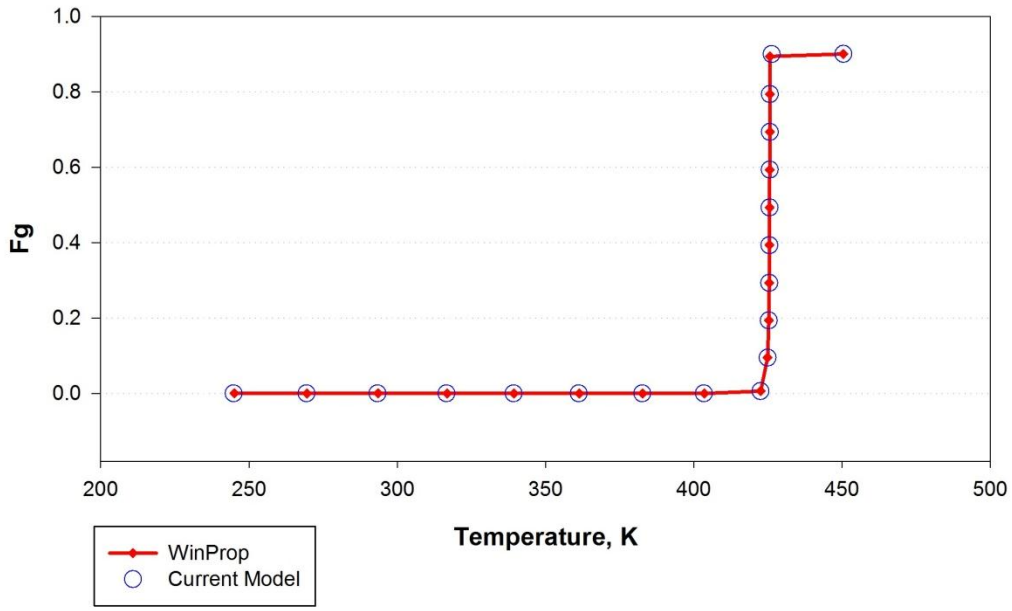

Figure 4-19: Variation of gas phase mole fraction versus temperature

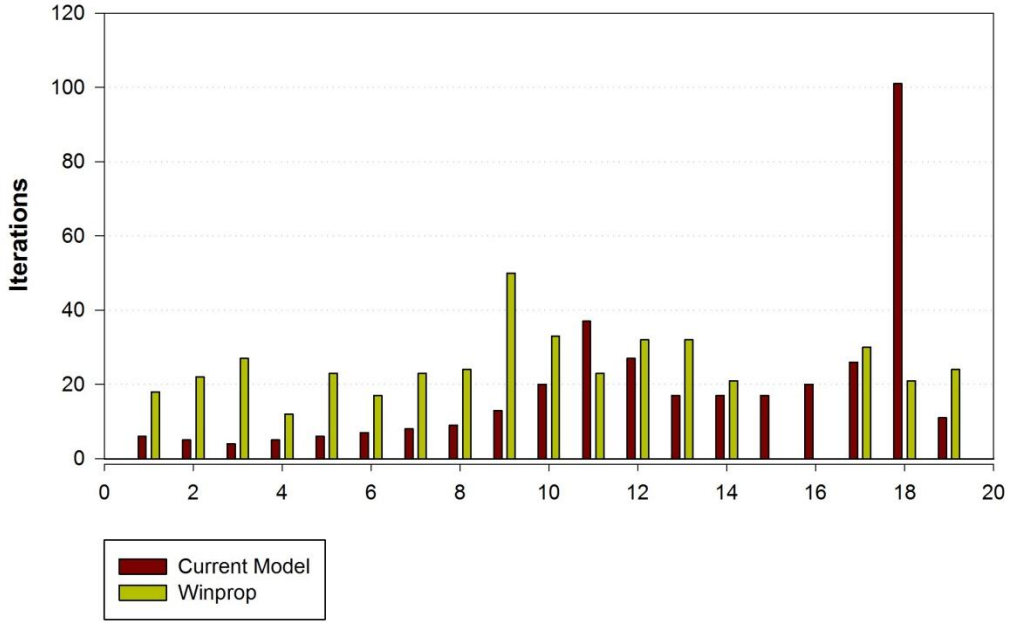

Figure 4-20: Number of iterations at each point of this study versus CMG Winprop

4.9.1.2 Test 2: mixture with Z(H_2O) = 98.982%

In the second test, global mole fraction of water was increased to 98.982% and global mole fraction of bitumen was decreased to 0. 698%. Global mole fraction of C1 and C6 and operating pressure remained unchanged. The synthetic mixture was tested against the range of total enthalpies from -40000 J/mol to 32000 J/mol with 6000 J/mol increment. This case is more difficult than the first case due to higher global mole fraction of water and existence of traces of low volatile hydrocarbon in the mixture. In this situations three phases equilibrium occurs in a very narrow window of temperature.

Figure 4-21 shows the results of the current model versus the results of CMG Winprop. The results show a good agreement between two methods. Sensitivity of both model to initial guess of both models to calculate phase splitting and temperature calculation was tested. The hybrid scheme of Agarwal et al. (1991) was selected in CMG Winprop.

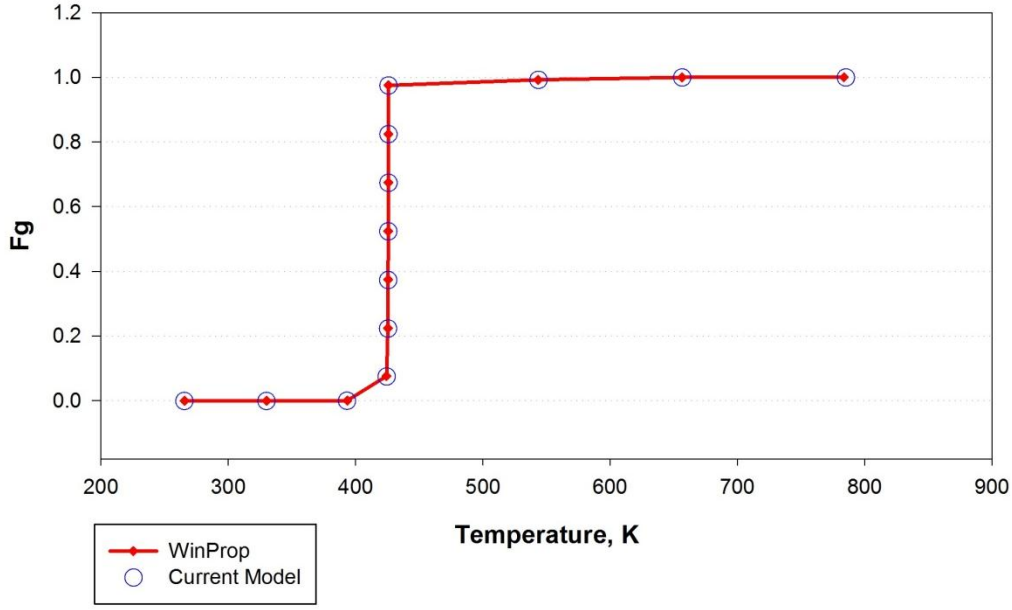

Figure 4-21: Variation of gas phase mole fraction versus temperature

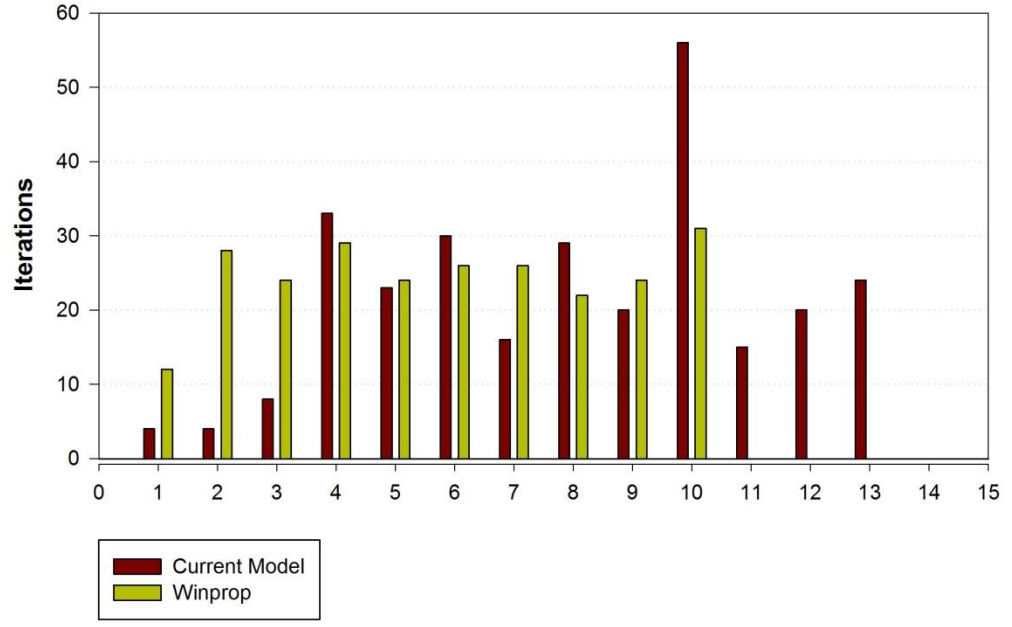

Figure 4-22: Number of iterations at each point of this study versus CMG Winprop

In this test case, hybrid method of Agarwal et al. (1991) was not able to find the solution for the last three points with the initial guess of 288.15 K. However the current model shows no sensitivity to initial guess. In terms of number of iteration at some points the current model has better performance and at some points CMG Winprop performs less number of iterations to reach to the solution. These are only for the points that CMG Winprop was able to converge to the solution with the hybrid scheme.

4.9.2 *Case 2: mixture (H_2O/C8/C13/C24/C61)*

In this case fluid mixture information was extracted from example 5-6 of Brantferger's dissertation (1991) and it was modified for use in this comparison. The mixture contains water and four other components. Fluid properties and ideal heat capacity coefficients are presented in Table 4-11. The given pressure was equal to 500 kPa. This fluid mixture was also tested over a wide range of total molar enthalpies and phase identification and splits are calculated by the current method. All of hydrocarbon components have low equilibrium ratios and have low volatility. Therefore the three phase equilibrium happens in a very narrow boiling point region. In fact the three phase equilibrium region is similar to a water and dead oil mixture system and such systems are most difficult cases to handle, but unfortunately these are the dominant cases in thermal processes.

All of the binary interaction coefficients are equal to zero for this example. The robustness of the current method and also its sensitivity to the initial guess were investigated for this mixture. Brantferger (1991) used this fluid mixture as one the test cases for their thermal compositional simulator.

Table 4-11: Composition and component properties for Case 2

Component	MW	Pc(kPa)	Tc(K)	ω	Mole fraction
H_2O	18.015	22120.00	647.370	0.344	0.6904
C8	116.000	3482.00	575.780	0.400	0.1379
C13	183.000	2337.00	698.000	0.840	0.0868
C24	337.000	1207.00	821.300	1.070	0.0629
C61+	858.000	779.00	1010.056	1.330	0.0220

Component	C_{P1}	C_{P2}	C_{P3}	C_{P4}
H_2O	32.240	0.001924	0.00001055	-3.596E-09
C8	-1.23E+01	6.65e-1	-2.52e-4	0
C13	-5.080	9.97e-1	-4.14e-4	0
C24	-5.690	1.840000	-7.64e-4	0
C61+	0.123	4.750000	-1.95e-3	0

4.9.2.1 Test 1: mixture with $Z(H_2O) = 69.04\%$

In the first test, the same global mole fraction as original data was used. Water global mole fraction is equal to 69.04% and the mixture was tested for a wide range of molar enthalpies. In this case total molar enthalpy varies from -20000 J/mol to 0.0 J/mol with 4000 J/mol increment and from 0.0 J/mol to 66000 J/mol with 6000 J/mol increment and pressure is equal to 500 kPa. Both simulators were able to find the solution with the initial guess of 288.15 K for this case. The hybrid method of Agarwal (1991) was used in this test. Figure 4-23 shows the vapor molar fraction versus the temperature and the fluid mixture passes through the LW/LVW/LV regions. The results of two methods show very close match.

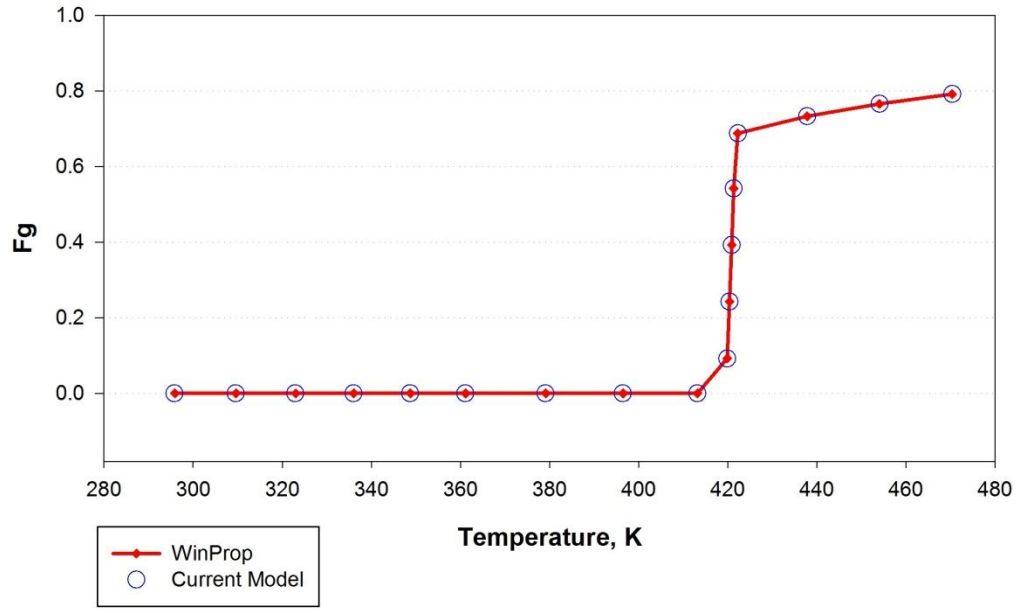

Figure 4-23: Variation of gas phase mole fraction versus temperature

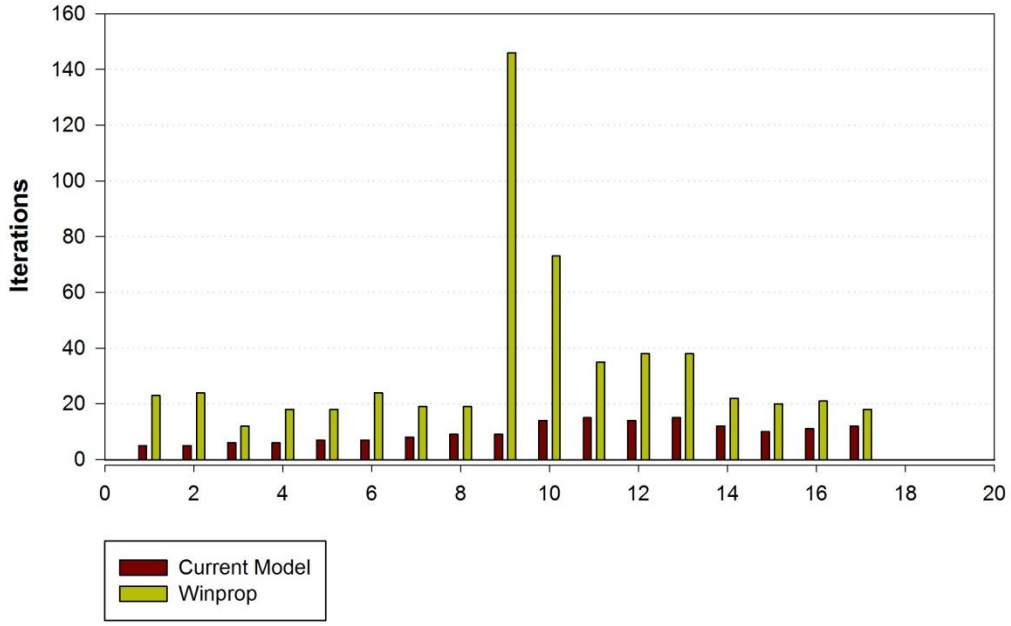

Figure 4-24: Number of iterations at each point of this study versus CMG Winprop

The numbers of iteration with the initial guess of 288.15 K for these two simulators are plotted in the Figure 4-24 and the current model has less number of iterations in all cases. It is very important to consider that the current model does not use any stability analysis and Agarwal's method (1991) is based on the stability test. Therefore, if the number of iteration for Agarwal's method (1991) is higher the number of stability test is also higher. Therefore each Newton's iteration of Agarwal's method computationally is more expensive than the developed method

4.9.2.2 Test 2: mixture with Z(H_2O) = 96.904%

In the second test, the global mole fraction for water component was increased and the global mole fractions of other components were decreased to 1.379%, 0.868%, 0.629%, and 0.22% respectively. Pressure remained unchanged and total molar enthalpy varies from -30000 J/mol to 46000 J/mol with 6000 J/mol increment. This case is more difficult than the first test case and it can seriously challenge both simulators. Figure 4-25 shows the phase molar fraction versus the temperature for this case. The results are almost identical and VLW phase region happens in a very narrow window of temperature.

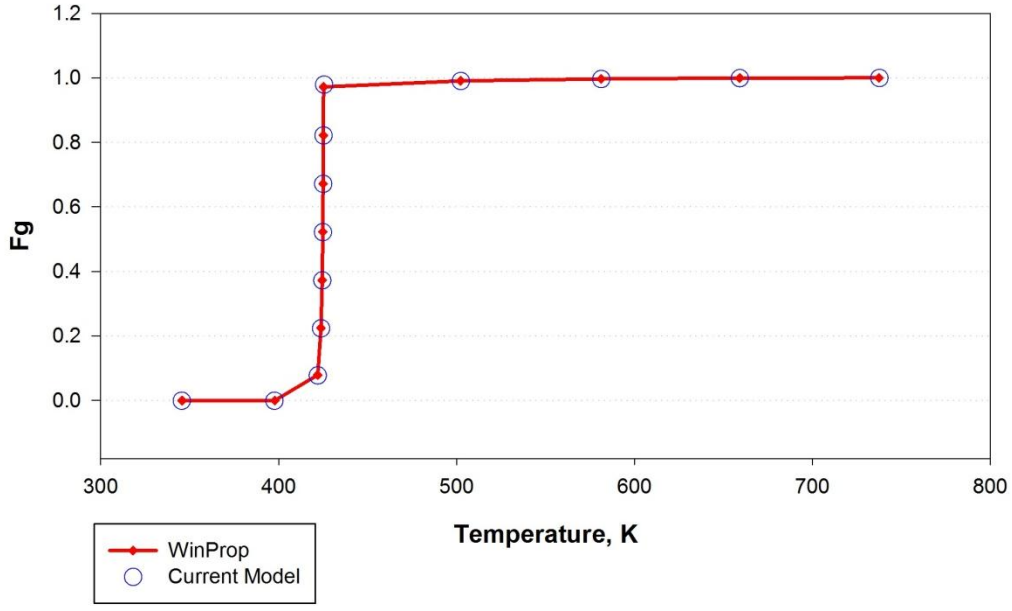

Figure 4-25: Variation of gas phase mole fraction versus temperature

In this case the hybrid method of Agarwal et al. (1991) was not able to converge for last seven points and the Newton method with better initial guess was required. This case is more challenging and difficult to converge to the solution. However the current method was able to handle all the test points with the same initial guess equal to 288.15 K. The Current model takes fewer number of iteration for all the converged cases in comparison with the Agarwal et al.'s hybrid method (1991).

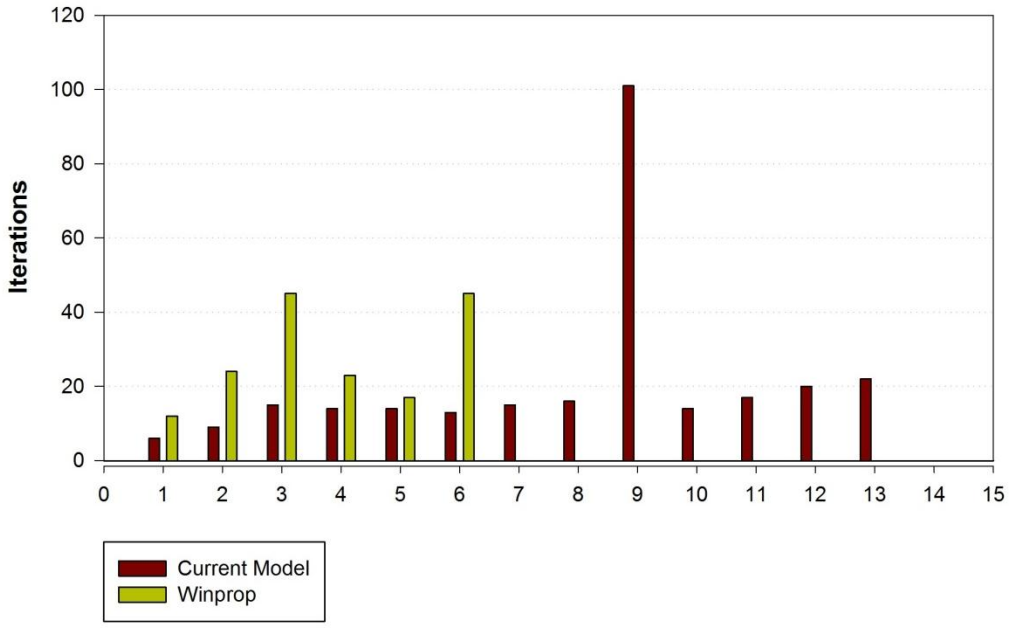

Figure 4-26: Number of iterations at each point of this study versus CMG Winprop

4.9.3 *Case 3: mixture (H_2O/C6/C10/C15)*

In this case, the fluid mixture was extracted from Case 3 of chapter 4 of Varavei's dissertation (2009). The fluid properties and ideal heat capacity coefficient for each component is presented in the Table 4-12 and it is taken from CMG Winprop package. The binary interaction coefficients and global mole fractions of each component in the feed are also presented in Table 4-12.

Table 4-12: Composition and component properties for Case 3

Component	MW	Pc(kPa)	Tc(K)	ω	Mole fraction
H_2O	18.015	22047.230	647.3	0.344000	0.790
C6	86.178	3288.847	507.5	0.275040	0.002
C10	134.000	2534.013	622.1	0.443774	0.003
C15	206.000	1849.090	718.6	0.651235	0.205

Component	C_{P1}	C_{P2}	C_{P3}	C_{P4}
H_2O	33.75536	-0.00594	2.24E-05	-9.96E-09
C6	-5.95528	0.533519	-0.0002	0
C10	-25.1949	0.859989	-0.00035	0
C15	-31.5697	1.291896	-0.00052	0

Binary Interaction Coefficients	H_2O	C6	C10	C15
H_2O	0			
C6	0.48	0		
C10	0.48	0.002866	0	
C15	0.48	0.010970	0.002657	0

Similar to the last examples, global mole fraction of water component in the mixture is changed and the mixture was tested for a wide range of total molar enthalpies.

4.9.3.1 Test 1: mixture with $Z(H_2O) = 79.0\%$

In the first test case, global mole fraction of water is equal to 79% and the mixture was tested at given pressure equal to 500 kPa. The mixture is in LW region at low enthalpies and by increasing the total molar enthalpy, the vapor phase appears and three phase region VLW happens. As energy of system increases furthermore, water phase disappears and two phase equilibrium VL occurs for a wide range of temperature. As it is shown in Figure 4-27 results of the current simulator is in good agreement with the CMG Winprop.

In this case both simulator ware able to find the phase splitting at all energies and they are not sensitive to the initial guess which was equal to 288.15 K. In this example, the current algorithm takes less number of iteration compare to hybrid method of Agarwal et al. (1991) except for last two points. The total molar enthalpy varies from -47000 J/mol to 55000 J/mol with 6000 J/mol increment.

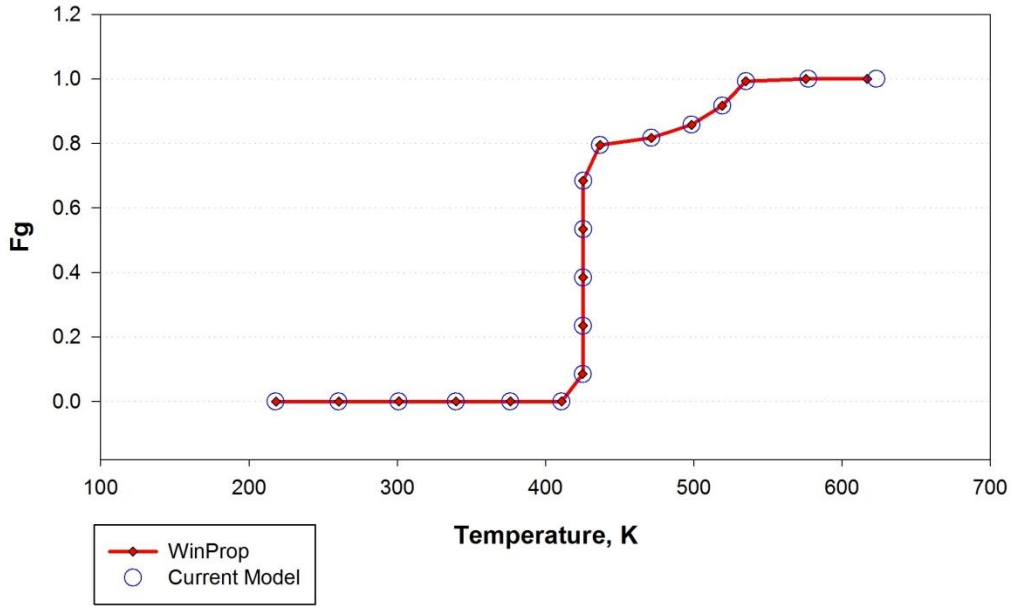

Figure 4-27: Variation of gas phase mole fraction versus temperature

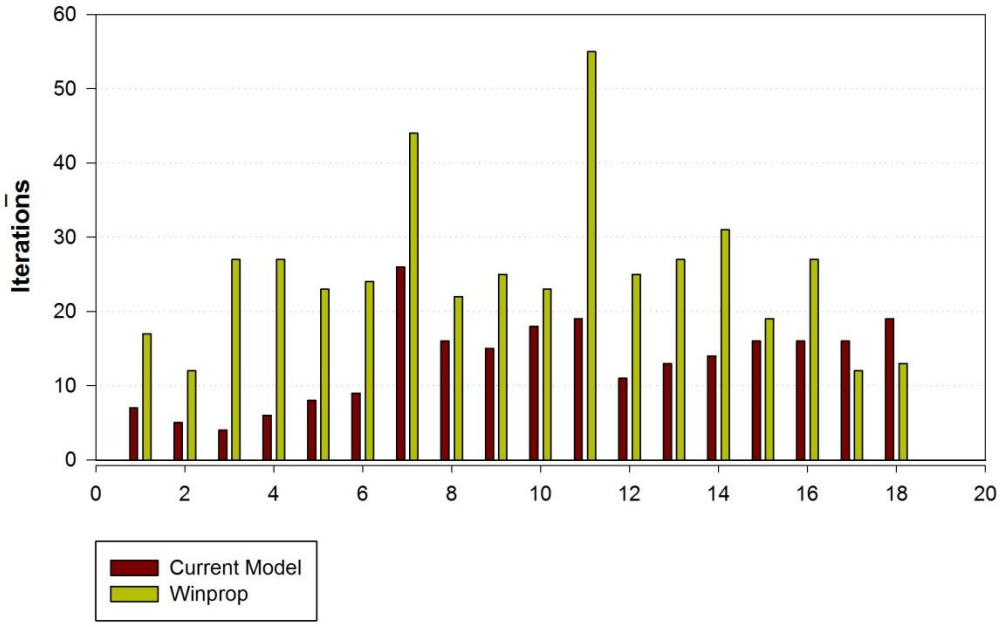

Figure 4-28: Number of iterations at each point of this study versus CMG Winprop

4.9.3.2 Test 2: mixture with $Z(H_2O)$ = 99.0%

The same mixture but with higher global mole fraction for water phase is tested in this case. Global mole fraction of C15 was decreased to 0.5% and global mole fraction of C6 and C10 remained unchanged. The same given pressure and initial guess for temperature is used. The total molar enthalpy varies from -47000 J/mol to 19000 J/mol with 6000 J/mol increment. The CMG Winprop hybrid scheme failed to converge with this initial guess for last three points and their second scheme with better initial guess was used. The results of two simulators are compared in Figure 4-29. The results are very close except for one point (the fifth point with total enthalpy equal to -23000 J/mol). The current model shows three phase system VLW with temperature equal to 423.5416 K, however the hybrid model of CMG Winprop shows two phase LW region and with temperature equal to 420.4007 K. The current method and CMG Winprop hybrid method converged to the solution with 29 and 98 iterations respectively.

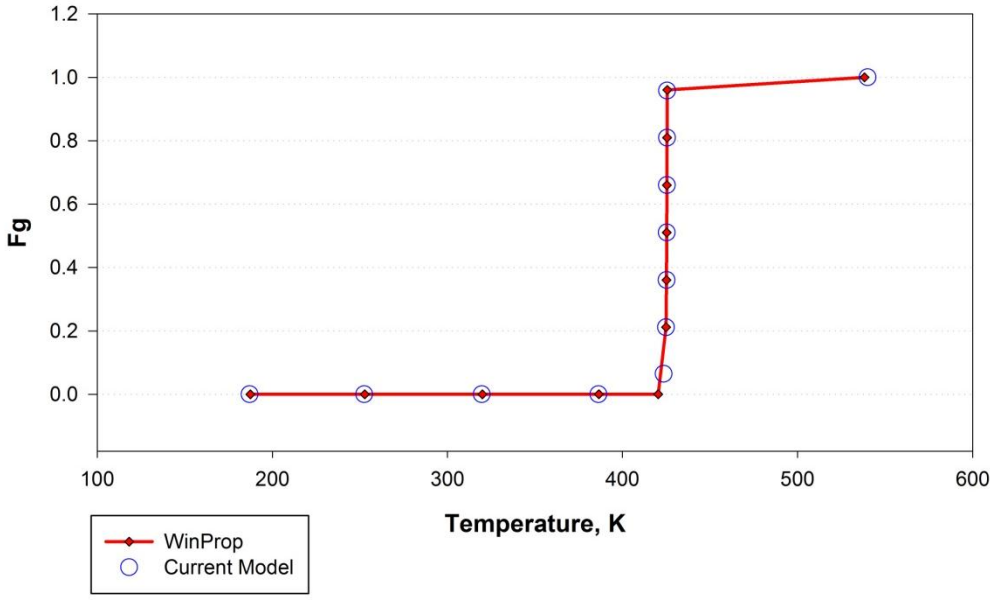

Figure 4-29: Variation of gas phase mole fraction versus temperature

The results of this special point are reported in Table 4-13. CMG Winprop scheme 2 with better initial guess was used to check the solution of isenthalpic flash calculation at this point and the final solution was similar to the result of current model. In fact vapor phase appears at temperature equal to 423.5493 K. This enthalpy is close to the phase boundary enthalpy and these situations are usually difficult to converge.

Table 4-13: Phase fraction of three different schemes

Model	Total Molar Enthalpy, J/mol	Temperature, K	Phase mole fraction			Iteration
			W	L	V	
Current	-23000	423.5416	.9294	.0062	.06444	29
Winprop Hybrid	-23000	420.4007	.9302	.0698	.000	98
Winprop Scheme 2	-23000	423.5493	.9289	.0062	.06486	42

This example shows that the current model was able to capture the phase appearance very close to boundary. Figure 4-30 shows results of current model and CMG Winprop. In this plot the vapor phase fraction for the fifth point is taken from the second scheme. The number of iteration for the current method and CMG Winprop hybrid's scheme are plotted in Figure 4-31. The current model takes fewer numbers of iteration to converge with the 288.15 K initial guess for temperature compare to CMG Winprop hybrid's scheme.

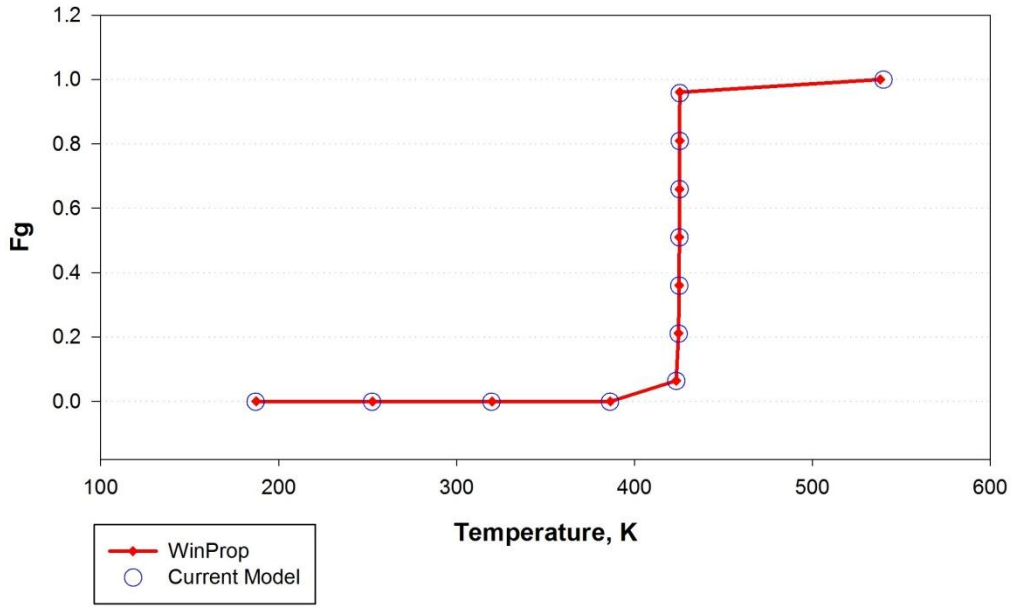

Figure 4-30: Variation of gas phase mole fraction versus temperature

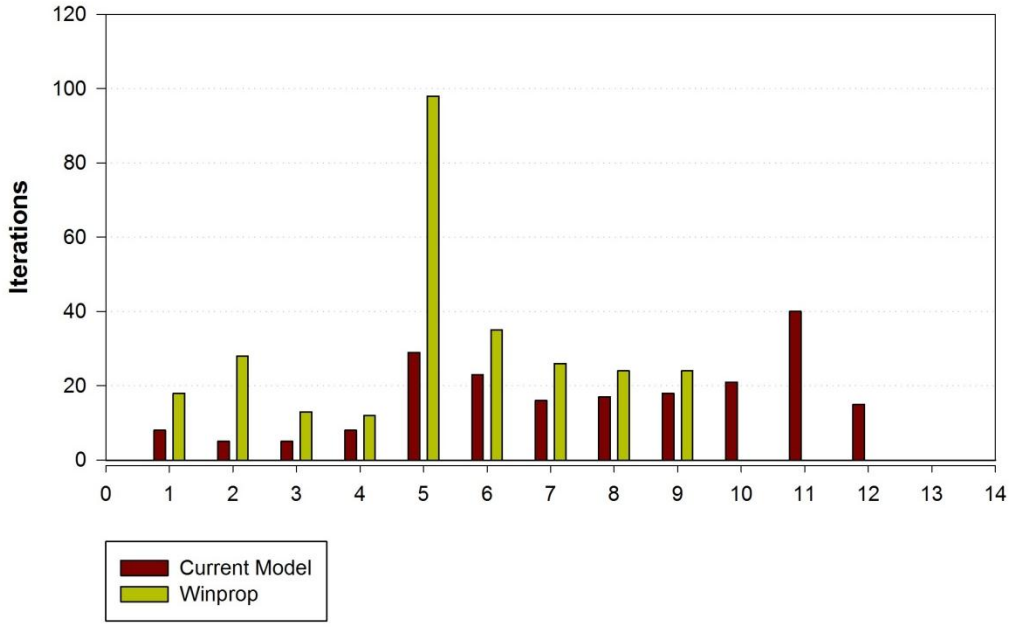

Figure 4-31: Number of iterations at each point of this study versus CMG Winprop

Chapter Five: **SIMULATOR VALIDATION AND VERIFICATION**

The purpose of this chapter is to verify and validate the results of this numerical simulator against the well-known analytical problems. In some cases where there is no analytical model available, this simulator is tested against the commercial reservoir simulators or standard published problems like the Aziz's et al. (1987) fourth SPE problems.

The current simulator has several functionalities and features as outlined below.

- Conductive and convective heat and mass flow
- Heat loss to overburden and underburden
- Sink/Source heaters
- Sink/Source multilayer, directional wellbore model with different well constraints;
    - BHP control
    - Rate control
- Two different PVT packages to handle thermodynamic properties of fluid
- K-Value option
- EOS option (PR or SRK EOS)

All of these features are very important in the performance of any thermal compositional reservoir simulator and they must be verified and validated before running any complex process such as ES-SAGD or SAGD.

5.1 **Case 1: Buckley-Leverett (1942) problem**

To confirm the ability of this simulator to model displacement of a non-wetting phase by a wetting phase, the simulator results were compared with the analytical solution of the Buckley-Leverett (1942) problem. The Buckley-Leverett (1942) problem is an isothermal, incompressible, two phase flow problem in a one dimensional domain and the solution is obtained by using method of characteristics. Water is injected at constant rate at one end and oil

is produced from the opposite end under constant bottom-hole pressure. This test verifies the convective mass flow feature of the simulator.

The following equations express mathematical formulations of this problem and its boundary and initial conditions;

$$\phi \frac{\partial S_w}{\partial t} + v \frac{df_w}{dS_w} \frac{\partial S_w}{\partial x} = 0 \qquad \textbf{5-1}$$

$$S_w\left(x, t=0\right) = S_{wr} \qquad \textbf{5-2}$$

$$S_w\left(x=0, t\right) = 1 - S_{or} \qquad \textbf{5-3}$$

$$f_w = \frac{1}{1 + \frac{k_{ro}}{\mu_o}\frac{\mu_w}{k_{rw}}}, \quad \theta = 0, P_c = 0 \qquad \textbf{5-4}$$

f_w is volumetric fractional flow of water phase, θ is the angle between displacement direction and the horizontal plane, P_c is the capillary pressure and v is the superficial flow velocity. By a simple mathematical procedure the location of front at any time can be calculated by the following expression;

$$x_{sw} = \frac{v}{\phi}\left(\frac{df_w}{dS_w}\right)_{S_w} t_{S_w} \qquad \textbf{5-5}$$

A case from published data was selected to validate the results of this simulator against the analytical solution of Buckley-Leverett (1942) problem. This case was chosen from Huang's Dissertation (2007). Table 5-1shows the input data of the displacement problem adapted from Huang's dissertation (2007).

As mentioned before, it is an isothermal problem; therefore water was injected at the same temperature as the initial reservoir temperature. To mimic incompressibility of the problem, compressibility of water and oleic phases are kept equal to zero and rock compressibility is very small. Figure 5-1 shows the results of the simulator versus analytical solution of Buckley-Leverett (1942) problem. There is a good agreement between them and the simulator was able to

produce the correct front location in this two phase water flooding problem. The front of numerical simulator is not as sharp as the analytical solution due to numerical dispersion plus first order upwind scheme that has been used for convective term of the conservation of mass equations.

Table 5-1: Reservoir properties for Buckley-Leverett (1942) problem Case 1

Number of grid blocks, (nx, ny, nx)	201,1,1
Dimension of grid blocks, (Δx, Δy, Δz), m	4.572E-3, 0.135, 0.135
Initial Conditions:	
Temperature, K	333.333
Pressure, kPa	551.581
Water viscosity, cp	0.860
Oil viscosity, cp	5.763
Residual oil saturation	0.200
Initial oil saturation	0.800
Irreducible water saturation	0.200
Initial water saturation	0.200
Reservoir Properties:	
Porosity	0.260
Pore volume compressibility, 1/kPa	0.000
Permeability, md	100.000
Well Conditions:	
Injection temperature, K	333.333
Water injection rate, PV/day	0.005
Producer BHP, kPa	413.685
Relative permeability constants:	
Oleic phase relative permeability end point	0.8
Oleic phase relative permeability exponent	2.0
Aqueous phase relative permeability end point	0.3
Aqueous phase relative permeability exponent	2.0

Fluid properties for Buckley-Leverett (1942) problem from Huang's dissertation (2007) are presented in Table 5-2;

Table 5-2: Fluid properties for Buckley-Leverett (1942) problem for Case 1

Component	MW	Density(kg/m^3)
H2O	18.015	712.260
OIL	400.000	586.160

Figure 5-1 shows a good agreement between the results of this simulator against the analytical solution at different times.

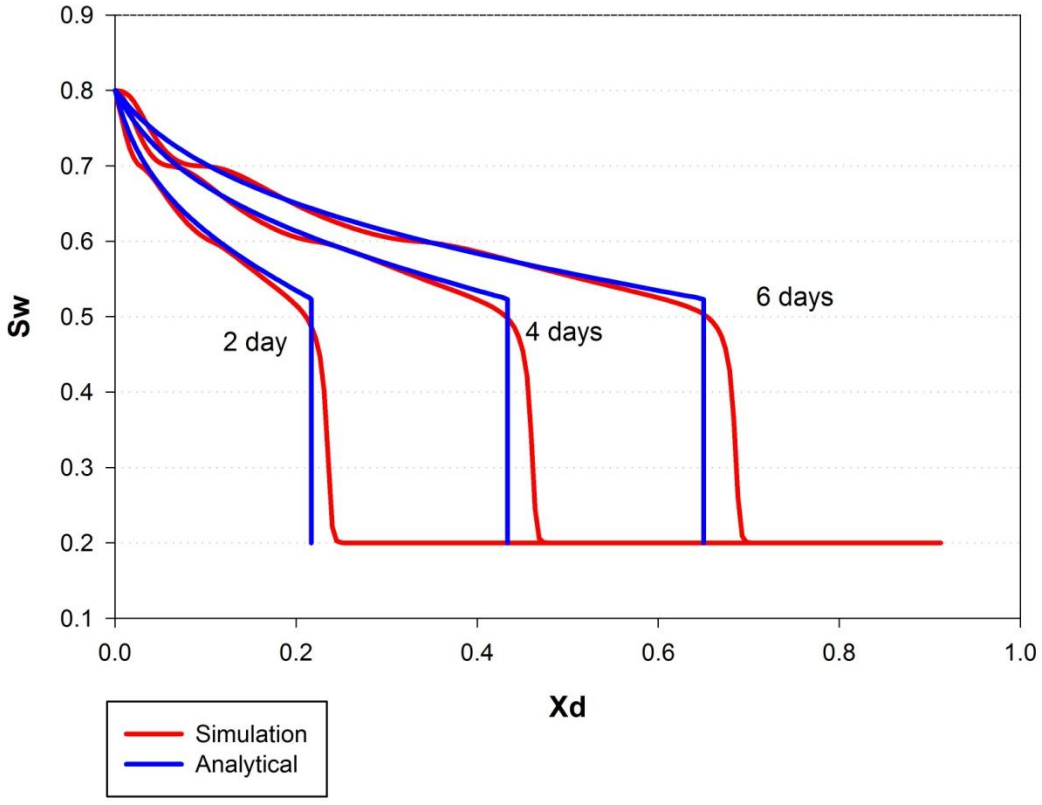

Figure 5-1: Numerical and analytical solution of Buckley-Leverett (1942) problem for Case 1

5.2 **Case 2: Lauwerier (1955) problem**

Heat loss to overburden and underburden has a direct impact on the energy efficiency of thermal processes such as SAGD, CSS and steam flooding. In this simulator Vinsome and Westerveld semi-Analytical model (1980) were used to model heat loss. In their original paper, Vinsome and Westerveld (1980) verified their model against the Lauwerier (1955) problem. It is one of the standard problems to validate convective and conductive heat flow of simulator and heat loss.

Lauwerier (1955) problem is a two dimensional problem of displacement of cold oil by hot water within a permeable zone. They solve conservation of energy equation for this problem under the following assumptions;

- Constant porosity, permeability, and thickness
- Thermal conductivity only in vertical direction
- Thermal conductivity of cap-rock and reservoir are equal
- Instantaneous thermodynamic equilibrium
- Constant specific heat of the fluids and reservoir rock

Conservation of energy in water layer is expressed as;

$$h_{pz}\rho_1 C_{p1}\frac{\partial T_1}{\partial t} + h_{pz} v \rho_w C_{pw}\frac{\partial T_1}{\partial x} - q_{loss} = 0 \qquad \textbf{5-6}$$

Where, h_{pz} is half of thickness of water bearing layer. Conservation of energy for overburden or oil bearing layer is expressed by;

$$\kappa_c \frac{\partial^2 T_2}{\partial z^2} = \rho_2 C_{p2}\frac{\partial T_2}{\partial t} \qquad \textbf{5-7}$$

These two equations are coupled by heat loss term in the first equation;

$$q_{loss} = \kappa_c \left.\frac{\partial T_1}{\partial z}\right|_{z=h_{pz}} \quad \textbf{5-8}$$

The boundary and initial conditions of this problem are;

$$T_1(x, t=0) = T_1(z, t=0) = T_{res} \quad \textbf{5-9}$$

$$T_1(x=0, t) = T_{inj} \quad \textbf{5-10}$$

By solving these two equations they developed an analytical solution for this problem as:

$$T_D = \frac{T_1 - T_{inj}}{T_{inj} - T_{ini}} = erfc \frac{X_D}{2\sqrt{Y_D(\tau_D - X_D)}} U(\tau_D - X_D) \quad \textbf{5-11}$$

Where;

$$X_D = \frac{\kappa_c x}{{h_{pz}}^2 v \rho_w C_{pw}} \quad \textbf{5-12}$$

$$\tau_D = \frac{\kappa_c t}{{h_{pz}}^2 \rho_1 C_{p1}} \quad \textbf{5-13}$$

$$Y_D = \frac{\rho_1 C_{p1}}{\rho_2 C_{p2}} \quad \textbf{5-14}$$

$$\rho_1 C_{p1} = (1-\phi)\rho_r C_{pr} + \phi(S_w \rho_w C_{pw} + S_o \rho_o C_{po}) \quad \textbf{5-15}$$

$$\rho_2 C_{p2} = (1-\phi)\rho_r C_{pr} + \phi\left(S_w \rho_w C_{pw} + S_o \rho_o C_{po}\right) \quad \textbf{5-16}$$

$U(\tau_D - X_D)$ is the unit step function which is equal to unity if $\tau_D > X_D$, otherwise zero. To validate results of this simulator against the analytical solution, two cases were selected. The first case is extracted from Brantferger dissertation (1991) and the second case from Varavei's dissertation (2009).

Figure 5-2 shows the temperature versus distance at different times of the solution for Lauwerier (1955) problem. The result shows a good agreement between the analytical and numerical computation of temperature profile and it verifies the implementation of Vinsome and Westerveld (1980) semi-analytical heat loss method.

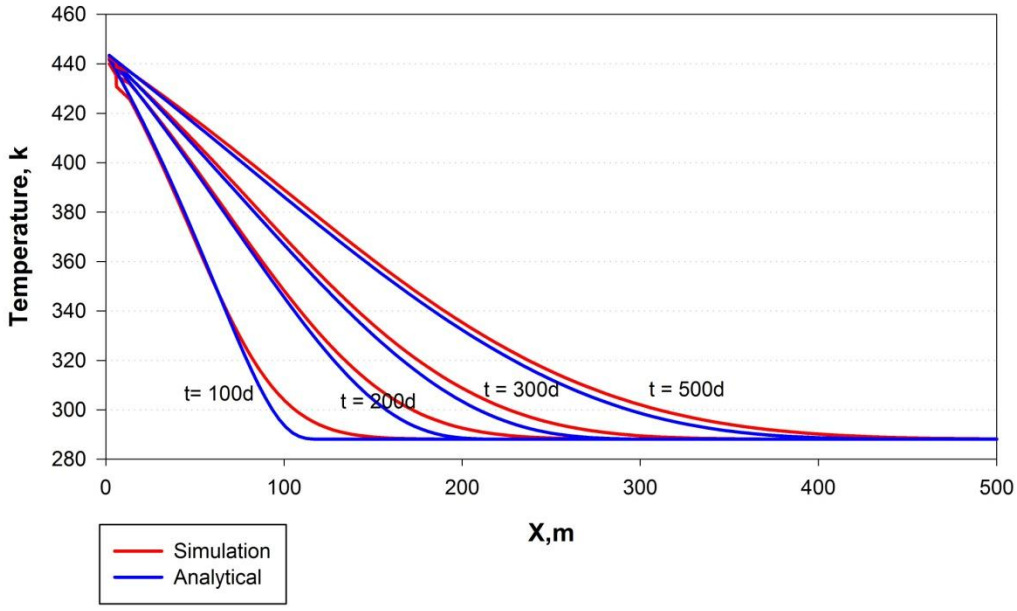

Figure 5-2: Numerical and analytical solution for Lauwerier (1955) problem Case 2, example 1

Table 5-3 shows the input data for oil and reservoir properties which is adopted from Brantferger dissertation (1991).

Table 5-3: Reservoir properties for Lauwerier (1955) problem

Number of grid blocks, (nx, ny, nx)	201,1,1
Dimension of grid blocks, (Δx, Δy, Δz), m	3.810, 0.305, 3.048
Initial Conditions:	
Temperature, K	288.150
Pressure, kPa	551.600
Water viscosity, cp	0.860
Oil viscosity, cp	5.763
Residual oil saturation	0.200
Initial oil saturation	0.010
Irreducible water saturation	0.200
Initial water saturation	0.990
Reservoir Properties:	
Porosity	0.260
Pore volume compressibility, 1/kPa	0.000
Permeability, md	10500.000
Cap rock thermal conductivity, kJ/m-day-K	218.000
Cap rock heat capacity, kJ/m^3-K	2350.000
Well Conditions:	
Injection temperature, K	444.444
Bottom-hole injection rate, m^3/day	0.816
Producer BHP, kPa	413.685
Relative permeability constants:	
Oleic phase relative permeability end point	0.8
Oleic phase relative permeability exponent	2.0
Aqueous phase relative permeability end point	0.3
Aqueous phase relative permeability exponent	2.0

Fluid properties for Lauwerier problem from Brantferger dissertation (1991);

Table 5-4: Reservoir fluid properties

Component	MW	Pc(kPa)	Tc(K)	ω	Oleic mole fraction
H2O	18.015	22120.000	647.370	0.344	0.000
Napoleum	16.000	4600.000	191.000	0.301	0.3978
Primol	645.800	924.000	787.150	0.540	0.6022

Varavei et al. (2009) also used Lauwerier (1955) model to verify their simulator ability to model heat loss. Table 5-5 lists the data was used in Varavei's dissertation (2009).

Table 5-5: Reservoir properties for Lauwerier (1955) problem

Number of grid blocks, (nx, ny, nx)	200,1,1
Dimension of grid blocks, (Δx, Δy, Δz), m	1.524, 3.048, 3.048
Initial Conditions:	
Temperature, K	288.150
Pressure, kPa	6894.757
Reservoir Properties:	
Porosity	0.350
Pore volume compressibility, 1/kPa	0.000
Permeability, md	10000.000
Cap rock thermal conductivity, kJ/m-day-K	218.000
Rock heat capacity, kJ/m^3-K	2350.000
Heat capacity ratio of fluid to rock	1.000
Well Conditions:	
Injection temperature, K	366.556
Injection rate, m^3/day	5.465
Producer BHP, kPa	6894.757

Figure 5-3 shows the dimensionless temperature profile of analytical solution versus the simulation results at different dimensionless times and the agreement is reasonably close and acceptable.

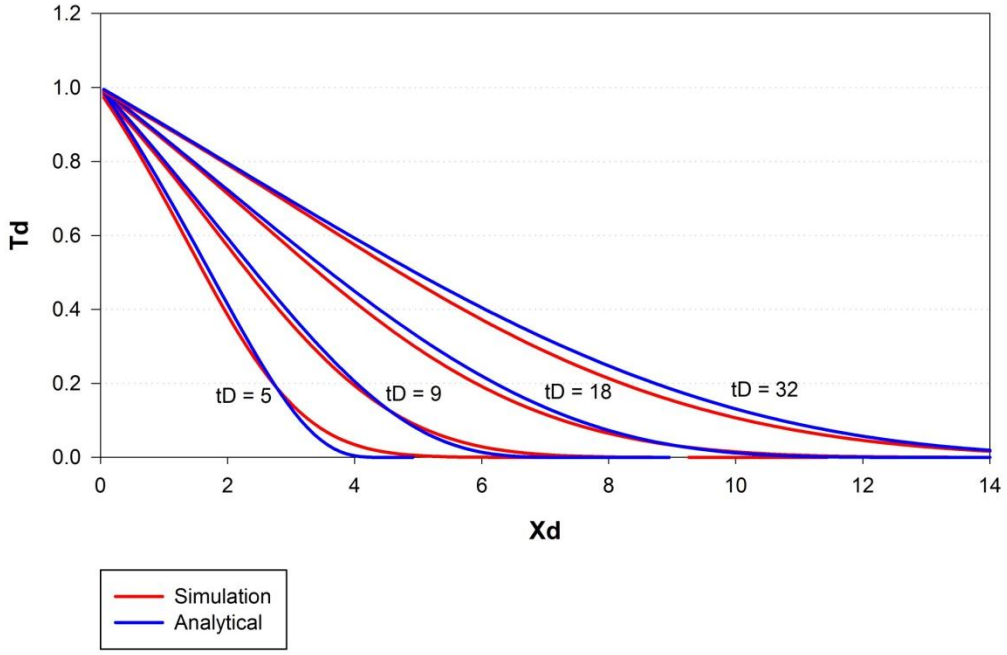

Figure 5-3: Numerical and analytical solution for Lauwerier (1955) problem Case 2, example 2

5.3 **Case 3: Fourth SPE comparative solution project: cyclic steam injection problem, Aziz et al. (1987)**

Thermal processes are complex problems and usually analytical solutions for these problems are available under very limiting conditions. In Fourth SPE comparative paper (Aziz et al. (1987)) three problems were simulated with several commercial simulators and their results were compared. In the first problem, steam is injected in three cycles into a reservoir from a vertical well and after a soaking period in each cycle, the heated oil is produced. The duration of each cycle is 365 days. Ten days for injection, one week of soaking time and 348 days of production.

It is a cylindrical model with 13 grids in r-direction and 4 grids in z-direction with different permeability in different layers. A vertical well is perforated in all four layers and it acts as both injector and producer.

Reservoir rock and fluid properties plus initial and operating condition are available in Table 5-6. The Corey type relative permeability curve is used in this simulation. Table 5-7 represents variation of dead oil viscosity versus temperature.

Table 5-6: Reservoir rock and fluid properties, initial and operating condition

Number of grid blocks, (nr, ny, nz)	13,1,4
Dimension of grid blocks, (Δr), m	0.900, 10x3.100, 12.200, 36.600
Dimension of grid blocks, (Δz), m	3.000, 6.100, 7.700, 7.600
Initial Conditions:	
Temperature, K	324.817
Pressure, kPa	517.000
Residual oil saturation w.r.t water	0.150
Initial oil saturation	0.550
Irreducible water saturation	0.450
Initial water saturation	0.450
Critical gas saturation	0.060
Residual oil saturation w.r.t gas	0.100
Oil Properties:	
Density @ SC, kgmol/m^3	1.580
Compressibility, 1/kPa	7.00E-7
Thermal expansion coefficient, 1/K	6.84E-4
Specific heat capacity, kJ/kgmol-K	1260.000
Molecular weight, kg/kgmol	600.000
Reservoir Properties:	
Porosity	0.300
Pore volume compressibility, 1/kPa	7.30E-5
Horizontal permeability, md	2000.000, 500.000, 1000.000, 2000.000
Vertical permeability, md	1000.000, 250.000, 500.000, 1000.000

Reservoir thermal conductivity, kJ/m-day-K	150.000
Cap rock thermal conductivity, kJ/m-day-K	150.000
Rock heat capacity, kJ/m^3-K	2347.000
Well Conditions:	
Injection temperature, K	505.377
Steam quality	0.700
Bottomhole injection pressure, kPa	6895.00
Maximum injection rate(CWE), m^3/day	158.987
Producer BHP, kPa	117.200
Maximum liquid production rate, m^3/day	158.987

Table 5-7: Variation of dead oil viscosity versus temperature

Temperature, K	Viscosity, cp
297.039	5780.000
310.928	1380.000
338.706	187.000
366.483	47.000
394.261	17.400
422.039	8.500
449.817	5.200
533.150	2.500

Figure 5-4 and 5-5 show the oil production rate and water production rate for all three cycles of this problem and its comparison with CMG STARS commercial simulator. The cyclic steam stimulation is a complex process and it tests and verifies not only the conductive and convective heat flow, convective mass flow and heat loss but also the ability of the wellbore model in handling combination of operating constraints.

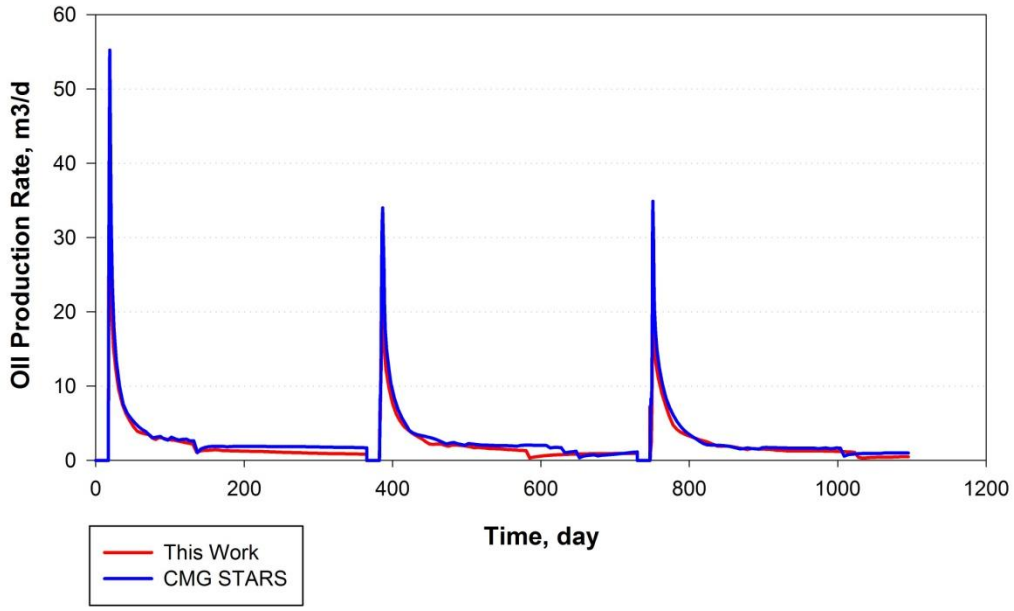

Figure 5-4: Oil production rate, SPE4-1A, this work vs. CMG STARS

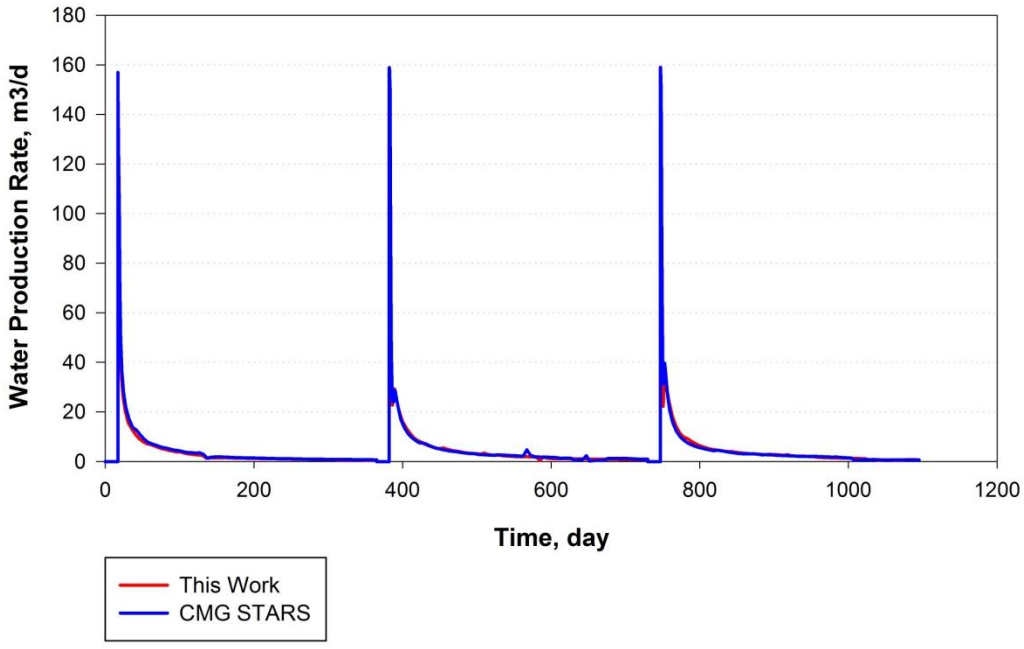

Figure 5-5: Water production rate, SPE4-1A, this work vs. CMG STARS

5.4 **Case 4: Fourth SPE comparative solution project: Steam displacement-Heavy Oil, Aziz et al. (1987)**

Displacement of non-distillable oil by steam in one-eighth element of symmetry of an inverted nine-spot pattern is simulated. Steam is injected from an injector and oil is produced from two producers. One of the purposes of this simulation was to compare the performance of different simulators in handling grid orientation effect. The nine point discretization is not available in the current simulator, therefore this model was run without this option in CMG STARS and the results of two simulators were compared. All of the fluid properties, rock properties, initial conditions, and relative permeability data are similar to the fourth SPE problem 1A (Aziz et al. (1987)). Steam is injected from bottom layer into the reservoir and oil is produced from all four layers of the edge and corner producers. The grid properties and operating conditions are listed in Table 5-8.

Table 5-8: Reservoir rock and operating condition

Number of grid blocks, (nx, ny, nz)	9,5,4
Dimension of grid blocks, (Δx), m	4.446, 7x8.891, 4.446
Dimension of grid blocks, (Δy), m	4.446, 3x8.891, 4.446
Dimension of grid blocks, (Δz), m	3.000, 6.100, 7.700, 7.600
Well Conditions:	
Injection temperature, K	505.377
Steam quality	0.700
Bottomhole injection pressure, kPa	6895.000
Maximum injection rate(CWE), m^3/day	5.962
Well radius, m	0.090
Producer BHP, kPa	117.200
Maximum liquid production rate, m^3/day	39.750, 19.875

Figure 5-6 and 5-7 compares the oil production and water production rates of this study versus CMG STARS.

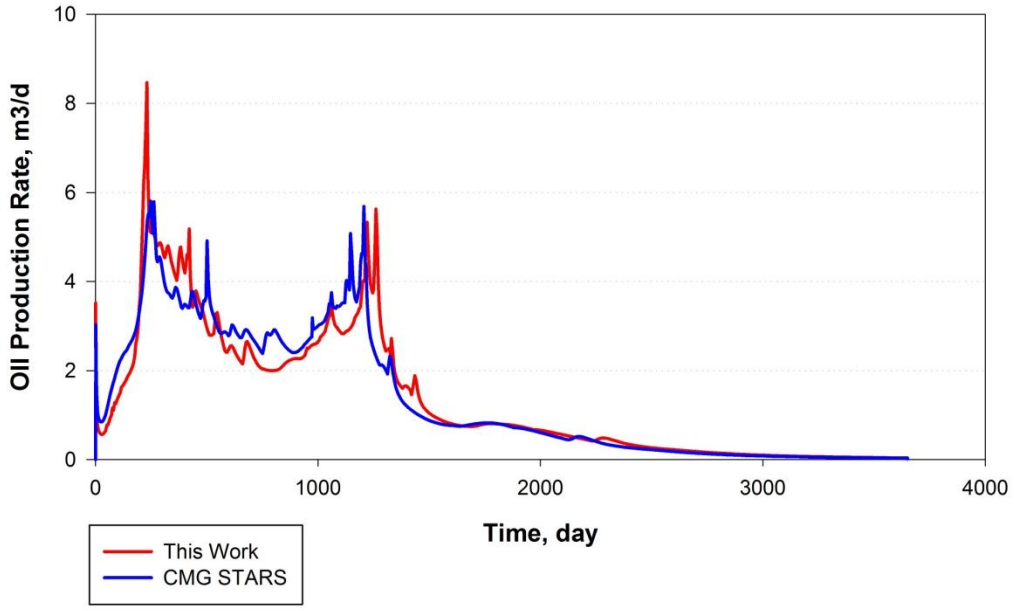

Figure 5-6: Oil production rate, SPE4-1B, this work vs. CMG STARS

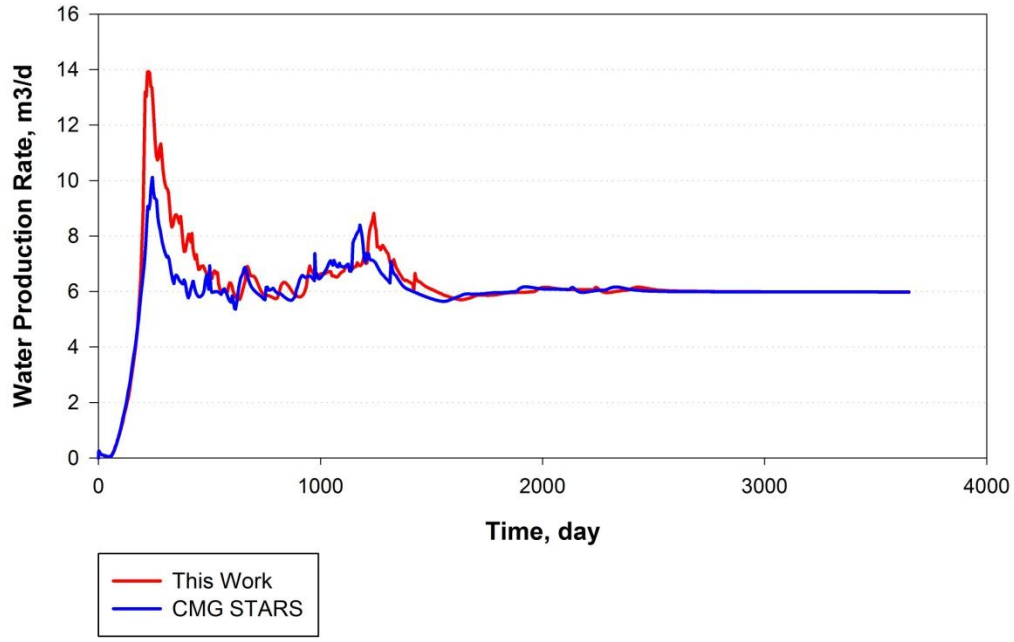

Figure 5-7: Water production rate, SPE4-1B, this work vs. CMG STARS

5.5 **Case 5: Steam-Assisted Gravity Drainage (SAGD) simulation in a 2-D model**

Simulation of SAGD process is different with the other thermal methods such as steam flooding since the major driving force is gravity instead of viscous force. In fact several driving mechanisms play role in this process and the combination of these driving forces makes a SAGD project successful and also challenging from point of view of numerical simulation.

A 2-D SAGD problem was chosen to test the capability of the current simulator in simulation of this process and the results were compared with CMG STARS commercial simulator. CMG STARS is a thermal compositional simulator and it handles thermodynamic equilibrium by using K-Values, therefore, we used the K-Value option of the current simulator in this comparison. The rock and fluid properties, operating conditions, initial conditions, and numerical properties of this model can be found in Table 5-9.

Figure 5-8 shows well configuration of a SAGD well-pair. Two horizontal wells, one on top of the other, are employed. The injector is located in layer 13 and it is perforated in 8 grids, grid number 2 to grid number 9 in x-direction. The producer is similar to the injector but it is located at layer 18. There is 5 meters vertical distance between these two wells and the producer is two meters above the base rock. Preheating process is 60 days and heaters are used to mimic this process. The heater properties can be found in Table 5-9. After preheating period is done, simulation switches to SAGD process for total simulation of 1700 days. Steam is injected at 488.15 K with the quality of 85 % with maximum injection pressure of 3500 kPa and maximum injection rate of 150 m^3/day (CWE).

The producer operates under minimum BHP equal to 500 kPa and maximum liquid rate equal to 450 m^3/day at surface condition. Figures 5-9 and 5-10 compare oil and water production rates of SAGD process between the results of this simulator and CMG STARS. The results are satisfactory and acceptable.

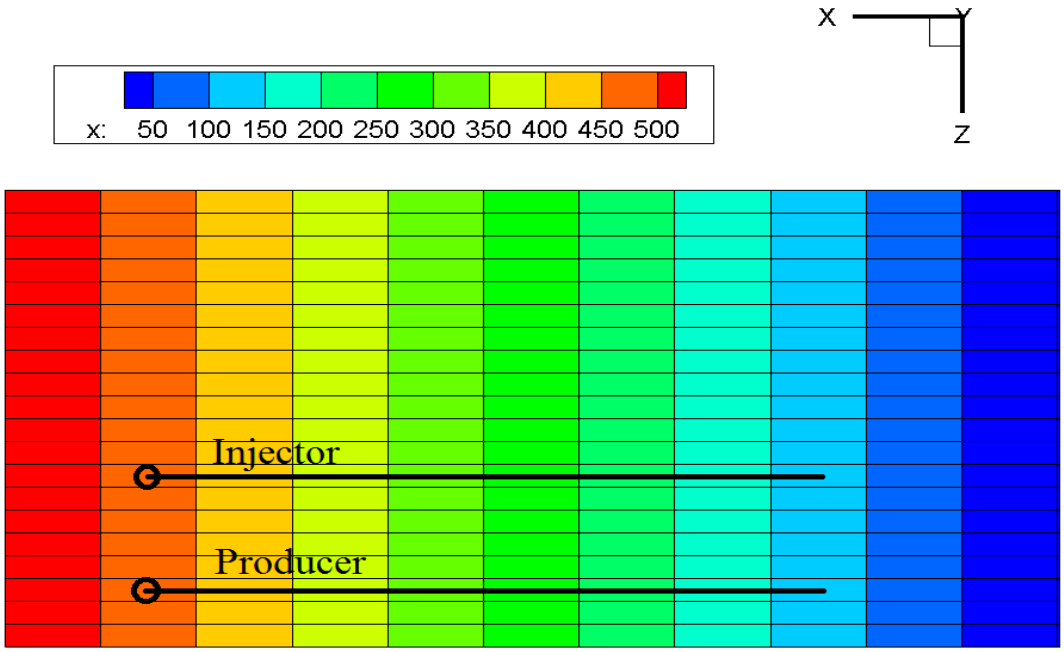

Figure 5-8: Schematic of a 2-D SAGD model with a horizontal well-pair (Injector & Producer)

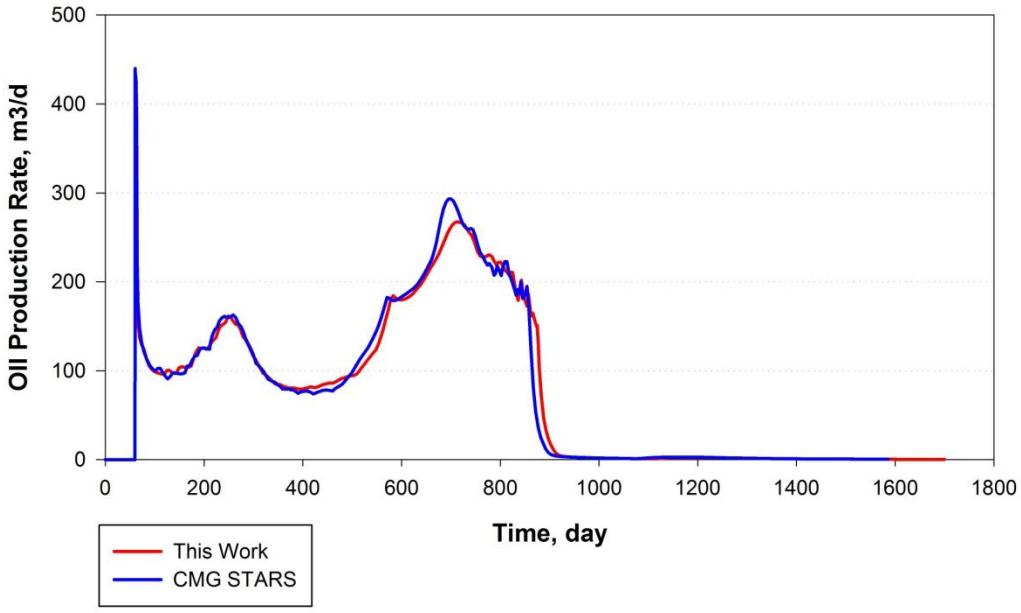

Figure 5-9: Oil production rate, 2-D SAGD process, this work vs. CMG STARS

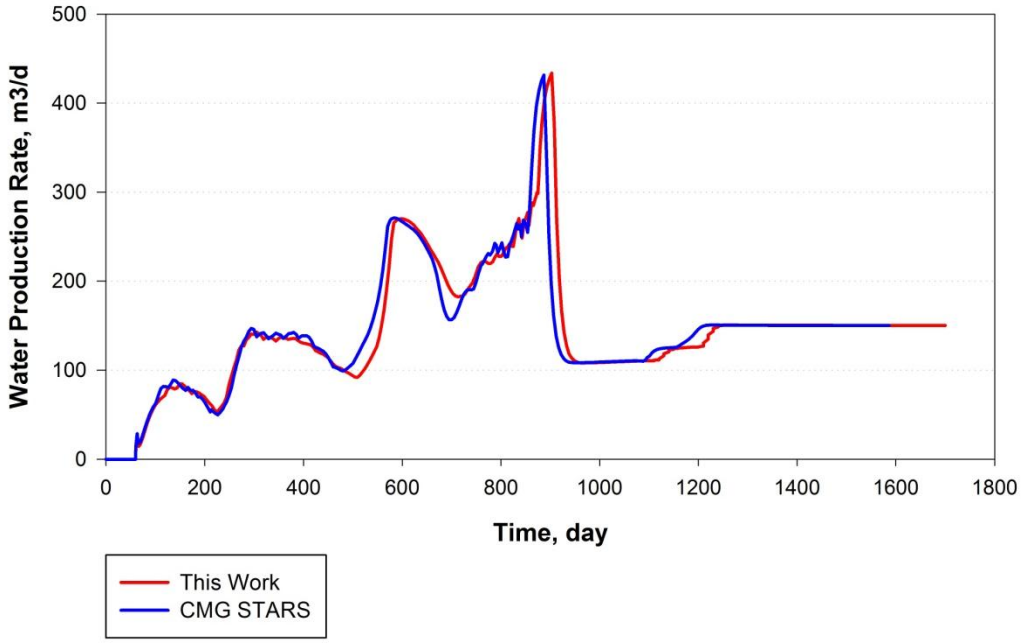

Figure 5-10: Water production rate, 2-D SAGD process, this work vs. CMG STARS

Table 5-9: Reservoir rock and fluid properties

Number of grid blocks, (nx, ny, nz)	11,1,20
Dimension of grid blocks, (Δx), m	50.00
Dimension of grid blocks, (Δy), m	76.00
Dimension of grid blocks, (Δz), m	1.00
Initial Conditions:	
Temperature, K	288.15
Pressure, kPa	500.00
Residual oil saturation w.r.t water	0.15
Initial oil saturation	0.85
Irreducible water saturation	0.15
Initial water saturation	0.15
Critical gas saturation	0.02
Residual oil saturation w.r.t gas	0.10

Reservoir Properties:	
Porosity	0.30
Pore volume compressibility, 1/kPa	1.00E-5
Horizontal permeability, md	4000.00
Vertical permeability, md	4000.00
Reservoir thermal conductivity, KJ/m-day-K	150.00
Cap rock thermal conductivity, KJ/m-day-K	150.00
Rock heat capacity, KJ/m^3-K	2350.00
Well Conditions:	
Injection temperature, K	478.15
Steam quality	0.85
Bottomhole injection pressure, kPa	3500.00
Maximum injection rate(CWE), m^3/day	150.00
Producer BHP, kPa	500.00
Maximum liquid production rate, m^3/day	450.00
Heater Properties:	
Heater energy rate, kJ/day-K	5.00E5
Heater maximum temperature, K	473.00

Table 5-10 represents fluid properties of 2-D SAGD model.

Table 5-10: Fluid properties

Component Name	Feed	Tc (K)	Pc (kPa)	CP, 1/kPa	CT, 1/K	MW
H_2O	0.000	647.000	22120.000	-----	----	18.015
CH_4	0.027	191.000	4600.000	7.028E-6	3.504E-3	16.043
HOIL	0.973	787.150	924.000	4.918E-7	2.612E-4	645.800

Component	C_{P1}	C_{P2}	C_{P3}	C_{P4}	HVR	Molar Density(kgmol/m^3)
H_2O	32.243	0.0	0.0	0.0	4820	----
CH_4	19.251	0.0	0.0	0.0	1556	18.061
HOIL	-22.383	0.0	0.0	0.0	8569	1.549

Table 5-11 represents variation of water and oleic component viscosity versus temperature.

Table 5-11: Variation of oleic component viscosity versus temperature

Temperature, K	Viscosity, cp		
	H_2O	CH_4	HOIL
278.15	1.092682	0.062250	1.48E+07
290.15	0.889337	0.057768	1.89E+06
302.15	0.735771	0.051032	323640.00
314.15	0.617601	0.045977	70470.00
326.15	0.525132	0.040667	18768.00
338.15	0.451677	0.035297	5923.00
350.15	0.392530	0.030044	2158.30
362.15	0.344317	0.025055	889.01
374.15	0.304575	0.020448	406.69
386.15	0.271481	0.016307	203.61
398.15	0.243667	0.012683	110.21
410.15	0.220090	0.009599	63.82
422.15	0.199948	0.007050	39.20
434.15	0.182616	0.005008	25.34
446.15	0.167602	0.003428	17.13
458.15	0.154515	0.002251	12.05
470.15	0.143042	0.001410	8.77
482.15	0.132930	0.000837	6.59
494.15	0.123974	0.000468	5.08
506.15	0.116005	0.000244	4.01
518.15	0.108882	0.000118	3.23
530.15	0.102491	5.15E-05	2.66
542.15	0.096733	2.03E-05	2.22
554.15	0.091527	7.03E-06	1.88

Equilibrium ratios of each component in K-Value approach is calculated from following equation which is function of temperature and pressure only;

$$K_i\left(P,T\right)=\left(\frac{kv_1}{P}+kv_2\cdot P+kv_3\right)\exp\left(\frac{kv_4}{T-kv_5}\right) \quad \textbf{5-17}$$

where, kv_1 to kv_5 are different constants that must be defined for each component. Table 5-12 show the k-value coefficients of each pure component;

Table 5-12: K-values of each pure component

Component	kv_1, kPa	kv_2, 1/kPa	kv_3	kv_4, K	kv_5, K
H_2O	0.0000	0.0	0.00	0.00	0.0
CH_4	0.4391E5	0.0	1.97	-4121.51	0.0
HOIL	1.4077E6	0.0	0.00	-6121.51	111.8

Table 5-13: The relative permeability curves for three phases

SW	Krw	Krow	SL	Krog	Krg
0.1500	0.0000	1.0000	0.2500	0.2000	0.0000
0.1850	0.0005	0.9900	0.2956	0.1758	0.0039
0.2000	0.0011	0.9800	0.3412	0.1531	0.0156
0.2500	0.0051	0.9400	0.3869	0.1320	0.0352
0.3000	0.0125	0.9000	0.4325	0.1125	0.0625
0.3500	0.0237	0.8250	0.4781	0.0945	0.0977
0.4000	0.0389	0.7500	0.5238	0.0781	0.1406
0.4500	0.0582	0.6400	0.5694	0.0633	0.1914
0.5000	0.0818	0.5600	0.6150	0.0500	0.2500
0.5500	0.1100	0.4650	0.6606	0.0383	0.3164
0.6000	0.1500	0.3700	0.7062	0.0281	0.3906
0.6510	0.2110	0.2986	0.7519	0.0195	0.4727
0.7000	0.2700	0.2300	0.7975	0.0125	0.5625
0.7500	0.3600	0.1610	0.8431	0.0070	0.6601
0.8000	0.4500	0.0920	0.8888	0.0031	0.7656
0.8500	0.5700	0.0460	0.9344	0.0008	0.8789
0.9000	0.6900	0.0000	0.9800	0.0000	1.0000
0.9500	0.8450	0.0000			
1.0000	1.0000	0.0000			

The current simulator was tested against several analytical and numerical models. In this tests different elements and functionalities of developed simulator such as; heat loss, wellbore model, convective heat and mass flow and conductive heat transfer were tested and it was able to provide satisfactory results in variety of tests.

Chapter Six: **SIMULATION RESULTS AND DISCUSSIONS**

In this chapter several models representing SAGD and ES-SAGD processes are simulated and the results are compared with the commercial simulator, then EOS approach results versus K-Value approach results from current simulator are compared to investigate the effect of different properties and equilibrium ratios on thermal processes.

Expanded-Solvent SAGD is a hybrid method in which a small amount of solvent is added to injected steam to enhance the oil recovery and cumulative steam oil ratio. In ES-SAGD process, injected steam transfers its remaining latent heat to the bitumen at the edge of chamber and condensed, at the same time solvent mixes with the bitumen due to its solubility in the oil phase and its condensation. As a result of dual actions of temperature and solvent dilution, bitumen becomes more mobile and diluted and it flows toward the production well under gravity with less resistance. Adding solvent to steam also reduces the overall steam chamber temperature by reducing the vapor pressure of steam chamber, therefore it directly reduces the amount of heat loss to overburden and under-burden and it helps to improve the cumulative steam oil ratio at the end of the process.

Several scenarios were designed to investigate the effect of using EOS on the simulated performance of ES-SAGD. First we start with a base case, which is a 2-D model of the SAGD process. This case will be tested to see the effect of EOS on the modeling of PVT properties and enthalpy of the system and its effect on oil recovery and the energy balance of the process.

The following tolerances were used for convergence of Newton-Raphson method in all of the simulations in this section:

- Pressure: 50.00 (kPa)
- Saturation: 0.05 (m^3/m^3)
- Mole fraction: 0.05 (mol/mol)
- Temperature: 5.00 (K)
- Enthalpy: 200.00 (J/mol)

6.1 **Case 1: Base case 2-D SAGD model, this work vs. CMG STARS**

The reservoir simulation model is a 2-D homogeneous and isotropic model with constant porosity, permeability and initial water and oil saturation and contains a single SAGD well-pair. Fluid properties, rock properties, heat loss properties, and rock-fluid properties are extracted from Gates et al. (2007) paper and are presented in Table 6-1. The vertical distance between injector and producer is 5 m and production well is located 2.0 m higher than the base rock.

Steam is injected with the quality of 0.8 at 478.15 K into the reservoir and the injection well operates based on the maximum injection pressure of 2300 kPa. Producer is operating under minimum BHP of 1000 kPa and it is constrained to maximum steam production rate of 10 m^3/day (CWE). To establish thermal communication between the injector and producer, a preheating period of three months was modeled by using heaters. After the thermal communication was established, the wells are switched to regular SAGD mode for 1500 days of simulation.

Table 6-1: Reservoir and fluid properties of Case 1

Number of grid blocks, (nx, ny, nx)	30,1,32
Dimension of grid blocks, (Δx, Δy, Δz), m	2x10.00 26x4.00 2x10.00, 100.00, 1.00
Initial Conditions:	
Temperature, K	288.150
Pressure, kPa	500.000
Initial oil saturation	0.892
Initial water saturation	0.108
Reservoir Properties:	
Porosity	0.297
Pore volume compressibility, 1/kPa	1.400E-5
Horizontal permeability, md	4264.000
Vertical permeability, md	852.000
Rock thermal conductivity, kJ/m-day-K	660.000
Water thermal conductivity, kJ/m-day-K	53.500

Oil thermal conductivity, kJ/m-day-K	11.500
Gas thermal conductivity, kJ/m-day-K	5.000
Rock heat capacity, kJ/m^3-K	2600.000
Well Conditions:	
Well radius, m	0.110
Steam injection rate (CWE), m^3/day	200.000
Bottom hole injection pressure, kPa	2300.000
Steam quality	0.800
Injection temperature, K	478.150
Producer BHP, kPa	1000.000
Maximum steam production rate (CWE), m^3/day	10.000
Heater Properties:	
Heater rate, kJ/day-K	5.000E5
Maximum temperature, K	458.150

Component	MW	Pc(kPa)	Tc(K)	ω	Oleic mole fraction
H_2O	18.0150	22054.397	647.370	0.344	0.000000000
C1	16.000	4600.390	190.550	0.008	0.009302326
C6	86.000	3289.160	507.400	0.275	0.013953488
BITUMEN	507.000	999.110	976.000	1.123	0.976744186

Component	C_{P1}	C_{P2}	C_{P3}	C_{P4}	HVR
H_2O	34.49057816	-0.014255189	4.73116E-05	-3.56672E-8	4820
C1	37.93010615	-0.068408604	0.000272446	-2.38987E-7	0
C6	-5.967610614	0.534622954	-0.000202459	6.494e-8	0
BITUMEN	-19.84748243	3.026702365	-0.001136662	3e-7	0

Table 6-2 represents variation of water and oleic component viscosity versus temperature.

Table 6-2: Oleic component viscosity versus temperature for Case 1

Temperature, K	Viscosity, cp			
	H_2O	C1	C6	Bitumen
283.15	1.3110	98.060	0.3415	1.50E+06
293.15	1.0050	72.880	0.3086	2.81E+05
303.15	0.8004	55.640	0.2808	6.75E+04
313.15	0.6543	43.500	0.2571	1.98E+04
323.15	0.5518	34.710	0.2366	6873.000
333.15	0.4714	28.200	0.2189	2744.000
343.15	0.4066	23.280	0.2034	1233.000
353.15	0.3570	19.500	0.1898	612.100
363.15	0.3182	16.540	0.1778	330.800
373.15	0.2828	14.180	0.1671	192.200
398.15	0.2227	10.080	0.1451	63.760
423.15	0.1848	7.518	0.1281	27.430
448.15	0.1586	5.828	0.1147	14.240
473.15	0.1394	4.656	0.1039	8.387
498.15	0.1238	3.813	9.50E-02	5.430
523.15	0.1117	3.186	8.77E-02	3.758
548.15	0.1005	2.707	8.15E-02	2.739
573.15	9.13E-02	2.400	7.80E-02	2.075
598.15	8.41E-02	2.400	7.80E-02	2.075

The relative permeability curves for three phases are presented in the Figure 6-1.

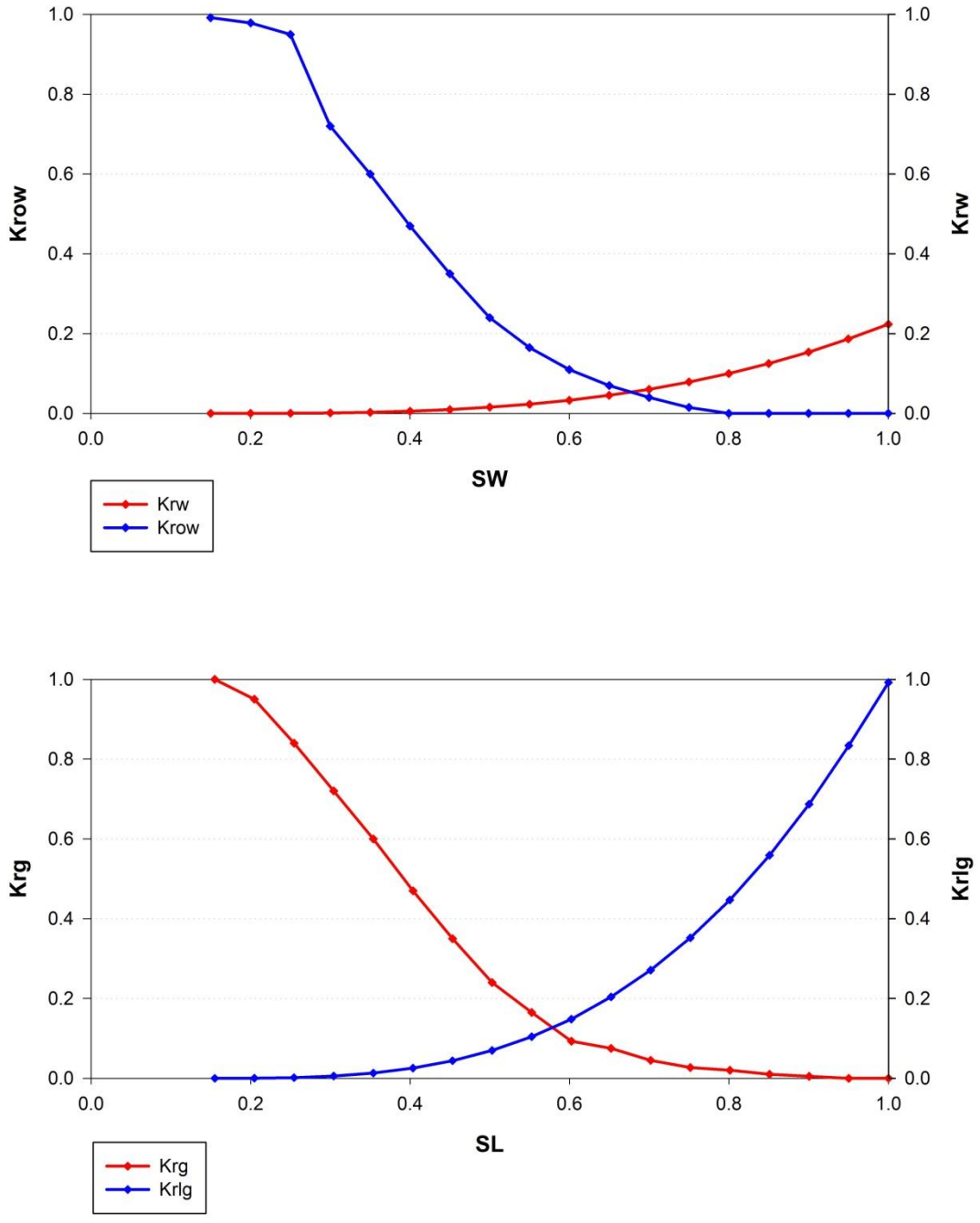

Figure 6-1: Relative permeabilities for Case 1

Table 6-3 shows the k-values coefficients of each pure component;

Table 6-3: K-Value coefficients of different component for Case 1

Component	kv_1, kPa	kv_2, 1/kPa	kv_3	kv_4, K	kv_5, K
H2O	0.0	0.0	0.0	0.0	0.0
C1	4.36376e5	0.0	0.0	-879.84	2.16
C6	1.0062e6	0.0	0.0	-2697.55	48.78
BITUMEN	1.0062e6	0.0	0.0	-9697.55	8.78

Table 6-4 represents fluid properties of 2-D SAGD model.

Table 6-4: Fluid properties for K-Value approach

Component Name	Vshift	ρ_{ref} ($kgmol/m^3$)	CP, 1/kPa	CT, 1/K
H_2O	0	---	-----	----
C1	0	18.140	5.302E-06	1.697E-03
C6	0	7.397	1.958E-06	1.629E-04
BITUMEN	0	1.375	3.407E-07	7.029E-06

Figure 6-2 shows the oil production rate, water production rate, and water injection rate for 1500 days of simulation respectively. First, the results are compared with CMG STARS results and there is a quite good match between them. This model is used as the base case for the rest of this chapter. In each case only necessary sections of data file are changed to investigate different mechanisms.

After the results of K-Value approach were compared against the CMG STARS results, the same model was run with EOS approach and results of EOS approach are compared with the K-Value approach.

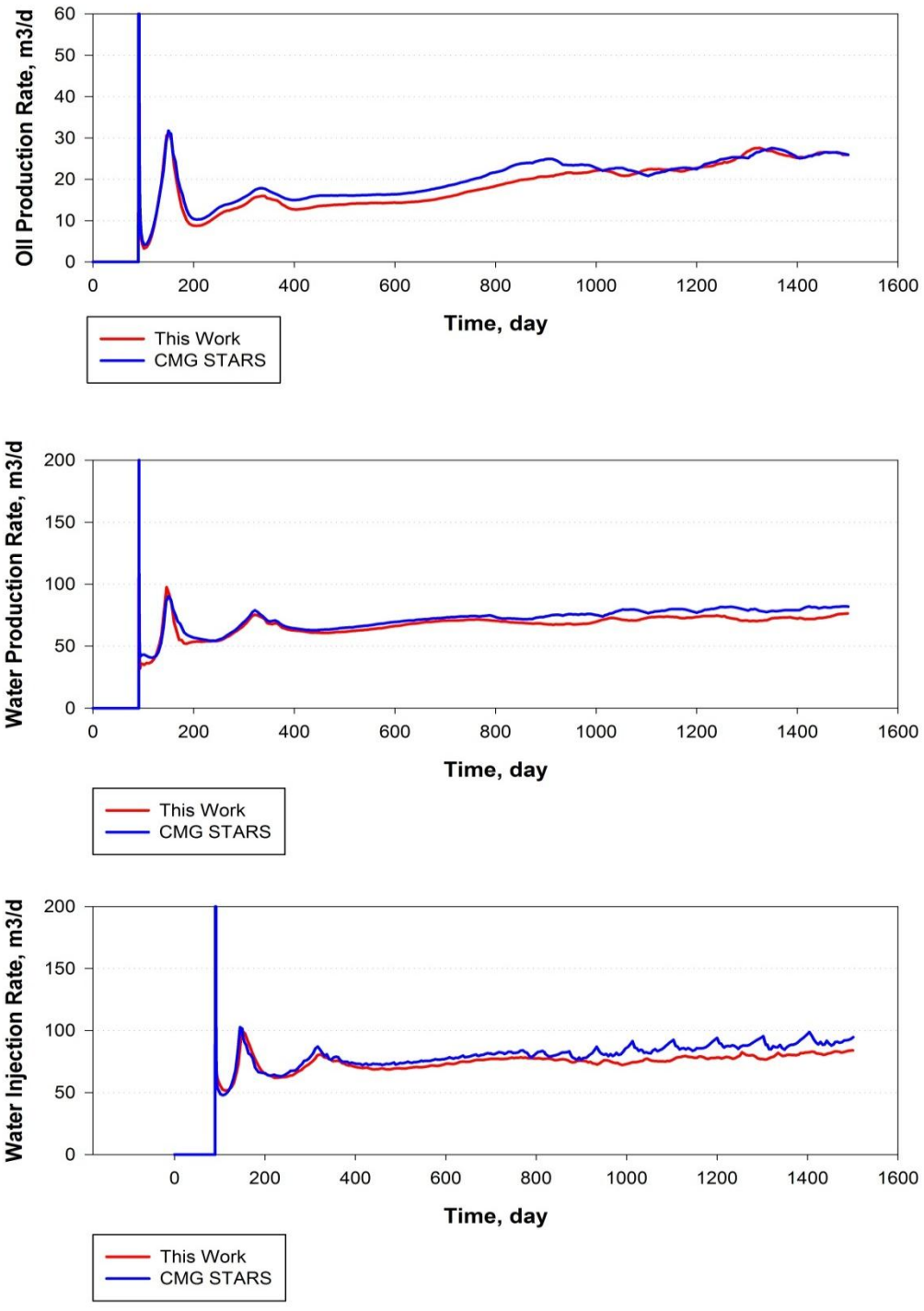

Figure 6-2: Production and injection rate for SAGD process, Case 1, this work vs. CMG STARS

6.2 **Case 2: 2-D SAGD model, EOS vs. K-Values**

This case is identical to the base case except for handling phase split and property calculations, where SRK equation of state was used. The main objective of this case was to compare the effect of PVT properties calculation from correlations versus equation of state on the predicted performance of SAGD process.

To have a fair comparison, all the component properties for K-Value approach were calculated in CMG Winprop PVT Package. SRK equation of state was used in CMG Winprop and component properties such as thermal expansion, reference density, compressibility factor and equilibrium ratios were calculated. Then these properties were used in K-Value approach.

In EOS approach the latter properties are calculated internally at each Newton's iteration level. Figure 6-3 shows oil and water production rate for SAGD process with K-Value compare to the case of EOS. The results don't show a major difference between the water production and injection rate and oil production rate of EOS approach versus K-Value approach. This case is a good example to show that the results of the K-Value approach with correlations are not too different from the EOS approach for pure steam injection.

6.3 **Case 3: 2-D model, ES-SAGD vs. SAGD**

In this case, hexane is injected at 2% of volume with steam at the same operating condition of the base case and all of the physical properties of the model are the same as the base case. The main objective of this test was to compare the results of EOS approach for both ES-SAGD and SAGD processes. The oil production rate, water production rate and water injection rate are presented in the Figure 6-4. It is clear that co-injection of hexane and steam enhanced the oil production rate. This effect has been both numerically and practically proven in field tests as well as in laboratory scale experimental studies (Leaute (2002), Leaute and Carey (2007), Rivero and Mamora (2002), and Nasr and Isaacs (2001)).

6.4 **Case 4: 2-D ES-SAGD model, EOS vs. K-Values**

In this case, solvent is co-injected with steam at ratio of 2% of the volume in CWE. All of physical properties and operating conditions are identical with the base case. The main objective of this simulation was to see the effect of adding solvent on the oil recovery and compare the performance of EOS approach versus the K-Value approach. Figure 6-5 presents oil and water production and water injection rate for ES-SAGD process. The difference between EOS approach and K-Value approach is more pronounced when solvent is added to the injected steam. Figure 6-5 shows that the oil production of K-Value approach is a little bit higher than the EOS approach in this case. Another fact is that in K-Value approach oil production rate is faster than the EOS approach, a closer look at the oil production rate shows that the all of the peaks of oil production rate in K-Value approach happens almost 100 days sooner than the EOS approach.

Figure 6-6 shows cumulative oil production, water production and water injection of ES-SAGD process for EOS approach and K-Value approach. It shows that the EOS approach produces less amount of oil at surface condition for almost the same amount of injected water in comparison with the K-Value approach.

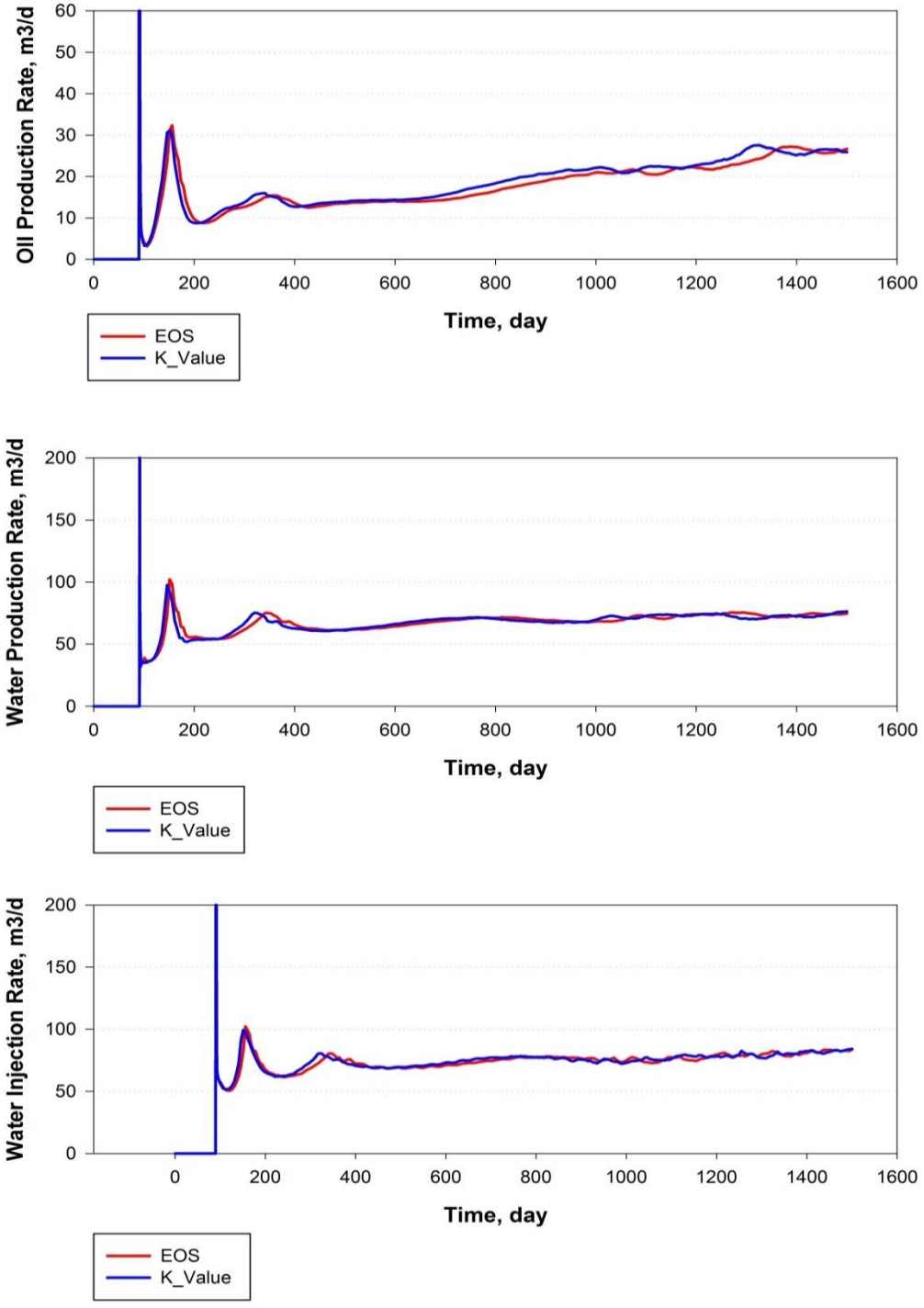

Figure 6-3: Oil production rate, water production and injection rate for K-Value and EOS

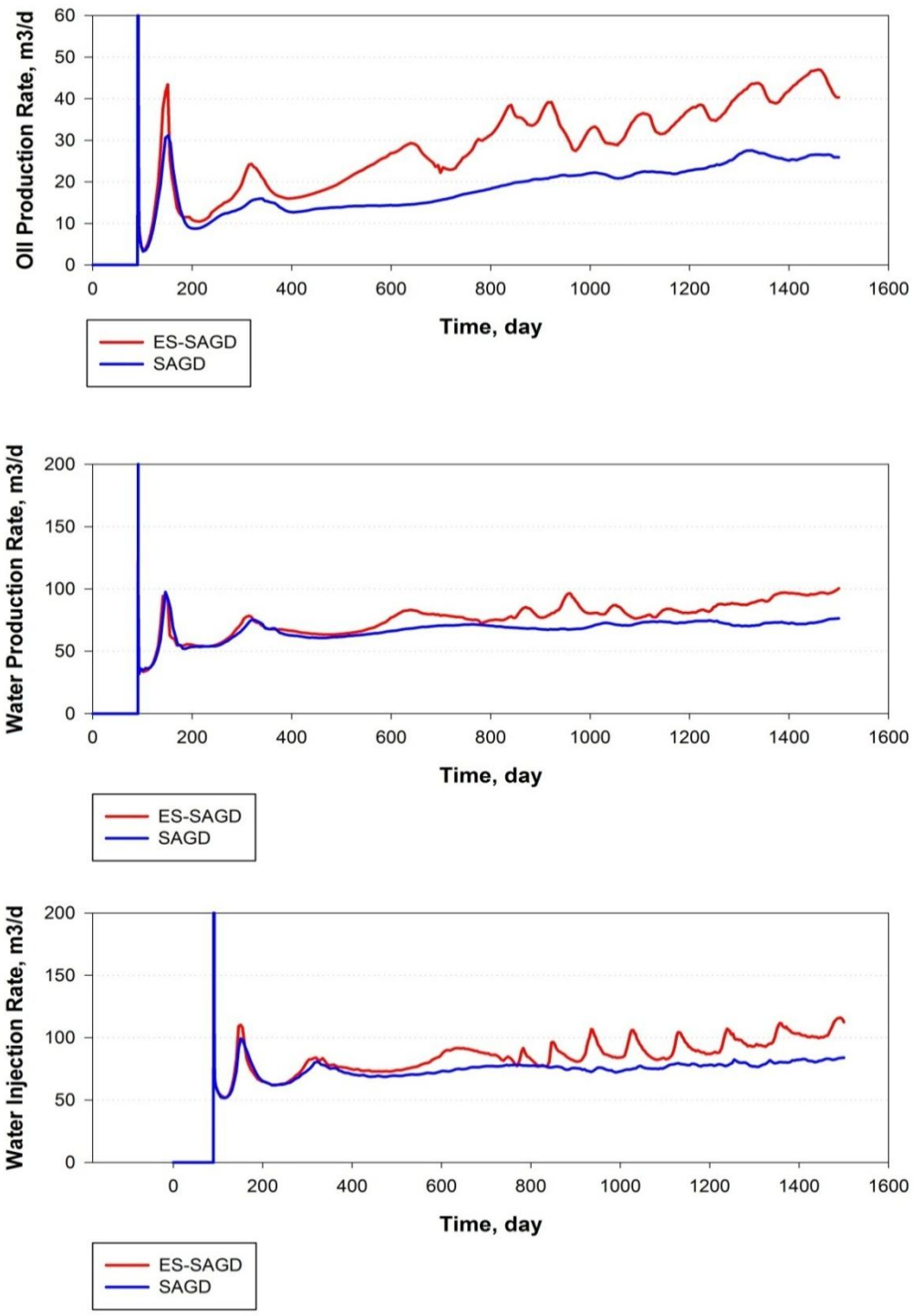

Figure 6-4: Oil production rate, water production and injection rate ES-SAGD vs. SAGD

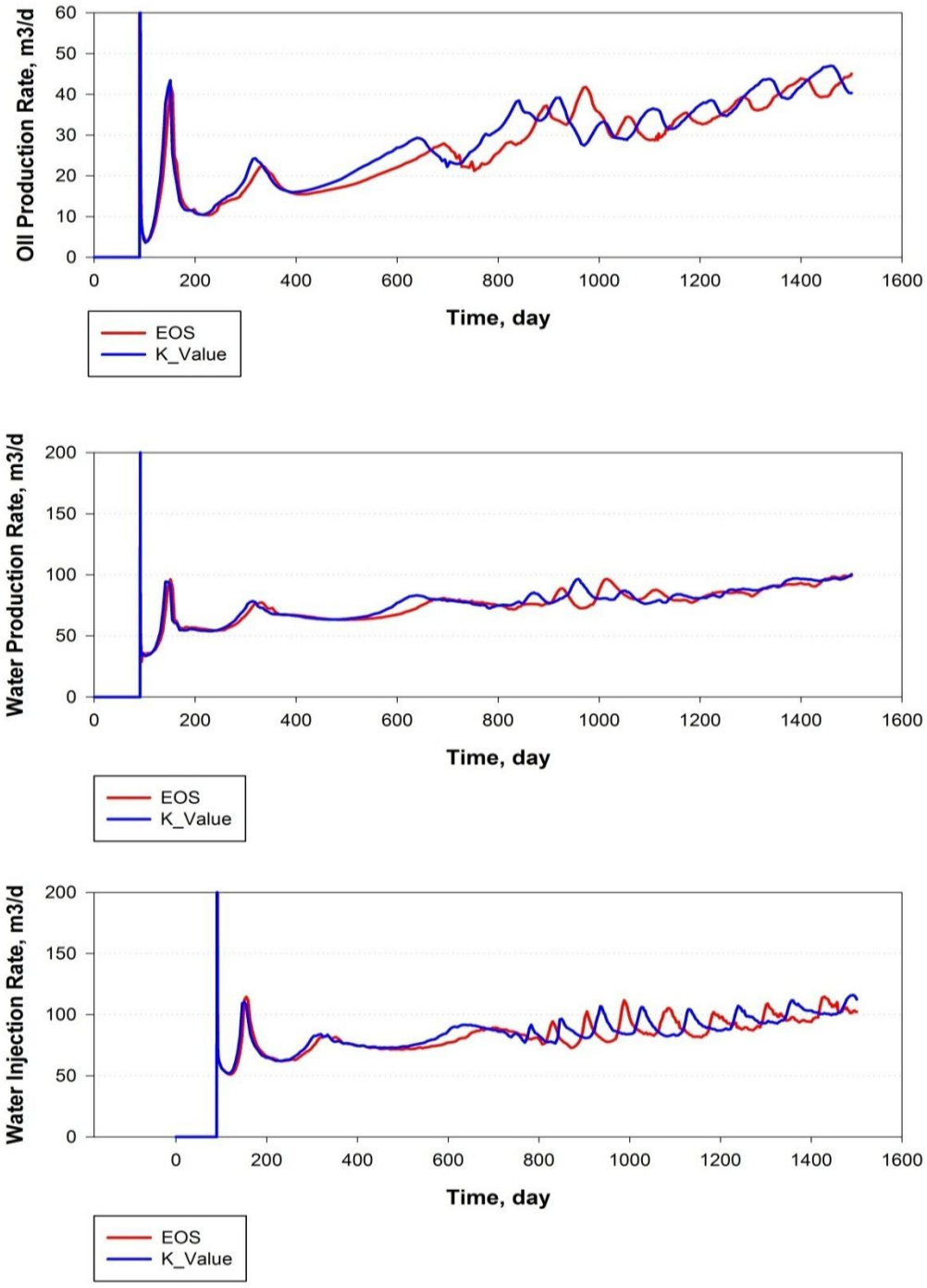

Figure 6-5: Oil production rate, water production and injection rate for ES-SAGD process, EOS vs. K-Value

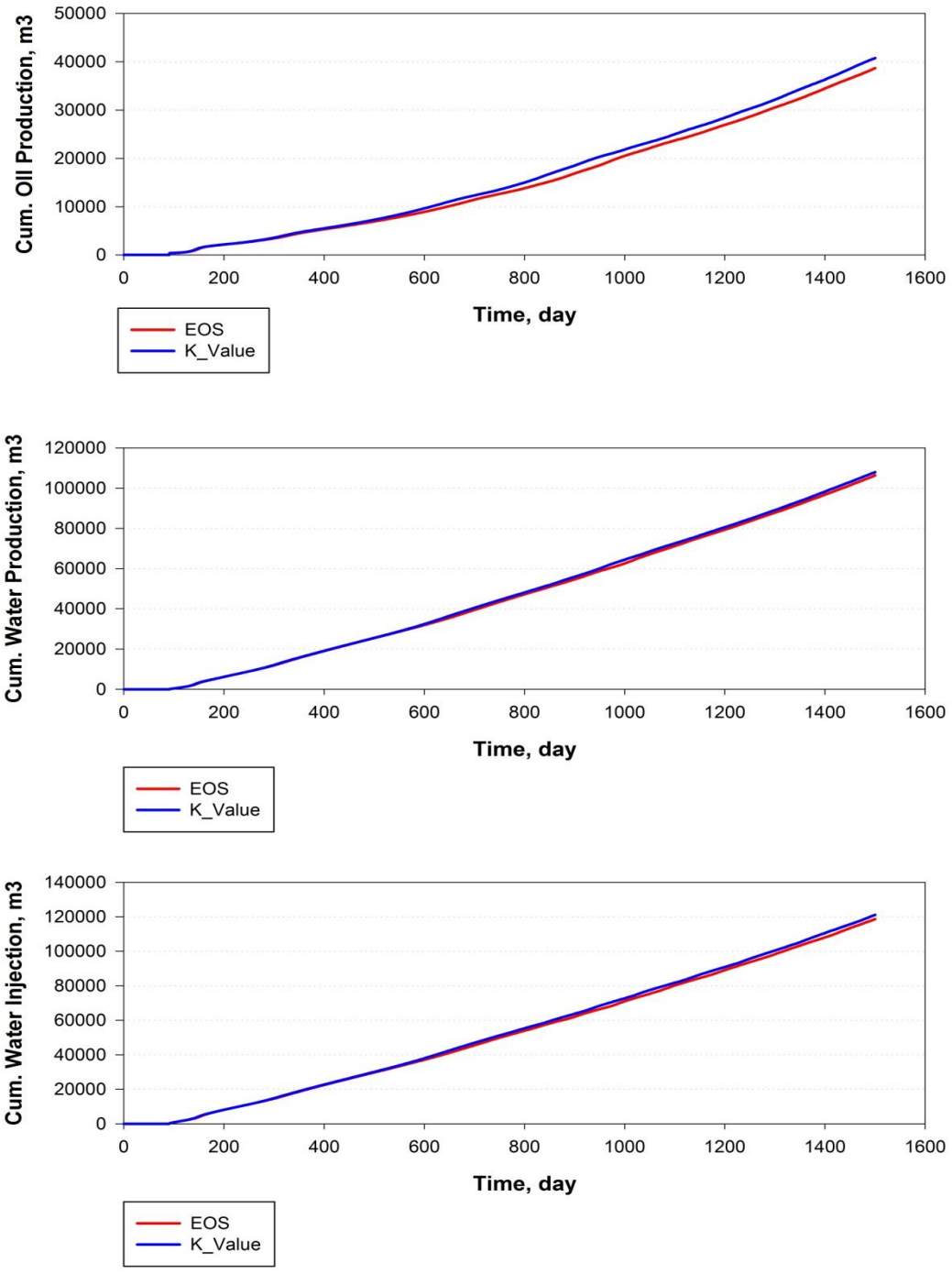

Figure 6-6: Cumulative oil production and water production and injection for ES-SAGD process, EOS vs. K-Value

Figure 6-8 to 6-12 shows temperature, gas saturation, oil saturation, water saturation and solvent mole fraction in oleic phase at different time of ES-SAGD process in 2-D domain, respectively. The latter properties are results of EOS approach. The time sequence is 602.8 days, 955.4 days, 1209 days, and 1500 days. The most interesting plot is the solvent mole fraction in oleic phase, which is always high at the edge of steam chamber. Hexane saturation properties are very similar to water and it condenses almost at the same temperature as water condenses.

Higher amount of hexane in oleic phase at the edge of steam-solvent chamber enhances the viscosity reduction further more than only steam injection and this is the main reason for higher oil recovery in comparison with pure steam injection. As it is shown in Figure 6-12 the solvent mole fraction in oleic phase in some grid blocks at the edge of steam-solvent chamber reaches to 0.9 which is very high. A grid block investigation was performed to investigate its effect on equilibrium ratios of different components.

6.5 **Grid block level investigation**

In this section a detailed comparison at grid level is performed. Equilibrium ratio of components, component mole fraction of oleic phase and temperature of each grid block is plotted versus time. The major goal of this investigation is to observe variation of these properties versus time for several grid blocks and compare their behaviour. For this purpose the same dataset was run in two different modes, once in EOS mode and once in the K-Value mode. Equilibrium ratios, oleic mole fraction of components and temperature of grid blocks are extracted and plotted against time. Several grid blocks from different part of steam chamber in different layers were selected for this comparison. Figure 6-7 shows location of selected grid blocks in the reservoir and respect to the location of injector and producer. The selected blocks are above injector and after 1500 days of simulation all of them are inside the steam chamber area.

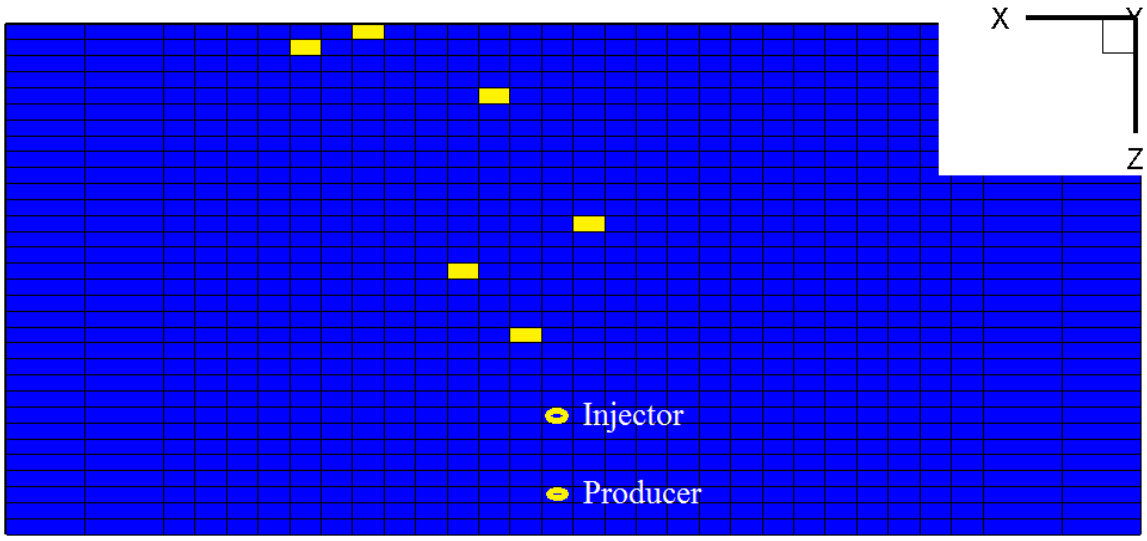

Figure 6-7: Location of selected grid blocks with respect to the well locations

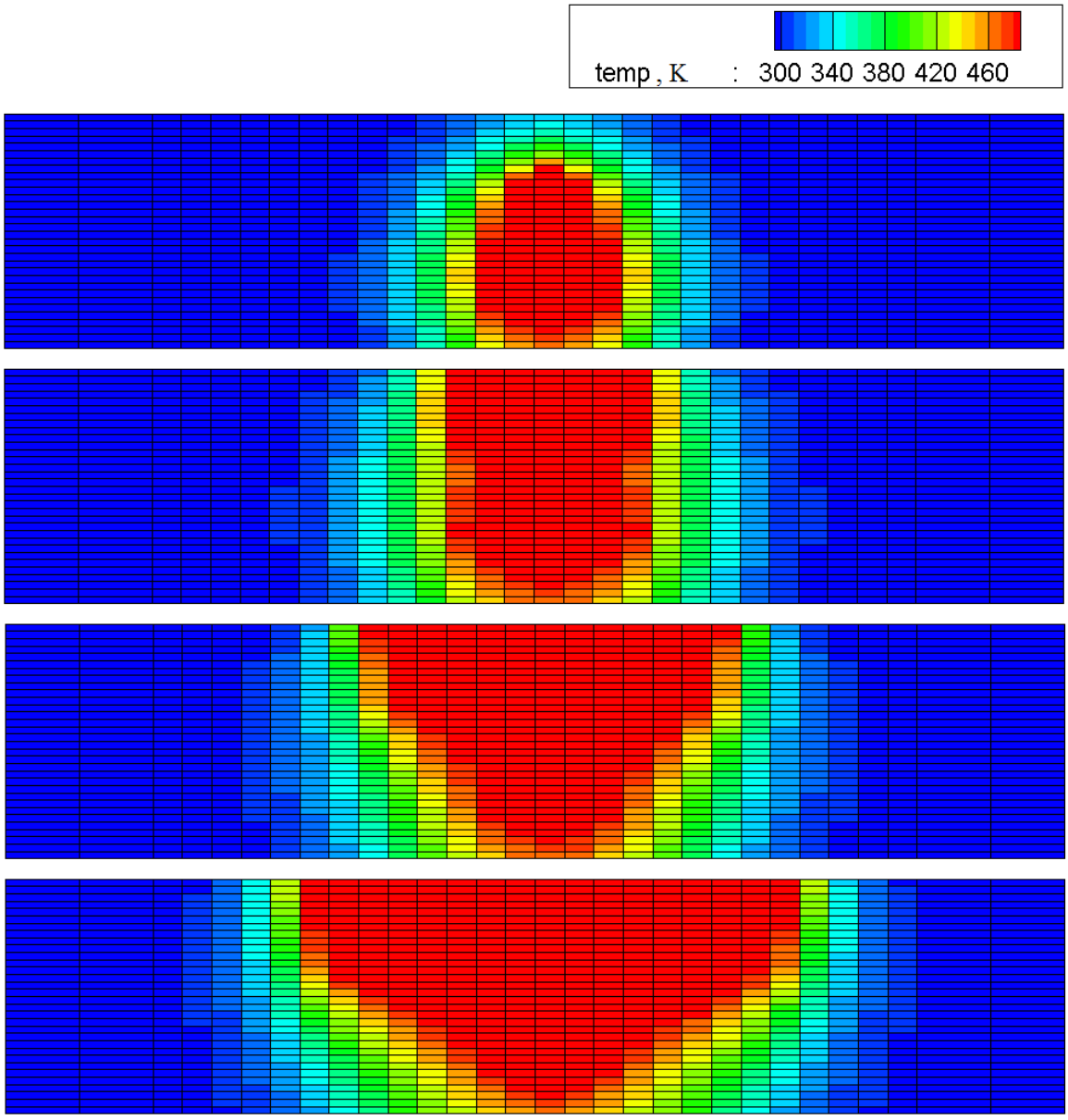

Figure 6-8: Temperature profile at different times for ES-SAGD process

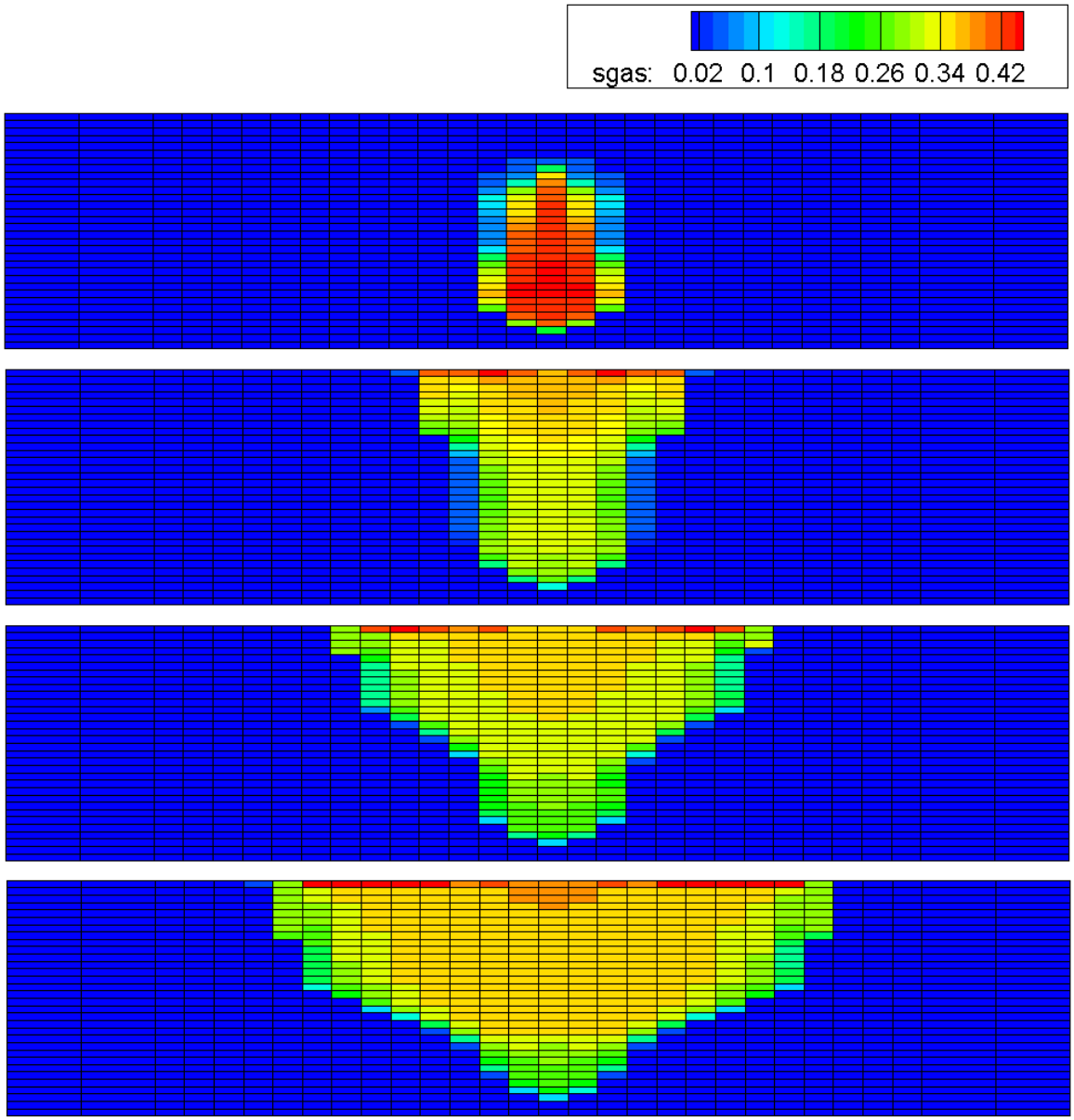

Figure 6-9: Gas saturation profile at different times for ES-SAGD process

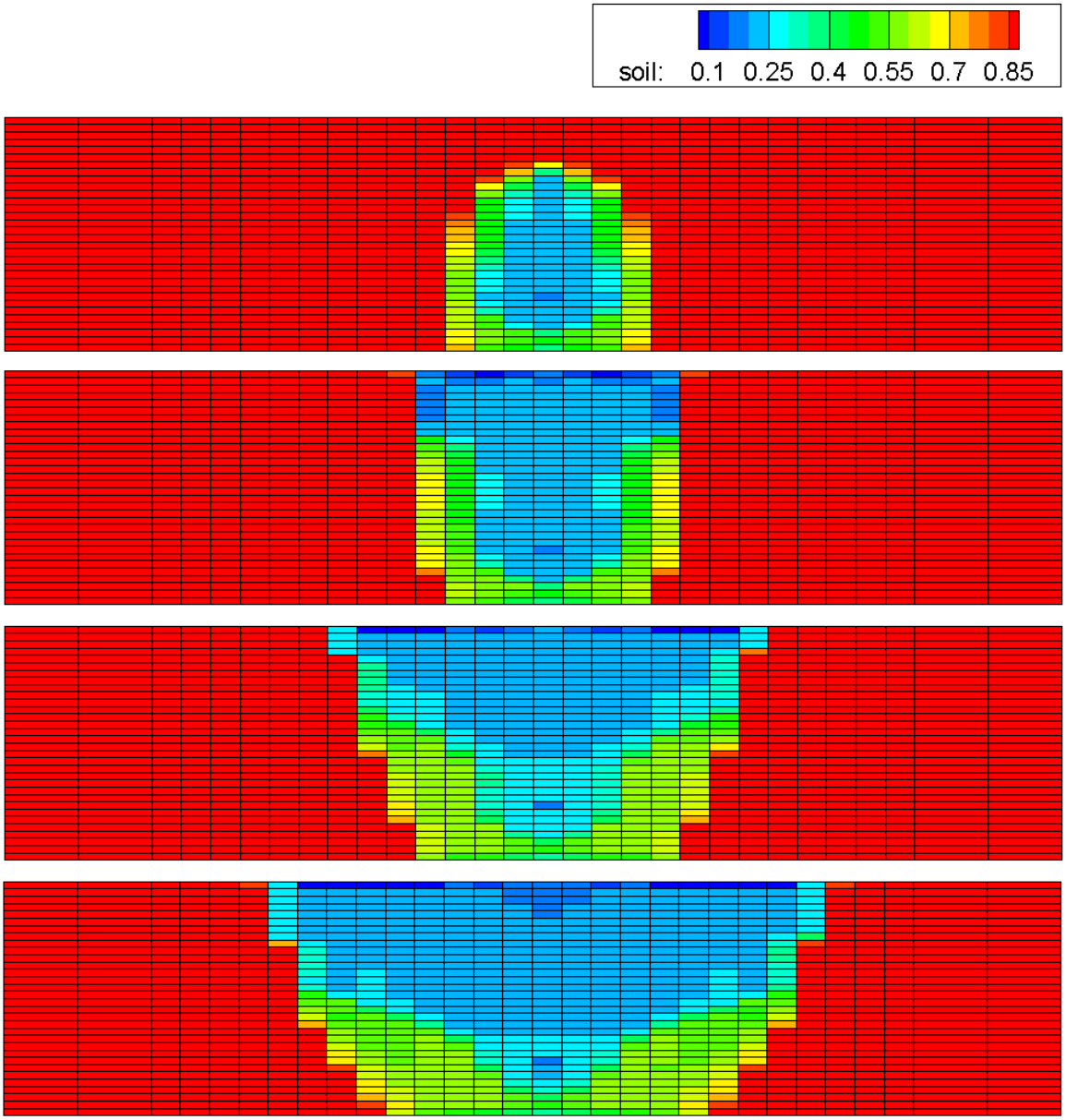

Figure 6-10: Oil saturation profile at different times for ES-SAGD process

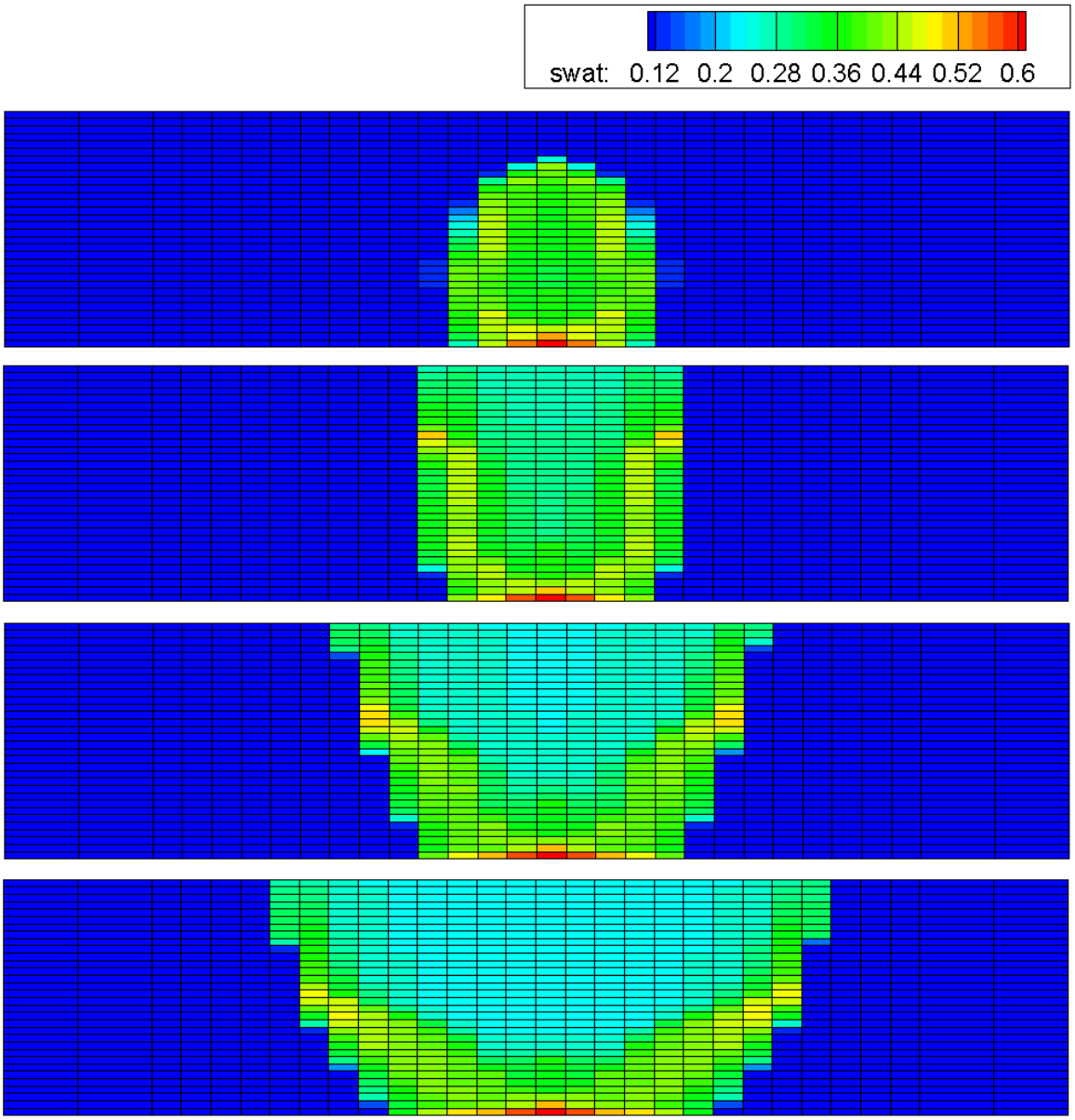

Figure 6-11: Water saturation profile at different times for ES-SAGD process

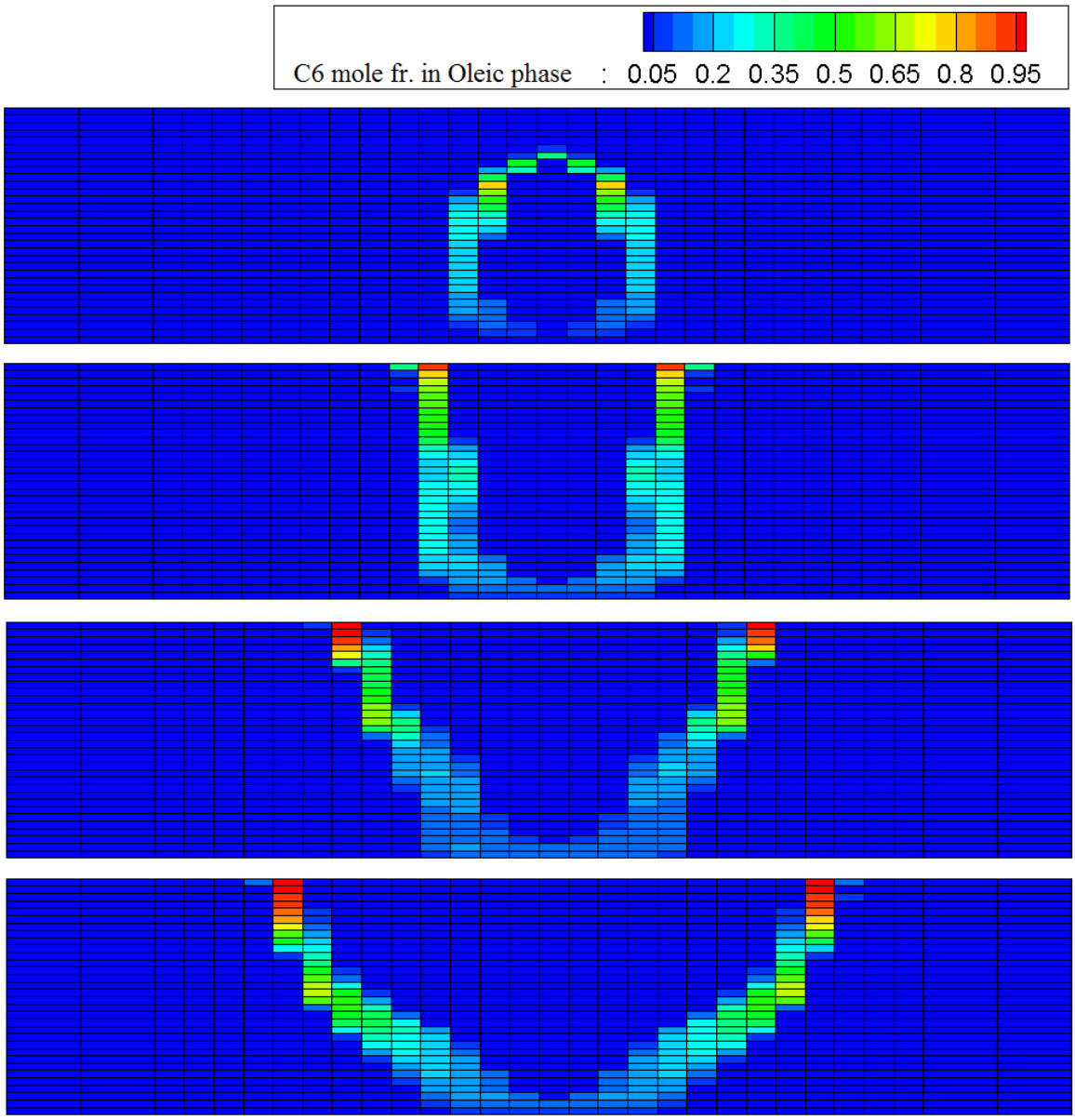

Figure 6-12: Hexane mole fraction in oleic phase profile at different times for ES-SAGD process

6.5.1 *Grid block (14, 1, 20)*

Figure 6-13 shows equilibrium ratios of different components, component mole fraction in oil phase and temperature variation with time for this grid block (14, 1, 20) in EOS approach respectively. The same properties are also presented in Figure 6-14 for K-Value approach. As it is seen, the equilibrium ratio for each component in K-Value approach exactly follow the temperature variation however the dependency of equilibrium ratio to both composition and temperature is more clear in EOS approach. In K-Value approach the equilibrium ratio of C1 is two times bigger than that in the EOS approach.

The other observation reveals that the solubility of H_2O in oleic phase is not negligible and its mole fraction in oleic phase varies from very small number ~ 1.E-3 to 0.1at high temperatures. In K-Value approach the mutual solubility between aqueous phase and oleic phase is neglected. These two phases are assumed to be absolutely immiscible in most of commercial software i.e. ECLIPSE Thermal. In CMG STARS user can specify liquid-liquid K-Values.

Figures 6-13 and 6-14 show variation of component mole fractions in oleic phase versus time for two approaches and in the EOS approach the mole fraction of water in oleic phase is not negligible.

Temperature variation is similar for both approaches but in the K-Value approach, 3-phase temperature starts at lower value in comparison with the EOS approach. The main reason is using higher equilibrium ratio for each component in the K-Value approach, therefore gas phase appears sooner than in the EOS approach. Since gas phase appears sooner in the K-Value approach, then steam chamber grows faster. Steam chamber growth has direct relationship with the rate of oil production of ES-SAGD process, therefore oil production rate in K-Value approach is faster than in the EOS approach. This is the main reason behind the higher production observation in Case 4.

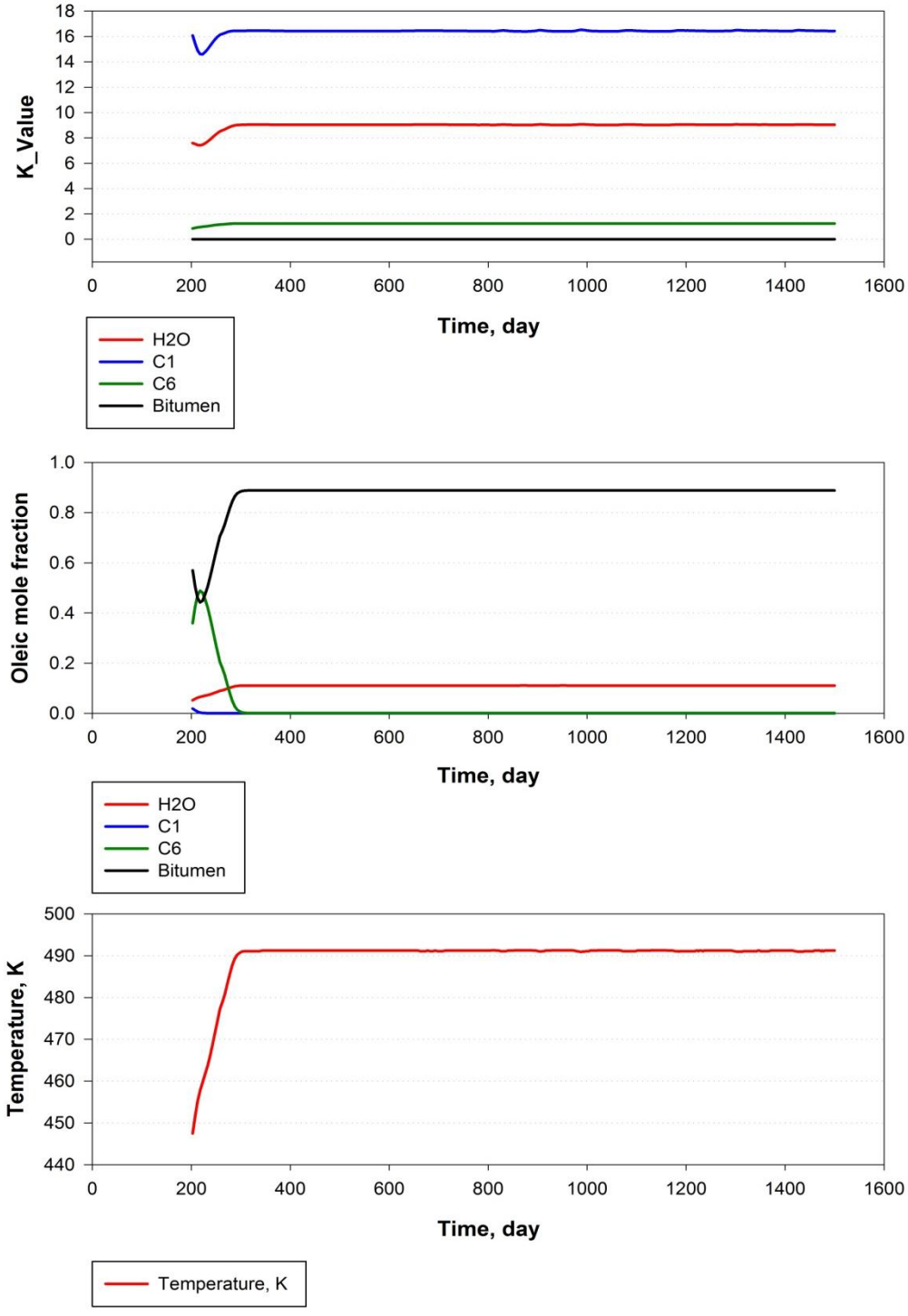

Figure 6-13: Equilibrium ratios, mole fractions in oleic phase and temperature versus time for grid block (14, 1, 20) in EOS approach

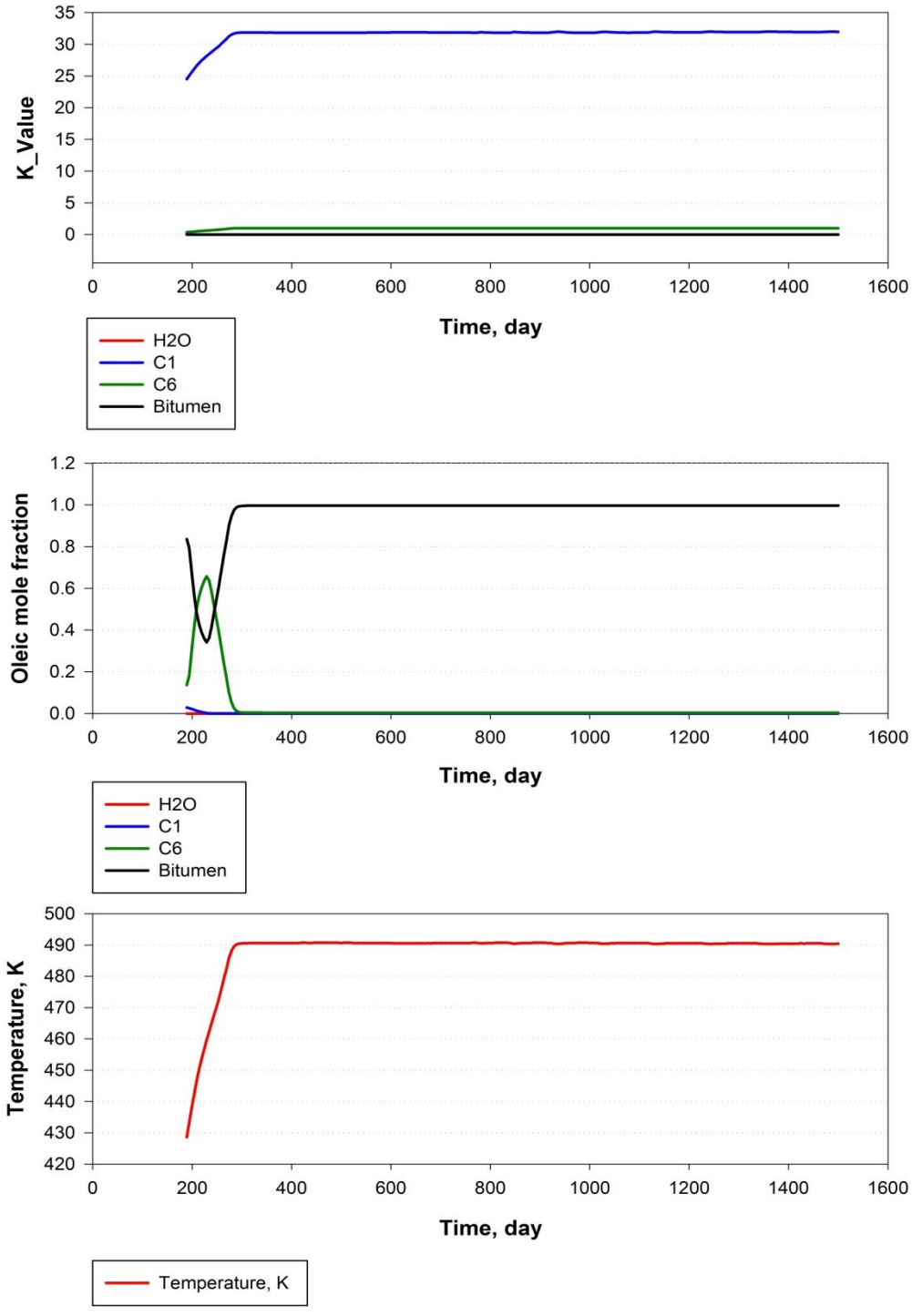

Figure 6-14: Equilibrium ratios, mole fractions in oleic phase and temperature versus time for grid block (14, 1, 20) in K-Value approach

6.5.2 *Grid block (9, 1, 1)*

Variation of equilibrium ratio with composition is more pronounced in this grid block due to higher variation of component mole fraction in the oleic phase with time. Temperature variation also affects the final equilibrium ratios. The mole fraction of injected solvent varies from small amounts up to 90% in the EOS approach and up to 98% in the K-Value approach in this grid block. When steam chamber grows and passes this grid block the global mole fractions in this grid block reach to almost steady state condition. Unlike EOS approach equilibrium ratios in K-Value approach only changes with temperature and variation of component does not affect them. This is clearly seen in Figure 6-16.

In all of the grid blocks which were investigated this behaviour is repeated. When the grid block is at the edge of steam-solvent chamber the variation of components is higher and it will change the equilibrium ratio of components. When the corresponding grid block is not at the edge of steam chamber and it is inside the steam chamber, then the grid block reaches to pseudo steady-state condition and equilibrium ratios remain unchanged. This phenomenon is presented in Figure 6-15.

K-Values are presented here when there are 3-phases coexisting in the grid block. In this grid block and all of selected grid blocks gas phase in K-Value approach appears sooner than the EOS approach due to higher equilibrium ratio for volatile components. For example in this grid block gas phase appears after 1000 days of simulation in EOS approach, however it starts at 900 days in K-Value approach. Grid block temperature is equal to saturation temperature of grid block and is equal to 340 K in EOS approach compared to 320 K in K-Value approach.

The same behaviour happens in the rest of selected grid blocks too and they are presented in this section to validate that the equilibrium ratios are changing with temperature, pressure and composition whenever composition changes are significant. It also confirms that the solubility of water in oil phase at high temperature is not negligible and must be considered in thermal processes. Using equilibrium ratios which are only functions of temperature and pressure is definitely not enough when solvent is added to the system. Calculated saturation temperature of a

grid block in K-Value approach may be higher or lower than the thermodynamically correct one depending on the values of equilibrium ratios.

Figures 6-17 to 6-24 present variations of equilibrium ratio, component mole fraction in oleic phase and temperature of the other selected grid blocks, for both EOS and K-Value approaches. The following additional grid blocks were selected in this study; (12,1,16), (7,1,2), (16,1,13), (13,1,5).

However, employing an equation of state to calculate the thermodynamic properties did not have a huge impact on the oil production rate, water production, and water injection rate in this example. Nonetheless, this grid to grid level analysis shows that the K-Value approach could provide incorrect phase splitting and equilibrium ratios in comparison with the EOS approach.

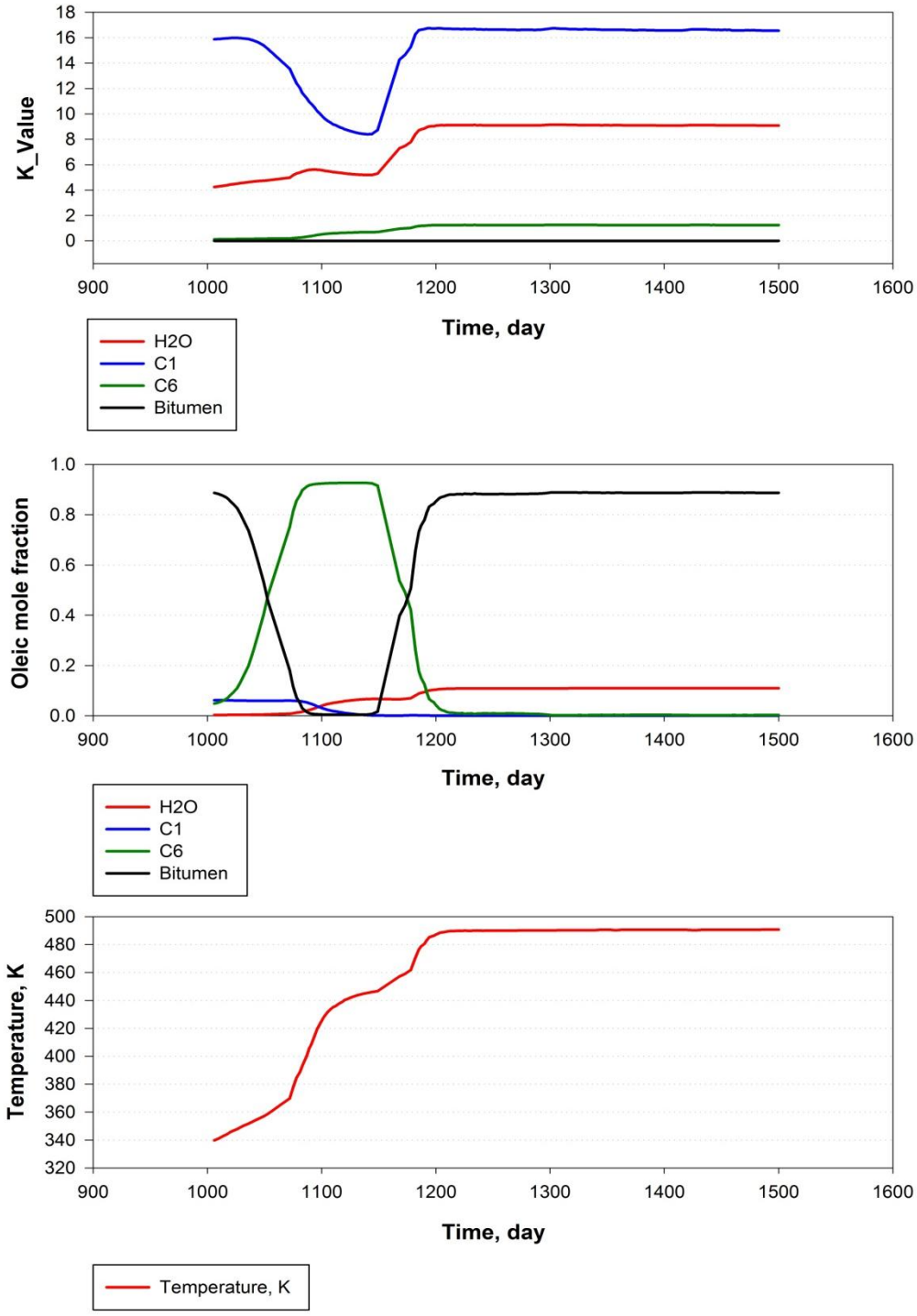

Figure 6-15: Equilibrium ratios, mole fractions in oleic phase and temperature versus time for grid block (9, 1, 1) in EOS approach

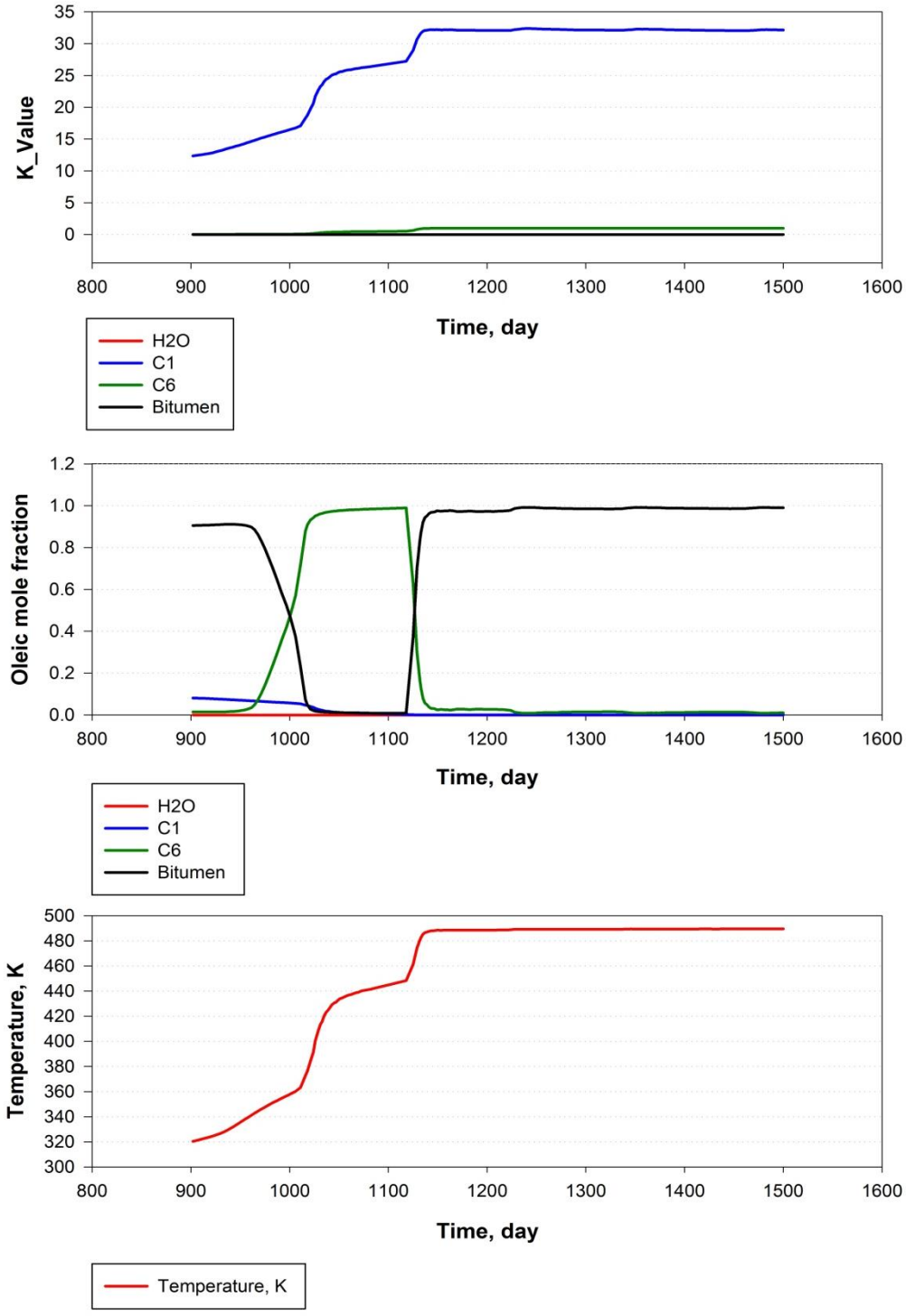

Figure 6-16: Equilibrium ratios, mole fractions in oleic phase and temperature versus time for grid block (9, 1, 1) in K-Value approach

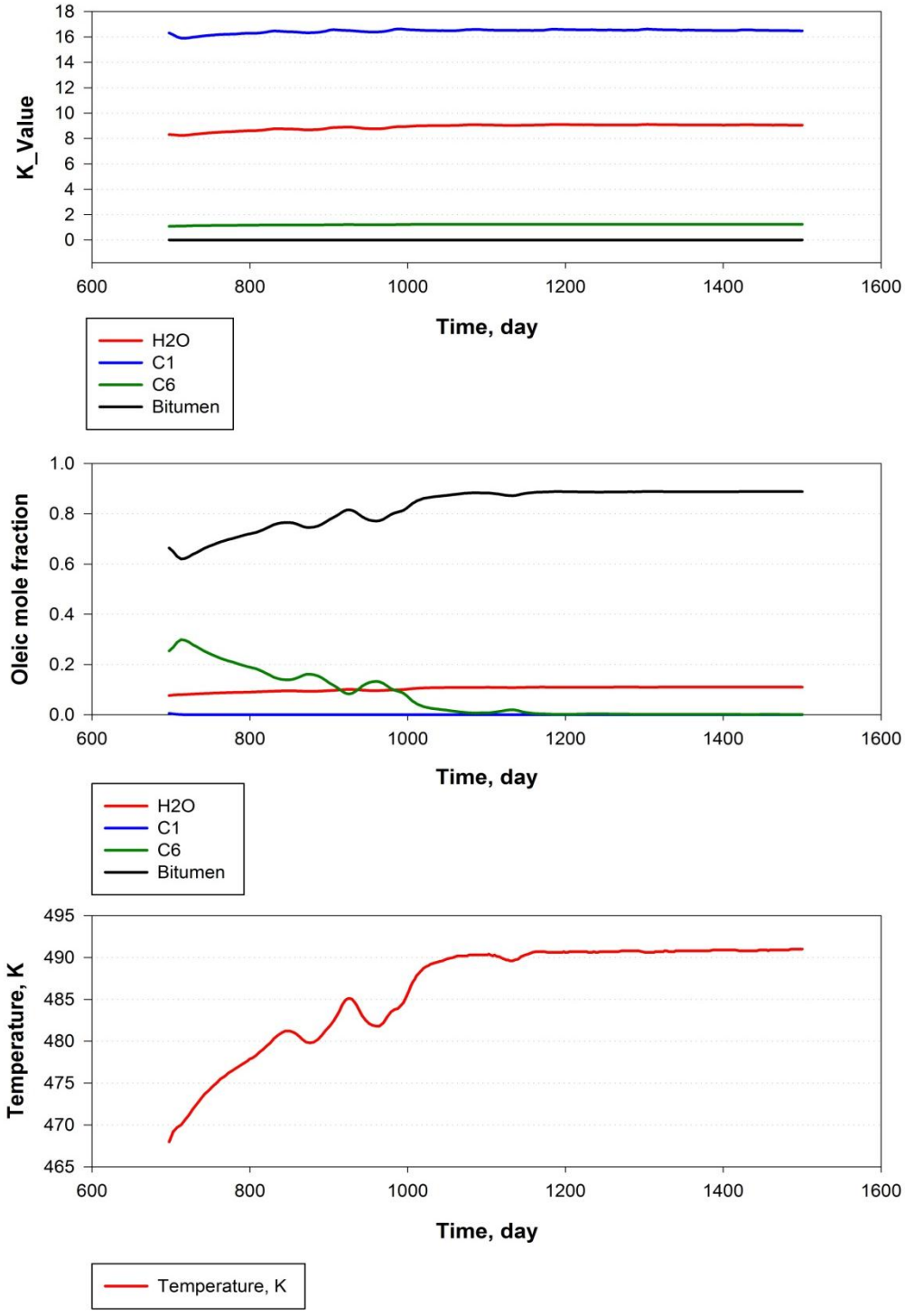

Figure 6-17: Equilibrium ratios, mole fractions in oleic phase and temperature versus time for grid block (12, 1, 16) in EOS approach

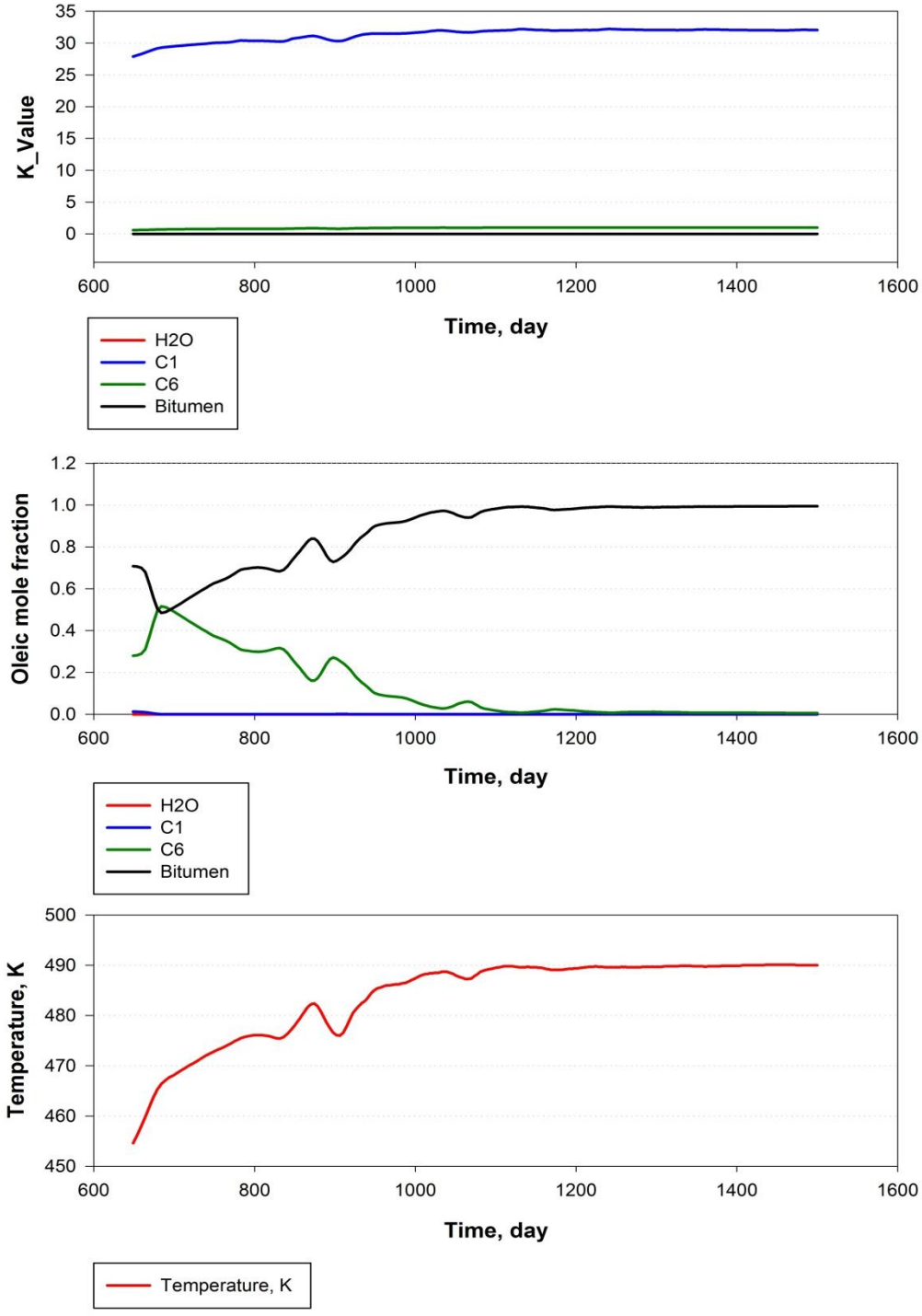

Figure 6-18: Equilibrium ratios, mole fractions in oleic phase and temperature versus time for grid block (12, 1, 16) in K-Value approach

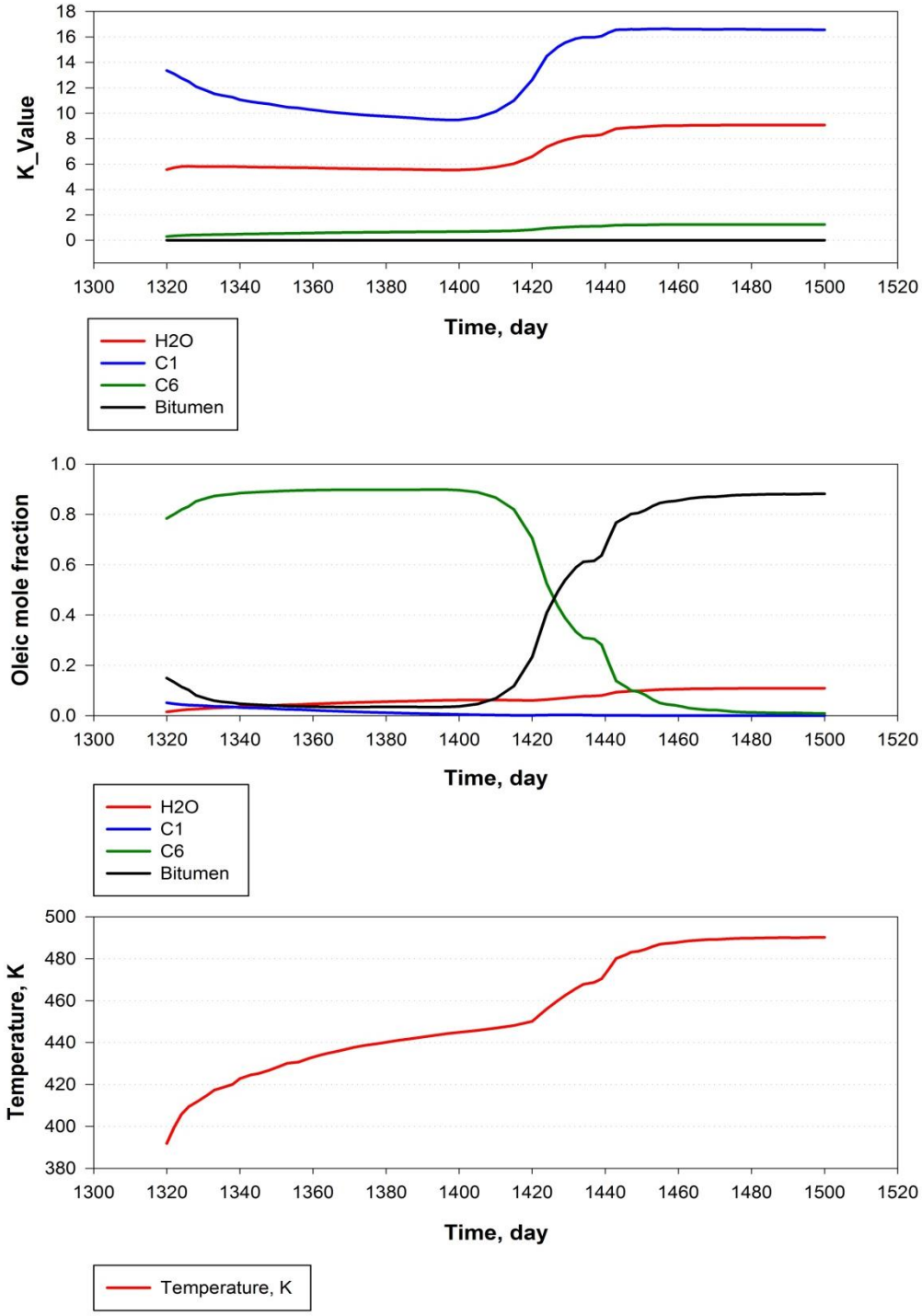

Figure 6-19: Equilibrium ratios, mole fractions in oleic phase and temperature versus time for grid block (7, 1, 2) in EOS approach

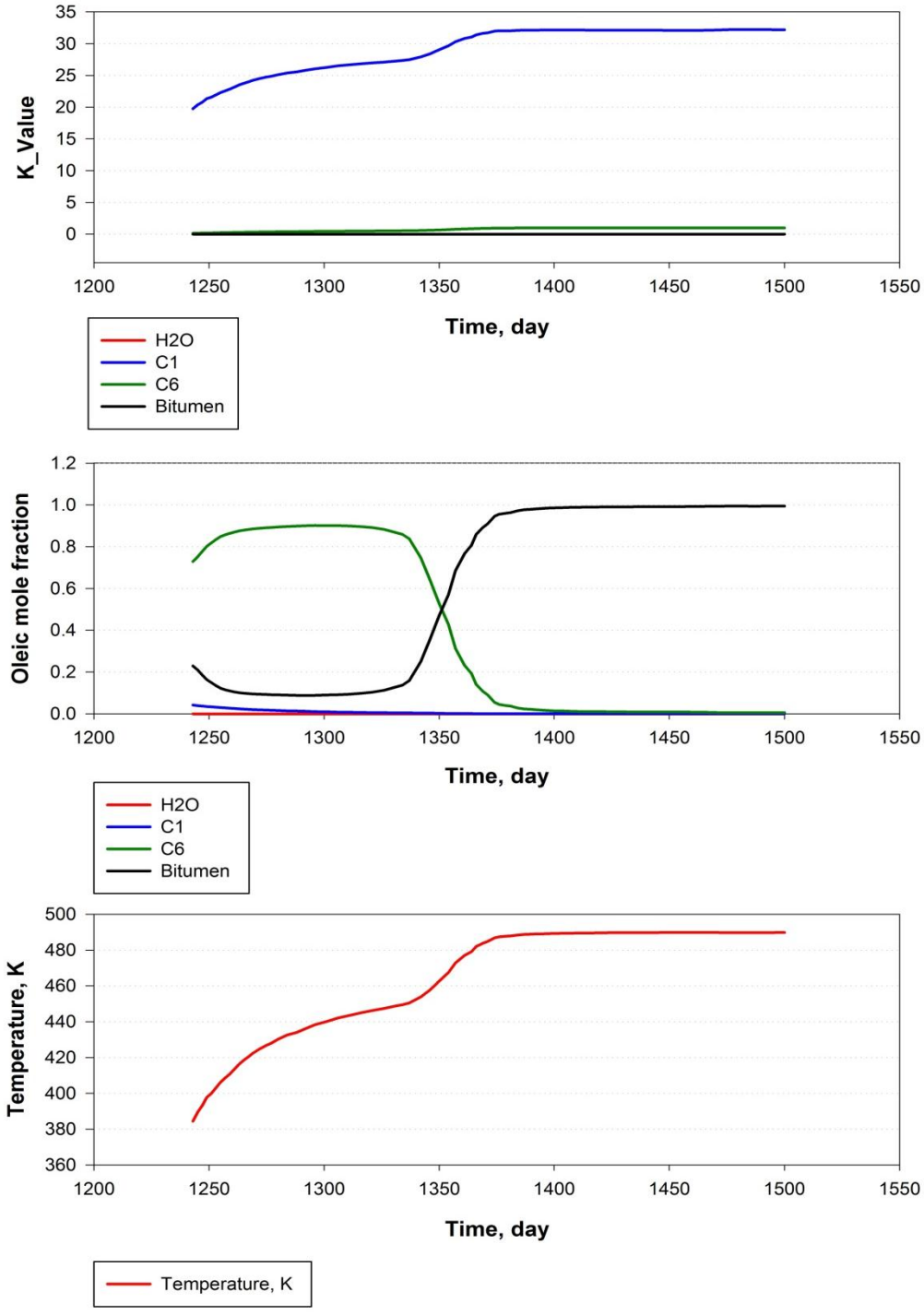

Figure 6-20: Equilibrium ratios, mole fractions in oleic phase and temperature versus time for grid block (7, 1, 2) in K-Value approach

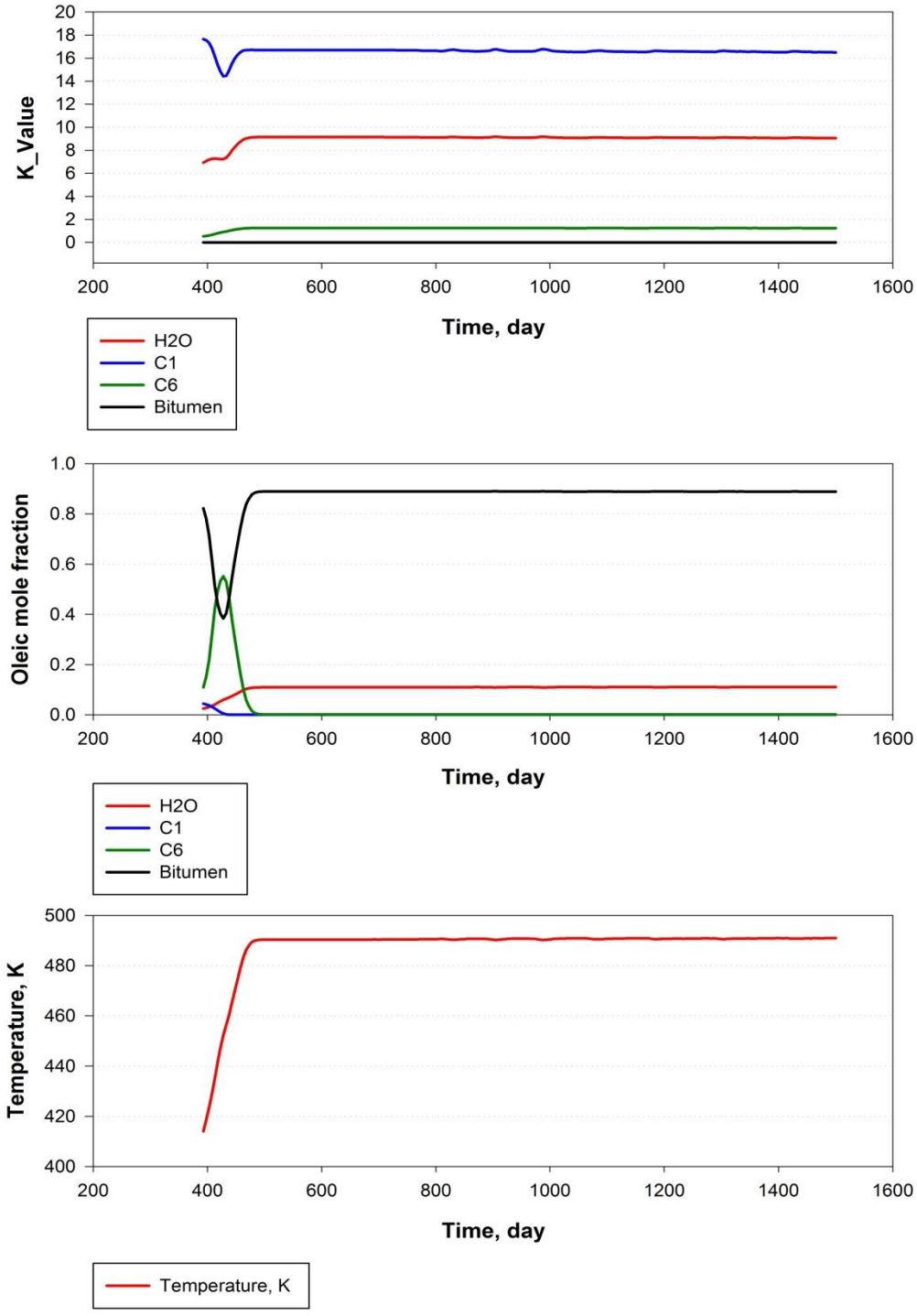

Figure 6-21: Equilibrium ratios, mole fractions in oleic phase and temperature versus time for grid block (16, 1, 13) in EOS approach

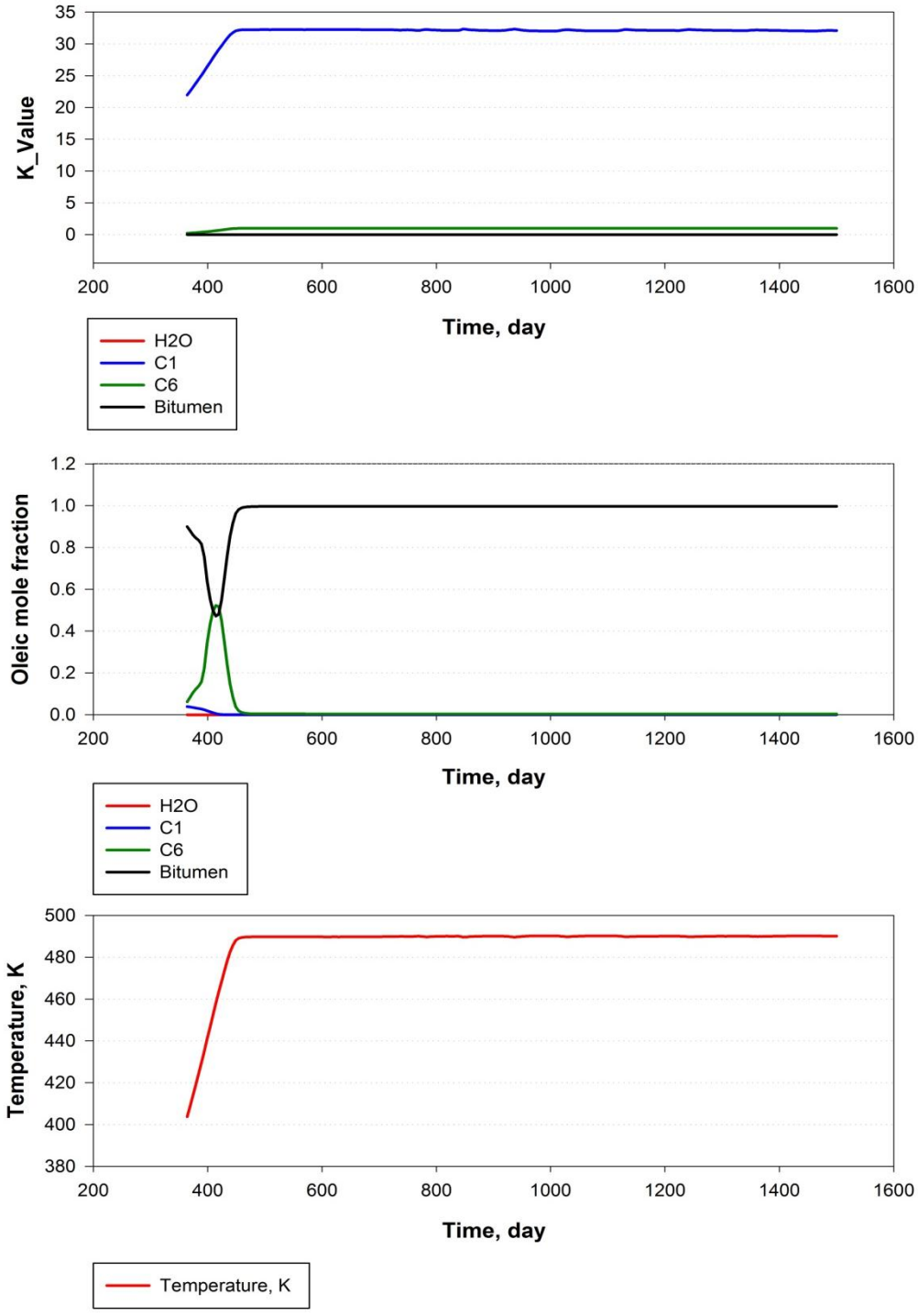

Figure 6-22: Equilibrium ratios, mole fractions in oleic phase and temperature versus time for grid block (16, 1, 13) in K-Value approach

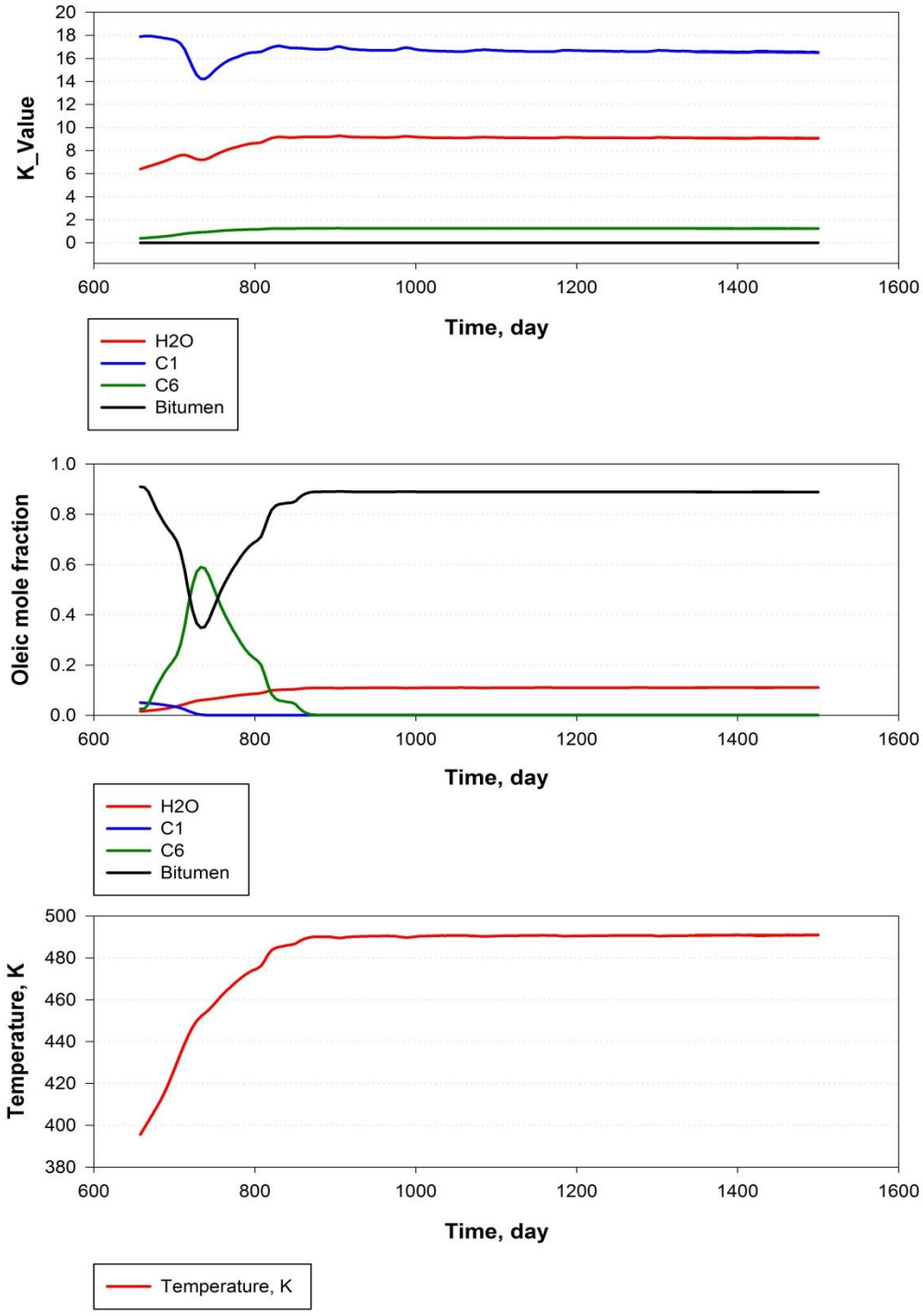

Figure 6-23: Equilibrium ratios, mole fractions in oleic phase and temperature versus time for grid block (13, 1, 5) in EOS approach

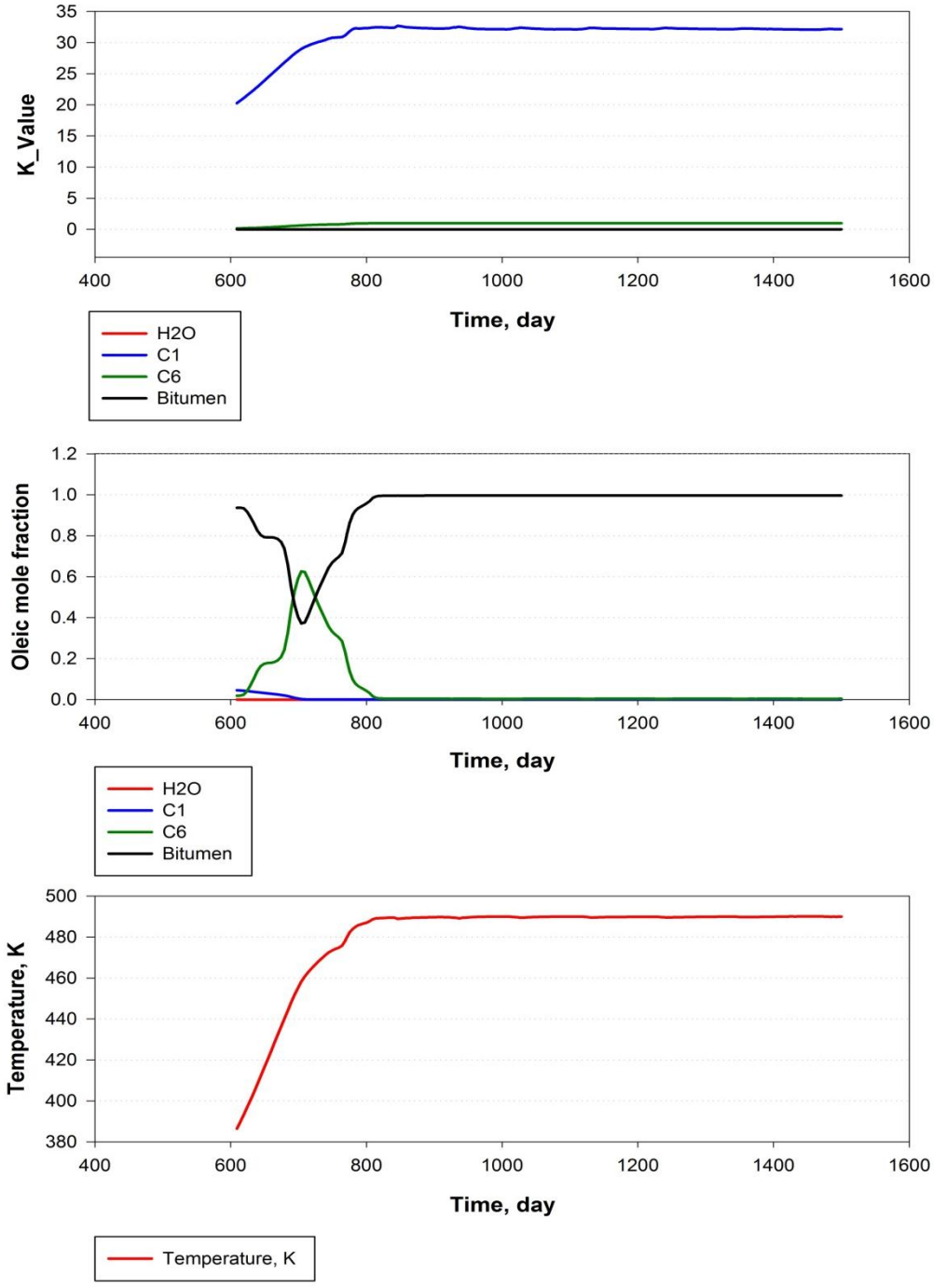

Figure 6-24: Equilibrium ratios, mole fractions in oleic phase and temperature versus time for grid block (13, 1, 5) in K-Value approach

6.6 **Case 5: 2-D ES-SAGD model, PR EOS vs. SRK EOS**

In this case, Peng-Robinson and SRK equations of state were used in two different ES-SAGD cases with solvent ratio of 2 percent. The main goal of this test was to investigate the effect of different EOS type on the results of simulations. Figure 6-25 presents oil production rate, water production and injection rates for these two runs. It shows that the results are slightly different for the two equations of states. The main reason is the different treatment of liquid phase property calculations. If volume shift is used to correct the properties of liquid phase specifically density, the results might be closer to each other.

6.7 **Case 6: 2-D ES-SAGD model, solvent ratio effect**

In this test three different levels of hexane addition to steam at 2, 4 and 6 volume% were tested and the results are compared. The main objective of this test was to see the effect of higher amount of solvent co-injection on the performance of ES-SAGD process. As it is shown in Figure 6-26 the oil production rate increases by increasing percentage of co-injected solvent. Adding more solvent to the steam decreases oil viscosity more and the process takes advantage of viscosity reduction by both heat and solvent transport from the injected fluid to the reservoir oil, and consequently it enhances the ultimate oil recovery of process and improves cumulative steam to oil ratio of the system.

Figure 6-27 presents cumulative oil production and water production for all three cases. The cumulative oil production for case with 6% is more than that for 4% and the case of 4% is higher than the 2%.

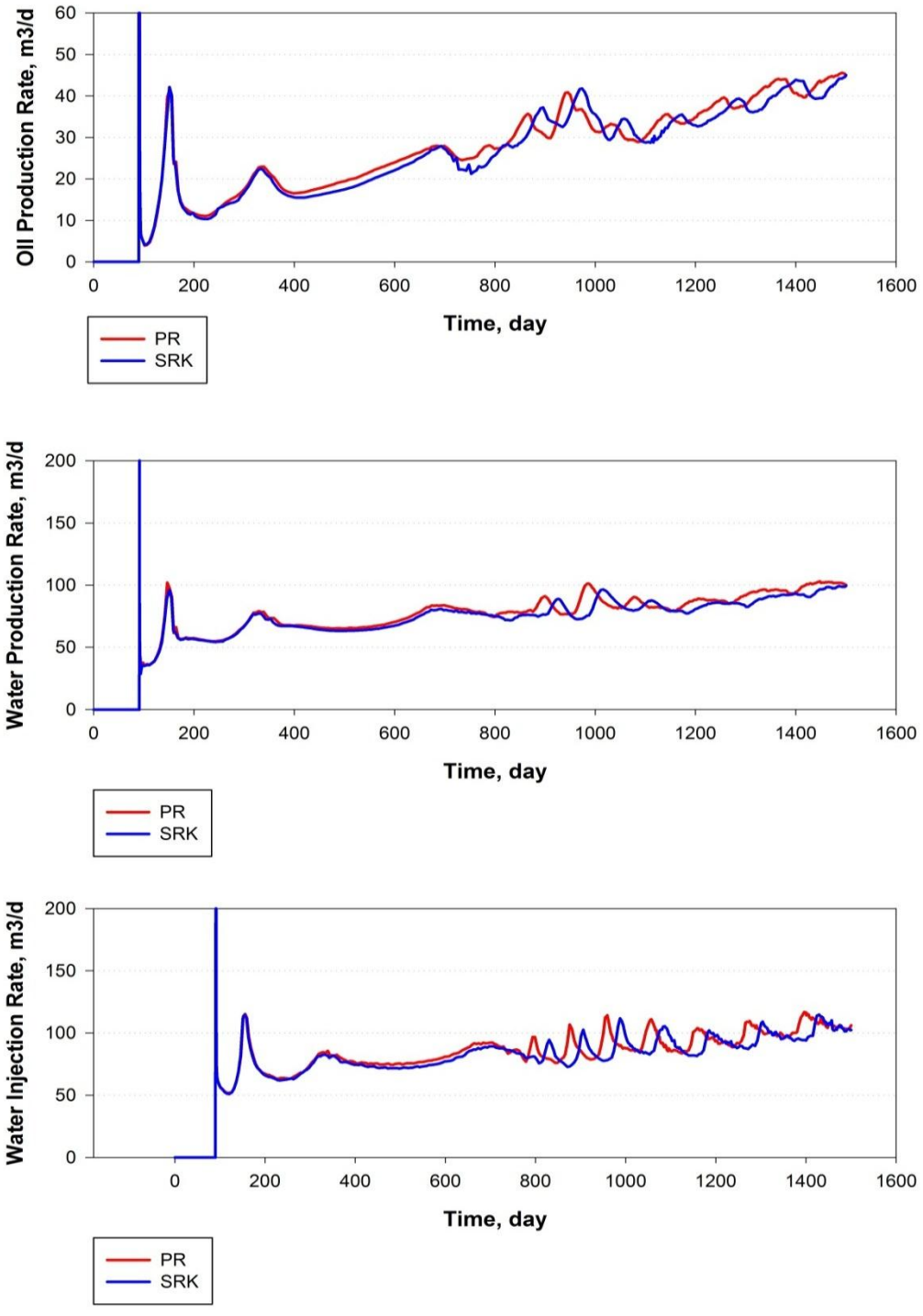

Figure 6-25: Production and injection rates for ES-SAGD case. SRK EOS vs. PR EOS

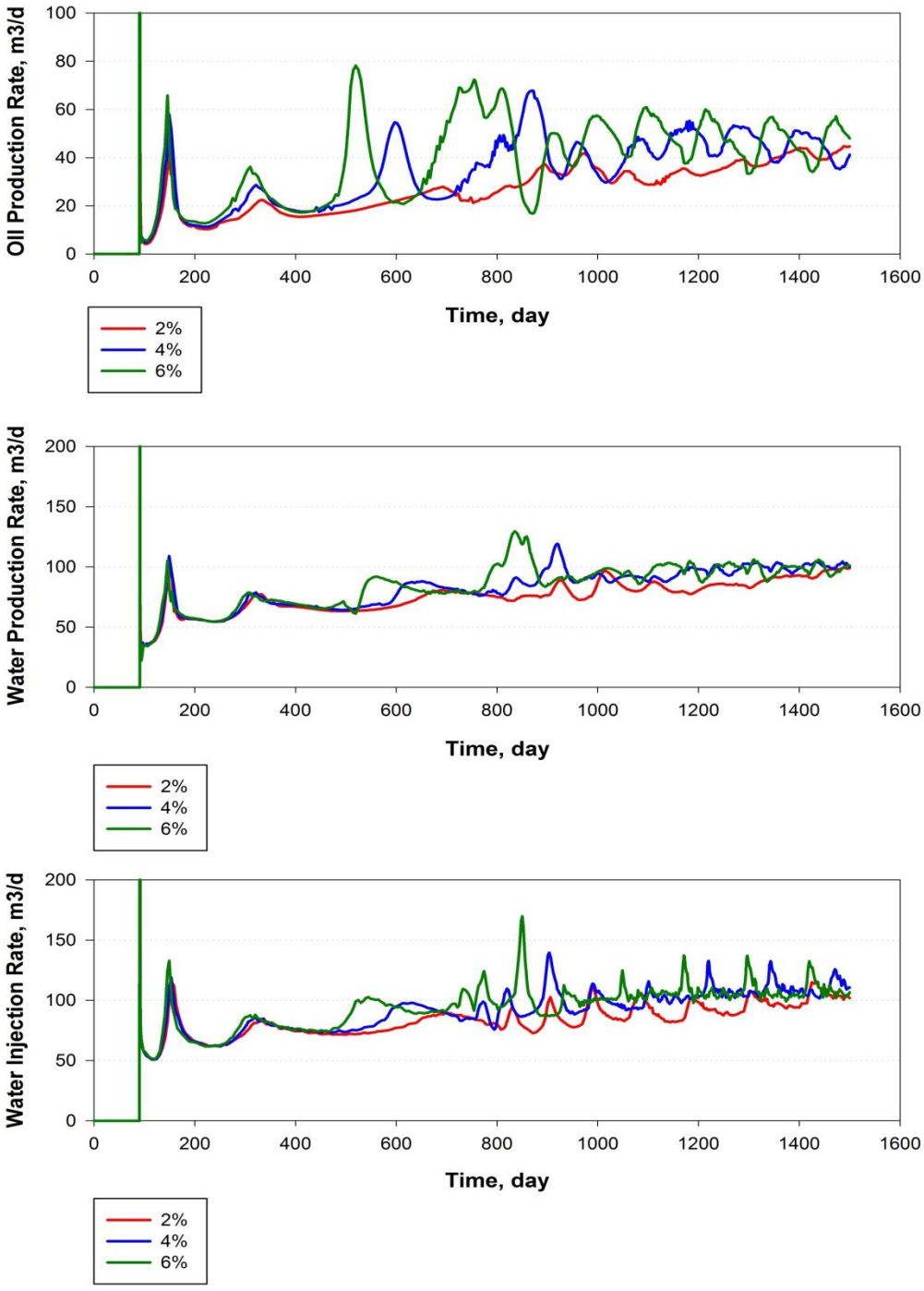

Figure 6-26: Production and injection rates for different solvent ratios

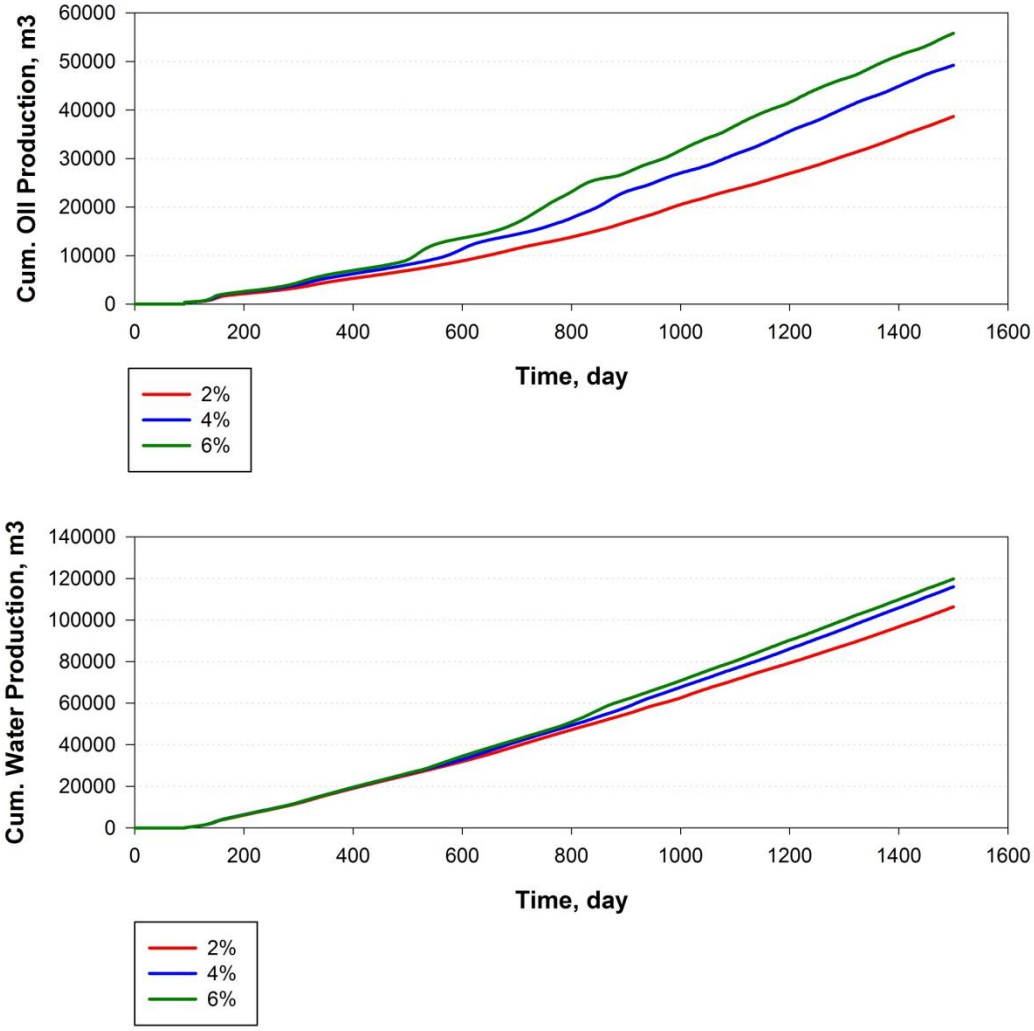

Figure 6-27: Cumulative oil and water production for different solvent ratios

6.8 **Case 7: Molecular diffusion effect**

Effect of molecular diffusion is tested in this case. The solvent is co-injected to the reservoir with steam in low percentages and it helps enhancement of viscosity reduction. The co-injected solvent mixes with bitumen by, dissolution followed by diffusion and dispersion.

In the all previous cases the molecular diffusion was assumed to be negligible since in most of field scale cases it is generally smaller than the numerical dispersion of the system. In this case we try to test this assumption. This case is exactly similar to case 3, but with molecular diffusion coefficient of 2.0E-4 and 2.0E-3 m^2/day for hexane.

Figure 6-28 shows the oil production rate, water production rate, and water injection rate, respectively. The results of no diffusion are compared with the two molecular diffusion cases. The results show there is no significant change on the oil production or injection rate by adding molecular diffusion to the ES-SAGD process in the field scale simulations. In the field scale simulations, the numerical dispersion with the used grid size is higher than the physical diffusion. In order to capture the real effect of diffusion on the simulation the grid size needs to be reduced, therefore number of grid blocks will increased and sometimes it becomes computationally impractical.

This model also was run in CMG STARS and same results were obtained. The effect of mechanical dispersion was not investigated in this study since this feature has not been completed yet. Mechanical dispersion could make an impact on the results but it will be investigated only in future extension of this work.

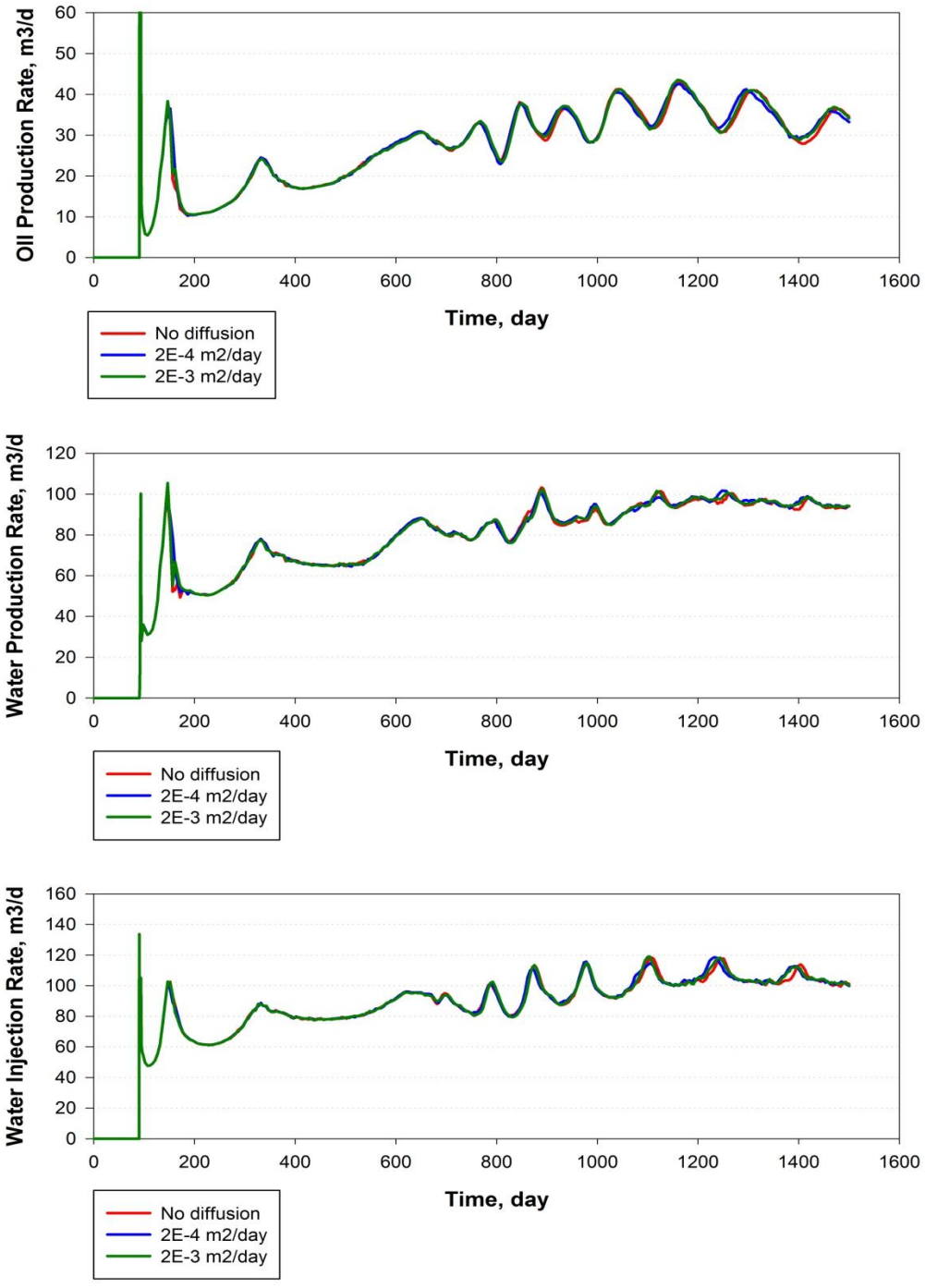

Figure 6-28: Production and injection rate of ES-SAGD process for different diffusion coefficients

6.9 **Case 8: Synthetic fluid with five component**

In this case, another fluid model is used in a 2-D model. Fluid properties, rock properties, heat loss properties, and rock-fluid properties are extracted from Brantferger dissertation (1991) and are presented in Table 6-5. The reservoir simulation model is a 2-D homogeneous and isotropic model with constant porosity, permeability and initial water and oil saturation and contains a single SAGD well-pair. The vertical distance between injector and producer is 5 m and the production well is located 2 m above the base rock.

Steam is injected with the quality of 0.85 at 478.15 K into the reservoir and it operates based on the maximum injection rate of 100 m^3/day CWE and the producer is operated under minimum BHP of 1000 kPa with constraint of no more than 10 m^3/day CWE steam rate. To establish thermal communication between the injector and producer, a preheating period of two months was modeled by using heaters. After the thermal communication was established, the wells are switched to regular SAGD mode for 700 days of simulation. The main objective of this case was to test another fluid model other than the base case fluid and compare the simulation results of EOS based simulation against the K-Value based simulation.

Table 6-5: Reservoir and fluid properties of Case 8

Number of grid blocks, (nx, ny, nx)	21,1,20
Dimension of grid blocks, (Δx, Δy, Δz), m	4.000, 50.000, 1.000
Initial Conditions:	
Temperature, K	288.150
Pressure, kPa	500.000
Initial oil saturation	0.939
Initial water saturation	0.061
Reservoir Properties:	
Porosity	0.300
Pore volume compressibility, 1/kPa	1.400E-5
Horizontal permeability, md	4000.000
Vertical permeability, md	2000.000

Well Conditions:	
Well radius, m	0.110
Steam injection rate (CWE), m^3/day	200.000
Bottomhole injection pressure, kPa	2500.00
Steam qulaity	0.850
Producer BHP, kPa	1000.000
Maximum steam production rate (CWE), m^3/day	10.000
Heater Properties	
Heater rate, kJ/day-K	1.000E5
Maximum temperature, K	453.000

Component	MW	Pc(kPa)	Tc(K)	ω	Oleic feed
H_2O	18.015	22120.000	647.370	0.344	0.000000000
C8	116.000	3482.000	575.780	0.400	0.071059441
C13	183.000	2337.000	698.000	0.840	0.086563305
C24	337.000	1207.000	821.300	1.070	0.073966441
C61+	858.000	779.000	1010.056	1.330	0.768410914

Component	C_{P1}	C_{P2}	C_{P3}	C_{P4}
H_2O	32.21218	0.003829	3.18E-05	-1.44E-08
C8	-12.28450	1.330218	-0.00076	0
C13	-5.078580	1.993745	-0.00124	0
C24	-5.684770	3.681697	-0.00229	0
C61+	0.122826	9.50287	-0.00586	0

Table 6-6 represents variation of water and oleic component viscosity versus temperature.

Table 6-6: Variation of oleic component viscosity versus temperature

Temperature, K	Viscosity, cp				
	H_2O	C8	C13	C24	C61+
283.15	1.3110	98.060	0.3415	3.415	5.50E+06
293.15	1.0050	72.880	0.3086	3.086	2.81E+05
303.15	0.8004	55.640	0.2808	2.808	6.75E+04
313.15	0.6543	43.500	0.2571	2.571	1.98E+04
323.15	0.5518	34.710	0.2366	2.366	6873.00
333.15	0.4714	28.200	0.2189	2.189	2744.00
343.15	0.4066	23.280	0.2034	2.034	1233.00
353.15	0.3570	19.500	0.1898	1.898	612.10
363.15	0.3182	16.540	0.1778	1.778	330.80
373.15	0.2828	14.180	0.1671	1.671	192.20
398.15	0.2227	10.080	0.1451	1.451	63.76
423.15	0.1848	7.518	0.1281	1.281	27.43
448.15	0.1586	5.828	0.1147	1.147	14.24
473.15	0.1394	4.656	0.1039	1.039	8.39
498.15	0.1238	3.813	9.50E-02	0.950	5.43
523.15	0.1117	3.186	8.77E-02	0.877	3.76
548.15	0.1005	2.707	8.15E-02	0.815	2.74

The relative permeability curves for three phases are similar to the base case. All of the properties that are similar to the base case can be found in the Table 6-1 and 6-2. Figure 6-29 presents oil production rate, water production rate and water injection rate for this case and its comparison with the K-Value approach. As the Figure 6-29 shows, there is not much difference between the results of these two different approaches since steam is dominant and all oleic components are non-volatile. This fluid mixture is very similar to water and dead oil mixture.

In the other test, solvent C8 was added as additive to steam with different ratios, i.e. 2% and 10% and the results were compared with the pure steam case. Addition of C8 to the steam improves

oil recovery as the injected ratio increases. Figure 6-30 represent the oil production rates of all three cases.

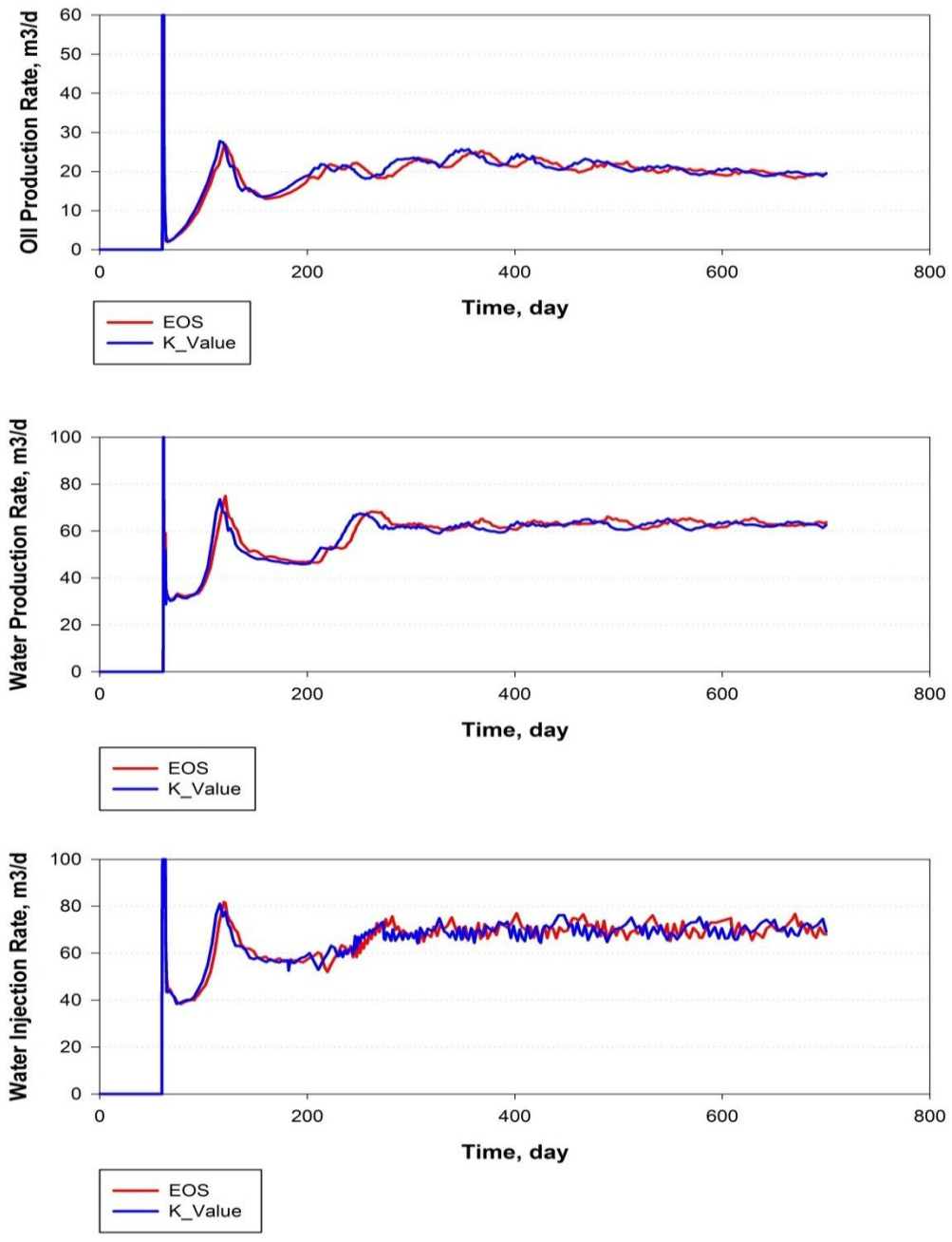

Figure 6-29: Production and injection rates of SAGD process, EOS vs. K-Value

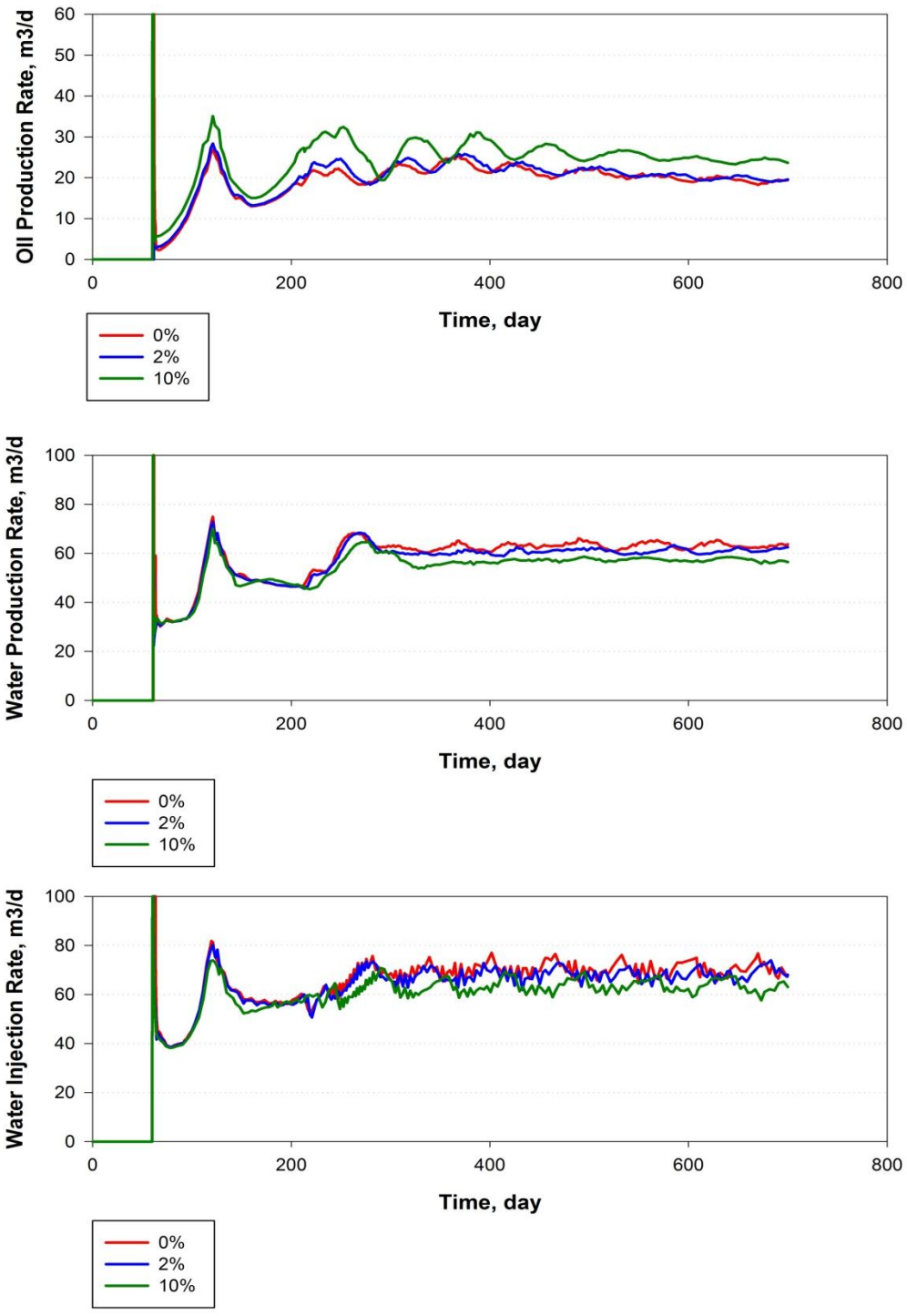

Figure 6-30: Production and injection rate of ES-SAGD process for different solvent ratios

6.10 **Case 9: Synthetic fluid with six component**

The last case uses a fluid mixture with several pseudo components. This mixture consists of water, methane, n-heptane and three more pseudo components. The fluid properties are extracted from Badamchizadeh et al. (2011) paper and they are presented in Table 6-7. The fluid properties were slightly modified to make it suitable to use in a thermal compositional simulator. The reservoir simulation model is a 2-D homogeneous and isotropic model identical with the base case. All of rock-fluid properties are taken from the base case and the same well configuration and spacing is used.

Steam is injected with the quality of 0.8 at 458.15 K into the reservoir and the injector operates based on the maximum injection rate, the producer is operated under minimum BHP of 1000 kPa and constrained to maximum of 10 m^3/day CWE steam rate. To establish thermal communication between the injector and producer, a preheating period of three months was modeled by using heaters. After the thermal communication was established, the wells are switched to regular SAGD mode for 1500 days of simulation. The main objective of this case was to test another fluid model with volatile and non-volatile components and compare the simulation results of EOS based simulation against the K-Value based simulation.

Similar to the base case, SRK equation of sate was used in this simulation and CMG Winprop properties for thermal expansion, compressibility factor, reference molar density and equilibrium ratio were used in K-Value approach. Reference enthalpy of system was calculated at the initial reservoir temperature.

Table 6-7: Reservoir and fluid properties of Case 9

Initial Conditions:	
Temperature, K	283.150
Pressure, kPa	500.000
Initial oil saturation	0.849
Initial water saturation	0.151
Well Conditions:	
Well radius, m	0.110
Steam injection rate (CWE), m^3/day	200.000
Bottomhole injection pressure, kPa	2500.000
Steam qulaity	0.800
Injection temperature, K	458.150
Producer BHP, kPa	1000.000
Maximum steam production rate (CWE), m^3/day	10.000
Heater Properties	
Heater rate, kJ/day-K	5.000E4
Maximum temperature, K	458.150

Component	MW	Pc(kPa)	Tc(K)	ω	Oleic feed
H_2O	18.015	22054.397	647.37	0.344	0.000000000
nC7	100.205	2735.775	540.2	0.351	0.000599985
C1	16.043	4600.155	190.6	0.008	0.008399990
C11-C28	305.509	1703.757	826.12749	0.721	0.297999973
C29-C45	505.590	1311.297	955.4321	1.000	0.618699944
C46+	863.921	834.134	1222.0442	1.518	0.074300007

Component	C_{P1}	C_{P2}	C_{P3}	C_{P4}
H_2O	34.4905782	-0.0142552	4.73E-05	-3.57E-08
nC7	-9.7070371	0.69606943	-0.0003998	1.02E-07
C1	37.9301062	-0.0684086	0.00027245	-2.39E-07
C11-C28	-58.156128	1.86177618	-0.0007698	0
C29-C45	-74.250572	2.95272034	-0.0012026	0
C46+	-36.838282	4.88550304	-0.0018791	0

Table 6-8 represents variation of water and oleic component viscosity versus temperature.

Table 6-8: Variation of oleic component viscosity versus temperature

Temperature, K	**Viscosity, cp**					
	H_2O	**nC7**	**C1**	**C11-C28**	**C29-C45**	**C46+**
278.15	1.10129497	0.80102	0.015307	204.03	96236	4.48E+13
293.939	0.82183203	0.60865	0.021105	71.302	13925	4.25E+11
309.729	0.63185301	0.48804	0.02837	30.421	2874.4	9108500000
325.518	0.49834614	0.39639	0.036809	15.213	786.77	373370000
341.308	0.40177045	0.32389	0.046112	8.6231	269.37	25761000
357.097	0.33014401	0.26959	0.056096	5.3887	110.08	2702900
372.887	0.27583263	0.22768	0.066604	3.6408	51.887	399100
388.676	0.2338484	0.19449	0.077523	2.6195	27.468	78015
404.466	0.20082505	0.16763	0.088777	1.9835	15.998	19233
420.255	0.17445098	0.14548	0.10032	1.5658	10.087	5752.2
436.045	0.15309235	0.12688	0.11208	1.2792	6.7963	2023.2
451.834	0.13558172	0.11098	0.12397	1.075	4.8439	815.97
467.624	0.12106206	0.097083	0.13584	0.92478	3.6215	369.72
483.413	0.10890089	0.084581	0.14746	0.81147	2.8211	185.1
499.203	0.09861898	0.072769	0.15851	0.72442	2.2778	101.06
514.992	0.08985313	0.060262	0.16863	0.65801	1.9015	59.622
530.782	0.08232065	0.23982	0.18261	0.50526	1.3483	31.066
546.571	0.0758025	0.23986	0.19012	0.45041	1.1639	20.397
562.361	0.07012419	0.23856	0.19585	0.40402	1.0232	14.067
578.15	0.06514802	0.23577	0.19956	0.36444	0.9131	10.124

The relative permeability curves for three phases are similar to the base case. All of the properties that are similar to the base case can be found in the Table 6-1 and 6-2. Figure 6-31 presents oil production rate, water production rate and water injection rate for this case and its comparison with the K-Value approach. As the Figure 6-31 shows, there is not much difference between the results of these two different approaches.

In the next step C7 is added as steam additive with 5 percent solvent ratio in an ES-SAGD process. Simulation was run in both EOS and K-Value approach. Then the results of ES-SAGD case from both EOS and K-Value approach are compared to see the effect of EOS on the final results. Figure 6-32 presents oil production rate, water production rate and water injection rate for both approaches. Unlike the previous examples at the end of simulation, oil production rate, water production rate and water injection rate of EOS approach is higher than the K-Value approach. A closer look at Figure 6-33 reveals that the deviation started around 900 days of simulation.

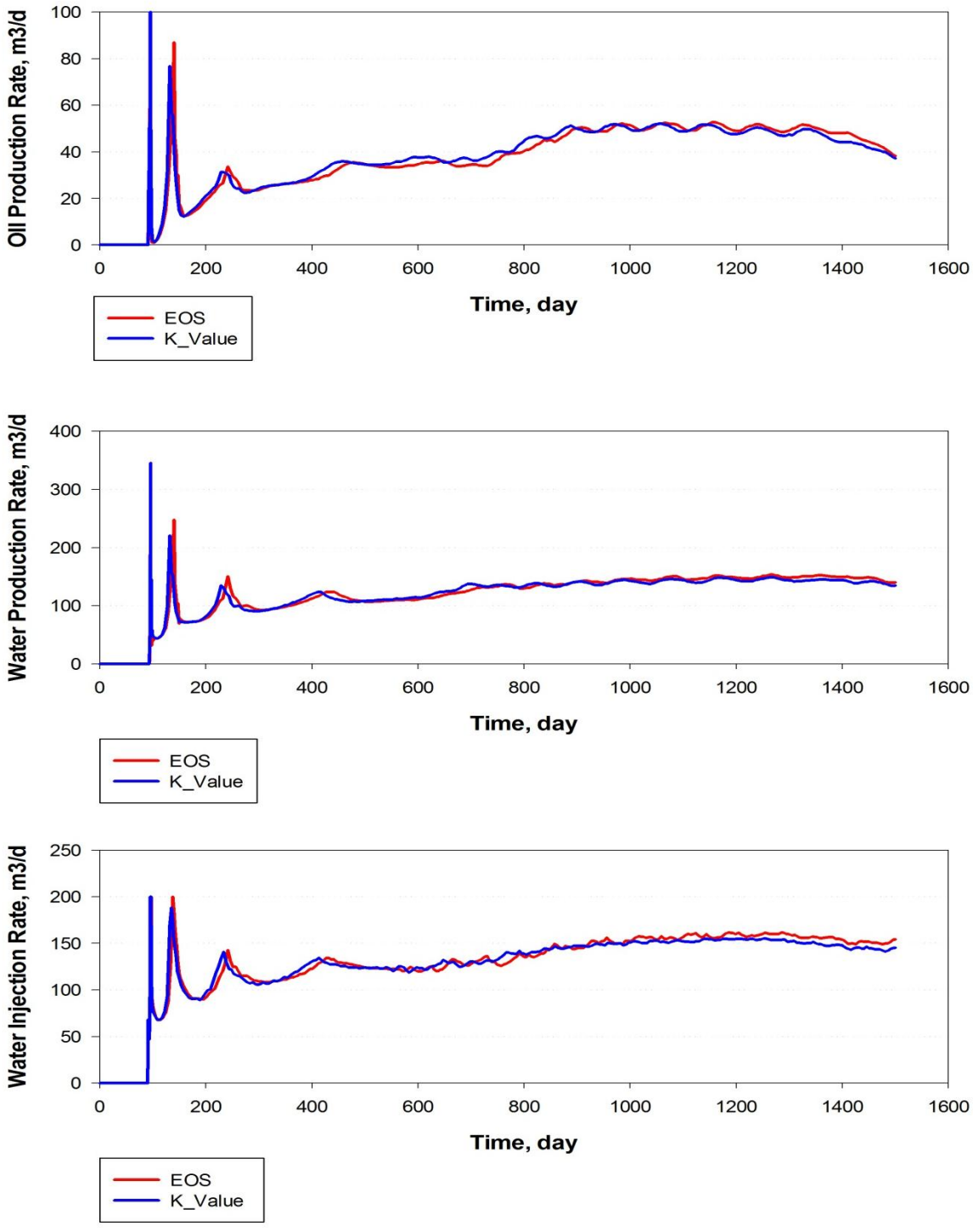

Figure 6-31: Production and injection rate of SAGD process, EOS vs. K-Value

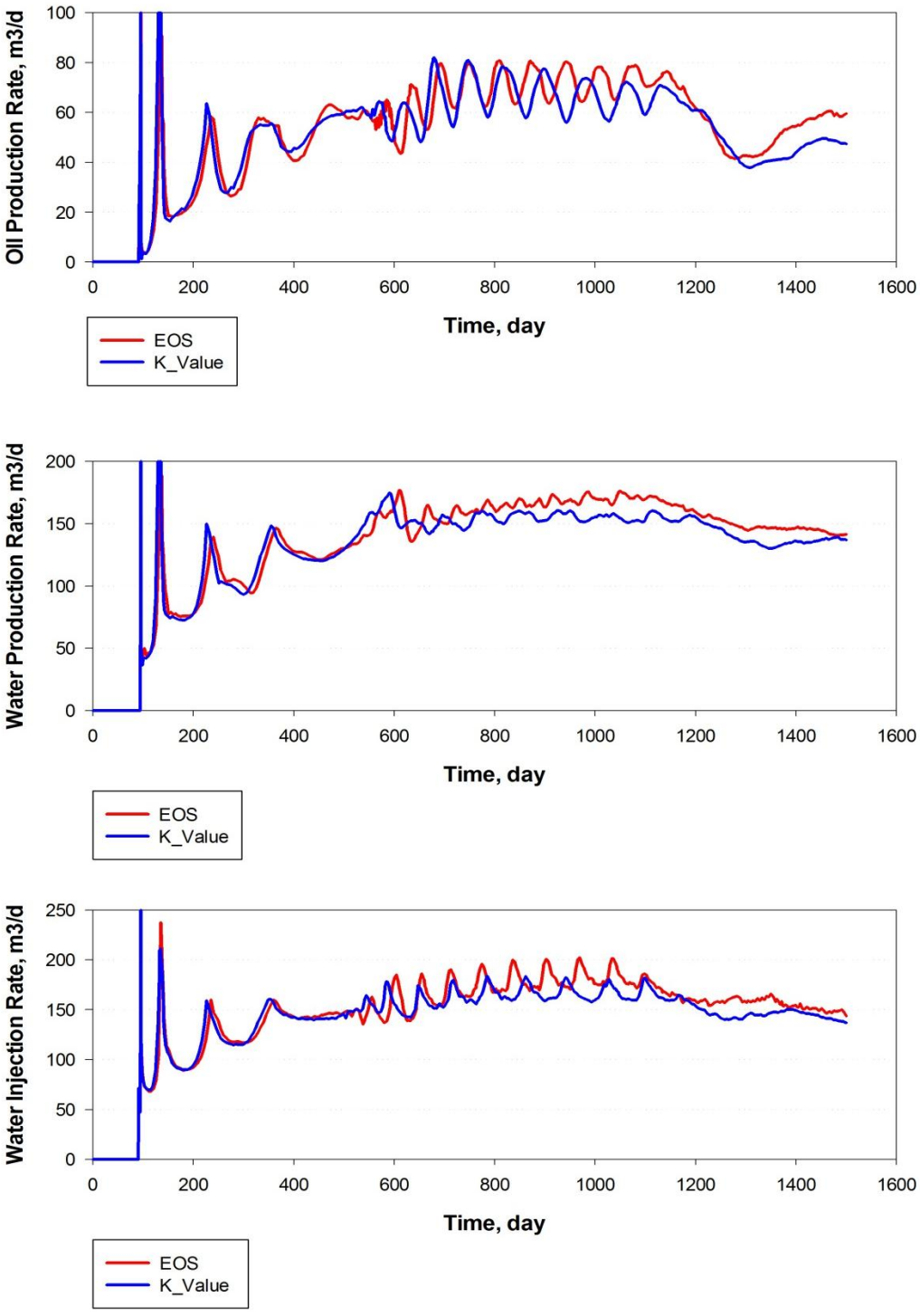

Figure 6-32: Production and injection rate of ES-SAGD process, EOS vs. K-Value

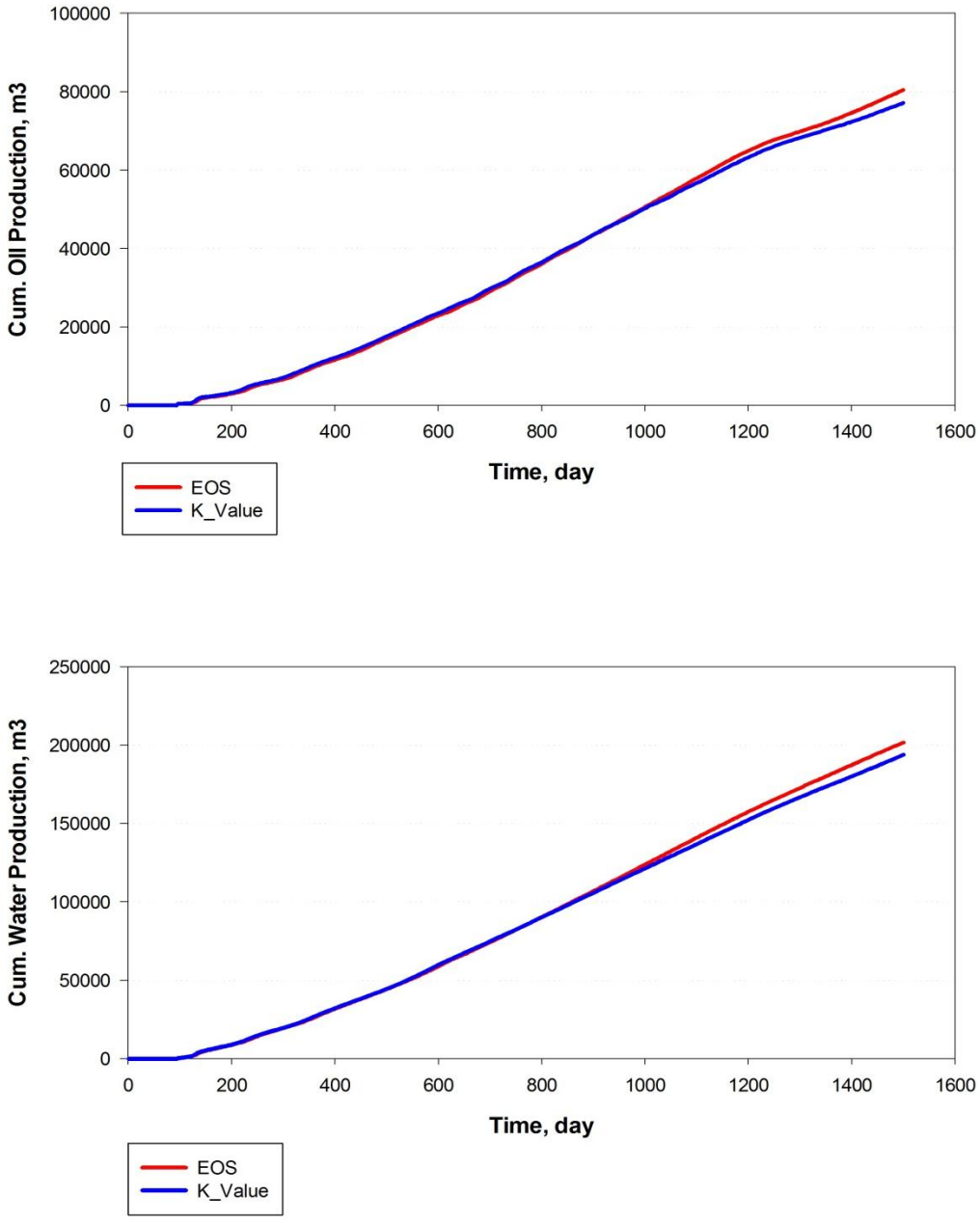

Figure 6-33: Cumulative oil and water production rate of ES-SAGD process, EOS vs. K-Value

Chapter Seven: **CONCLUSIONS AND RECOMMENDATIONS**

This dissertation has presented an investigation of the effect of using an equation of state based PVT model instead of the K-Value based model in numerical simulation of thermal and hybrid processes such as SAGD and ES-SAGD. This study and its contribution are divided into two major categories. First, a new isenthalpic multiphase flash calculation suitable for thermal compositional simulator was developed. Second, the isenthalpic multiphase flash calculation was accommodated in the thermal compositional simulator and a new thermal compositional simulator capable of computing the thermodynamic properties of fluids by equation of state was developed. In the next two sections more details will be provided.

7.1 **Isenthalpic multiphase flash calculations**

The new flash method was shown to have both speed and robustness which is crucial for a thermal compositional simulator and its results are as accurate as the currently available algorithms. This new method which works based on the negative flash concept was validated and tested against commercial PVT packages. The results are in very good agreement with the results of current standard methods. The biggest advantage of this new method is that it is completely independent of stability analysis and therefore it is computationally less expensive than the current methods.

The new isenthalpic multiphase flash calculation method shows it is capable of handling difficult situations such as narrow boiling point regions, phase appearance and phase disappearance, which are common in thermal and hybrid processes.

The new method is not sensitive to the initial guess for temperature. Good initial guess for temperature is very important in many current isenthalpic flash calculations, specifically for schemes that use Newton's method to solve energy and material balance equations simultaneously. In all tests of the new scheme that were presented in this dissertation, the same initial guess for temperature was used.

Another important feature of this method is that the equilibrium ratios are initialized with the Wilson correlation (1969) and it worked in all of the presented examples. It is worth mentioning that any method of initialization could be used with the current method, but it was unnecessary in our cases.

7.2 **EOS based 3-D thermal compositional simulator**

A new numerical simulator was developed in this study to enable us to quantify the effect of some of thermodynamic properties on the performance of thermal and hybrid processes. The new model is a three dimensional, three phase thermal compositional reservoir simulator capable of solving mass transfer equation of different components in the system and the energy equations. It is suitable for simulating any kind of thermal and non-thermal processes. All of thermodynamic properties are calculated from its PVT package and therefore it provides thermodynamically consistent calculations.

The simulator also has capability of running in two different modes. User can specify EOS or K-Value mode to simulate thermal and hybrid processes.

The results of this study shows that equilibrium ratios of different component vary with compositions of different phases and it is not always right to use correlation which are only function of temperature and pressure.

The mutual solubility of water in oil phase is not negligible at high temperature and it must be considered in simulations. The results of this simulator show that the solubility of water component could be as high as 10 mole percent in oleic phase. On the other hand the solubility of other component in aqueous phase was negligible in all of the presented cases.

The EOS provides us with better and more accurate calculation of phase properties and it has a significant effect on the final recovery of the hybrid processes. It also affects the time of appearance or disappearance of phases in grid blocks and breakthrough events could happen at different times.

It was shown in the grid to grid level analysis of the EOS and K-Value approaches that the mole fraction of components in oleic phase remains unchanged during the life of steam injection processes. When steam appears in a grid block, usually the temperature remains at the steam saturation temperature and the equilibrium ratios also remain unchanged. In hybrid processes where, a small amount of solvent is added to the steam, the most significant variations happens at the edge of steam chamber, but when the grid block is not at the edge of steam chamber, the equilibrium ratios remain more or less unchanged.

7.3 **Recommendations for future works**

Currently this model has only diffusion coefficient in mass transfer equations. Mechanical dispersion is an important feature in processes like VAPEX, Hot VAPEX, and lab scale hybrid processes and should be added to the current model.

The current model only simulates non-reactive processes and it cannot be used to simulate processes such as in-situ combustion, coal gasification, and foamy oil reservoirs. It is necessary to add a reaction term to the conservation equations in order to simulate the latter processes.

This simulator has been written in a way that the further development would be easy to add to the main code. For example it is easy to change this model to handle any type of boundary conditions. The commercial simulators are volumetric and users need to define pseudo wellbores at boundary of reservoir to mimic the effect of boundary. Therefore this software could be used as a platform for any future academic development.

REFERENCES

Abdalla, A., and Coats, K. "A Three-Phase Experimental and Numerical Simulation Study of the Steam Flood Process." *Paper SPE 3600 presented at Fall Meeting of the Society of Petroleum Engineers of AIME*, New Orleans, Louisiana, 3-6 October 1971.

Abou-Kassem, J. H. (1996). "Practical considerations in developing numerical simulators for thermal recovery." *Journal of Petroleum Science and Engineering*, 15(2), 281-290.

Abou-Kassem, J.H., and Aziz, K. (1985). "Handling of phase change in thermal simulators." *Journal of petroleum technology*, 37(09), 1,661-1,663.

Abou-Kassem, J. H., and Aziz, K. "Grid orientation during steam displacement." *Paper SPE 10497 presented at SPE Reservoir Simulation Symposium*, New Orleans, Louisiana, 31 January-3 February 1982.

Agarwal, R. K., Li, Y.-K., Nghiem, L. X., and Coombe, D. A. (1991). "Multiphase multicomponent isenthalpic flash calculations." *Journal of Canadian Petroleum Technology*, 30(03), 69-75.

Amirijafari, B., and Campbell, J. M. (1972). "Solubility of gaseous hydrocarbon mixtures in water." *Society of Petroleum Engineers Journal*, 12(01), 21-27.

Aziz, K., Ramesh, A., and Woo, P. (1987). "Fourth SPE comparative solution project: comparison of steam injection simulators." *J. Pet. Technol*, 39(12), 1576-1584.

Aziz, K., and Settari, A. (1986). *Fundamentals of reservoir simulation*: Elsevier Applied Science Publishers New York.

Badamchizadeh, A., Kohse, B. F., and Kumar, A. "Modeling of Asphaltene Precipitation Due to Steam and n-alkane Co-injection in the ES-SAGD Process." *Paper SPE 149411 presented at Canadian Unconventional Resources Conference*, Calgary, Alberta, 15-17 November 2011.

Baker, L. E., Pierce, A. C., and Luks, K. D. (1982). "Gibbs energy analysis of phase equilibria." *Society of Petroleum Engineers Journal*, 22(05), 731-742.

Behie, A. and Forsyth Jr., P.A. "Practical Considerations for Incomplete Factorization Methods in Reservoir Simulation." *Paper SPE 12263 presented at SPE Symposium on Reservoir Simulation*, San Francisco, California, 15-18 November 1983.

Boston, J., and Britt, H. (1978). "A radically different formulation and solution of the single-stage flash problem." *Computers & Chemical Engineering*, 2(2), 109-122.

Brantferger, K. M. (1991). *Development of a thermodynamic consistent, fully implicit, compositional, equation-of-state, steam flood simulator*, PhD Thesis, The University of Texas at Austin, Austin, Texas.

Buchanan, W.L. "Simulating steam additive EOR processes." *Paper SPE 13522 presented at SPE Reservoir Simulation Symposium*, Dallas, Texas, 10-13 February 1885.

Buckley, S., and Leverett, M. (1942). "Mechanism of fluid displacement in sands." *Trans. AIME*, 146(01), 107-116.

Calsep, PVTsim, Version 20.0, Houston, Texas, 2012.

Chan, M., and Sarioglu, G. "Numerical Modelling of Cyclically Steamed and Fractured Oil-Sand Reservoirs." *Paper SPE 22369 presented at International Meeting on Petroleum Engineering*, Beijing, China, 24-27 March 1992.

Chien, H. H. Y. (1994). "Formulations for three-phase flash calculations." *AIChE journal*, 40(6), 957-965.

Chien, M., Yardumian, H., Chung, E., and Todd, W. "The formulation of a thermal simulation model in a vectorized general purpose reservoir simulator." *Paper SPE 18418 presented at SPE Symposium on Reservoir Simulation*. Houston, Texas, 6-8 February 1989.

Chung, K., and Butler, R. (1988). "Geometrical Effect of Steam Injection on the Formation of Emulsions in the Steam-Assisted Gravity Drainage Process." *Journal of Canadian Petroleum Technology*, 27(01), 36-42.

Cicek, O. and Ertekin, T. "Development and Testing of a New 3D Field Scale Fully Implicit Multi-Phase Compositional Steam Injection Simulator," *Paper SPE 35516 presented at European 3D Reservoir Modeling Conference*, Norway, April 1996.

Computer Modeling Group Ltd, STARS User's Guide, 2013.10, 2013.

Computer Modeling Group Ltd. WINPROP, Phase Property Program, User's Guide, 2013.

Coats, K. (1976). "Simulation of steamflooding with distillation and solution gas." *Society of Petroleum Engineers Journal*, 16(05), 235-247.

Coats, K., George, W., Chu, C., and Marcum, B. (1974). "Three-dimensional simulation of steamflooding." *Society of Petroleum Engineers Journal*, 14(06), 573-592.

Coats, K. H. (1978). "A highly implicit steam flood model." *Society of Petroleum Engineers Journal*, 18(5), 369-383.

Coats, K. H. (1980). "In-situ combustion model." *Society of Petroleum Engineers Journal*, 20(06), 533-554.

Corey, A. T. (1954). "The interrelation between gas and oil relative permeabilities." *Producers monthly*, 19(1), 38-41.

Crookston, R., Culham, W., and Chen, W. (1979). "A numerical simulation model for thermal recovery processes." *Society of Petroleum Engineers Journal*, 19(01), 37-58.

Das, S. "Diffusion and dispersion in the simulation of Vapex process." *Paper SPE 97924 presented at SPE International Thermal Operations and Heavy Oil Symposium*. Calgary, Alberta, 1-3 November 2005.

Das, S. K., and Butler, R. M. (1996). "Diffusion coefficients of propane and butane in Peace River bitumen." *The Canadian Journal of Chemical Engineering*, 74(6), 985-992.

Das, S. K., and Butler, R. M. (1998). "Mechanism of the vapor extraction process for heavy oil and bitumen." *Journal of Petroleum Science and Engineering*, 21(1), 43-59.

ECLIPSE Technical Description, Schlumberger, February 2010

Farouq-Ali, S. M. "Multiphase multidimensional simulation of in-situ combustion" *Paper SPE 6896 presented at SPE Annual Fall Technical Conference and Exhibition*. Denver, Colorado, 9-12 October 1977.

Ferrer, J., and Farouq-Ali, S. M. (1977). "A Three-Phase Two-Dimensional Compositional Thermal Simulator for Steam Injection Processes." *Journal of Canadian Petroleum Technology*, 16(01).

Forsyth Jr, P., Rubin, B., and Vinsome, P. (1981). "The Elimination of the Constraint Equation And Modelling of Problems With a Non-condensable Gas In Steam Simulation." *Journal of Canadian Petroleum Technology*, 20(04), 63-68.

Garthoffner, E.H. "The role of oil-in-water emulsions in thermal oil recovery processes." *Paper 7952 presented at SPE California Regional Meeting*. Ventura, California, 18-20 April 1979.

Gates, I. D. (2007). "Oil phase viscosity behaviour in expanding-solvent steam-assisted gravity drainage." *Journal of Petroleum Science and Engineering*, 59(1), 123-134.

Glandt, C. A. and Chapman, W.G. (1995). "Effect of Water Dissolution in Oil Viscosity." *SPE Reservoir Engineering*, 10(01), 59-64.

Grabowski, J. W., Vinsome, P. K., Lin, R. C., Behie, G., and Rubin, B. "A fully implicit general purpose finite-difference thermal model for in situ combustion and steam." *Paper SPE 8396 presented at SPE Annual Technical Conference and Exhibition*, Las Vegas, Nevada, 23-26 September 1979.

Griswold, J., and Kasch, J. (1942). "Hydrocarbon-water solubilities at elevated temperatures and pressures." *Industrial & Engineering Chemistry*, 34(7), 804-806.

Heidemann, R. A. (1974). "Three-phase equilibria using equations of state." *AIChE Journal*, 20(5), 847-855.

Heidman, J., Tsonopoulos, C., Brady, C., and Wilson, G. (1985). "High-temperature mutual solubilities of hydrocarbons and water. Part II: Ethylbenzene, ethylcyclohexane, and n-octane." *AIChE journal*, 31(3), 376-384.

Huang, C. K. (2009). *Development of a General Thermal Oil Reservoir Simulator under a Modularized Framework*, PhD Thesis, The University of Utah, Utah.

Huang, C.-K., Yang, Y.-K., and Deo, M. D. "A new thermal-compositional reservoir simulator with a novel" equation line-up" method." *Paper SPE 110219 presented at SPE Annual Technical Conference and Exhibition*, Anaheim, California, 11-14 November 2007.

Iranshahr, A., Voskov, D. V., and Tchelepi, H. A. "Phase Equilibrium Computations Are No Longer the Bottleneck in Thermal Compositional EOS Based Simulation." *Paper SPE 119166 presented at SPE Reservoir Simulation Symposium*, Woodlands, Texas, 2-4 February 2009.

Ishimoto, K. (1985). *One-dimensional fully implicit compositional model for steam flooding*. M.Sc. Thesis, University of Texas at Austin.

Ito, Y. "One dimension computer model for simulating oil recovery by steam flooding", M.Sc. Thesis, Department of Chemical and Petroleum engineering, University of Calgary, Calgary, Alberta, January, 1977.

Karmaker, K., and Maini, B. B. "Experimental investigation of oil drainage rates in the VAPEX process for heavy oil and bitumen reservoirs." *Paper SPE 84199 presented at SPE Annual Technical Conference and Exhibition*, Denver, Colorado, 5-8 October 2003.

Lapene, A., Nichita, D. V., Debenest, G., and Quintard, M. (2010). "Three-phase free-water flash calculations using a new Modified Rachford–Rice equation." *Fluid Phase Equilibria*, 297(1), 121-128.

Lauwerier, H. (1955). "The transport of heat in an oil layer caused by the injection of hot fluid." *Applied Scientific Research, Section A*, 5(2-3), 145-150.

Leaute, R., and Carey, B. (2007). "Liquid addition to steam for enhancing recovery (LASER) of bitumen with CSS: Results from the first pilot cycle." *Journal of Canadian Petroleum Technology*, 46(9), 22-30.

Leaute, R. P. "Liquid addition to steam for enhancing recovery (LASER) of bitumen with CSS: Evolution of technology from research concept to a field pilot at Cold Lake." *Paper SPE 79011 presented at SPE International Thermal Operations and Heavy Oil Symposium and International Horizontal Well Technology Conference*, Calgary, Alberta, 4-7 November 2002.

Luo, S., and Barrufet, M. (2005). "The Effect of Water-in-Oil Solubility on Oil Reservoir in the Steam-Injection Process." *SPE Reservoir Evaluation & Engineering*, 8(06), 528-533.

McKetta, J. J., and Katz, D. L. (1948). "Methane–n-butane–water system in two-and three-phase regions." *Industrial & Engineering Chemistry*, 40(5), 853-863.

Michelsen, M. L. (1982). "The isothermal flash problem. Part I. Stability." *Fluid Phase Equilibria*, 9(1), 1-19.

Michelsen, M. L. (1982). "The isothermal flash problem. Part II. Phase-split calculation." *Fluid Phase Equilibria*, 9(1), 21-40.

Michelsen, M. L. (1987). "Multiphase isenthalpic and isentropic flash algorithms." *Fluid phase equilibria*, 33(1), 13-27.

Mifflin, R., Watts, J., and Weiser, A. "A Fully Coupled Fully Implicit Reservoir Simulator for Thermal and Other Complex Reservoir Processes." *Paper SPE 21252 presented at SPE Symposium on Reservoir Simulation*, Anaheim, California, 17-20 February 1991.

Naccache, P.F. "A fully-implicit thermal reservoir simulator." *Paper SPE 37985 presented at* SPE Reservoir Simulation Symposium, Dallas, Texas, 8-11 June 1997.

Nasr, T. N., and Isaacs, E. E. (2001). "Process for enhancing hydrocarbon mobility using a steam additive." U.S. Patents.

Nelson, P. (1987). "Rapid phase determination in multiple-phase flash calculations." *Computers & chemical engineering*, 11(6), 581-591.

Nelson, W. L. (1956). "Solubility of water in oil." *Oil & Gas J*, 140.

Nutakki, R., Firoozabadi, A., Wong, T., and Aziz, K. "Calculation of Multiphase Equilibrium for Water-Hydrocarbon Systems at High Temperature." *Paper SPE 17390 presented at SPE Enhanced Oil Recovery Symposium*, Tulsa, Oklahoma, 16-21 April 1988.

Peaceman, D. W. (1983). "Interpretation of well-block pressures in numerical reservoir simulation with nonsquare grid blocks and anisotropic permeability." *Society of Petroleum Engineers Journal*, 23(03), 531-543.

Peng, D. Y., and Robinson, D. B. (1976). "Two and three phase equilibrium calculations for systems containing water." *The Canadian Journal of Chemical Engineering*, 54(5), 595-599.

Prausnitz, J. M., Anderson, F., Grens, E., Eckert, C., Hsieh, R., and O'connell, J. (1980). *Computer calculations for multicomponent vapor-liquid and liquid-liquid equilibria*: Prentice-Hall Englewood Cliffs, NJ.

Rachford Jr, H., and Rice, J. (1952). "Procedure for use of electronic digital computers in calculating flash vaporization hydrocarbon equilibrium." *Journal of Petroleum Technology*, 4(10), 19-3.

Reid, R. C., Prausnitz, J. M., and Poling, B. E. (1987). *The properties of gases and liquids*.: 4th Ed.,McGraw-Hill Co., New York, NY

Rivero, J., and Mamora, D. "Production acceleration and injectivity enhancement using steam-propane injection for Hamaca extra-heavy oil." *Paper SPE 75129 presented at SPE/DOE Improved Oil Recovery Symposium*, Tulsa, Oklahoma, 13-17 April 2002.

Rubin, B., and Buchanan, W. L. (1985). "A general purpose thermal model." *Society of Petroleum Engineers Journal*, *25*(02), 202-214.

Rubin, B., and Vinsome, P. (1980). "The Simulation of the In-Situ Combustion Process in One Dimension Using a Highly Implicit Finite-Difference Scheme." *Journal of Canadian Petroleum Technology*, 19(04).

Saad, Y. (1990). *SPARSKIT: A basic toolkit for sparse matrix computations*. Moffet Field, California: Research Institute for Advanced Computer Science, NASA Ames Research Center.

Saad, Y., and Schultz, M. (1986). "GMRES: A Generalized Minimum Residual Algorithm for solving non-symmetric linear systems." *SIAM Journal on scientific and statistical computing*, *7*(03), 856-869.

Shutler, N. D. (1969). "Numerical, Three-Phase Simulation of the Linear Steamflood Process." 9(2), 232-246.

Shutler, N. D. (1970). "Numerical Three-Phase Model of the Two-Dimensional Steamflood Process." 10(4), 405-417.

Soave, G. (1972). "Equilibrium constants from a modified Redlich-Kwong equation of state." *Chemical Engineering Science*, 27(6), 1197-1203.

Stateva, R. P., and Tsvetkov, S. G. (1994). "A diverse approach for the solution of the isothermal multiphase flash problem. Application to vapor-liquid-liquid systems." *The Canadian Journal of Chemical Engineering*, 72(4), 722-734.

Stone, H. (1973). "Estimation of three-phase relative permeability and residual oil data." *Journal of Canadian Petroleum Technology*, 12(04).

Stone, T. W., and Nolen, J. S. "Practical and robust isenthalpic/isothermal flashes for thermal fluids." *Paper SPE 118893 presented at SPE Reservoir Simulation Symposium*, The Woodland, Texas, 2-4 February 2009.

Tang, Y., and Saha, S. (2003). "An efficient method to calculate three-phase free-water flash for water-hydrocarbon systems." *Industrial & engineering chemistry research*, 42(1), 189-197.

Trangenstein, J. "Minimization of Gibbs free energy in compositional reservoir simulation." *Paper SPE 13520 presented at SPE Reservoir Simulation Symposium*, Dallas, Texas, 10-13 February 1985.

Trangenstein, J. A. (1987). "Customized minimization techniques for phase equilibrium computations in reservoir simulation." *Chemical Engineering Science*, 42(12), 2847-2863.

Tsonopoulos, C., and Wilson, G. (1983). "High-temperature mutual solubilities of hydrocarbons and water. Part I: Benzene, cyclohexane and n-hexane." *AIChE journal*, 29(6), 990-999.

Varavei, A. (2009). *Development of an Equation-of-State Thermal Flooding Simulator*, PhD Thesis, The University of Texas at Austin, Austin, Texas.

Varavei, A., and Sepehrnoori, K. "An EOS-Based Compositional Thermal Reservoir Simulator." *Paper SPE 119154 presented at SPE Reservoir Simulation Symposium*, The Woodland, Texas, 2-4 February 2009.

Vinsome, P. " A numerical description of hot-water and steam drives by the finite-difference method." *Paper SPE 5248 presented at* Fall Meeting of the Society of Petroleum Engineers of AIME, Houston, Texas, 6-9 October 1974.

Vinsome, P., and Westerveld, J. (1980). "A Simple Method for Predicting Cap And Base Rock Heat Losses In Thermal Reservoir Simulators." *Journal of Canadian Petroleum Technology*, 19(03).

Wilson, G. M. "A modified Redlich-Kwong equation of state, application to general physical data calculations." *Presented at 65th National AIChE Meeting, Cleveland, Ohio, May 1969*.

Yaws, C., Pan, X., and Lin, X. (1993). "Water solubility data for 151 hydrocarbons." *Chemical Engineering (New York);(United States)*, 100(2).

Yazdani, A. (2007). *Physical and numerical modeling of permeability and drainage height effects in Vapex*, PhD Thesis, University of Calgary, Calgary, Alberta, Canada.

Yazdani, A., and Maini, B. B. (2005). "Effect of Height and Grain Size on the Production Rates in the Vapex Process: Experimental Study." *SPE Reservoir Evaluation & Engineering*, 8(03), 205-213.

Youngren, G. K. (1980). "Development and application of an in-situ combustion reservoir simulator." *Society of Petroleum Engineers Journal*, 20(01), 39-51.

APPENDIX A

Derivatives of SRK equation of state with respect to temperature, pressure and component mole number

SRK compressibility Factor:

$$F = Z^3 - Z^2 + \left(A - B - B^2\right)Z - AB = 0 \qquad \textbf{A. 1}$$

Derivatives of compressibility factor with respect to pressure:

$$\frac{\partial F}{\partial Z} = 3Z^2 - 2Z + \left(A - B - B^2\right) \qquad \textbf{A. 2}$$

$$\frac{\partial F}{\partial A} = Z - B \qquad \textbf{A. 3}$$

$$\frac{\partial F}{\partial B} = -\left(1 + 2B\right)Z - A \qquad \textbf{A. 4}$$

$$\frac{\partial Z}{\partial P} = -\frac{\left(\frac{\partial F}{\partial A}\frac{\partial A}{\partial P} + \frac{\partial F}{\partial B}\frac{\partial B}{\partial P}\right)}{\frac{\partial F}{\partial Z}} \qquad \textbf{A. 5}$$

Derivatives of compressibility factor with respect to temperature:

$$\frac{\partial Z}{\partial T} = -\frac{\left(\frac{\partial F}{\partial A}\frac{\partial A}{\partial T} + \frac{\partial F}{\partial B}\frac{\partial B}{\partial T}\right)}{\frac{\partial F}{\partial Z}} \qquad \textbf{A. 6}$$

Derivatives of compressibility factor with respect to mole number:

$$\frac{\partial Z}{\partial n_k} = -\frac{\left(\frac{\partial F}{\partial A}\frac{\partial A}{\partial n_k} + \frac{\partial F}{\partial B}\frac{\partial B}{\partial n_k}\right)}{\frac{\partial F}{\partial Z}} \qquad \textbf{A. 7}$$

where,

$$\frac{\partial B}{\partial P} = \frac{B}{P} \qquad \textbf{A. 8}$$

$$\frac{\partial A}{\partial P} = \frac{A}{P} \qquad \textbf{A. 9}$$

$$\frac{\partial B}{\partial T} = -\frac{B}{T} \qquad \textbf{A. 10}$$

$$\frac{\partial A}{\partial T} = A\left(\frac{1}{a}\frac{\partial a}{\partial T} - \frac{2}{T}\right) \qquad \textbf{A. 11}$$

$$\frac{\partial B}{\partial n_k} = \frac{P}{RT}\frac{\partial b}{\partial n_k} \qquad \textbf{A. 12}$$

$$\frac{\partial A}{\partial n_k} = \frac{P}{R^2T^2}\frac{\partial a}{\partial n_k} \qquad \textbf{A. 13}$$

$$\frac{\partial b}{\partial n_k} = \frac{b_k - b}{N_j} \qquad \textbf{A. 14}$$

$$\frac{\partial a}{\partial n_k} = \frac{1}{N_j}\left(\frac{\partial a}{\partial x_k} - 2a\right) \qquad \textbf{A. 15}$$

$$\frac{\partial a}{\partial x_k} = 2\sum_{i=1}^{nc} x_i\sqrt{a_i a_k}\left(1 - d_{ik}\right) \qquad \textbf{A. 16}$$

$$\frac{\partial a}{\partial T} = -\frac{R\sqrt{\Omega_a}}{2\sqrt{T}}\sum_i\sum_k x_i x_k\left(m_k\sqrt{a_i\frac{T_{ck}}{P_{ck}}} + m_i\sqrt{a_k\frac{T_{ci}}{P_{ci}}}\right)\left(1 - d_{ij}\right) \qquad \textbf{A. 17}$$

$$\frac{\partial d_{ij}^{'}}{\partial T} = \frac{1}{a}\left[\frac{\partial}{\partial T}\left(\frac{\partial a}{\partial x_k}\right) - d_{ij}^{'}\frac{\partial a}{\partial T}\right] \qquad \textbf{A. 18}$$

$$\frac{\partial d_{ik}^{'}}{\partial n_k} = \frac{2\sqrt{a_i a_k}\left(1 - d_{ik}\right)}{aN_j} - d_{ik}^{'}\left(\frac{1}{N_j} + \frac{1}{a}\frac{\partial a}{\partial n_k}\right) \qquad \textbf{A. 19}$$

SRK fugacity coefficient:

$$\ln\varphi_i = \frac{b_i}{b}(Z-1) - \ln(Z-B) + \frac{A}{B}\left(\frac{b_i}{b} - d_{ij}^{'}\right)\ln\left(\frac{Z+B}{Z}\right) \qquad \textbf{A. 20}$$

Derivatives of fugacity coefficient with respect to Pressure:

$$\frac{\partial \ln\varphi_i}{\partial P} = \frac{b_i}{b}\frac{\partial Z}{\partial P} - \frac{\left(\frac{\partial Z}{\partial P} - \frac{\partial B}{\partial P}\right)}{Z-B} + \frac{A}{B}\left(\frac{b_i}{b} - d_{ij}^{'}\right)\left[\frac{\partial B}{\partial P} - \frac{B}{Z}\left(\frac{\partial Z}{\partial P}\right)\right]\left(\frac{1}{Z+B}\right) \qquad \textbf{A. 21}$$

Derivatives of fugacity coefficient with respect to Temperature:

$$\frac{\partial \ln\varphi_i}{\partial P} = \frac{A}{B}\left(\frac{b_i}{b} - d_{ij}^{'}\right)\left[\frac{\partial B}{\partial T} - \frac{B}{Z}\left(\frac{\partial Z}{\partial T}\right)\right]\left(\frac{1}{Z+B}\right) \qquad \textbf{A. 22}$$

$$\frac{\partial \ln\varphi_i}{\partial T} = \frac{b_i}{b}\frac{\partial Z}{\partial T} - \frac{\left(\frac{\partial Z}{\partial T} - \frac{\partial B}{\partial T}\right)}{Z-B} +$$

$$\left[\frac{1}{B^2}\left(\frac{b_i}{b} - d_{ij}^{'}\right)\left(B\frac{\partial A}{\partial T} - A\frac{\partial B}{\partial T}\right) - \frac{A}{B}\frac{\partial d_{ij}^{'}}{\partial T}\right]\ln\left(\frac{Z+B}{Z}\right) +$$

$$\frac{A}{B}\left(\frac{b_i}{b} - d_{ij}^{'}\right)\left[\frac{\partial B}{\partial T} - \frac{B}{Z}\left(\frac{\partial Z}{\partial T}\right)\right]\left(\frac{1}{Z+B}\right) \qquad \textbf{A. 23}$$

Derivatives of fugacity coefficient with respect to component mole number:

$$\frac{\partial \ln \varphi_i}{\partial n_k} = \frac{b_i}{b}\left[\frac{1}{b}\frac{\partial b}{\partial n_k}(1-Z)+\frac{\partial Z}{\partial n_k}\right]-\frac{\left(\frac{\partial Z}{\partial n_k}-\frac{\partial B}{\partial n_k}\right)}{Z-B}+$$

$$\left[\frac{1}{B^2}\left(\frac{b_i}{b}-d_{ij}^{'}\right)\left(B\frac{\partial A}{\partial n_k}-A\frac{\partial B}{\partial n_k}\right)-\frac{A}{B}\left(\frac{b_i}{b^2}\frac{\partial b}{\partial n_k}+\frac{\partial d_{ij}^{'}}{\partial n_k}\right)\right]\ln\left(\frac{Z+B}{Z}\right)+$$

$$\frac{A}{B}\left(\frac{b_i}{b}-d_{ij}^{'}\right)\left[\frac{\partial B}{\partial n_k}-\frac{B}{Z}\left(\frac{\partial Z}{\partial n_k}\right)\right]\left(\frac{1}{Z+B}\right) \qquad \textbf{A. 24}$$

SRK molar enthalpy:

$$h-h^0 = RT(Z-1)+\frac{T\,\partial a/\partial T-a}{b}\ln\left(\frac{Z+B}{Z}\right) \qquad \textbf{A. 25}$$

Derivative of molar enthalpy with respect to Pressure:

$$\frac{\partial h}{\partial P} = RT\frac{\partial Z}{\partial P}+\frac{1}{b}\left(a-T\,\partial a/\partial T\right)\left[\frac{\partial Z}{\partial P}\left(\frac{B}{Z}\right)-\frac{\partial B}{\partial P}\right]\left(\frac{1}{Z+B}\right) \qquad \textbf{A. 26}$$

Derivative of molar enthalpy with respect to Temperature:

$$\frac{\partial h}{\partial T}-\frac{\partial h^0}{\partial T}=R\left(Z-1+T\frac{\partial Z}{\partial T}\right)+\frac{1}{b}\left(T\,\partial^2 a/\partial T^2\right)\ln\left(\frac{Z+B}{Z}\right)+$$

$$\frac{1}{b}\left(a-T\,\partial a/\partial T\right)\left[\frac{\partial Z}{\partial T}\left(\frac{B}{Z}\right)-\frac{\partial B}{\partial T}\right]\left(\frac{1}{Z+B}\right) \qquad \textbf{A. 27}$$

Derivative of molar enthalpy with respect to Component mole number:

$$\frac{\partial h}{\partial n_k}-\frac{\partial h^0}{\partial n_k}=RT\frac{\partial Z}{\partial n_k}-\frac{1}{b}\left(\frac{\partial a}{\partial n_k}-T\frac{\partial}{\partial n_k}\left(\partial a/\partial T\right)-\frac{a-T\,\partial a/\partial T}{b}\frac{\partial b}{\partial n_k}\right)\ln\left(\frac{Z+B}{Z}\right)+$$

$$\frac{1}{b}\left(a-T\,\partial a/\partial T\right)\left[\frac{\partial Z}{\partial n_k}\left(\frac{B}{Z}\right)-\frac{\partial B}{\partial n_k}\right]\left(\frac{1}{Z+B}\right) \qquad \textbf{A. 28}$$

where,

$$\frac{\partial h^0}{\partial n_k}=h_k^0 \qquad \textbf{A. 29}$$

$$\frac{\partial h^0}{\partial T}=C_p^0 \qquad \textbf{A. 30}$$